# Annual report of the ISTC Contact Expert on Accelerator Driven Transmutation projects
# Year 2002

During our last meeting in Karlsruhe, January 2002 – see Minutes from Karlsruhe meeting (Appendix 1) – following decisions and action plans were decided.

## I. CEG decided to put the following priority recommend on the ISTC projects

| Project Number | Shorttitle | Funding priority by CEG |
|---|---|---|
| **2267** | **SAD-project - Creation of Subcritical Assembly Driven by Proton Accelerator in Dubna** | **high/1** |
| **2213** | **Fission Cross Sections of Tungsten Isotopes** | **high/2** |
| **2253** | **Investigation of the delayed neutron characteristics** | **high/3** |
| **2199** | Neutron cross-sections and level densities for fission-products Th, 233U | low at the moment |
| **2224** | ECO-FRIENDLY HIGH-POWER LINACS | to be reviewed by accelerator experts |
| **2257** | Proton accelerator based intense source of radioactive ions for nuclear physics experiments. | to be reviewed by accelerator experts |
| **2299** | Experimental and theoretical research of the basic parameters…. | Beyond the competence of CEG |
| **2405** | Experimental researches of nuclear-physics characteristics of materials essential for the processes of weapon plutonium …. | low at the moment! |

1) **Project #2267 - SAD** has been approved. C. Broeders, E. Gonzales, Ff. Mellier (earlier – Roland Soule) and W. Gudowski are actively collaborating with this project. V. Bhatnagar is also involved in this collaboration. Working plan is under approval process. In April 2002 V. Bhatnagar and W. Gudowski participated in the first preparatory meeting. See *Appendix 2* for Minutes from this meeting.
*Appendix 3* presents the status of the SAD-project - #2267

2) **Project #2213** has not been approved – further interactions with D. Gambier needed. Again on the agenda of CEG in Brussels.
*Appendix 4* presents a final report of the project #1309 showing competence and quality of the research work done by the Khlopin's group applying for the project #2213. Project #1309 is in a way a predecessor of the project #2213

3) **Project #2253** has not been approved. Should be reevaluated in Brussels and consulted with USA – Los Alamos is being interested. Shared funding should be an option.

4) **Project #2405** has not been approved following our request to see the results of the predecessor-project # 1145. Final report and status of the TENDL library has been reported to the CEG (see my e-mail with the whole document) and now is in hands of CEG experts.

## II. Status reports of on-going projects

**#1372 - Complex radiochemical and activation analysis of long-life nuclear waste transmutation in fast reactors and in the beams of high energy accelerators**

Proper links to the European projects have been established, project experts participate regularly in European data project meetings, prof. Brandt and dr. Westmeier collaborate avctively with this project.
Status of the project is reported in the Appendix 5.
The multi-national team of experimentalists worked very smoothly together.
However there are some problems, both inside the two main participating laboratories, IPPE-Obninsk and JINR-Dubna, as well as in collaboration between them. There are some delays in realizing the project plan and some difficulties in performing planned experiments.
It is quite probable that three radioactive waste nuclides mentioned in the ISTC-contract, namely $^{241}$Am, $^{234}$U, and $^{238}$Pu may not be allowed as targets around the JINR accelerators, as they are definitively too radioactive. The suggestion from prf. Brandt is to turn to study of **$^{239}$Pu**, instead of $^{241}$Am, $^{234}$U and $^{238}$Pu.

**#1606 - Experimental Mock-Up of Molten Salt Loop of Accelerator-Based Facility for Transmutation of Radioactive Waste and Conversion of Military Plutonium**

Progress meeting took place, after some problems and cancellation (Attention – some general organizational solution should be adopted to avoid problems related to visas, invitations, hotels, etc. To be suggested by the Chairman during the meeting!) 16-18 December, 2002 in Moscow.
**Conclusions:** The work done in the frame of ISTC-1606 project is evaluated by the European collaborators (A. Rieneski, W. Gudowski, M. Hugon and M. Delpech) as a good work, getting the information, having experimental values for the salt properties, for the processing of the salt.

The loop is build seriously and the test program is already defined. The loop will be transfer soon to Snezhnisk/Chelyabinsk. The project is performing what was expected with good exchanges between Russian teams and European teams.

In Appendix 6 the travel report and conclusions of the meetings are given in details.

**# 2048 - Improvement of corrosion resistance of constructional steels**
(prepared by a "prinicipal " collaborator Georg Mueller)
The main goal of the project is to develop a surface treatment process for steels to improve their corrosion resistance in liquid lead alloys at high temperatures (550 -650° C) and critical oxygen activities (high and low). The project started at May, 1st 2002. In March 2002 a ´Kick Off´ meeting was organized by the project leader in St. Petersburg with participation of all collaborating Institutions from Europe (FZK, CEA, CIEMAT). During this meeting it was agreed that Western steels (T91, HT9 and 1.4970) should be investigated as reference material within this project. In accordance to the work plan two technical quarter reports were prepared by the participants and delivered to ISTC. Development of the program and methods of experimental investigations was completed. After several experimental tests it was decided to proceed as follows: deposition of precoatings at the vacuum arc facility BULAT and additional at magnetron type coating devices; electron-beam processing of samples at the GESA-1 and GESA-2 electron beam accelerators; tests in liquid lead and lead-bismuth in stagnant melts (FXT-0, FXT-1 and FXT-2 facilities), under conditions of free convection (KP-2 loop) and in the circulating non isothermal test benches with forced circulation of lead and lead-bismuth (IPPE – CU-1 and CU-2 loops, CRISM Prometey X2 and X6 loops); creep and durability tests (test benches X5 and X2 with the tensile-testing machine R5). Requirements to samples to be tested at these facilities have been worked out as well as procedures for post-corrosion investigations. For the surface alloy process four different coatings Al, Al+Y, Al+Si, Al+Si+Y are under investigation. First screening tests in stagnant and flowing melts at 650 °C and different oxygen activities (a=1, 10-3 and 10-5) were performed. A preliminary design study of a full scale cylindrical electron beam facility for treatment of claddings was finished. At present the works are somewhat in advance to the corresponding time schedule of the technical work plan.

In Appendix 7 minutes from the kick-off meeting in St. Petersburg, 25.03.02 – 26.03.02, can be found.

**# 2068 Development and demonstration of HLW partitioning technology with the use of phosphorylated calixarenes.**

Objectives achieved up to date follow the timeline from the workplan. In the first year the study on extraction properties of phosphorylated calixarenes and simulated phosphine oxides was started.

Appendix 8 gives a detail status report together with 3 quarterly reports.

**#B70 – part 2 "Experimental Research of Transmutation of Fission Products and Minor Actinides in a Thermal Neutron Spectrum Subcritical Assembly Driven with a Neutron Generator"**

This project is also well integrated into the European collaboration network and has also important links to IAEA activities.
The following experiments with external sources (DD),(DT) have been performed:

1. Measurements of $k_{eff}$ for $N_{rods}$ equal to 280;
2. Multiplication factors $K_{src}$ for $N_{rods}$ equal to 280 with different neutron sources $S_0(E,r,z)$;
3. Reactivity changes $\Delta\rho$ ($\rho=(k_{eff}-1)/k_{eff}$) due to removal 4 central fuel rods (Nrods= 280 and 276) (The measurements with pulse DT neutrons have been performed $\tau = 7\mu s$)
4. Measurements of the following reaction rates inside the experimental channels of the core (Nrods = 280) $^{115}In(n,)^{116}In$, $^{19}F(n,2n)^{18}F$, $^{63}Cu(n,2n)^{62}Cu$, $^{27}Al(n,p)^{27}Mg$, $^{27}Al(n,\alpha)^{23}Na$, $^{65}Cu(n,2n)^{64}$, $^{56}Fe(n,p)^{56}$,Mg, $^{54}Fe(n,p)^{54}Mg$, $^{59}Co(n,p)^{59}Fe$, $^{59}Co(n,\alpha)^{56}Fe$ (external source - DT neutrons).
5. Measurements of neutronics of the assembly without uranium fuel driven with a neutron generator working in (D,D) and (D,T) - modes and with Cf -252 source, placed at different positions of the assembly. (Measurements of spatial distribution of neutron flux density in experimental channels of the core and of the reflector).
6. Measurements of the external source multiplication factor of the sub-critical assembly $M = (1-k_s)-1$ for the DD, DT neutrons and neutrons Cf - 252 source located at different positions in the assembly at the subcriticality level that corresponds to number of fuel pins 280.

Appendix 9 gives a more detailed status report of the Yalina experiments.

**#2002 - "Experimental and theoretical studies of the yields of residual product nuclei produced in thin Pb and Bi targets irradiated by 40-2600 MeV protons"**

Project 2002 is underway according to the scheduled workplan. Tentative processing of the irradiation results for natural Pb at 600 MeV have been completed.
A design of a facility that will ensure automatic replacement of irradiated samples has been finished. The facility has been designed for operating with two Ge detectors, with a table for placing samples between the detectors. With the facility in actual operations, the realization of all of our projects will be much facilitated.
This project is very well integrated with European and worldwide nuclear data projects. Very good cooperation with CEG.

In Appendix 10 three quarterly reports for 2002 are given.

III. Project #559 - 1 MW molten Pb-Bi spallation target. (Chairman's headache!!)

The target complex TC-1 has arrived at the University of Nevada Las Vegas (UNLV) campus. The intent of UNLV is to utilize this target complex as a significant component of a multi-year lead-bismuth (LBE) technology development program. The goal of UNLV is a research program that contributes to the international programs while remaining true to the fundamental goal of all Universities: The training and education of students

A meeting of the Molten Metal Target Advisory Committee took place in Las Vegas July 31 – August 2 2002. Minutes of this meeting are given in Appendix 11. One of the suggestions of the meeting was to diossolve the Advisory Group and collaborate with UNLV in a frame of very diffuse define international collaboration (like NEA/OECD or similar). Waclaw Gudowski opposed very strongly to this idea and suggested to continue collaboration through the existing collaboration network, i.e. Molten Metal Advisory Group and our Contact Expert Group. The meeting approved this idea.

**R&D Recommendations for continued 1MW target collaboration:**

After completing this 2-year combined program of TC-1 operations and supporting fundamental research, UNLV must make decisions based on its own institutional needs and interests, coupled with available funding and the status of related LBE technology developments outside UNLV. Based on current knowledge the following decision tree is foreseen:

1) Add corrosion chemistry control and measurement capabilities to TC-1.

2) Add a test section to TC-1. Most likely, this entails removing the target itself from TC-1 and replacing it with some geometry suitable for tests of interest that have arisen from the ongoing capabilities development.
3) Perform contaminant transport experiments. Such experiments may permanently exclude future use of TC-1.
4) Visual inspection of the TC-1 primary circuit surfaces, metallography and/or another investigations of primary circuit structure materials.
5) Abandon TC-1 in favor of re-use of key components in another facility (pump, flow meter, heat exchanger, instruments, etc.)

Clearly, 1 and 2 can be performed without destruction, but 3, 4 can limit future use of the system or will lead to TC-1 renewal end 5 means the end of TC-1 life.

**Capabilities Development and Research Recommendations**

During this meeting, a variety of possible research topics were suggested. Some of the topics listed below were extracted from a preliminary Test Plan document for UNLV, crafted by Ning Li, Samir Moujaes and Joachim Knebel.

1) Flow measurement techniques: Magnetic, ultrasonic, and the application of classic or innovative techniques to high temperature liquid metals.
2) Pressure measurements.
3) Continuous level measurements. Currently, point measurements are typically made using continuity-type probes. A continuous measurement using optical or other techniques would improve control and operation of LBE facilities.
4) Gas flow in liquid LBE: The entrainment and movement of bubbles; buoyancy effects.
5) Contaminant species transport and deposition in flowing LBE.
6) Oxygen control and measurement. In advance of possibly installing a system in TC-1, benchtop tests could be performed to study effects of gas feed rates and temperature on establishing objective oxygen concentrations, and the stability of oxygen concentrations and oxygen sensors with time.
7) Corrosion modelling and mass transfer model verification.
8) Heat transfer measurements including unusual geometries where no correlations have been developed, typical of most window designs. It is a significant fact that in window cooling both thermal and momentum boundary layers are never fully developed.
9) Ultrasonic and radiographic non-destructive inspection of structures.
10) Benchmark experiments for CFD codes and turbulence models for low Pr number flow.
11) Scaled testing of new LBE system concepts, such as gas-assisted pumping and windowless targets.

**Conclusions**

CEG's continued in 2002 its successful activities with significantly increased intensity of the interactions with ISTC projects.
Most of the objectives set during the meeting in Karlsruhe have been achieved.
For the coming year some we should put some efforts into following activities:

1) Continue and further develop contacts with ISTC projects of interest
2) Improve communication with ISTC Office in Brussels, continue good collaboration with ISTC Secretariat in Moscow.
3) Regain momentum in collaboration with USA, Japan and Korea. Stimulate development of "driving forces" and incentives for such collaboration
4) Further efforts into experimentally oriented projects. Take care about 559-target.
5) *To be continued after discussion in Brussels…*

**Contact Expert Group (CEG) on ISTC ADS projects**

**Summary Records of the Fifth (or Second EU CEG) Meeting**

**Forschungszentrum, Karlsruhe**

**February 1, 2002**

Meeting began with very interesting visits to ITU and KALLA-Laboratory at FZK on January 31.

## I. Welcome and approval of the agenda

W. Gudowski, Chairman of the CEG, welcomed the participants and invited them to introduce themselves. M. Hugon was kindly ask to be the Secretary. M. Hugon reminded that he had been nominated Secretary for one year only, but accepted to be Secretary for this meeting only.
List of the participants, the CEG members and a few guests is given (see p. 10 of Attachment 1).
The agenda was approved (see Attachment 1).

## II. Review of the CEG activities in 2001

1. Minutes of the fourth CEG meeting in Stockholm in January 2001 (see Attachment 2)

W. Gudowski presented first a CEG Annual Report for 2001 (see Attachment 3) and then reported and reviewed the action plan decided during the fourth CEG meeting in Stockholm in January 2001. Most of the tasks and actions have been successfully completed and do not require any further activities.

The actions were:

1. M. Hugon is responsible for preparation of the minutes of this meeting – **completed.**
2. W. Gudowski contacts co-ordinator of n-TOF-ND-ADS project informing him about **# 1749 - closed by the CEG on ADTT.**
3. W. Gudowski and J. Blomgren inform co-ordinator of HINDAS project on **# 1971 – done.**
4. W. Gudowski initiates talks with US–partners on 50-50 financing of **# 1971 – project financed by USA.**
5. W. Gudowski will ask the Japanese to have access to the results of the project #**1828, which is funded by Japan – to be done again.** He will also send the proposal for information to the co-ordinator of the FP5 n-TOF-ND-ADS project.

6. W. Gudowski takes action on **# 1755**: suggests Mr. Finck, be the driving force of this project and will send proposal to the co-ordinator of the FP5 MUSE project for consultation – **closed by the ISTC Governing Board.**
7. W. Gudowski will send proposal **# 1886** to the co-ordinator of the FP5 SPIRE project and to Mr. G. Bauer (PSI) for consultation - **closed by the ISTC Governing Board.**
8. W. Gudowski will send the proposal **#2048** to the co-ordinator of the FP5 TECLA project for consultation – **done.**
9. C. Broeders will assess the whole proposal **# 2048** and its cost, which seems to be very high – **completed, proposal accepted for funding by the Governing Board.**
10. C. Broeders (FZK) will be the monitor for project **# 1372** – **project not yet signed by ISTC**. He has made the link with Mr. F. Kaeppeler (FZK), who participates to the n-TOF-ND-ADS – **done.**
11. W. Gudowski will discuss matching funds for **# 1372** with USA and Japan. Once accepted, this project should be coupled to the FP5 n-TOF-ND-ADS project – **project financed by EU only.**
12. M. Hugon together with Mr. J.-F. Dozol (CEA) will monitor **# 2068 – STCU # Rus-09 (j) – project STCU # Rus-09 (j) started on 1 January 2002, but project # 2068 not yet signed by ISTC.**
13. W. Gudowski will discuss matching funds from Japan and USA for **# 2002**. Looks after coupling with the FP5 HINDAS project - **project financed by EU only, started on 1 January 2002.**

2. Project **# 1606**: Molten salt technology for radwaste and Pu treatment

The kick-off meeting of this project was held in the closed city of Snezhinsk in the province of Chelyabinsk on May 31 - June 1, 2001. The record of decisions is given in Attachment 3.1

M. Hugon mentioned that Western collaborators should maintain funding on long-term R&D projects, such as the molten salt loop, when it is installed in one of the hot cells in Snezhinsk. In the past, experiments for fusion studies have been built in closed cities with ISTC funds, but have been subsequently abandoned because of change of interest of the financing parties (in this case, European countries).

This project should be linked through the CEG with the ISTC project # 1486 (Cascade sub-critical molten salt reactor for RW transmutation), which is funded by the USA and Japan. The link could be achieved directly by the Kurchatov Institute, which is participating in both projects. **No link has been established yet !!!**

Project # 1606 is coupled to the FP5 concerted action MOST (molten salt reactor) in the area of "Safety and efficiency of future systems". V. Ignatiev (KI) was invited at the second meeting of the MOST project in Cadarache on 21-22 January 2002.

3. Project **# 559**: Pilot flow lead-bismuth target of MW power for ADS

The ISTC Molten Metal Target Advisory Group met on November 12 from 8 p.m. to10 p.m. during the AccApp/ADTTA'01 conference in Reno (Nevada). This EU-

Russian-US advisory group was set up 3 years ago in the framework of ISTC project # 559 (funded by USA (500 000$), EC (250 000$) and Sweden (250 000$)). Its objective is to monitor the progress of the fabrication and test of a liquid lead-bismuth target in Obninsk and its subsequent transfer to the LANSCE facility in Los Alamos to study its coupling with the linac.

The participants were made aware that the cost for the installation of the target in the LANSCE facility was 20 million $ and that LANL had no such funding available. An alternative solution proposed by the USA was to install the target in the University of Nevada in Las Vegas (UNVL) as an installation to train students on lead corrosion and thermodynamics without irradiation. UNLV is willing to invest 2 million $ per year during 4 years for this.

A task force was up with H. Ait Abderhaim (SCK.CEN) and J. Knebel (FZK) to propose a joint EU-US programme for the target. Meanwhile, H. Ait Abderhaim has expressed a strong interest to install the target in SCK.CEN Mol.

## III. Presentation on ISTC projects

1. Proposal **#2048:** Improvement of Corrosion Resistance of Constructional Steels in Liquid Pb and Pb-Bi Alloys by Means of Their Surface Modification with the Help of Pulsed Electron Beams and Protective Coatings

The original proposal, which was first unofficially submitted at the last CEG meeting, was assessed by C. Broeders. A new proposal has been prepared with a reduced cost (640 000 $) and has been sent to the second Governing Board meeting of 2001. It has been accepted for funding and the work plan sent to ISTC.

Rusanov (IPPE Obninsk) reported on the objectives of the project, which are to study the corrosion of pre-coated steels in liquid lead alloys at 550-650 °C. V. Engelko (NIIEA St Petersburg) explained how to put a 20 μm aluminium coating on the steel surface with an intense pulsed electron beam.

The foreign collaborators of this project are G. Müller (FZK), CIEMAT and CEA.

*Action on G. Müller:* ISTC project **# 2048** should be coupled to the FP5 TECLA project and be associated with the TESTRA cluster on technological support for transmutation.

A participant asked whether the stability of the protective coating to radiation was improved by the electron beam treatment.

G. Heusener questioned whether irradiation of certain lead isotopes was creating dangerous isotopes. If it is true, then a process is needed to separate those lead isotopes.

*Action on V. Engelko:* Find out if it is possible to get the data on generation of dangerous isotopes from Pb-Bi cooled reactors used in submarines.

2. ISTC related nuclear data projects in Russia

S. Yavshits (KI) made a summary of the ISTC funded projects on nuclear data for transmutation. A table including 50 proposals submitted to ISTC for funding in this area was distributed by L. Tocheny (ISTC). These project proposals cover the energy range 1eV-3GeV and have different status: non funded proposals, completed projects, on-going projects, projects still under negotiation and proposals to be submitted to the ISTC Governing Board. The large number of ISTC proposals related to different aspects of nuclear data are finished, on-going, or proposed (for spallation reactions in target, for transmutation reactions in reactors and subcritical blankets, driven by accelerator or fusion driver - within thermal, fast and very fast neutron spectrum.
Initialisation of the projects is often quite chaotic, not always based on a principle of "suply-and-demand". There are virtually no coordination between Proposals – proposals are in principle in competiotion and there are no working mechanisms to enforce a natural coordination. It is therefore recommended to create a special short-term ISTC project (using e.g. the model of monography projects) with the following objectives:

1. Review and summary of the all ISTC-funded nuclear data projects. If scientifically motivated other projects not funded by ISTC (like so called back-ground results, library activities – as for example photonuclear data coordinated by IAEA) could be also included.
3. Review of the implementation of the final results of data projects – like contribution to nuclear data libraries, avaiability from nuclear data libraries, new nuclear data files etc.
4. In collaboration with nuclear data community – updating "The High priority request list for nuclear data at low and intermediate energies" Formulation of recommendations for further nuclear data focus of ISTC projects.

Experts from relevant Russian institutes should be participating in this project in order to guarantee its broad scope (to CEG knoweledge most active isntitutes are IPPE, ITEP, JINR, Arzamas, Khlopin RI, Kurchatov, MIFI, NIKIET + some more)
Moreover, CEG strongly recommends to publish the set of selected nuclear detat related papers under the ISTC label with results of completed projects in a special issue of e.g. "Nuclear Instruments and Methods".

*Actions on L. Tocheny:*
- What is the situation of TENDL ? This data base was promised in project ISTC # 1145
- In order to be useful, the data obtained in the ISTC projects funded by the EU should be delivered to the JEFF Committee for evaluation. This will allow to find out the gaps and possible overlaps with FP5 projects. Similarly, the data coming from the projects funded by Japan (JAERI - JENDL), KOREA (KAERI) and USA should be sent to the relevant data libraries.
- There should be co-ordination between the Russian institutes providing nuclear data. CJD Obninsk is the nuclear fission data centre in Russia, but KRI St Petersburg proposes to make a web page for nuclear data.
- The results obtained in the ISTC projects on nuclear data should be published in the journal "Nuclear Instruments and Methods".

3. Proposal # **2267**: Creation of Sub-critical Assembly Driven by Proton Accelerator (SAD)

The SAD project at JINR in Dubna is indirectly linked to the FP5 MUSE project through the University of Mining and Metallurgy (UMM) of Krakow (Poland). UMM is an assistant contractor to KTH, a principal contractor of the MUSE project.

The SAD project is at present funded by CEA, CIEMAT, FZK and KTH. Its aim was to prepare proposal # **2267**: Creation of Sub-critical Assembly Driven by Proton Accelerator (SAD). The purpose of this proposal is the development and construction of an experimental installation (SAD) using the existing 660 MeV synchro-phasotron proton accelerator in JINR and a sub-critical MOX fuel blanket. The present conceptual design of the experimental sub-critical assembly in Dubna (SAD) is based on a core with a nominal thermal power of 15-20 kW. This corresponds to a multiplication coefficient keff=0.95 and an accelerator beam power of 0.5 kW.

The proposal is co-ordinated by JINR Dubna and has NIKIET Moscow, Mayak Ozersk, GSPI Moscow and VNIIM Moscow as partners. The total cost of this 3-year project is 1 750 000 $, of which 1 200 000 $ are requested to ISTC. The rest of the funding will be provided by JINR and its member states.

A joint seminar was organised with FZK/IRS, where V. Shvetsov presented the on going SAD-related experiments in Dubna and the SAD project proposal **# 2267.** This seminar provided background information for evaluation of project **# 2267**.

The SAD experiment is different from the MUSE experiment by the size of the installations, the neutron producing target and the power level of the sub-critical core. SAD is a compact experiment with a one-meter diameter and 60 cm high core and a real lead target producing neutrons, whereas MUSE has a very large core without target (the neutron energy is 14 MeV). In addition, the power level of the sub-critical core is 15-20 kWth in SAD and a few 100 Wth in MUSE. Therefore the SAD experiment appears to be complementary to MUSE.

SAD project may become the first experimental facility proving feasibilty of coupling a real spallation source with a subcritical core. Data obtained on specific MOX fuel, Pb targets and coolants will serve as a gold mine of data for validation of the codes and improving simulation tools for transmutation systems. Moreover, this expertiment will deliver very valuable shielding data for intermediate and high energy neutrons.

## IV. Evaluation of new ISTC proposals

The results of the evaluation are given in the group ranking table indicating the funding priority (see Attachment 4).

**# 2199: Neutron cross-sections in the resonance energy range and nuclear level densities for fission products, Th, $^{233}$U**

This proposal is not supported for funding by the CEG at this moment. There are 2 Korean collaborators (Pohang and Kyungpook Universities) and one European (TU Delft. CEG Chairman will consult this projects with Korean colleagues.

*Action on W. Gudowski:*
Consult # 2199 with Korea, contact TU Delft.

**# 2213: Measurements of proton- and neutron-induced fission cross sections of separated tungsten isotopes and natural tungsten in 50-200 MeV energy region**
This proposal is supported for funding by the CEG with high-medium priority (2nd in the group ranking). Once accepted, it could be linked the FP5 HINDAS project.

**# 2224: New generation eco-friendly high-power ion linear accelerators**
This proposal is not supported for funding by the CEG. It will be sent by S. Monti to Pagani and A. Müller for advice.

*Action on S. Monti:*
Send proposal #2224 to Pagani and A. Müller for advice.

**# 2253: Investigation of the delayed neutron characteristics from the fission of compound nuclei $^{233}$Th, $^{234}$U, $^{235}$U, $^{244}$Am, $^{238}$Np, $^{246}$Cm, $^{233}$Pa, $^{234}$Pa, $^{240}$Np, Np at the excitation energies from 5 to 20 MeV**
This proposal is supported for funding by the CEG with medium priority (3rd in the group ranking). At present, no experimental work is performed on delayed neutrons both in FP5 and ISTC.

**# 2257: Proton accelerator based intense source of radioactive ions for nuclear physics experiments**
This proposal is not supported for funding by the CEG. It should be sent to accelerator specialists for evaluation.

**# 2267: Creation of Sub-critical Assembly Driven by Proton Accelerator (SAD)**
This proposal is supported for funding by the CEG with the highest priority (1st in the group ranking).

**# 2299: Experimental and theoretical research of the basic parameters of interaction of intense relativistic nuclear beams with matter**
This proposal is not supported for funding by the CEG. It should be sent to accelerator specialists for evaluation.

**# 2405: Experimental researches of nuclear physics characteristics of materials essential for the processes of weapon plutonium utilisation and radioactive wastes transmutation**
This proposal is not supported for funding by the CEG. As the previous project # 1145 of the same team was completed at the end of July 2001, the final report should be first sent to the CEG prior to evaluation. This project was financed by the USA and had Japan with JAERI as foreign collaborator.

## V. Re-evaluation of ISTC proposals evaluated during the Fourth CEG meeting

The results of the re-evaluation are given in the revised group ranking table established during the Fourth CEG meeting in Stockholm (see Attachment 4).

**# 1749: Measurements of the cross sections of fast and resonance neutrons induced fission of minor actinides for their transmutation with accelerator-driven systems**
This proposal is closed by the CEG on ISTC ADS projects.

**# 1755: Experimental study of fast and fast-thermal accelerator driven systems on the basis of BFS-1 – microtron complex**
This proposal was already closed by the ISTC Governing Board.

**# 1828: Measurements of the Prompt Neutron Spectra of Minor Actinides. Fast Neutron Induced Fission of $^{241}$Am and $^{243}$Am, Thermal Neutron Induced Fission of $^{243}$Cm**
This proposal is funded by Japan.
*Action on W. Gudowski:*
The Chairman will ask again the Japanese to have access to the results of this interesting project. They are of interest for the FP5 n-TOF-ND-ADS project.

**# 1886: Investigations of the irradiation and thermomechanical endurance of the beam window of ADS neutron generating target**
This proposal was already closed by the ISTC Governing Board.

**# 1971: Neutron Induced Fission Cross-Sections of $^{240}$Pu, $^{243}$Am and W in the Energy Range 1 – 200 MeV**
This proposal is funded by USA.
*Action on W. Gudowski:*
The Chairman will ask the Americans to send the data of this project, which are of interest for the FP5 HINDAS project.

## VI. Short report on project # 559: Pilot flow lead-bismuth target of MW power for ADS

This point was added to the agenda shortly before the meeting to discuss the possibility of installing the target in SCK.CEN in Mol, as proposed by H. Ait Abderhaim (see Section II.3). P. Kupschus reported that for the MYRRHA project, which is only funded by SCK.CEN, there are two options to use the target loop for licensing purposes: (i) as a demonstration experiment or (ii) run corrosion experiments under conditions relevant to MYRRHA. The first possibility is excluded, because the loop is too small.

A. Rusanov (IPPE Obninsk) felt that it would be very difficult to use the target for other purposes than for irradiation.

L. Tocheny and the CEG encouraged SCK.CEN to discuss with IPPE Obninsk and DOE. Before making a proposal to install the target in Mol, SCK.CEN will ask IPPE whether it is possible or not to export the target to Mol rather than to Las Vegas. If yes, a cost estimate will be made in about six weeks. If the price is acceptable, a proposal will be made.

*Action on Kupschus:*
Prepare an option for #559 target experiments at Mol,

## VII. Links between ISTC and EU FP5 funded projects

The possible links between EU FP5 projects on advanced options for partitioning and transmutation and ISTC projects/proposals are identified as indicated in Figure 1 (see caption very carefully).

## VIII. FINAL RECOMMENDATION on highest priority projects (see Excel recommendation table for more detail information – Attachment 4)

**The highest priority:**

### # 2267: Creation of Sub-critical Assembly Driven by Proton Accelerator (SAD)

The SAD experiment has a special importance for the European partners being very complementary to the MUSE experiment and offering important enhancements by using a real spallation target driven by 660 MeV accelerator. The size of the installations, the neutron producing target and the power level of its sub-critical core make this installation very suitable and convenient for many interesting experiments.
SAD project may become the first experimental facility proving feasibilty of coupling a real spallation source with a subcritical core. Data obtained on specific MOX fuel, Pb targets and coolants will serve as a gold mine of data for validation of the codes and improving simulation tools for transmutation systems. Moreover, this expertiment will deliver very valuable shielding data for intermediate and high energy neutrons.
Moreover, a focus on Pb reflector/coolant makes this experiment very important for the European projects TECLA, MEGAPIE and XADS.
FZK, KTH, CEA and CIEMAT have already put significant efforts to design this experiment and to fund some preliminary experiments related to SAD.

**Next highest priorioty**:

### # 2213: Measurements of proton- and neutron-induced fission cross sections of separated tungsten isotopes and natural tungsten in 50-200 MeV energy region

Khlopin's group has a long time experience of a very successful collaboration with Uppsala University, running interesting nuclear data projects on Uppsala accelerator. Moreover, projects run by this group are well integrated into the European projects and in reality Khlopin group acts already now as a subcontractor (funded by ISTC through #1309) to HINDAS project. This group has a unique competence (missing in

European groups) in neausrements techniques for fission induced by very high energy neutrons.

**Third priority:**

**# 2253: Investigation of the delayed neutron characteristics from the fission of compound nuclei $^{233}$Th, $^{234}$U, $^{235}$U, $^{244}$Am, $^{238}$Np, $^{246}$Cm, $^{233}$Pa, $^{234}$Pa, $^{240}$Np, Np at the excitation energies from 5 to 20 MeV**

At present, no experimental work is performed on delayed neutrons neither in FP5 nor in ISTC, however this data are very important for designing transmutation systems. We support this project and we shall integrate it into BASTRA cluster.

## IX. Diverse issues

W. Gudowski proposed to change the name of the CEG to **CEG on ISTC Transmutation projects**. A revised veriosn a the White paper is attached in Attachment 5.

G. Heusener wished well to the CEG members because it was his last CEG meeting before his retirement next May. Dr. Heusener stressed also that it would be very important to reinvigorate a close collaboration with USA , Japan and Korea.

**CEG acknowledges and appreciates very much EU/ISTC travel support for our Russian guests for this meeting.**

## X. Summary of ACTION PLAN

***V. Engelko***

*Action on V. Engelko:*

Find out if it is possible to get the data on generation of dangerous isotopes from Pb-Bi cooled reactors used in submarines.

***W. Gudowski***

The Chairman will ask again the Japanese to have access to the results of the project #1828. They are of interest for the FP5 n-TOF-ND-ADS project.

The Chairman will ask the Americans to send the data of this project, which are of interest for the FP5 HINDAS project.

Consult # 2199 with Korea, contact TU Delft.

***P.Kupschus***

Prepare an option for #559 target experiments at Mol,

***S. Monti***

Contact accelerator experts – Pagani and Mueller to get review on the proposal #2224

***G. Müller***

ISTC project **# 2048** should be coupled to the FP5 TECLA project and be associated with the TESTRA cluster on technological support for transmutation.

***L. Tocheny***:

- What is the situation of TENDL ? This data base was promised in project ISTC # 1145
- In order to be useful, the data obtained in the ISTC projects funded by the EU should be delivered to the JEFF Committee for evaluation. This will allow to find out the gaps and possible overlaps with FP5 projects. Similarly, the data coming from the projects funded by Japan should be sent to JENDL.
- There should be co-ordination between the Russian institutes providing nuclear data. CJD Obninsk is the nuclear fission data centre in Russia, but KRI St Petersburg proposes to make a web page for nuclear data.
- The results obtained in the ISTC projects on nuclear data should be published in the journal "Nuclear Instruments and Methods".

Waclaw Gudowski Michel Hugon

**Minutes**
**Meeting on the Status of the SAD Project held on April 9, 2002, LIT JINR.**

At the meeting the following persons were present:

1. W.Gudowski, RIT, Stockholm, Sweden
2. V.Bhatnagar, Research Directorate General, European Commission, Brussels, Belgium.
3. V.N.Shvetsov, FLNP, JINR, Dubna, Russia
4. A.Polanski, LIT, JINR, Dubna, Russia
5. V.S.Barashenkov, LIT, JINR, Dubna, Russia
6. A.N.Sosnin, LIT, JINR, Dubna, Russia

**SAD fuel issues:**

*Short info provided by V. Shvetsov:*

Manufacturing of the fuel elements will take 2 years, however paperwork and design procedures are to be started tomorrow after the decision to approve the project is taken.

The MAYAK factory is reliable and there are little doubts that the time sche3dule will be kept. The factory is the main producer of the fuel elements for the liquid metal cooled fast reactors in operation in the country; manufacturing of the fuel elements is well developed. Up to now there are no limitation on the distribution of fuel inside the fuel element: each rod will be well certified; x-ray proved scheme of the fuel density distribution will be provided for each rod as well as the isotope composition of each separate fuel element.

The first interactions with designers indicate that a vertical setup of the assembly is preferable because horizontal position requires a lot of special loading machinery to serve the installation during the operation, e.g. pneumatic loading systems which cost a lot. Installation must be equipped with minimal amount of tools because of the limitations on the project funding. However, the vertical composition requires special beam line bending the trajectory of the beam. Available at JINR bending magnets are cheap but has a small bending angle and therefore one needs several of them to bend a beam by 90 degrees.

One single bending magnet is not available, neither can be purchased in a frame of a SAD budget. There may be a chance to find such a magnet "on loan" from the western collaborators. Such magnet will probably have weight of 40 tons and bending radius of about 4 meters.

W. Gudowski will investigate an option with a single bending magnet.

There are advantages and disadvantages of a vertical setup. For example: in case of the vertical setup a beam dump is not needed however it is not clear if safety assessment will show that an emergency horizontal beam stop will not be needed for protection against the bending magnet failure. Thickness of the shielding will also decrease in vertical setup. A horizontal setup gives much better access for experimentalists, is cheaper and simpler. However it will require, as mentioned, a lot of special, non standard, loading machinery to serve the installation during the operation.

An option with the bending angle of the magnet of about 60 degrees will be also assessed; such magnet will be much cheaper and one can use available magnets to further turn the beam. No cryogenic systems must be introduced, because of the complexity and the need to build the supporting technical infrastructure.

The choice of the setup must be done soon after deep going analyses and consultations with western partnerts. Close ties with existing accelerator facilities must be established very soon (Saturne, Los Alamos etc.) in order to optimize the design and use existing competence and expertise.

A 50 page project description with cost estimation of materials and manufacturing has been prepared by V.N.Shvetsov's report. It has proposed that V.N.Shvetsov should prepare a 2-3 page summary of this report.

*Discussion:*

An issue of fuel cassettes (bundles). Should they be used ? The answer is "Yes" however cassettes will not have the steel walls in order to decrease the amount of iron in the core. Total length of the cassettes is 80 cm. Perhaps a single intermediate grid should be introduced into the cassettes. For the horizontal core setup there will be a serious risk of "compactation effect" in case of grid failures.

There have been some discussions with CEA-Cadarache (R. Soule) on CEA participation and assistance in SAD experiments. For example the supply of very small fission chambers have been discussed. Most of the decisions on what equipment will be needed have to be done very soon to accommodate this into the design.

To assess the final design and to help in calculations during a design stage of SAD a SAD advisory group has been suggested. This group will be lead by the chief designer from NIKIET, Lopatkin, and suggested members are: C. Broeders (FZK), R. Soule (CEA-Cadarache), E. Gonzales (CIEMAT), W. Gudowski (KTH) and A. Polanski (JINR). V.N.Shvetsov will supervise the whole set of efforts in calculations.

*What is a procedure and a timetable for licensing of SAD?*

Authorities issuing the license need special sets of papers on general design, safety, substantiation of safety proving reliability of the installation. The first volume of this set is prepared by NIKIET, the second one – by GSPI (general project including substantiation of the buildings, walls, ceilings, roofs, equipment, shielding, falling planes etc). After these 2 volumes are ready we can approach the 6 Russian ministries responsible for taking the final decision to build the installation. Some of the papers for the vertical design are ready. The licensing procedure can be started immediately. V.N.Shvetsov plans to start the process next week and he is to draw a timetable of these activities to control the flow.

**ACTION PLAN:**

Better contacts with the MUSE, n-TOF, MEGAPIE projects and other groups must be established as soon as possible. Some measurements methodologies developed in European projects like calorimetric methods should be adopted in SAD. Responsible – **V. Shvetsov**

Some actions need to be undertaken to inform the JINR member states about SAD-expriment. V. Shevtsov is negotiating with Czech Rep., Bulgaria, Roumania and Poland to contribute with 30000 USD per year per country. Responsible V**. Shevtsov, A. Polanski**

**V.N.Shvetsov** will distribute the new version of the project and perhaps a 2-3 pages list of the equipment you have or you want to use. Westerners could be helpful and it can be beneficial for JINR.

V.Bhatnagar andM.Hugon will be added into the list of the SAD project official collaborators. V.Bhatnagar will supervise the licensing activities.

W. Gudowski is responsible for organizing the SAD Advisory Group.

W. Gudowski V. Shvetsov

# STATUS OF THE SAD PROJECT
# ISTC Project #2267
# January 22, 2003

As the preparation of the ISTC-JINR official contract is not finished yet the operations under the project carried preparatory character. So by forces of initiative groups of the employees of the organizations – participants the conceptual project of the SAD installation, prepared in 2001 was redesigned. The basic SAD data were negotiated between JINR, design institutes and IA "Mayak"

## SAD Basic Data

SAD basic features are determined with "Phasotron" JINR proton accelerator and usage as a basic fuel elements (FE) serially released in Russia MOX FE of a BN-600 reactor. Rather modest proton current of accelerator (maximum value is 3.2 μA) positions the SAD facility within the section of prototype installation between zero power facilities and industrial scale ones, which are designed now. Basic data are listed in following tables.

Table 1: SAD basic data

| | |
|---|---|
| Thermal power | 15 ÷ 20 kWt |
| Protons energy | 660 MeV |
| Beam power | 0.75 ÷ 1 kWt |
| Proton beam / target orientation | Vertical |
| Fuel elements orientation | Vertical |
| Criticality coefficient | $k_{eff}$ <0.95 |
| Fuel | MOX, $UO_2$ + $PuO_2$ |
| Cladding tubes maximum temperature | 400° C |
| Spallation target | Replaceable: Pb, Pb-Bi, W |
| Reflector | Pb |
| Coolant | Air |

Proton accelerator parameters are listed in Table 2.

Table 2 : Parameters of JINR Phasotron

| | |
|---|---|
| Intensity of the extracted proton beam: | 3.2 μA ($1.997 \cdot 10^{13}$ protons/s) |
| Beam emittance: | $\Sigma_x = p\,(5.1 \pm 2.3)\ cm \cdot mrad$ |
| | $\Sigma_y = p\,(3.4 \pm 1.4)\ cm \cdot mrad$ |
| Time structure | |
| Fast extraction | |
| Frequency | 250 Hz |
| FWHM | 20 μs |
| Number of protons in pulse | $0.8 \cdot 10^{11}$ |
| Slow extraction | |
| Frequency | 250 Hz |
| Pulse width | 3500 μs |
| Beam microstructure | |
| Micropulse FWHM | 10 ns |
| Micropulse period | 70 ns |

SAD fuel properties, negotiated with Mayak and VNIINM are listed in

Table 3: SAD fuel properties

| | |
|---|---|
| Fuel composition | $(UO_2 + PuO_2)$ |
| U and Pu fraction % by mass | ≤ 87.6 |
| $^{239}$Pu fraction weight % from all Pu isotopes | ≥ 95.0 |
| $^{235}$U fraction % from all U isotopes* | ≤ 0.4 |
| Relative $PuO_2$ fraction weight %* | ≤ 30.0 |
| Density* | 10.0 – 10.7 g/cm$^3$ |

*- parameters will be specified during FE technical project stage

SAD facility will be equipped with experimental channels permitting installation and extraction in different parts of subcritical assembly, reflector and shielding different detectors and isotopic samples. At present time SAD potential user are requested to propose their requirements for locations, dimensions and design features of such channels.

## SAD Allocation and Composition

SAD facility will be located in new building will be constructed in a gap (18 meters width) between existing accelerator and YASNAPP-2 buildings (Figure 1).

General layout of the installation now supposes proton beam injection from the bottom of installation after 110° turn with strong bending magnets. So proton beam heats the target from below and it's necessary to have rather thick beam stop in straightforward i.e. top direction. The biological shielding properties will be determined by the highest neutron energy. The preliminary view of the SAD beamline general layout is shown at *Figure 2*. Initially horizontal beam is deflected 20 degrees downwards inside accelerator hall and then turns 110° and hits spallation target, located inside fuel blanket. Such an allocation permits to avoid safety problems with possible water accidents, which exist in the case of beam injection from the top of the core. These problems are: accidental core flood with bending magnet cooling water or flood with a water from the nearest water reservoir in the case of accidental break of dam.

Estimated volume of the structural concrete necessary to satisfy requirements of radioprotection standards in initial GSPI composition drawings was about 3000 cubic meters (***Figure 3***). Now preliminary calculations of the exposure rate behind YASNAPP-2 wall with different shielding thickness (point 6.2 of the time schedule) were made and there are strong indications that concrete shielding thickness in side and top directions (red arrow on ***Figure 3***) could be decreased at least by factor 1.5 – i.e. necessary volumes will be decreased correspondingly by factor more than 3.

## SAD Beam Line Magnetic Elements

Several meetings with Romanian authorities at JINR were devoted to Romania participation in SAD project. There is preliminary agreement that 8° bending magnets, quadruple lenses and corrective magnets for proton beam line will be manufactured and delivered to JINR within Romania contribution to JINR budget. Cost estimation of

this part is k$ 200-250, which is about ¾ of total beamline cost. Visit for preparation of corresponding agreement is planned for middle of February 2003.

## SAD Fuel

Mayak manufactured necessary amount of the $PuO_2$, request on $UO_2$ was sent to Electrostal machinery plant. Fuel pellets technology research efforts started.

## SAD General Project

Second version of the initial technical proposal was distributed between project participants in November 2002. Negotiations on the project areas of responsibility are in progress and third/final version of the general technical proposal will be prepared in February 2003. This activity represents point 1 of the time schedule.

Certified design organization, responsible for SAD control system was chosen and introduced into project workplan.

Measurements of the exposure rate outside accelerator hall were performed at different configurations of the collimators in beam extraction area (point 6.1 of the time schedule).

## SAD Core Project

Necessary calculations (point 5.1 of the time schedule) and initial data on SAD core (point 5.2 of the time schedule) are partly prepared by NIKIET.

# Project Workplan

Project workplan will be finally prepared in February 2003 and Contract between ISTC and JINR could be signed in March 2003.

Figures:

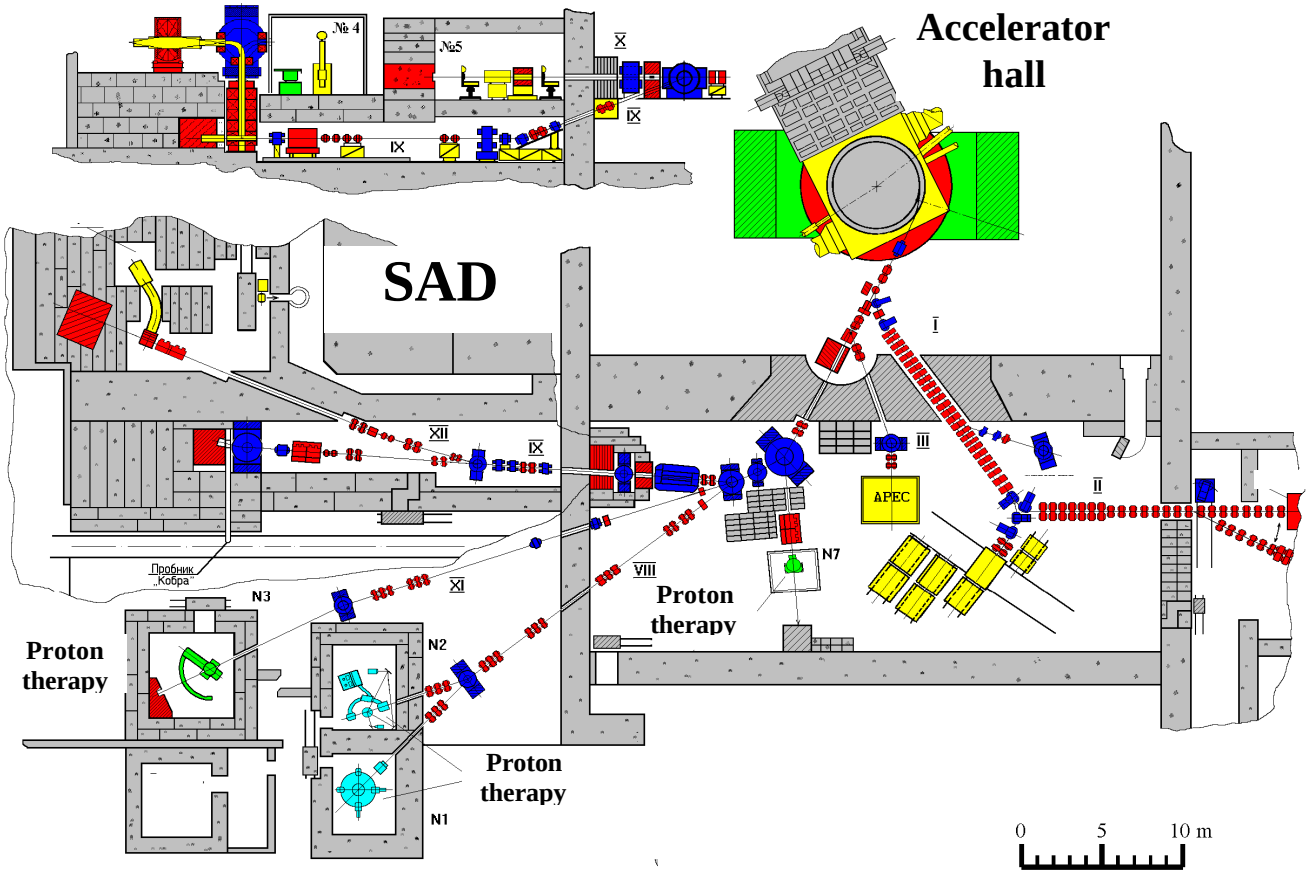


*Figure 1 General plan view of the JINR "Phasotron" accelerator complex (in the left upper corner side view of the neutron/meson therapy complex). SAD facility will be constructed between accelerator and YASNAPP-2 buildings.*

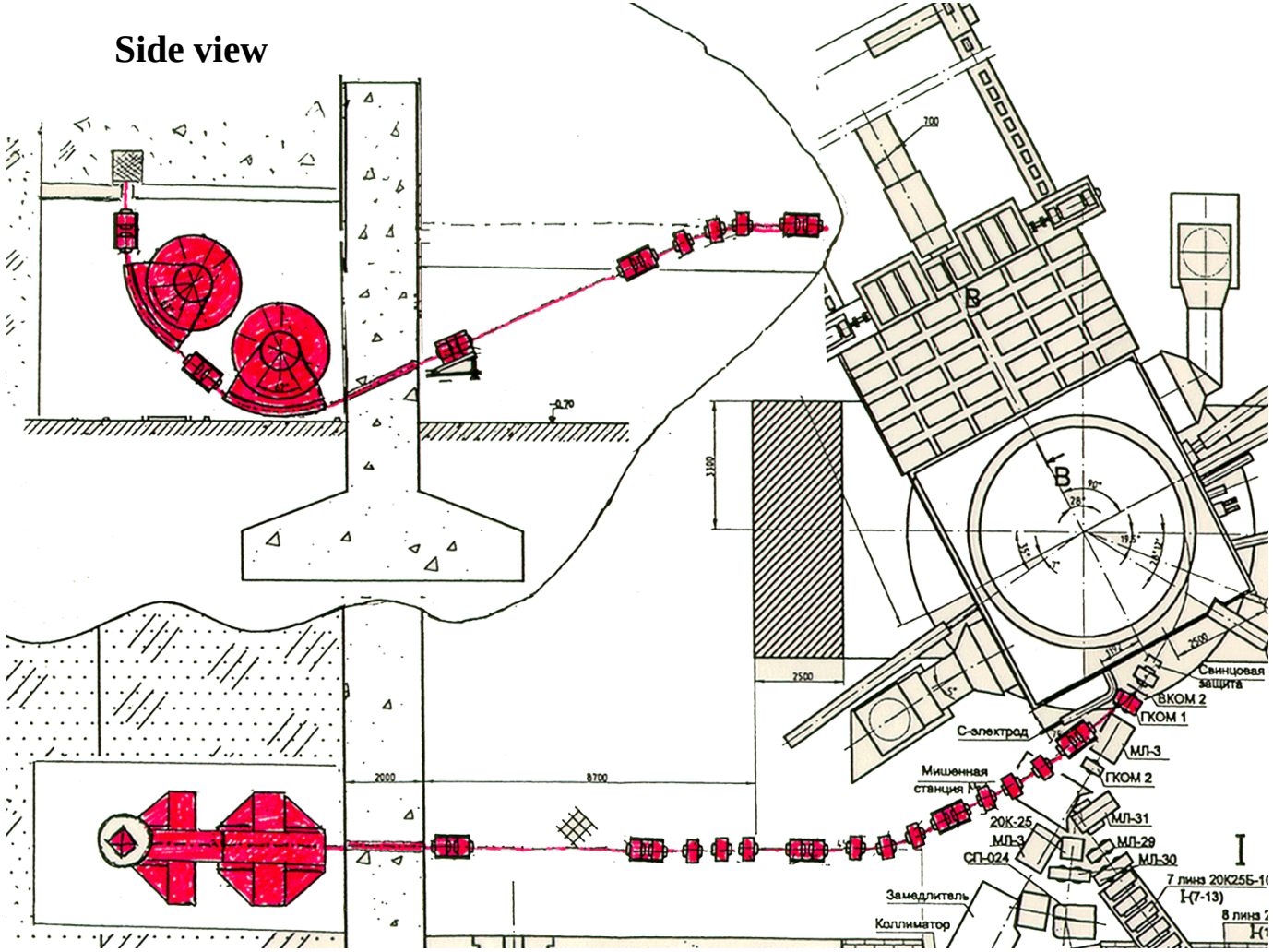


*Figure 2: SAD proton beamline with two 60° magnets*

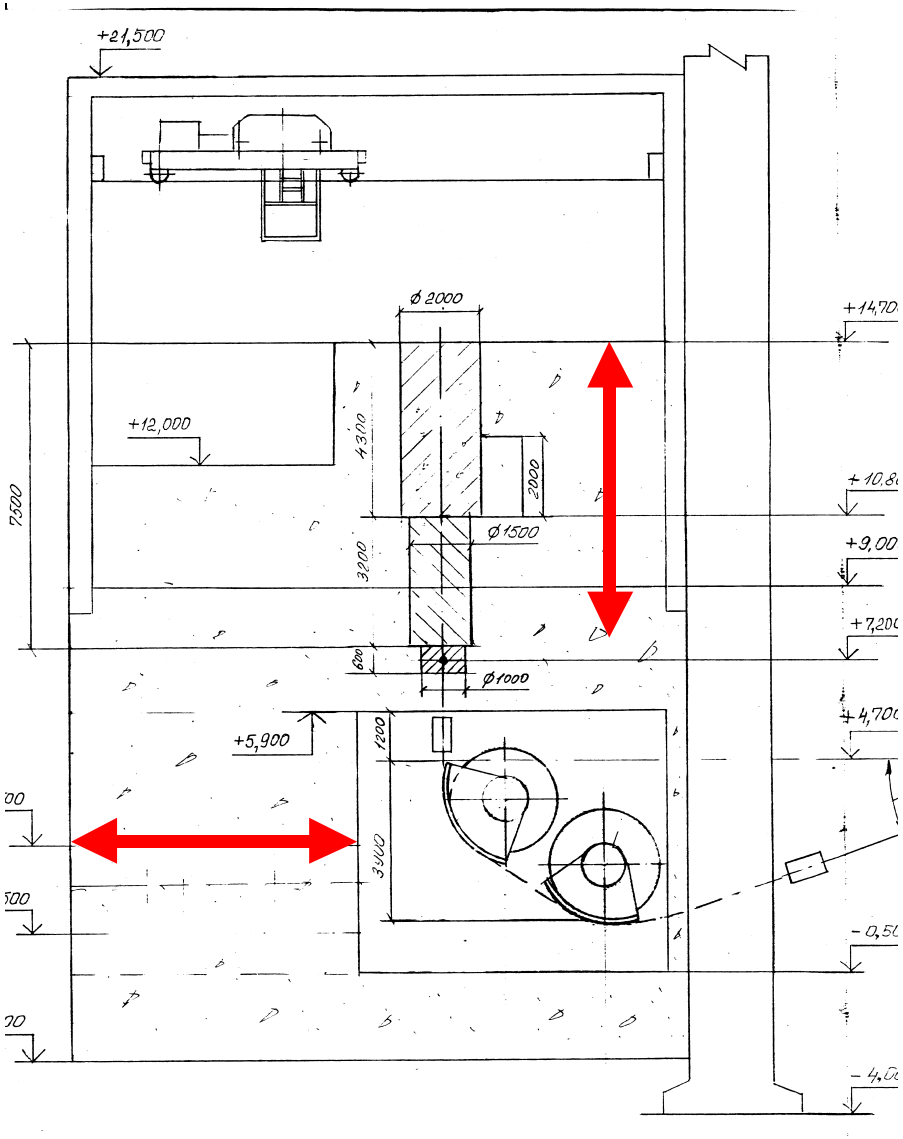


*Figure 3: see text*

**ISTC 1309-99**

**Unrestricted Summary**
**Final Report**
**Project ISTC 1309-99**

# Measurements and Comparison of Proton- and Neutron-Induced Fission Cross Sections of Lead and Neighboring Nuclei in the 20-200 MeV Energy Region.

**(From 1 December 1999 to 30 November 2002 for 36 months )**

**Vilen Pavlovich Eismont**
**(Project Manager)**
**V.G.Khlopin Radium Institute**

**Director General**

**of V.G. Khlopin Radium Institute**

**A.A. Rimski-Korsakov**

**Project Manager**

**V.P. Eismont**

**November 2002**

**This work was supported financially by European Community and performed under the contract to the International Science and Technology Center (ISTC), Moscow**

**ISTC 1309-99**

# Measurements and Comparison of Proton- and Neutron-Induced Fission Cross Sections of Lead and Neighboring Nuclei in the 20-200 MeV Energy Region.

(From 1 December 1999 to 30 November 2002 for 36 months )

Vilen Pavlovich Eismont
(Project Manager)
V.G.Khlopin Radium Institute

The goal of the present Project is the development of the nuclear database for calculation of the key parameters of neutron production targets of the accelerator driven systems (ADS). For this the fission cross sections of the lead isotopes $^{204, 206, 207, 208}$Pb, as well as of $^{209}$Bi and $^{205}$Tl have been measured at the proton and neutron beams of the cyclotron of the T. Svedberg Laboratory of the Uppsala University (Uppsala, Sweden).The fission cross sections have been determined for $^{nat}$Pb and $^{209}$Bi (monoisotope) as most prospective materials for the neutron production targets of ADS. Neutron-induced fission cross sections for all lead isotopes and $^{205}$Tl and proton-induced fission cross sections for $^{204}$Pb and $^{205}$Tl (above about 60 MeV) have been obtained for the first time. Obtained dependences of the fission cross sections on the nucleon energy and difference of these dependences for isotopes under study give the base for extracting of fundamental parameters of the fission process and their connection with excitation energy and nuclear structure and thus for creating of the fission models being adequate to the reality and computer codes for theory and practice.

Keywords: experiment, fission cross section, fission fragment angular distribution, separated lead isotopes, $^{204, 206, 207, 208}$Pb, $^{209}$Bi, $^{205}$Tl, protons, quasi-monoenergetic neutrons, intermediate energy, nuclear data, new technology, accelerator.

* Russia, 194021, St.-Petersburg, 2-y Murinskiy Pr. 28,
Telephone /Fax: (812) 247-57-49
e-mail: 105@atom.nw.ru

**ISTC 1309 - 99**

The work was performed together with the follow institutes and collaborators:

## 1. Institutes.

V.G.Khlopin Radium Institute,
Russia, 194021, St.-Petersburg, 2-y Murinskiy Pr. 28,
Telephone /Fax: (812) 247-57-49
e-mail: 105@atom.nw.ru

## 2. Foreign collaborators.

**Name:** Uppsala University, Department of Neutron Research
**Address:**
**City:** Uppsala
Country: Sweden
Zip Code: Box 525,SE-75121
**Name of Signature Authority:** Prof. Jan Kallne
**Tel:** +46 18 471 23 94
**Fax:** +46 18 471 38 53
**E-mail:** jan.kallne@tsl.uu.se
**Name of Contact Person:** Assoc. Prof. Jan Blomgren
**E-mail:** Jan.Blomgren @tsl.uu.se

**Name:** Forschungszentrum Karlsruhe
**Address:**
**City:** Karlsruhe
Country: Germany
Zip Code: Postfach 3640, 76021
**Name of Signature Authority:** Dr. G. Heusener
**Tel:** +49 7247 825510
**Name of Contact Person:** Dr. C.H.M. Broeders
**Tel:** +49 7247 822484
**Fax:** +49 7247 823484
**E-mail:** Cornelis.Broeders@ike.fzk.de

**Name:** European Commission, MO75 5/55
**Address:**
**Street:** Rue de la Loi/Wetstrat, 200
**City:** Brussels
Country: Belgium
Zip Code: 1049
**Name of Signature Authority:** Dr. Michel Hugon
**Tel:** +32 2 296 57 19
**Fax:** +32 2 295 49 91
**E-mail:** michel.hugon@dg12.cec.be
**Name of Contact Person:** Dr. Michel Hugon
**Tel:** +32 2 296 57 19
**Fax:** +32 2 295 49 91
E-mail: **michel.hugon@dg12.cec.be**

The goal of the present Project is the development of the nuclear database for calculation of the key parameters of neutron production targets of the accelerator driven systems (ADS). For this the fission cross sections of the lead isotopes $^{204, 206, 207, 208}$Pb, as well as of $^{209}$Bi and $^{205}$Tl have been measured at the proton and neutron beams of the cyclotron of the T. Svedberg Laboratory of the Uppsala University (Uppsala, Sweden).The fission cross sections have been determined for $^{nat}$Pb and $^{209}$Bi (monoisotope) as most prospective materials for the neutron production targets of ADS.

The use of new detectors of fission fragment lies in the basis of technical approach to solving problems of the project. First of all it relates to non-traditional technique of the fission fragment detection – thin-film breakdown counters (TFBC), which have been developed at Radium Institute. This method has an advantage of threshold registration of the fission fragments under the condition of intense fluxes of weakly-ionizing particles. At the same time, TFBC give out a fast pulse signal, that allows to use the time-of-flight method. Another type of detectors, using in the project, is a multisectional ionization chamber with Frisch grids. In the intermediate energy region this detector was used for the first time. It is also adopted for the time-of-flight method. In addition to the fission cross section measurement with high and accurately determined detection efficiency of the fragments, this method allows measurement of the fragment angular distributions.

Neutron-induced fission cross section measurements (with a help of ionization chamber and thin-film breakdown counters) were carried out relatively to the $^{238}$U fission cross section. The standard $^{238}$U fission cross section [A.D. Carlson *et al.*, "Update to Nuclear Data Standards for Nuclear Measurements", summary report on a Consultants meeting at the IAEA Headquarters, Vienna, 2-6 December 1996, ed. by H. Wienke and published as report INDC(NDS)-368 (April 1997)] was used for absolutization of the relative results. Proton-induced fission cross section measurements (with a help of thin-film breakdown counters) were carried out both relatively to the both the $^{209}$Bi and $^{238}$U fission cross sections using the known data on these cross sections and absolutely – by means of determination of the proton fluence with the help of monitor reactions of the (p, xpyn)-type.

In the table 1 the absolute neutron-induced fission cross sections of all nuclei under study (obtained using the method of ionization chamber) are presented.

**Table 1**. The absolute fission cross section (mb) of tallium-205, lead isotopes and bismuth-209 (IC) induced by intermediate energy neutrons.

| $E_n$ | $^{205}Tl$ | $^{204}Pb$ | $^{206}Pb$ | $^{207}Pb$ | $^{208}Pb$ | $^{nat}Pb$ | $^{209}Bi$ |
|---|---|---|---|---|---|---|---|
| **MeV** | **Mb** | **mb** | **mb** | **mb** | **mb** | **mb** | **mb** |
| **34.7±1.4** | 0.025±0.017 | 0.46±0.13 | 0.08±0.04 | 0.035±0.024 | 0.029±0.022 | 0.048±0.025 | 0.37±0.07 |
| **46.3±1.1** | – | 2.58±0.15 | 0.79±0.06 | 0.51±0.04 | 0.28±0.04 | 0.49±0.05 | 2.70±0.12 |
| **65.4±0.9** | 0.97±0.08 | 11.1±0.7 | 5.1±0.3 | 3.28±0.22 | 2.33±0.17 | 3.32±0.24 | 12.3±0.7 |
| **96.0±1.4** | 4.73±0.26 | 30.3±1.7 | 15.2±0.9 | 11.2±0.6 | 8.2±0.5 | 10.9±0.7 | 28.8±1.7 |
| **133.6±1.9** | 7.9±0.7 | 46.2±3.4 | 24.2±1.8 | 18.2±1.4 | 14.3±1.1 | 18.0±1.5 | 43.3±3.3 |
| **173.9±1.9** | 11.1±1.6 | 61.7±4.8 | 38.7±3.1 | 35.3±2.5 | 23.9±1.8 | 30.5±2.4 | 66.6±3.8 |

In tables 2 and 3 the fission cross section ratios for all nuclei under study to the fission cross section of $^{209}Bi$ obtained by IC and TFBC are presented correspondingly.

**Table 2.** Proton-induced fission cross sections of lead isotopes and thallium relatively $^{209}Bi$ (IC).

| $E_n$[MeV] | $^{205}Tl$ | $^{204}Pb$ | $^{206}Pb$ | $^{207}Pb$ | $^{208}Pb$ | $^{nat}Pb$ |
|---|---|---|---|---|---|---|
| **34.7±1.4** | 0.067±0.047 | 1.260±0.440 | 0.223±0.120 | 0.098±0.069 | 0.077±0.059 | 0.133±0.080 |
| **46.3±1.1** | - | 0.970±0.060 | 0.298±0.024 | 0.193±0.017 | 0.105±0.015 | 0.183±0.018 |
| **65.4±0.9** | 0.079±0.006 | 0.904±0.048 | 0.414±0.022 | 0.266±0.016 | 0.189±0.012 | 0.270±0.017 |
| **96.0±1.4** | 0.164±0.008 | 1.050±0.055 | 0.526±0.026 | 0.394±0.017 | 0.290±0.015 | 0.380±0.018 |
| **133.6±1.9** | 0.181±0.012 | 1.070±0.054 | 0.557±0.029 | 0.418±0.023 | 0.331±0.020 | 0.415±0.024 |
| **173.9±1.9** | 0.17±0.023 | 0.934±0.056 | 0.580±0.034 | 0.529±0.031 | 0.360±0.024 | 0.458±0.030 |

**Table 3.** Neutron-induced fission cross sections of lead isotopes and thallium relatively $^{209}$Bi (TFBC).

| $E_n$ [MeV] | $^{204}$Pb | $^{206}$Pb | $^{207}$Pb | $^{208}$Pb | $^{nat}$Pb | $^{205}$Tl |
|---|---|---|---|---|---|---|
| **34.7±1.4** | 1.04±0.09 | 0.17±0.02 | 0.13±0.02 | 0.029±0.007 | | 0.020±0.007 |
| **46.1±1.2** | 1.06±0.05 | 0.32±0.02 | 0.19±0.01 | 0.082±0.005 | 0.20±0.01 | 0.067±0.004 |
| **66.4±0.9** | 1.02±0.05 | 0.45±0.02 | 0.29±0.01 | 0.202±0.008 | 0.30±0.01 | 0.105±0.005 |
| **73.4±1.0** | | | | 0.219±0.019 | 0.32±0.03 | |
| **89.5±0.8** | 1.06±0.08 | 0.49±0.03 | 0.37±0.03 | 0.28±0.02 | | 0.16±0.01 |
| **95.0±1.4** | 0.98±0.05 | 0.49±0.02 | 0.36±0.02 | 0.30±0.01 | 0.38±0.01 | 0.164±0.006 |
| **111.0±1.1** | 1.06±0.09 | 0.55±0.04 | 0.46±0.03 | 0.33±0.02 | | 0.204±0.016 |
| **133.0±1.9** | 1.00±0.06 | 0.59±0.03 | 0.44±0.02 | 0.31±0.01 | 0.42±0.02 | 0.23±0.01 |
| **144.0±1.8** | 1.02±0.07 | 0.65±0.04 | 0.50±0.03 | 0.39±0.02 | 0.46±0.03 | 0.25±0.01 |
| **173.9±1.9** | 1.00±0.04 | 0.61±0.02 | 0.47±0.02 | 0.37±0.01 | 0.51±0.02 | 0.25±0.01 |

In the table 4 and 5 the relative proton-induced fission cross sections and in the table 6 – the absolute proton-induced fission cross sections (obtained using the TFBC technique) are presented.

**Table 4.** Proton-induced fission cross sections of lead isotopes and thallium relatively $^{209}$Bi.

| E?,MeV | $^{204}$Pb | $^{206}$Pb | $^{207}$Pb | $^{208}$Pb | $^{nat}$Pb | $^{205}$Tl |
|---|---|---|---|---|---|---|
| **64±2** | 1.12±0.09 | 0.52±0.04 | 0.36±0.03 | 0.25±0.02 | -- | 0.17±0.01 |
| **94±2** | 1.05±0.12 | 0.58±0.06 | 0.52±0.06 | 0.37±0.04 | -- | 0.20±0.03 |
| **167±2** | 1.05±0.06 | 0.57±0.08 | 0.52±0.02 | 0.44±0.03 | 0.54±0.04 | 0.34±0.02 |

**Table 5.** Proton-induced fission cross section of $^{209}$Bi relatively to $^{238}$U.

| E?,MeV | $^{209}$Bi |
|---|---|
| **64±2** | 0.018±0.001 |
| **167±2** | 0.086±0.004 |

**Table 6.** Proton-induced fission cross sections of $^{209}$Bi $^{204,206,207,208}$Pb and $^{205}$Tl.

| E? , MeV | $^{209}$Bi, mb | $^{204}$Pb, mb | $^{206}$Pb, mb | $^{207}$Pb, mb | $^{208}$Pb, mb | $^{205}$Tl, mb |
|---|---|---|---|---|---|---|
| **47.5±0.5** | 9.3±0.9 | -- | -- | -- | -- | 0.86±0.09 |
| **49.2±0.5** | 11.3±1.1 | -- | -- | ---- | -- | 1.14±0.11 |
| **97.5±2.0** | 100±10 | 106±10 | 49±5 | -- | -- | 18±2 |
| **177.3±1.2** | 162±16 | 179±18 | 97±10 | 79±8 | 73±8 | 50±5 |

The data on the fission cross sections of $^{204,206,207,208}$Pb and $^{205}$Tl to the fission cross section of $^{209}$Bi obtained by both methods coincide within the accuracy of the uncertainties. The accuracy of the absolute neutron cross sections of $^{nat}$Pb and $^{209}$Bi measured by IC and the proton fission cross sections of the same nuclides measured by TFBC is about 10%.

Due to its practical importance, the fission cross sections of $^{nat}$Pb and $^{209}$Bi were fittted by the follow functions:

$\sigma_f$ ($^{nat}$Pb+n)= 50.1×exp-(127/E)$^{1.5}$ [mb], $\sigma_f$ ($^{nat}$Pb+p)= 113×exp-(99.9/E)$^{1.7}$ [mb],

$\sigma_f$ ($^{209}$Bi+n)= 101×exp-(109/E)$^{1.5}$ [mb], $\sigma_f$ ($^{209}$Bi+p)= 197×exp-(86.2/E)$^{1.7}$ [mb],

where ? – neutron energy, MeV.

The formulas are available for the region ?=25-180MeV, the weight-average deviation of the experimental points from the curve is not more than the uncertainties of the measurements.

The data of our neutron fission cross sections measurements of these nuclides practically coincide with the data of the follow works Staples, P.W. Lisowski, and N.W. Hill, *APS/AAPT Conference*, Washington, April 18-21, 1995; *Bull. Am. Phys. Soc*. **40**, 962 P. (1995); Updated data, Private communication by P. Staples (1996); O. Shcherbakov, A. Donets, A. Evdokimov, A. Fomichev, T. Fukahori, A. Hasegawa, A. Laptev, V. Maslov, G. Petrov, S. Soloviev, Y. Tuboltsev and A. Vorobyev, *Journal of Nuclear Science and Technology*, Supplement 2, August 2002, pp.230-233, Proceedings of the International Conference on Nuclear Data for Science and Technology, October 7-12, 2001, Tsukuba, Japan, vol.1.], ?? ????????? ???? ?????? ?????? [R. Nolte, M.S. Allie, P.J. Binns, F.D. Brooks, A. Buffler, V. Dangendorf, K. Langen, J.-P. Meulders, W.D. Newhauser, F. Ross and H. Schuhmacher, *Journal of Nuclear Science and Technology*, Supplement 2, August 2002, pp.311-314, Proceedings of the International Conference on Nuclear Data for

Science and Technology, October 7-12, 2001, Tsukuba, Japan, vol.1. The maximum deviation from our data (for $^{209}$Bi at neutron energy 97 MeV) is about 20%. The data on proton fission cross sections coincide with well-known published data.

Neutron-induced fission cross sections for all lead isotopes and $^{205}$Tl and proton-induced fission cross sections for $^{204}$Pb and $^{205}$Tl (above about 60 MeV) have been obtained for the first time.

The obtained dependences of the fission cross sections on the nucleon energy and difference of these dependences for isotopes under study give the base for extracting of fundamental parameters of the fission process and their connection with excitation energy and nuclear structure and thus for creating of the fission models being adequate to the reality and computer codes for theory and practice.

The detail comparison of proton and neutron cross sections of lead allows to conclude that the observed exceeding of fission cross sections in the proton reaction in a crucial manner connects not with the features of the mechanism of the nucleon interaction with the nucleus (??????? ???????), but with the higher fissility of the nuclei produced in this case (???????? ??????? ???????).

## List of publications.


**1. "Measurement and Comparison of Proton- and Neutron-Induced Fission Cross-section of Lead and Neighboring Nuclei in the 20-200MeV Energy Region for Improvement of Nuclei Models and Concepts of Accelerator Driven Systems".**

V.P. Eismont, A.G. Mitryukhin, V.S. Oplavin, I.V. Ryzhov, A.N. Smirnov, S.M. Solovjev, G.A., Tutin, H. Condè, N. Olsson, O. Jonson, P.-U. Renberg.

TSL Progress Report 2000-2001 Ed. A. Ingemarsson, Uppsala University (2002), p. 42.

**2. "An ionization chamber with Frisch grids for studies of high-energy neutron-induced fission".**

G.A. Tutin, I.V. Ryzhov, V.P. Eismont, A.V. Kireev, H. Condé, K. Elmgren, N. Olsson, P.-U. Renberg.

Nuclear Instruments and Methods in Phys. Res., A 457(2001), p. 646.

**3. "Proton- and Neutron-Induced Fission Cross Sections and Fission Probability in the Intermediate Energy Region".**

A.N. Smirnov, V.P. Eismont, I.V. Ryzhov, H. Condè, N. Olsson, P.-U. Renberg and A.V. Prokofiev.

Journal of NUCLEAR SCIENCE and TECHNOLOGY, Supplement 2. Proc. of Intern Conf. On Nuclear Data in Science and Technology 7-12 Oct, 2001, Tsukuba, Ibaraki, Japan, ed. K. Shibata, Atomic Energy Society of Japan, Japan Atomic Energy Research Institute vol. 1, p 238.

**4. "Measurements of Neutron-Induced Fission Cross Sections of Pb and Bi at Intermediate Energies".**

I.V. Ryzhov, G.A., Tutin, V.P. Eismont, A.G. Mitryukhin, V.S. Oplavin, S.M. Solovjev, H. Condè, N. Olsson and P.-U. Renberg.

Journal of NUCLEAR SCIENCE and TECHNOLOGY, Supplement 2. Proc. of Intern Conf. On Nuclear Data in Science and Technology 7-12 Oct, 2001, Tsukuba, Ibaraki, Japan, ed. K. Shibata, Atomic Energy Society of Japan, Japan Atomic Energy Research Institute vol. II, p 1410.

**5. "Angular Anisotropy of Nucleon-Induced Fission of Heavy Nuclei at Intermediate Energies".**

[1]A.N. Smirnov, [1]V.P. Eismont, [1]A.V. Prokofiev, [1]I.V. Ryzhov, [1]A. Tutin, [2]H. Conde, [2]N. Olsson.

Journal of NUCLEAR SCIENCE and TECHNOLOGY, Supplement 2. Proc. of Intern Conf. On Nuclear Data in Science and Technology 7-12 Oct, 2001, Tsukuba, Ibaraki, Japan, ed. K. Shibata, Atomic Energy Society of Japan, Japan Atomic Energy Research Institute vol. 1, p 299.

**6. "Fragment Angular Anisotropy in the $^{232}$Th(n,f) and $^{238}$U(n,f) Reactions at Intermediate Energies".**

I.V. Ryzhov, G.A. Tutin, V.P. Eismont, M. S. Onegin, H. Condé and N. Olsson.

Journal of NUCLEAR SCIENCE and TECHNOLOGY, Supplement 2. Proc. of Intern Conf. On Nuclear Data in Science and Technology 7-12 Oct, 2001, Tsukuba, Ibaraki, Japan, ed. K. Shibata, Atomic Energy Society of Japan, Japan Atomic Energy Research Institute vol. 1, p 295.

**7. "Intermediate Energy Neutron Induced Fission Cross Sections for Perspective Neutron Production Target in ADS".**

A.N. Smirnov, V.P. Eismont, A.V. Prokofiev, I.V. Ryzhov, A. Tutin, H. Conde, N. Olsson.

Sixth Information Exchange Meeting on Actinide and Fission Product Partitioning and Transmutation, Madrid, Spain, 11-13 December,2000, OECD-NEA(NDS), p.117 and CD ROM publication: paper P-36.

**8. "Nucleon-Induced Fission Cross Sections for ADS Needs".**

V.P. Eismont, N.P. Filatov, I.V. Ryzhov, A.N. Smirnov, G.A. Tutin, J. Blomgren, H. Condé, N. Olsson.

Seventh Information Exchange Meeting on Actinide and Fission Product Partitioning and Transmutation, Jeju, Korea, October, 14-16, 2002, program and abstracts, p. 153.

**ISTC 1309-99**

**Final**
**Project Technical Report**
**of ISTC 1309-99**

# Measurements and Comparison of Proton- and Neutron-Induced Fission Cross Sections of Lead and Neighboring Nuclei in the 20-200 MeV Energy Region.

**(From 1 December 1999 to 30 November 2002 for 36 months)**

**Vilen Pavlovich Eismont**
**(Project Manager)**
**V.G.Khlopin Radium Institute**

**Director General**

**of V.G. Khlopin Radium Institute**

**A.A. Rimski-Korsakov**

**Project Manager**

**V.P. Eismont**

**November 2002**

---

**This work was supported financially by European Community and performed under the contract to the International Science and Technology Center (ISTC), Moscow**

**ISTC 1309-99**

# Measurements and Comparison of Proton- and Neutron-Induced Fission Cross Sections of Lead and Neighboring Nuclei in the 20-200 MeV Energy Region.

(From 1 December 1999 to 30 November 2002 for 36 months)

Vilen Pavlovich Eismont
(Project Manager)
V.G.Khlopin Radium Institute

The goal of the present Project is the development of the nuclear database for calculation of the key parameters of neutron production targets of the accelerator driven systems (ADS). For this the fission cross sections of the lead isotopes $^{204, 206, 207, 208}$Pb, as well as of $^{209}$Bi and $^{205}$Tl have been measured at the proton and neutron beams of the cyclotron of the T. Svedberg Laboratory of the Uppsala University (Uppsala, Sweden). The fission cross sections have been determined for $^{nat}$Pb and $^{209}$Bi (monoisotope) as most prospective materials for the neutron production targets of ADS. Neutron-induced fission cross sections for all lead isotopes and $^{205}$Tl and proton-induced fission cross sections for $^{204}$Pb and $^{205}$Tl (above about 60 MeV) have been obtained for the first time. Obtained dependences of the fission cross sections on the nucleon energy and difference of these dependences for isotopes under study give the base for extracting of fundamental parameters of the fission process and their connection with excitation energy and nuclear structure and thus for creating of the fission models being adequate to the reality and computer codes for theory and practice.

Keywords: experiment, fission cross section, fission fragment angular distribution, separated lead isotopes, $^{204, 206, 207, 208}$Pb, $^{209}$Bi, $^{205}$Tl, protons, quasi-monoenergetic neutrons, intermediate energy, nuclear data, new technology, accelerator.

* Russia, 194021, St.-Petersburg, 2-y Murinskiy Pr. 28,
Telephone /Fax: (812) 247-57-49

e-mail: 105@atom.nw.ru

**ISTC 1309 - 99**

The work was performed together with the follow institutes and collaborators:

## 1. Institutes.

V.G.Khlopin Radium Institute,
Russia, 194021, St.-Petersburg, 2-y Murinskiy Pr. 28,
Telephone /Fax: (812) 247-57-49
e-mail: 105@atom.nw.ru

## 2. Foreign collaborators.

**Name:** Uppsala University, Department of Neutron Research
**Address:**
**City:** Uppsala
Country: Sweden
Zip Code: Box 525,SE-75121
**Name of Signature Authority:** Prof. Jan Kallne
Tel: **+46 18 471 23 94**
Fax: **+46 18 471 38 53**
E-mail: **jan.kallne@tsl.uu.se**
**Name of Contact Person:** Assoc. Prof. Jan Blomgren
E-mail: **Jan.Blomgren@tsl.uu.se**

**Name:** Forschungszentrum Karlsruhe
**Address:**
**City:** Karlsruhe
Country: Germany
Zip Code: Postfach 3640, 76021
**Name of Signature Authority:** Dr. G. Heusener
Tel: **+49 7247 825510**
**Name of Contact Person:** Dr. C.H.M. Broeders
Tel: **+49 7247 822484**
Fax: **+49 7247 823484**
E-mail: **Cornelis.Broeders@ike.fzk.de**

**Name:** European Commission, MO75 5/55
**Address:**
**Street:** Rue de la Loi/Wetstrat, 200
**City:** Brussels
Country: Belgium
Zip Code: 1049
**Name of Signature Authority:** Dr. Michel Hugon
Tel: **+32 2 296 57 19**
Fax: **+32 2 295 49 91**
E-mail: **michel.hugon@dg12.cec.be**
**Name of Contact Person:** Dr. Michel Hugon
Tel: **+32 2 296 57 19**
Fax: **+32 2 295 49 91**
E-mail: **michel.hugon@dg12.cec.be**

**CONTENTS.** pages

Application (on 14 pages): Results on fission cross sections and fission fragment angular distributions prepared for the data EXFOR format.

# I. Introduction.

## I.1. The goal of the work.

Nuclear data, as quantitative characteristics of nuclear reactions, have become particularly important in the intermediate energy region. They are necessary for development of new concepts of nuclear energy production and transmutation of radioactive waste with the use of accelerators, as well as for design of shielding for accelerators and space apparatus, neutron and proton therapy, medical isotope production and many other applications. They are important also for the development of theory of nuclear interactions, nuclear structure and nuclear matter properties.

Predictive power of available theoretical models and computational codes in the intermediate energy region is estimated as ±50% in average, although calculations often differ from each other and from experimental data by 2-3 orders of magnitude [1,2]. Theoretical description becomes especially complicated in the energy region from a few tens of MeV to about 200 MeV, because of interference of collective and single-particle effects. Thus, it has been proposed to create files of experimental and evaluated data for the given energy region, similarly to the existing reactor-oriented databases for neutron-induced reactions below 20 MeV [3].

Lead target is considered as the most prospective one for accelerator-driven energy production and/or waste transmutation systems [4,5]. Another material under consideration is lead-bismuth eutectics [4], which loses to the pure lead because of higher induced activity but possesses better heating engineering characteristics. For calculations of key parameters of the lead targets (number and spectrum of emitted neutrons, prompt and residual radioactivity and heat release, radiation stability - in the case of solid target), nuclear data are needed for reactions induced in lead by intermediate energy protons and neutrons. In particular, fission reaction data are needed. In spite of comparatively low cross section (a few percents of total inelastic cross section), fission reaction leads to products with high energy release and, often, with long half-lives. It is estimated [6], that the contribution of the fission products to the overall residual activity of a lead target irradiated by 1.6-GeV protons amounts in 10-15% for cooling time of about year. Due to the above mentioned uncertainties in model calculations, as well as inaccurate benchmark experimental data, the estimation of the residual activity is very uncertain, in particular, the contribution to the activity from the fission process.

To obtain more reliable estimations, one needs new data on fission cross sections of lead and bismuth. Furthermore, the Bi(n,f) cross section is adopted as an important standard for neutron flux measurements in the energy region above 20 MeV [7], in particular for the

fulfillment of the data requests in the mentioned accelerator-driven technologies. The purpose of the proposed fission cross section measurements of the isotopes of lead and thallium (the neighbor of lead with lower Z) will be outlined below.

It is considered essential to perform the proton- and neutron-induced fission cross section measurements within a common experimental project and, as much as possible, with the use of the same experimental technique. Our earlier comparison of the proton and neutron cross sections showed interesting properties of the cross section ratio dependence on incident nucleon energy [8]. The analysis of these ratios was performed in terms of fission probability as a general physical basis that defines the fission process induced by protons and neutrons. Such an analysis allows obtaining the most realistic results.

However, measurements in the intermediate energy region are expensive and require much accelerator beam time, especially for monoenergetic neutrons with low beam fluxes. Thus, in parallel with the fulfillment of nearest practical needs, information has to be obtained for the development of theoretical models in the considered region of nucleus mass and projectile energy. The perspective of creation of a complete database can only be ensured by elaboration of adequate computational models. Except $^{nat}$Pb(n,f) and $^{209}$Bi(n,f) reactions, which have independent practical significance, as it was mentioned above, the study of the other reactions is directed to this goal. The thing is that due to the fast intranuclear cascade preceding fission a wide set of residual nuclei with charges and masses different from total Z and A of target and incident particle is occurred. Besides, the energy of residuals despite it is lower than initial energy introduced into nucleus can be enough to evaporate light particles (usually neutrons) with subsequent fission. In this case, known as emission fission, mass and energy of fissile nucleus is much less. It is generally accepted that before equilibrium stage when the fission channel is switched on there are pre-equilibrium processes also changing the characteristics of fissile nucleus. Thus it is necessary to take into account the fission of nuclei that are lighter than initial (composite) system: target + incident particle.

Fission of nuclei near Pb is of particular interest because the fissioning nuclei distribution includes systems with closed proton (Z=82) or neutron (N=126) shells as well as with both shells closed ($^{208}$Pb). Quantitative information about the role of shell effects in the stage of fission-neutron emission competition and possibly at the primary stage of nucleon-nucleus interaction can be obtained. The incompleteness of the left corner is not too distressing because the shell effects, for example, in the level density parameter, are, in general, symmetric relative to the filling numbers. It is evident that the influence of this quantum effect decreases when the incident particle energy increases due to the spreading of the mass and charge distributions of the residual nuclei and the increase of their excitation

energy (in the region from a few MeV to several tens of MeV). The description of the weakening of the shell effects with the energy increase is a theoretical problem that remains to be quantitatively solved. The proposed study will give new important information on this problem. Another quantum effect, namely the effect of incident particle isospin, can be of importance for a better description of particle-nucleus interaction at intermediate energies, and possibly for a better understanding of nuclear structure, as discussed below.

Some differences between neutron and proton induced fission reactions have been established already. Using both our own data ([9] - for protons, [10] - for neutrons) and reference data [11,12] we have compared proton and neutron induced fission cross sections for nuclei from Pb to Np in the projectile energy range from 40 to 450 MeV. The comparison indicates that the difference is not due to the Coulomb barrier influence only. For example, for nuclei lighter than $^{237}$Np (may be starting from $^{238}$U) the proton induced fission cross sections lie systematically above the neutron ones even in the projectile energy range $E_p \leq 35$ MeV, where Coulomb barrier essentially reduce the total inelastic cross sections. The difference increases with decreasing fissionability parameter $Z^2/A$ and decreases with increasing projectile energy (from $\approx 30$ for $E_{proj} \approx 20$ MeV to $\approx 2$ for $E_{proj} \approx 150$ MeV). At projectile energies above $\sim 200$ MeV the ratio of proton and neutron fission cross sections $\sigma_{pf}/\sigma_{nf}$ becomes constant and depends on fissionability parameter only according to the following empirical expression: $\sigma_{pf}/\sigma_{nf} = \exp [0.162(37 - Z^2/A)]$ (assuming that for $Z^2/A > 37$ $\sigma_{pf}/\sigma_{nf} = 1$). All the relations between fission cross sections noted above could be explained as a “memory” effect when the fissioning nucleus “remembers” which type of nucleon it interacted with. In other words the fissionability parameter $Z^2/A$ for the residual nuclei does not differ much from that of the compound nuclei despite the isospin dependence of the number of protons and neutrons ejected at the cascade stage. A quantitative estimation of the importance of the higher value of the fissionability parameter in the case of proton induced fission requires more accurate experimental data for inelastic proton and neutron cross sections.

Thus, the practice and theory (which in turn is useful for practice) require new and more accurate results for total and differential fission cross sections.

### 1.2. Expected Results

Using a spontaneous fission fragment sources ($^{252}$Cf) for tuning of the experimental setups and the TSL cyclotron (Sweden) for carrying out neutron and proton measurements with the help of both now existing and new created detection system the following results have been obtained:

1. The cross sections of $^{209}$Bi, $^{nat}$Pb, $^{208,207,206}$ Pb and $^{205}$Tl proton-induced fission at energies 20-180 MeV at five energy points have been measured in accordance with the working schedule approved by the leaders of the ISTC in May, 14, 2001.
2. The cross sections of $^{209}$Bi, $^{nat}$Pb, $^{208,207,206}$ Pb and $^{205}$Tl neutron-induced fission at energies 40-180 MeV at four eight energy points have been measured in accordance with the working schedule approved by the leaders of the ISTC in May, 14, 2001.
3. The comparison of the cross sections for neutron- and proton-induced fission and the analysis of results based on calculations of nuclear fissilities (as the ratio of fission cross section to the cross section of inelastic interaction) taking into account the dependencies of fissionability from nucleon content and excitation energy of fissile nuclei has been carried out.

Thus, both the experimental base and general physical basis for the creation of evaluated nuclear data files in energy range 20-200 MeV have been created. Moreover, new tests for nuclear models and their parameters will be performed and it in turn will provide the development of a reliable method of the fission cross section calculations for all nuclei being of interest for accelerator transmutation.

The measurements of cross sections in the case of proton-induced fission have been carried out using for determination of proton flux both the total collected charge and monitor reaction (for example, $^{27}$Al(p,3p3n)$^{22}$Na), in the case of neutron-induced fission the measurements will be carried out relative to fission cross section of $^{238}$U, the absolute values of which are determined using the cross section of n,p-scattering. Taking into account the errors of above mentioned methods of flux monitoring, the accuracy of determined absolute values of fission cross sections will be about 10%.

### 1.3. Technical Approach and Methodology.

There is a long-standing tradition of nuclear fission physics investigations at Khlopin Radium Institute. There is a team of highly qualified specialists, as well as the experimental arrangement, that already was used to study the nuclear fission induced by neutrons, protons, heavy ions at different accelerators in former USSR and abroad. This experience was used for carrying out the measurements and the analysis of data on fission cross sections, the information on which is inadequate, but which are needed to realize the projects on accelerator driven systems for radioactive waste transmutation and energy production.

The methodological approach was based on the use of accelerator, which produces both neutrons and protons, and on the use of non-traditional detection systems both now

existing and being worked out at KRI. In particular the multi-layer ionization chamber permits to measure the cross sections of 40-180 MeV neutron-induced fission of nuclei with low fissility due to its almost 100% detection efficiency and possibility to put in the targets with total mass up to 1 g. With the use of this equipment the significant part of new data was obtained and also repeated measurements for a number of nuclides will be performed in order to carry out the comparison analysis of the results obtained with neutrons and protons.

## 2. Methods and experiments.

### 2.1. Method of thin film breakdown counters.

**2.1.1.** Description of the experimental setup.

Measurements of intermediate energy proton- and neutron-induced fission cross sections of nuclei were carried out at the proton and quasi-monoenergetic neutron beams of the The Svedberg Laboratory (TSL) of the Uppsala University, Uppsala, Sweden.

General scheme of the beams formation and transport is presented in Fig. 2-1. The quasi-monoenergetic neutrons are produced by the reaction $^{7}$Li(p,n)$^{7}$Be The 25 - 180 MeV proton beam of the Gustaf Werner cyclotron is directed to a disc-shaped target of metallic lithium enriched up to of 99.98% by $^{7}$Li isotope. The thickness of the target depends on the energy of bombarding protons and is chosen from 4 to 15 mm as a compromise between requirements of the neutron beam intensity and energy resolution. After passage through the target the proton beam is deflected by two dipole magnets to the angle about 45° and focused onto a well-shielded carbon beam-dump placed at the end of an 8 m concrete tunnel. Neutrons are guided to the experimental room through a system of three collimators. A clearing magnet placed after the first collimator deflects charged particles produced in a vacuum terminating foil and along the collimator channel. The energy spectrum of the neutrons flying out from the target at angles close to 0° has a peak with the maximum energy from 21 to 174 MeV (depending on the proton beam energy) followed by a low-energy tail (down to parts of MeV) [13].

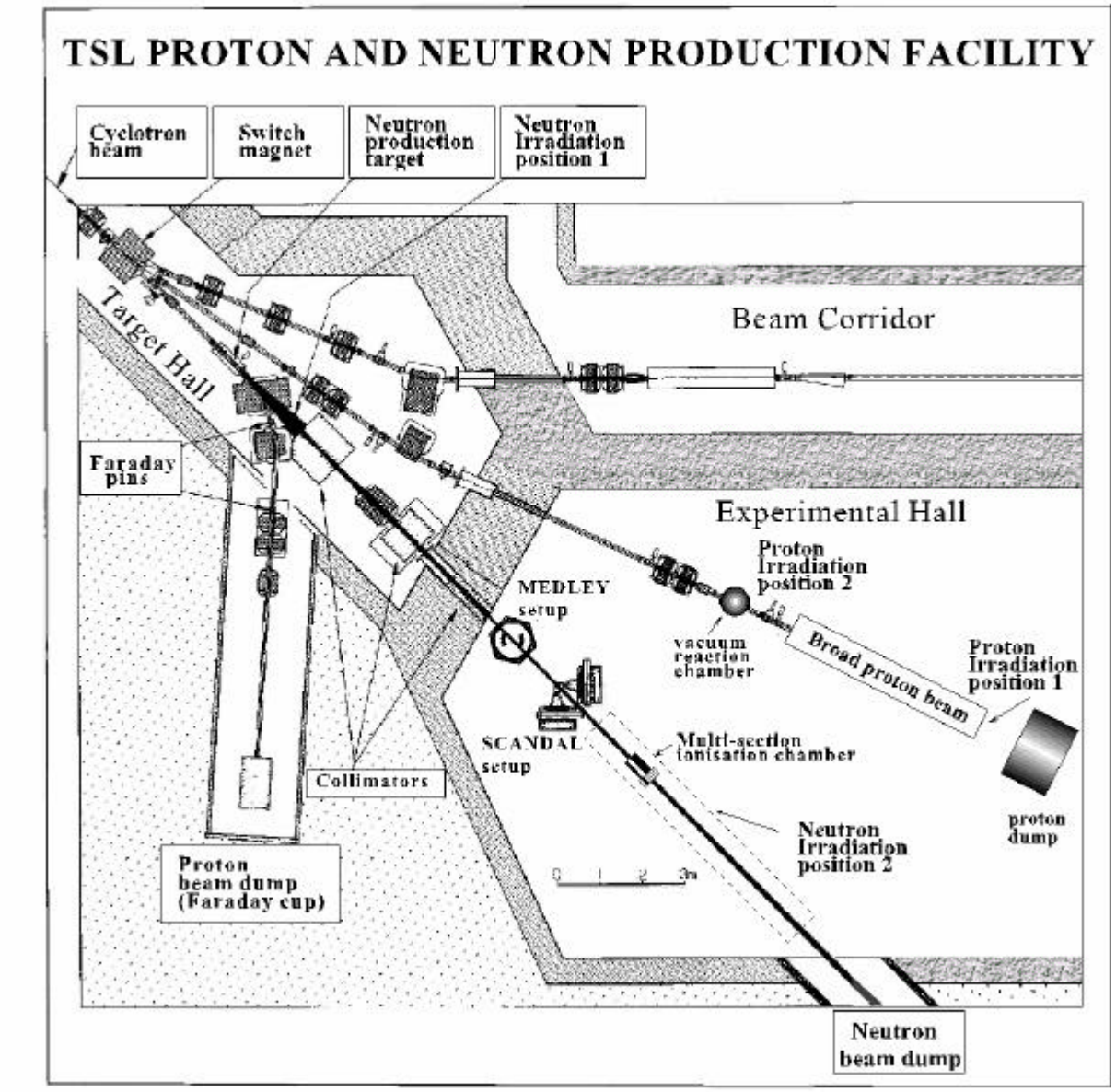


**Fig. 2-1.** The overview of the proton and neutron production facility of the The Svedberg Laboratory.

For measurements at protons the cyclotron beam is directed to another line, where an experimental vacuum chamber is placed. In the end of this line a dedicated device is installed for a wide proton beam formation [14]. The device consists of a special proton scatterer followed by collimator.

In order to provide minimal energy spread in the proton energy region 30 – 170 MeV the tantalum scattering foils are used with the thickness from 0.1 mm to 1 mm depending on the primary proton energy. Aluminum and stainless steel foils of 0.3 – 0.1 mm are used as materials for the exit window of proton beam line.

Measurements at neutrons and protons were carried out at the following irradiation positions:

a) neutron irradiation position 1 in the Target Hall at distances about 0.5 - 2 m from the lithium target at angles of 1 - 4° relative to the proton beam axis;
b) neutron irradiation position 2 in the Experimental Hall where a collimated neutron beam is conducted, possible distances from the lithium target are from 9 to about 16 m;
c) proton irradiation position 1 in the Experimental Hall, where the broad proton beam is formed;
d) proton irradiation position 2 in the experimental vacuum chamber placed at the beam line.

In order to improve the reliability of the results, the measurements of the relative fission cross sections with protons and neutrons were carried out in as much as possible identical beam conditions at the positions “a” and “c”. The main parameters of the proton and neutron beams are given in Tab. 2-1.

**Table2-1.**The main parameters of the proton and neutron beams.

| Parameter | Neutrons | Protons |
|---|---|---|
| **Energy (MeV)** | 35 - 174 (±2) | 30 - 170 (±2) |
| **Flux density (?? $^{-2}$*?$^{-1}$)** | (1-3)*$10^5$ | $10^5$-$10^6$ |
| **Distance from target (scatterer), m** | 1 – 2 | 3 |
| **Homogeneity of the profile in the sensitive area of the fission chambers** | 10% | 10% |
| **Contamination of other particles** | not more than 1% protons | not more than 1% neutrons |

In these positions the (n,f) and (p,f) cross sections of $^{204,206,207,208}$Pb, $^{nat}$Pb and $^{205}$Tl relative to the $^{209}$Bi ones were measured with the use of the same experimental fission chambers on the basis of the TFBC (see sect. 2.1.2.1). Measurements with neutrons have been carried at energies 35, 46, 66, 75, 90, 95, 111, 133, 144 and 174 MeV. Measurements with protons have been carried at energies 64, 94 and 167 MeV.

At the same time with the measurements at the position “a”, the measurements of the $^{209}$Bi(n,f) cross section relative to the $^{238}$U(n,f) ones at the neutron position “b” with the use the same type of the experimental chambers. The intensity of the collimated neutron beam at the (n,f) targets placed at about 10-12 m distances is $10^5$ - $10^6$ $s^{-1}$ (depending on the beam energy).

At the position “d”, the fission fragment angular distributions and the absolute (p,f) cross sections for $^{204,206,207,208}$Pb, $^{205}$Tl and $^{209}$Bi were measured with the use of the vacuum reaction chamber (see sect. 2.1.2.2). The measurements have been carried at proton energies about 50, 98 and 177 MeV. The maximal value of the proton beam current do not exceed 10nA that is limited by radiation safety conditions set for the accelerator Experimental Hall. Because of some technical problems, the minimal available energy of protons was limited by the value about 50 MeV.

**2.1.2.** Experimental chambers.

2.1.2.1. The experimental fission chambers for the relative measurements.

The universal chambers of mosaic type based on thin film breakdown counters (TFBC) being analogous to those used earlier [15] were used for the relative measurements both at neutrons and wide proton beam. The design of the fission chamber is shown in Fig. 2.2.

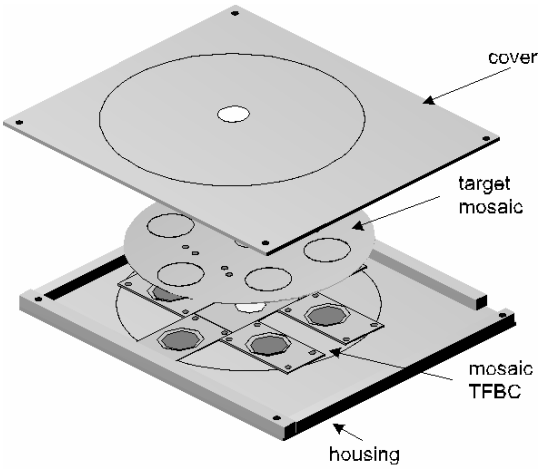


Fig. 2-2. The design of the fission chamber based on the TFBCs

The chamber includes 6 sandwiches placed symmetrically in a plane that is perpendicular to the incident particle beam direction. Each sandwich consists of a fissioning target and a TFBC placed close to the target surface. The sensitive surface of the TFBC is about 1 cm$^2$. The chamber housing is a non-evacuated rectangular box with the dimensions about 7 ? 92 ? 107 mm. The walls of the chamber are made of 1-mm thick duralumin, the entrance and exit windows are 58 mm in diameter and made of 0.2-mm thick aluminum foil. Due to the insignificant thickness of construction materials of the detectors, the targets and the windows, a share of intermediate energy neutrons scattered at the elements of the chamber is negligibly small. This allows to place a few chambers one after another and thus to perform

relative fission cross section measurements for a few target nuclides simultaneously. From 10 to 15 chambers were placed in the neutron flux simultaneously. The targets from the same material ($^{209}$Bi) were installed in the first and the last chambers for determination of the neutron scattering factor.

The number of chambers placed simultaneously in the wide proton beam were determined by the primary proton energy. Estimations and test measurements at 70 to 180 MeV protons have shown that the proton scattering factor allows measurements with up to 4 chambers simultaneously at the proton energies from 100 to 180 MeV without noticeable effect within statistical uncertainties and not more than 3 chambers at the proton energies below 80 MeV. Proton energy losses were not more that 5 MeV after passing of the chamber stack. These proton energy losses were taken into account as uncertainties of the average proton energy.

2.1.2.2. Experimental vacuum reaction chamber.

A vacuum chamber has been manufactured intended for measurements of absolute proton induced fission cross section and angular distribution of fission fragments at the focused proton beam with the use of the TFBC technique. The general view of the chamber is shown in Fig. 2-3.

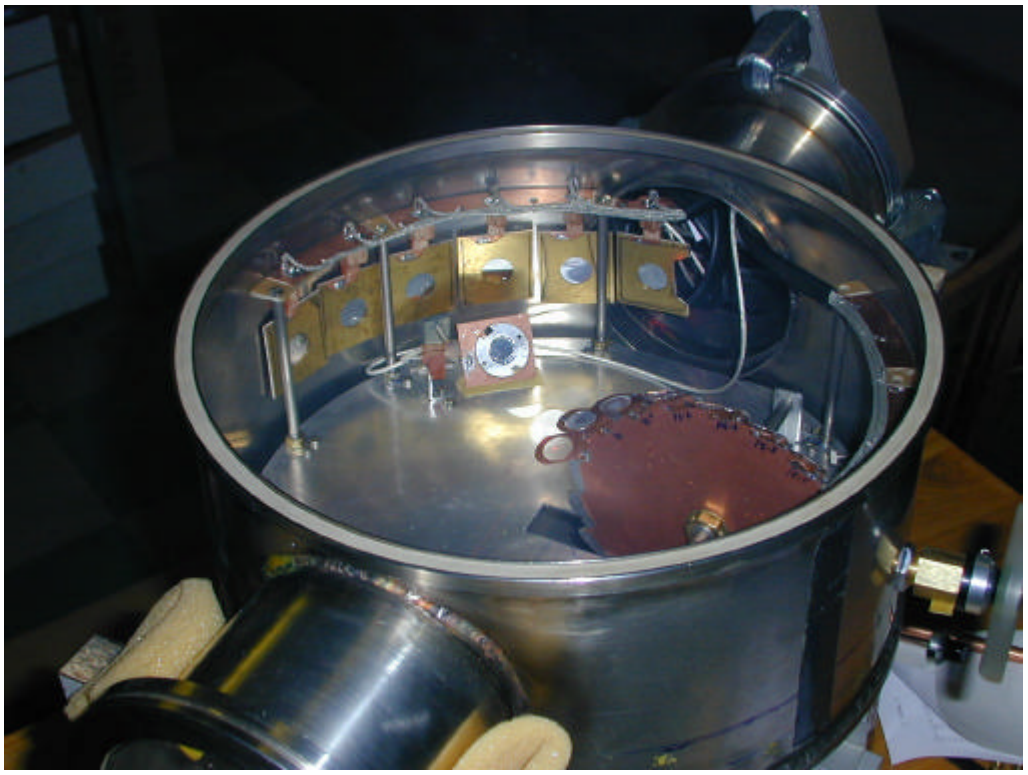

**Fig. 2-3.** The general view of the reaction vacuum chamber.

The chamber is about 28 cm in diameter and about 20 cm height. The chamber is made of stainless steel and supplied by two flanges a design and dimensions of which correspond to the flanges of proton beam line of the cyclotron.

In the chamber 12 TFBC are mounted. The sensitive surface of the TFBC is about 2 $cm^2$. The detectors are placed in the angle ranges of about 0°-90° (7.5°, 22.5°, 37.5°, 52.5°, 67.5°, 82.5°) and 90°-180° (97.5°, 112.5°, 127.5°, 142.5°, 157.5°, 172.5°) relatively to the beam direction. For simplifying of calibration procedure the sensitive surface of each detector was confined by a diaphragm with 14 mm in diameter. The commutation of the TFBCs with an electronic shaper and voltage supply is provided by means of shielded cables placing within the chamber and contacted with a special docking unit supplied with a vacuum multipin connector. The target block of the chamber is a rotating disk supplied with 20 target holders. The targets are placed at the angle 45° relatively to the beam direction. The rotation of the disk is provided from outside by means of vacuum input supplied with a multiturn counter, which guarantees precise positioning of the targets at the proton beam axis. The diameter of the beam spot formed by the focusing system at the target surface was about 5 mm that was controlled by video camera sets before and behind the chamber.

Double-side targets from lead isotopes ($^{204,206,207,208}$Pb), $^{205}$Tl and $^{209}$Bi were mounted in the target holders for measurements of angular distribution of fission fragments in a forward and backward hemisphere.

For measurement of the absolute (p,f) cross sections pairs of targets from corresponding isotopes were installed in the target holder divided by copper foil of the same area and of 0.1 mm thick for proton beam monitoring with the help of activation reactions on copper. Aluminum backings of the targets were used as the activation foils too (see sect. 2.1.5.2).

**2.1.3.** Electronics and computer software

A block scheme of the setup for measurement of the relative cross sections is shown in Fig. 2-4.

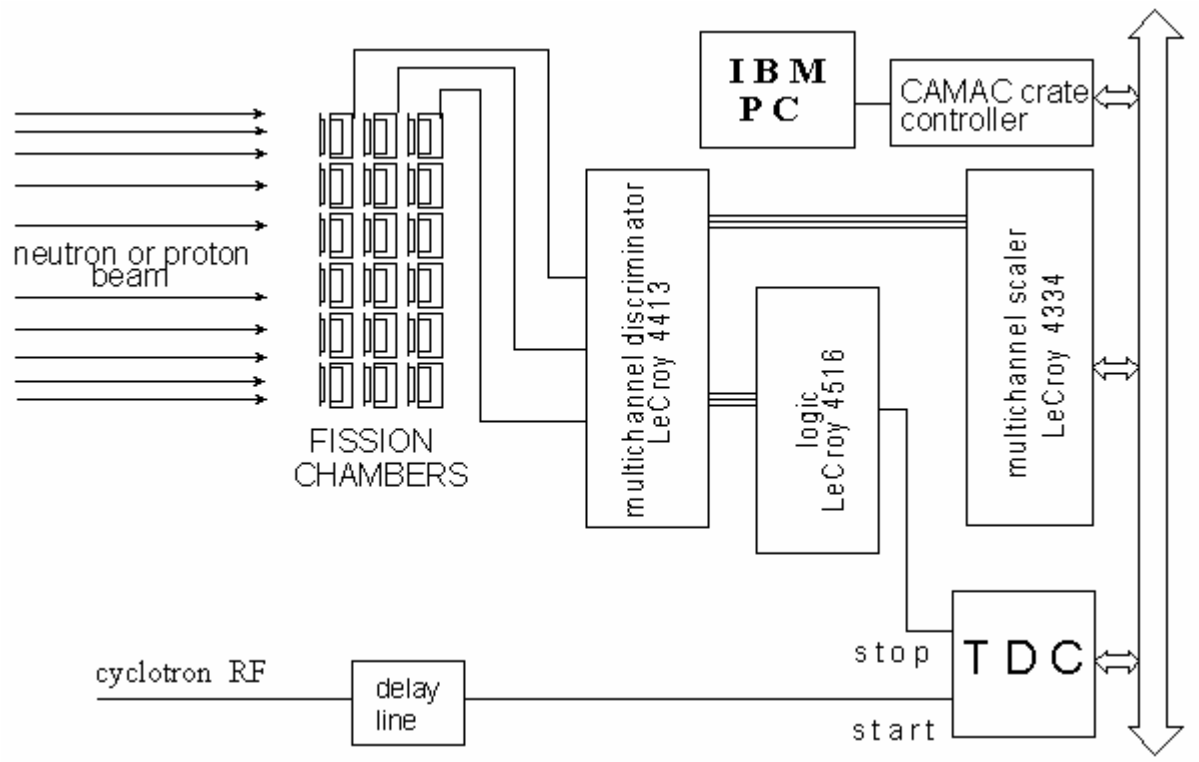


**Fig. 2-4**. The layout of the electronic system.

Electronics serving for registration and accumulation of information includes passive shaping circuits and the highly-integrated NIM and CAMAC modules:

- multi-channel fast discriminators LeCroy 4413 or LeCroy 4416B;
- multichannel pulse scaler LeCroy 4334;
- multichannel logic Fan-In/Fan-Out LeCroy 4516;
- time-to-digital converter (TDC);
- delay lines;
- CAMAC crate controller connected with an IBM PC.

The scheme provides registration and accumulation of information in a form of time-of-flight spectra of the fission events as well as in the form of time distributions of the sums of the fission events in equal time intervals from 28 fission chambers simultaneously.

The same scheme was used for measurements with the vacuum reaction chamber.

A computer software (code TFBCvNo) is a graphical user's interface made on a basis of "Windows 98". "Borland Delphi 3 for Windows" was used as a program environment. The new software is intended for the following functions in "on-line" mode:

- reading of registers of functional modules made in CAMAC standard;
- consecutive recording of information to HDD;

- accumulation and representation of the time-of-flight spectra of the fission events;
- separate accumulation of the events within and without the time window corresponding to the beam macropulse (that is needed for taking into account the background);
- rejection of the false events caused by pulse backgrounds from accelerator systems;
- monitoring of the primary proton beam by means of registration of the pulses from the proton beam current integrator;
- storage and protection of the accumulated data;
- automatic testing of the electronic modules;
- flexible tuning to a specific configuration of the electronic modules and fission chambers.
- preliminary processing of results of measurements.

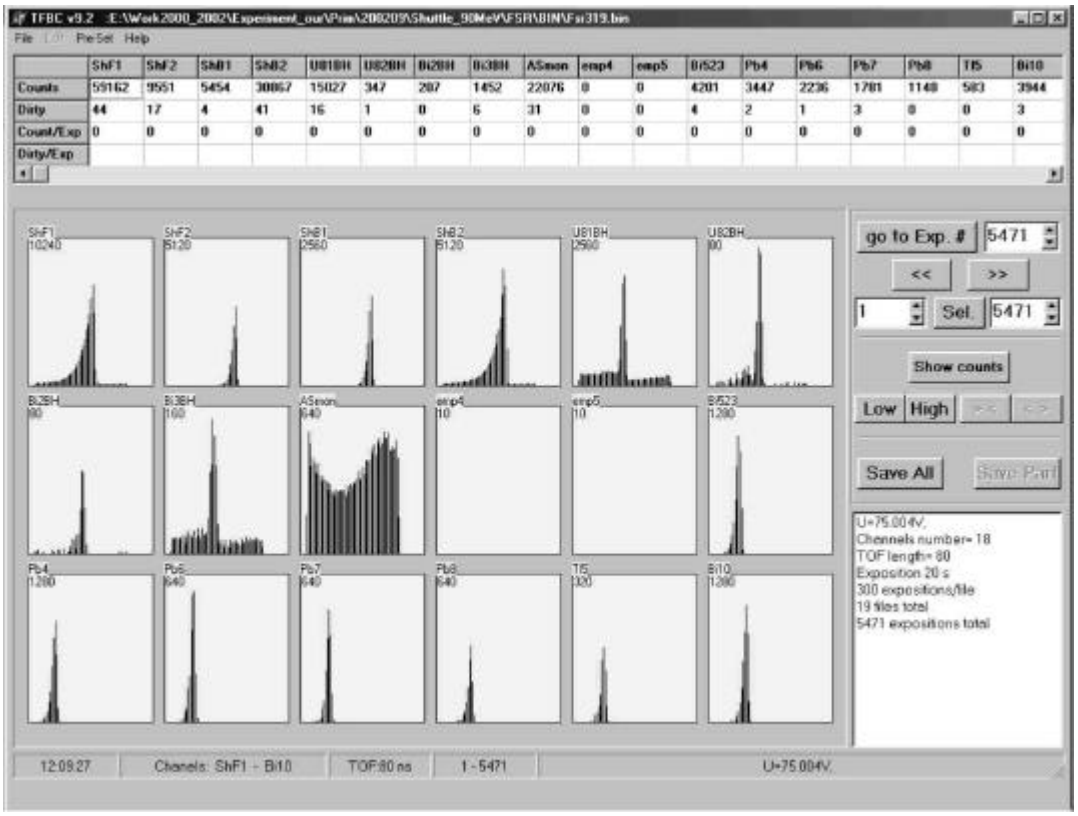


**Fig. 2-5**. Graphic user interface of the «TFBCv9.2» code.

Fig. 2-5. presents an exemplary screen with graphic and digital information for 18 fission chambers.

**2.1.4.** Targets.

The targets for the mosaic fission chambers and for the vacuum reaction chamber are the layers of fissioning materials deposited on the round aluminum foil backings of 0.1 mm

thick and of 1 $cm^2$ area. The targets were made by vacuum evaporation technique with the use of special design allowing a manufacturing up to 26 targets simultaneously with homogeneity not worse than 20% (for different targets). The targets were weighted with the accuracy not worse than 3% with the use of precise analytical balance. Enriched isotopic mixtures of lead, thallium (99.8% of $^{205}$Tl, 0.02% of $^{203}$Tl) and metallic bismuth (monoisotope $^{209}$Bi) were used to manufacture the targets. The data on isotopic composition of lead targets are shown in Table 2-2.

**Table 2-2**. Isotopic composition of lead targets

| **Isotope** | **Isotopic composition(%)** | | | |
|---|---|---|---|---|
| | **$^{208}$Pb** | **$^{207}$Pb** | **$^{206}$Pb** | **$^{204}$Pb** |
| **$^{208}$Pb** | 99.0±0.1 | 0.6 | 0.4 | <0.01 |
| **$^{207}$Pb** | 5.4 | 93.2±0.2 | 1.4 | <0.01 |
| **$^{206}$Pb** | 2.9 | 6.7 | 90.4±0.3 | - |
| **$^{204}$Pb** | 9.8 | 7.5 | 16.1 | 66.5±0.6 |
| **$^{nat}$Pb** | 52.4 | 22.1 | 24.1 | 1.4 |

Results of measurements for lead isotopes were corrected taking into account the isotopic contribution of the targets. An upper limit of admixture of actinides for lead isotopes, as well as for targets made from thallium and bismuth have been determined by means of analysis of results of measurement at 35 MeV neutrons and were not more 0.0001%.

**2.1.5.** Processing of results of the measurements.

2.1.5.1. Fission cross section ratios.

The following formula was used for a ratio of fission cross sections of nuclei X and Y:

$$\frac{\sigma_f(X)}{\sigma_f(Y)} = \frac{N(X)}{N(Y)} \frac{A(X)}{A(Y)} \frac{<\varepsilon_a^{sf} \rho>(Y)}{<\varepsilon_a^{sf} \rho>(X)} \frac{d_e(Y)}{d_e(X)} \frac{k_{peak}(X)}{k_{peak}(Y)}, \qquad (1)$$

where $\sigma_f$ is the fission cross section;

$N$ is the number of detected fission fragments;

$\varepsilon_a^{sf}$ is the absolute detection efficiency of TFBC for the fragments of spontaneous fission measured with the use of calibrated $^{252}$Cf source;

$\rho$ is the fissile target thickness;

$<\varepsilon_a^{sf} \rho>$ - is the product of the latter two quantities averaged over all sandwiches in the corresponding mosaic;

$A$ is the atomic weight of the nucleus;

$d_e$ is the calculated correction to the detection efficiency taking into account peculiarities of detection of the fragments from induced fission;

$k_{peak}$ is the share of the fission events induced by the high-energy peak neutrons. For proton-induced fission cross section ratios this correction is equal to 1.

The correction to the detection efficiency for the induced fission of nuclide X is described by the following expression:

$$d_e(X) = \frac{e_{ac}^{X}}{e_{ac}^{sf}}, \quad (2)$$

where $e_{ac}^{sf}$ and $e_{ac}^{X}$ are the calculated absolute detection efficiencies of the TFBC of the unitary square for the fragments of spontaneous and induced fission of nuclide X correspondingly.

Detection efficiency of the TFBC for fission fragments in a close (sandwich) geometry is a complex function of a large amount of parameters, related to physical properties of TFBC, physical properties of fission fragments and physical characteristics of fission reaction induced by nucleon of different energies.

A computer code for calculating the TFBC fission fragment detection efficiency has been elaborated. Semi-empirical dependences of the threshold voltage on fission fragment energy losses in $SiO_2$ and angle of incidence of fission fragments to the sensitivity surface of the detector were put into the basis of the code [16]. The code models the real process of fission fragment detection from both spontaneous fission and fission induced by intermediate energy nucleons. In the model the angular anisotropy and transferred longitudinal momentum generating angular distributions of fission fragments are taken into account. Fission fragment kinetic energy change due to the transferred momentum as well as the energy losses of fission fragments in the target material and their dependence on the fragment angular distribution are taken into account too.

The code input data are:

- Charge, mass and energy distributions of fission fragments taking into account the emission of pre-fission neutrons. Charge and mass distributions were calculated on the basis of the well-known systematics [17]. Fission fragment kinetic energies were calculated using the semi-empirical formula from the systematics [18]: $0.1189Z^2/A^{1/3}+7.3$.
- Fission fragments distributions of energy losses in $SiO_2$ and ranges in target materials calculated with tables [19].

- The values of fission fragments anisotropy and transferred to target nuclei longitudinal momentum for various incident nucleon energies tabulated on the basis of systematizations worked out in the [15, 20]

Different variants of the code allow calculating:

- the TFBC count characteristics (the dependences of absolute detection efficiency on operating voltage) for the close (sandwich) geometry;
- the TFBC count characteristics in far geometry for different mutual positions of target and detector;
- dependences of the detection efficiency on target thickness (at a preset operating voltage on TFBC and projectile energy);
- dependences of the detection efficiency on projectile energy (at a preset operating voltage and target thickness);
- dependences of the detection efficiency on angle of the fragment flying out from the target relatively to the particle beam direction.

Exemplary dependences of the absolute detection efficiency for fission fragments of different nuclei on the proton energy (at the same target thickness and applied voltage) and on the target thickness (at the proton energy 90 MeV) in the forward hemisphere are shown in Fig. 2-6.

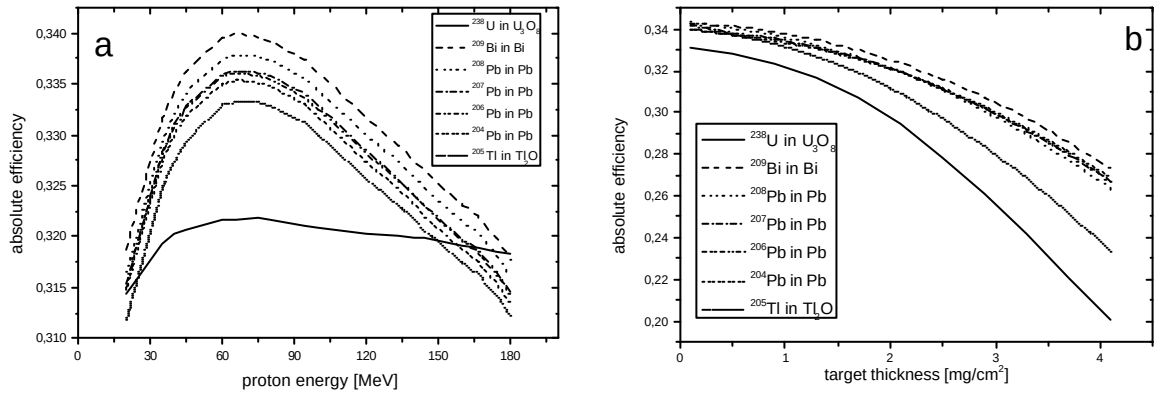


**Fig. 2-6.** Absolute detection efficiency in the forward hemisphere for fission fragments of different nuclei versus the proton energy (at the same target thickness and applied voltage) (a) and the target thickness (at the proton energy 90 MeV) (b).

The program was tested by means of comparison of calculations with results of different experiments on the investigation of the TFBC detection efficiency. First of all the modeling of

the main experiments on investigation of physical properties of the TFBC [16] has been carried out. Moreover the model calculation of number of special experiments being carried out for both the spontaneous fission fragments and at the proton and neutron beams of the TSL. In Fig. 2-7 (a,b,c) the examples are presented of the comparison of calculated counting characteristics of TFBC, the dependences of the efficiency on target thickness and the dependences of the ratio of efficiencies for forward and backward fission fragment detection on the energy of bombarding particles with the experimental results. The results of the test have shown that calculations with the use of the code agree well with the experimental results within uncertainties (uncertainties of the experimental data shown in the figure are from 3% to 7%).

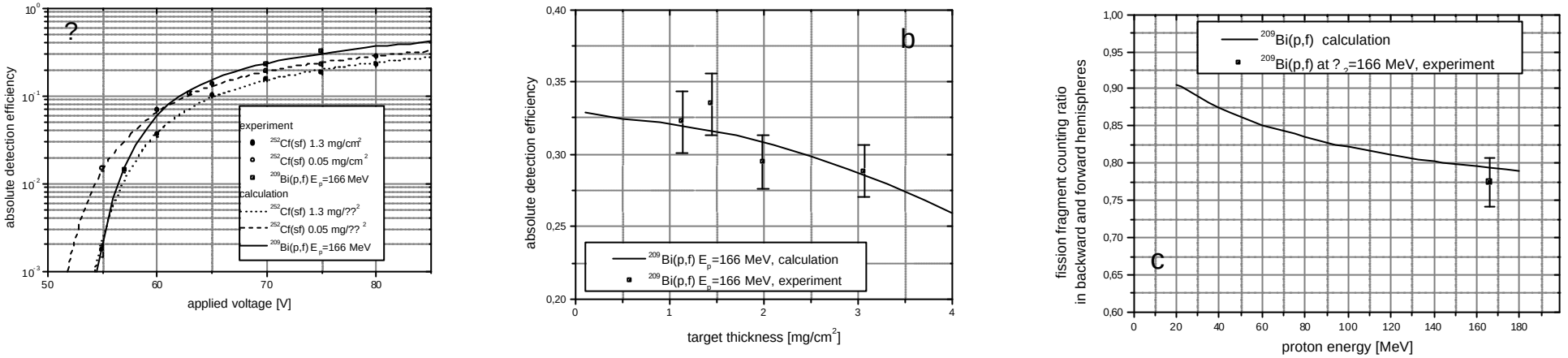


**Fig. 2-7. (a)** – Counting characteristics of the TFBC in the close geometry for the $^{252}$Cf spontaneous fission fragments, obtained for source with different effective thickness, and for fission fragments from the $^{209}$Bi(p,f) reaction at 166 MeV protons; (b) – Absolute detection efficiency for fission fragments from the $^{209}$Bi(p,f) reaction at 166 MeV protons versus target thickness; (c) - The dependences of the ratio of the detection efficiencies in backward and forward hemispheres of proton-induced fission fragment on the bombarding proton energy.

A practical testing of the program has been done in processing of the test experiments on measurements of proton-induced fission cross section ratios for number of heavy nuclei at the wide proton beam of the TSL. In Fig. 2-8 the results of measurement are presented together with the data of other authors [11] in the neighboring proton energy region. As it is seen from the figure the obtained result agree well within uncertainties (not more than 10%) with the data of earlier works.

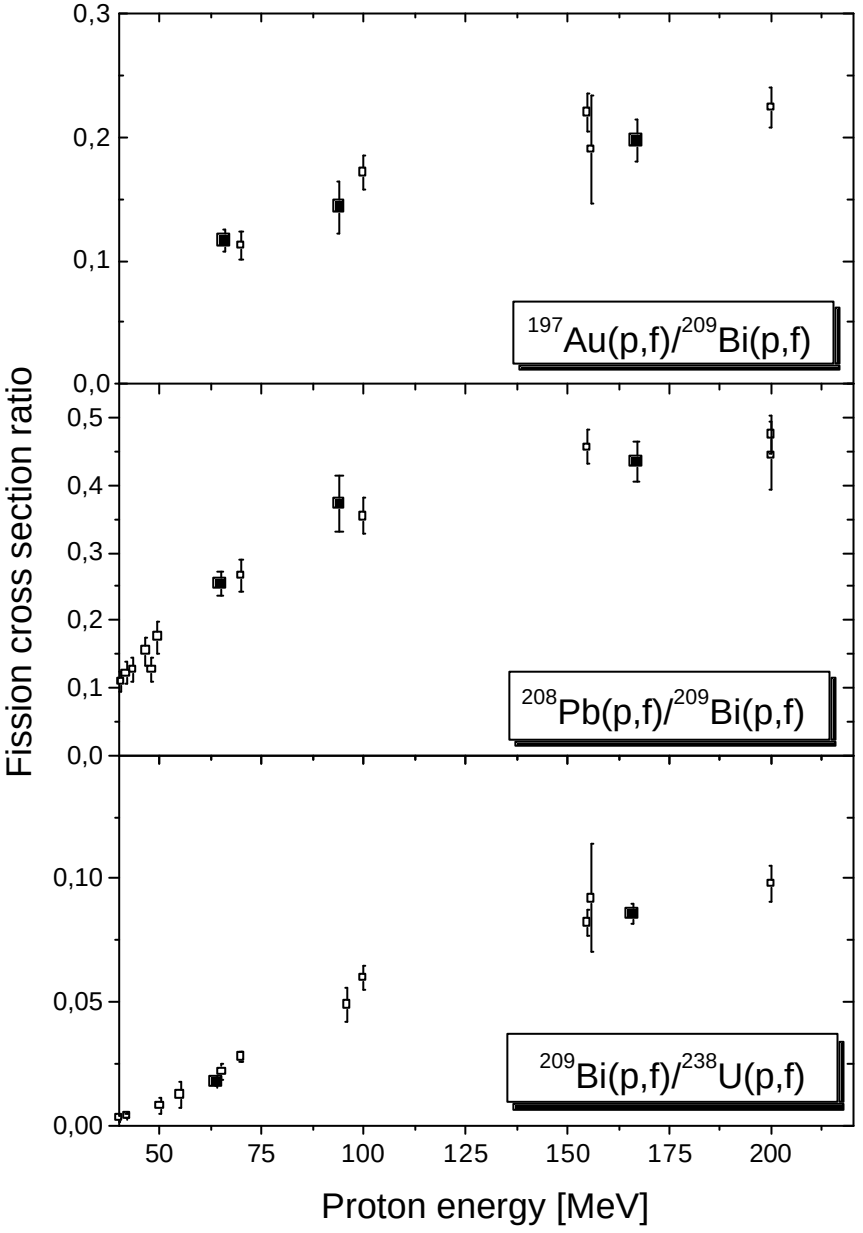


**Fig. 2-8.** Energy dependences of the $^{209}$Bi/$^{238}$U, $^{208}$Pb/$^{209}$Bi and $^{197}$Au/$^{209}$Bi proton-induced fission cross section ratios. The filled symbol is the result of the present work. The open symbols are the data extracted from compilation of literature experimental data [11].

With the help of the code described above the TFBC fission fragment detection efficiencies for close geometry have been calculated and tabulated for the $^{252}$Cf calibrating sources, for all working targets of isotopes of lead, thallium, bismuth, uranium and other nuclides of interest for the proton and neutron energies which are used for measurements at the beams of Gustaf Werner cyclotron of the TSL.

For calculation of corrections $k_{peak}$ software has been elaborated for modeling of time distribution of fission events measured at quasi-monoenergetic neutron beam with the use of the TFBC fission chambers. The code models a process of formation of the time distributions measured with the help of TDC taking into account peculiarities of time structure of the beams of the Gustaf Verner cyclotron of the TSL.

The input data and parameters are:

- The experimental database of the quasi-monoenergetic neutron spectra obtained with $^{7}$Li(p,n) reaction at different facilities (see, for example, [21]), containing more than 50 spectra for more than 10 peak neutron energies;
- Parameterizations of the (n,f) cross sections of heavy nuclei from Ta to U [15];
- Repetition frequency of the cyclotron RF signal;
- The length of the neutron flight distance;
- Time structure of the micropulse;
- Time resolution of the TFBC fission chamber.

The results of the model calculations for the $^{238}$U(n,f) and $^{209}$Bi(n,f) reactions at a peak neutron energy of 144 MeV measured at the neutron flight distance of 10 m (neutron irradiation position 2) are presented in Fig. 2-9..

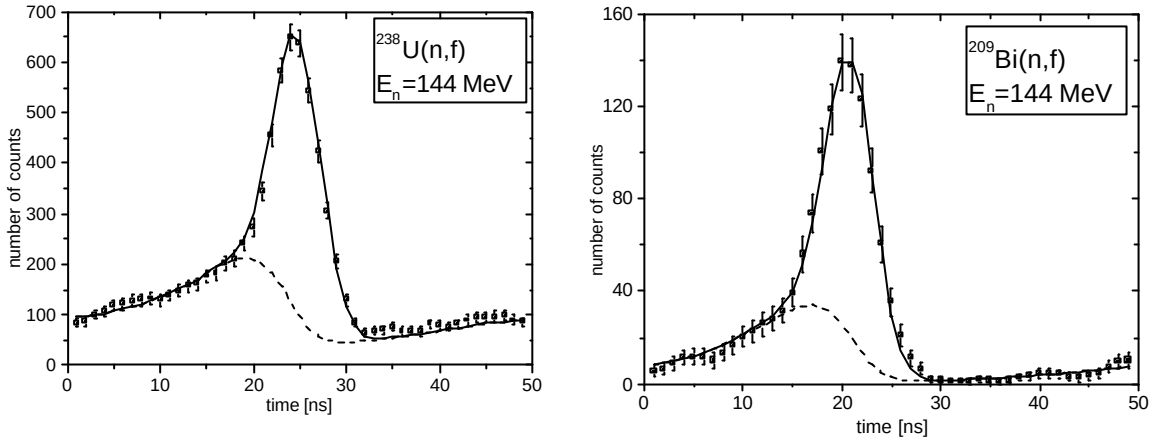


**Fig. 2-9.** Time distributions of fission events for the $^{238}$U(n,f) and $^{209}$Bi(n,f) reactions induced by neutrons with the peak energy 144 MeV. Solid points – experimental results, lines – model calculation. Dashed curves separate shares of fission events caused by the peak energy neutrons.

For the measurements at a short flight distance (neutron irradiation position 1) the time structure of the beam does not allow the decomposition to the “peak” and “low energy tail” components. Thus, the share of “peak” fissions has to be determined by an iterative unfolding procedure (see, for example, the work [22]). The input for the unfolding procedure has to include the neutron spectrum systematic and the relative fission reaction rates in as many neutron energy points as possible. Fig. 2-10 presents the exemplary decompositions of the time distributions of fission events for the $^{209}$Bi(n,f) and $^{208}$Pb(n,f) reactions at several neutron energies.

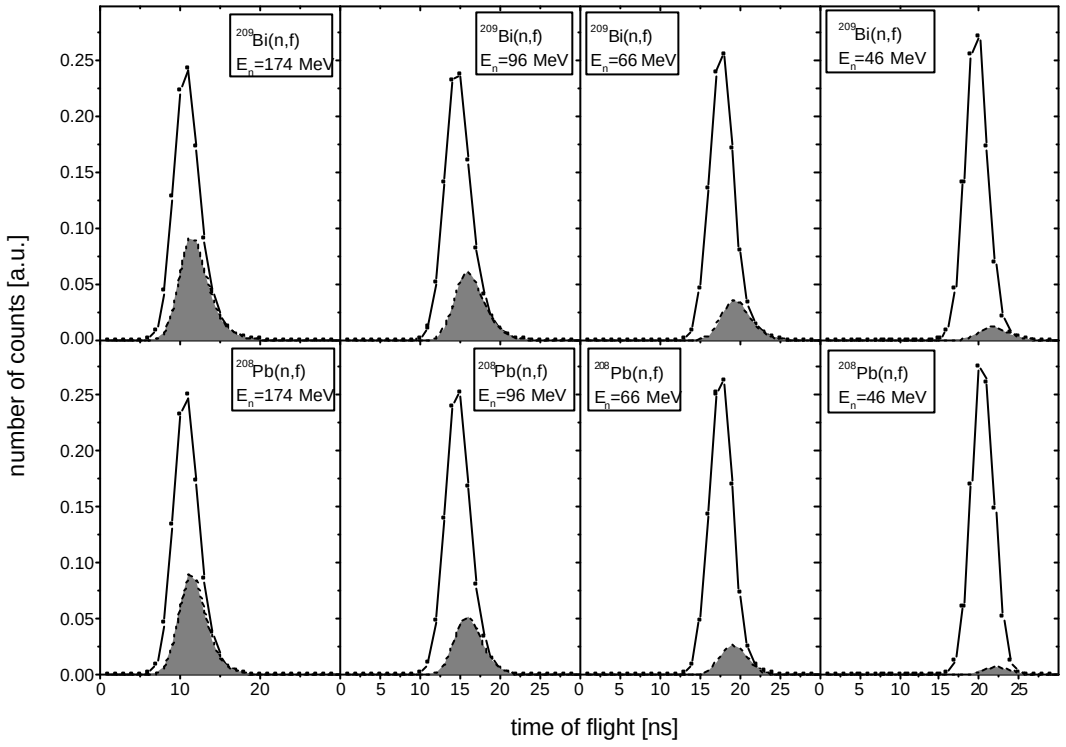


**Fig. 2-10.** Calculated time distribution of fission events for the $^{209}$Bi(n,f) and $^{208}$Pb(n,f) reactions at the neutron flight distance about 2 m and at several neutron energies. Filled areas show the shares of fission events induced by the low energy tail neutrons.

As a result of the usage of the iteration procedure for all nuclides under study the relative corrections $\frac{k_{peak}(X)}{k_{peak}(^{209}Bi)}$ have been obtained. The values of the corrections depend on both nuclide and neutron energy, the maximal value of the correction does not exceed 1.08

Uncertainties of the relative fission cross sections include the following components:

- statistic of counts for most proton and neutron energies is 1 – 3%, at neutron energies 35 and 46 MeV – from 30%(for $^{205}$Tl at 35 MeV) to about 5% (for $^{209}$Bi);
- error of the value of $< e_a^{sf} r >$ for the mosaic chambers is about 3%;
- error of the relative correction $\frac{k_{peak}(X)}{k_{peak}(Y)}$ for the bismuth - thallium region of nuclides does not exceed 1%, and for the $^{209}$Bi(n,f)/ $^{238}$U(n,f) ratio - 3% in the whole neutron energy range;

- error of the corrections ratio $\frac{d_e(Y)}{d_e(X)}$ for nuclides in the bismuth-thallium region does not exceed 1%, and for the $^{209}$Bi/$^{238}$U ratio is not more than 5% for the whole ranges of the projectile energy.

2.1.5.2. Fission fragment angular distributions and absolute proton-induced fission cross sections.

As it was mentioned above, measurements of the fission fragment angular distributions and the absolute proton-induced fission cross section were carried out in the vacuum reaction chamber at the proton energies 49, 98 and 177 MeV. The technique of activation foils was used for measurements of the proton flux using well known monitor reactions $^{nat}$Cu(p,xnp)$^{61}$Cu, $^{nat}$Cu(p,xn)$^{62}$Zn and $^{27}$Al(p,3pn)$^{24}$Na.

The angular distribution of fragments in the (p,f) reactions is:

$$W(q) \propto 1 + B\cos^2 q, \quad (3)$$

where $q$ is the angle between the fragment direction and the beam axis in the system of fissioning nucleus and $B = W'(0°)/W'(90°) - 1$ is the anisotropy factor.

The angular distribution (3) converted to the laboratory frame is (see, e.g., [23]):

$$W(q) \sim \left[1 + B(\cos q \sqrt{1 - h^2 \sin^2 q} - h \sin^2 q)^2\right] \frac{\left(h \cos q + \sqrt{1 - h^2 \sin^2 q}\right)^2}{\sqrt{1 - h^2 \sin^2 q}}, \quad (4)$$

where $h$ is the parameter connected with the linear momentum transfer (LMT) from the primary particle to the fissioning nucleus:

$$h = \frac{p_{||}}{2 p_{ff}}, \quad (5)$$

where $p_{||}$ is the average longitudinal component of the transferred linear momentum, and $p_{ff}$ is the average momentum of the fragment in the fissioning nucleus frame.

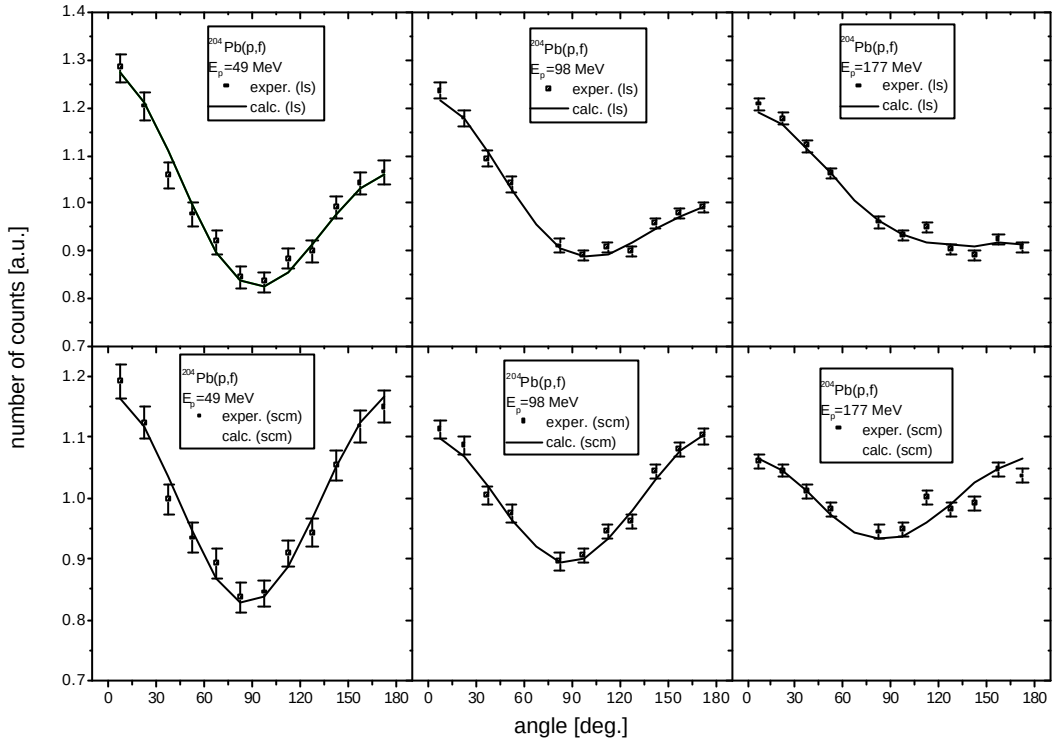


**Fig. 2-11.** The fission fragment angular distributions for $^{204}$Pb(p,f) reaction at proton energies 49, 98, and 177 MeV in the laboratory frame (upper row) and in the fissioning nucleus frame (lower row). Curves are the calculations using formulas (3) and (4).

Experimental angular distributions were fitted with the help of these expressions. Experimental and calculated angular distributions of fission fragments in the laboratory and fissioning nucleus frames for the $^{204}$Pb(p,f) reaction at proton energies 49, 98, and 177 MeV are presented in Fig. 2-11.

The absolute proton-induced fission cross sections were calculated using the following expression:

$$s_{pf}(X) = \frac{N(X)}{n(X) \cdot \Omega_{TFBC} \cdot k(q) \cdot \Phi_p}, \quad (6)$$

where $N(X)$ is the number of fission fragments registered by TFBC placed at the angle $q$ relative to the proton beam direction;

$n(X)$ is the number of the fissioning nucleus in the target per unit area;

$\Omega_{TFBC}$ is the solid angle within which the fragments reach the sensitive surface of the TFBC;

$k(q)$ is the correction of the solid angle for TFBC placed at the angle $q$ relative to the proton beam direction, and determining by the angular distribution of the fission fragments;

$\Phi_p$ is the fluence of protons within the target surface.

The calculated values of angular distribution obtained as the result of the fitting procedure of the experimental angular distributions were used as the corrections $k(q)$.

The values of the fluence $\Phi_p$ of protons were measured with the help of the monitor reactions on natural copper ($^{nat}$Cu(p,xnp)$^{61}$Cu and $^{nat}$Cu(p,xn)$^{62}$Zn) using special foils placed between fissile targets and reaction $^{27}$Al(p,3pn)$^{24}$Na using aluminum backing of the targets as the activation foils. After irradiation by protons γ-spectra of activated foils were measured using γ-spectrometer on a basis of a pure germanium. Processing of the γ-spectra was carried out using standard code "OXFORD PCA II".

The proton fluence was calculated using the following formula:

$$\Phi_p = \frac{S_{gpeak} \cdot l}{s_{(p,xnyp)} \cdot n_{Cu} \cdot e_{E_g}^{Ge} \cdot I_g \cdot [1 - \exp(-l t_o)] \cdot \{\exp[-l (t_1 - t_o)] - \exp[-l (t_2 - t_o)]\}}, \quad (7)$$

where $s_{p,xnyp}$ is one of the above mentioned reaction cross section;

$l$ is the decay factor of the formed nuclide ($^{61}$Cu, $^{62}$Zn or $^{24}$Na);

$S_{gpeak}$ is the area of γ-line selected from γ-spectrum of activated foil for the calculation;

$I_g$ is the absolute yield of the γ-line per decay;

$n_{Cu}$ is the number of nucleus in the activation foil;

$e_{E_g}^{Ge}$ is the absolute efficiency of the Ge-spectrometer for the energy of γ-line under consideration;

$t_o$ is the proton irradiation exposition;

$t_1$ is the time between the starting of irradiation by protons and starting of measurement of the γ-spectrum;

$t_2$ is the time between the starting of irradiation by protons and the end of measurement of the γ-spectrum.

The values of the $^{nat}$Cu(p,xnp)$^{61}$Cu, $^{nat}$Cu(p,xn)$^{62}$Zn or $^{27}$Al(p,3pn)$^{24}$Na reaction cross sections for the proton energies, at which the (p,f) cross section measurements have been measured, were extracted from EXFOR files by means of evaluation and interpolation of the tabulated cross section values.

Uncertainties of the absolute (p,f) cross sections include the following components:

- counting statistics for each of 12 TFBC is 1-3%;
- uncertainty of the target thickness is about 3%;
- uncertainty of the value of the solid angle is about 3%;
- uncertainty of correction $k(q)$ is not more than 3%;
- average sum error of the measurement and processing of γ-spectrum (uncertainties of $S_{gpeak}$, $e^{Ge}_{E_g}$ and $I_g$) did not exceed 3%;
- sum systematic component connected with values of cross sections $s_{p,xnyp}$ of activation reactions, the $^{61}$Cu, $^{62}$Zn and $^{24}$Na decay factors and thickness of the activation foils was about 9%;
- preliminary estimations have shown that the uncertainty connected with changes of the proton beam intensity during the irradiation did not exceed about 1%.

Thus the maximal uncertainty of the absolute (p,f) cross section is about 11%, while the average is close to 10%..

### 2.2. Multi-section Frisch-gridded ionization chamber method.

**2.2.1.** Advantages of the Frisch-gridded ionization chamber method.

The ionization chamber is represented by the most suitable detector of fission fragments at measurement fission cross sections on intermediate energy neutrons, as, having almost 100 % efficiency, practically has no restrictions in the size of a target from a fissional material. It is necessary to note, however, that the fission fragment energy distribution in the ionization chamber is garbled in the region of low energies by presence of light charged particles emitted from materials of the chamber and targets under bombardment of prompt neutrons, and the impurity and hardness of a spectrum of these particles increases with growth of neutron energy.

The ionization chamber with Frisch grids allows simultaneously measurement of fission fragment kinetic energy (in $2\times2p$ geometries) and emission angle with regard to the cathode normal of a charged particle emitted from the cathode plane. The detecting efficiency of fission fragments depends, mainly, on width of a fissile material layer, therefore, as a rule, is close to 100 % and can be determined with enough reliability. Besides, the ionization chamber owing to the constructive simplicity and pliability can be easily adapted to any experimental conditions.

The ionization chamber with Frisch grids was applied with success in the fission cross section and fission fragment angular distribution measurements of heavy nuclei (thorium - uranium) by the intermediate energy neutrons [15]. For weakly fissile nuclei in the field of a lead - bismuth the application of such chamber would require great expenses of accelerating time for achievement of sufficient statistical precision in the fission cross section measurements. To rise the counting rate of fission events usually go on a way of increase of target mass using multilayer thin - gap parallel-plane ionization chambers. However there is an inconsistency between an opportunity to obtain prompt time mark (electrical capacity of the chamber) and necessity to partition fission fragments and in product energy distributions. Light charged particles arise in interaction of prompt neutrons with upstream material in the chamber (value of chamber working gap).

We carried out experimentally direct matching in actual experimental conditions of the amplitude performances of the thin - gap parallel-plane ionization chamber and complete - gap ionization chamber with Frisch grid using targets made of a bismuth and lead (natural isotope composition) at the beam of the intermediate energy neutrons (95 MeV). It has shown advantage of last in fission cross section measurements of nuclei in the lead region by the intermediate energy neutrons. Thus the angular criteria were used for selection of fission events.

**2.2.2.** The design and peculiarity of working of the multi-section Frisch-gridded ionization chamber.

A multi-section ionization chamber has been designed and manufactured. The chamber is intended to measure the neutron-induced fission cross sections of weakly fissionable nuclei in lead region.

As one can see from Fig. 2-12, the chamber consists of seven units. Each unit constitutes a twin Frisch-gridded ionization chamber with a common cathode. Anodes of two adjacent chambers are common. The thin-walled cylindrical detector housing, with outer dimensions 500 mm (in length) and 200 mm (in diameter), is made of stainless steel and consist of vessel with flanges and two lids.

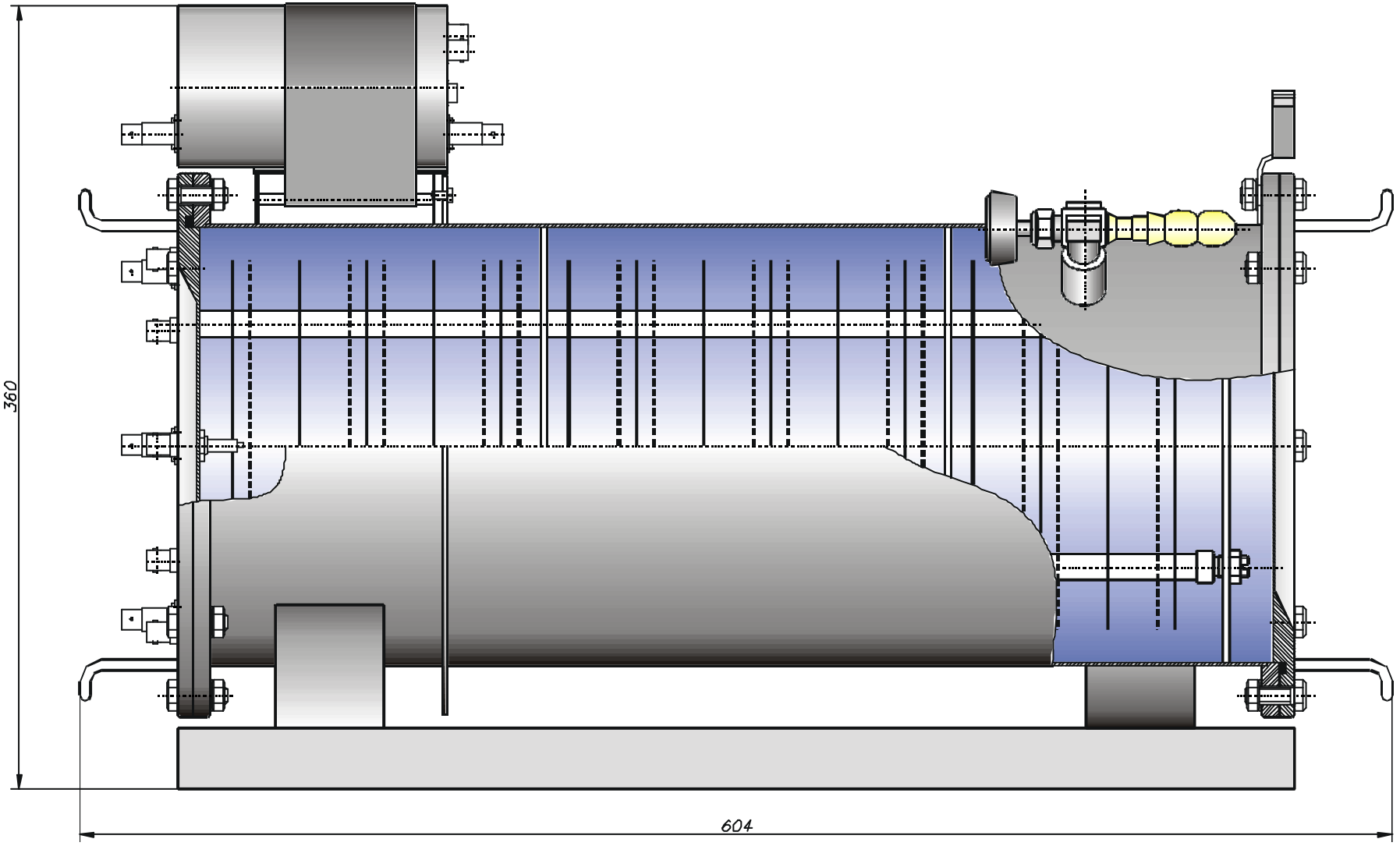


**Fig. 2-12.** Multi-section ionization chamber.

The anodes and cathodes are duralumin foils, 50 μm thick, sandwiched between two 1 mm duralumin rings with inner and outer diameters of 140 and 170 mm correspondingly. These rings are riveted together to hold the foils tightly stretched. Cathode foils are used as backings for the fissile targets. Maximum available target diameter is 80 mm.

The grids are mounted on the stainless steel rings with dimensions identical to mentioned above. The grids are made of parallel gilded molybdenum wires of 80 μm in diameter spaced by 1.25 mm.

The electrode assembly is held together with four insulating teflon rods. Fig. 2-13 shows that each rod consists of eight supporting bungs surrounded by teflon spacers. Rods are fixing between lid and ring. Such design enables quick access to and replacement of any cathode with fissile targets. The distance between the anode and the grid is 8 mm. The cathode to grid distance is 23 mm.

The gas mixture is composed of 90% argon and 10% methane (P-10). The chamber will operated at atmospheric pressure without a continuous gas flow.

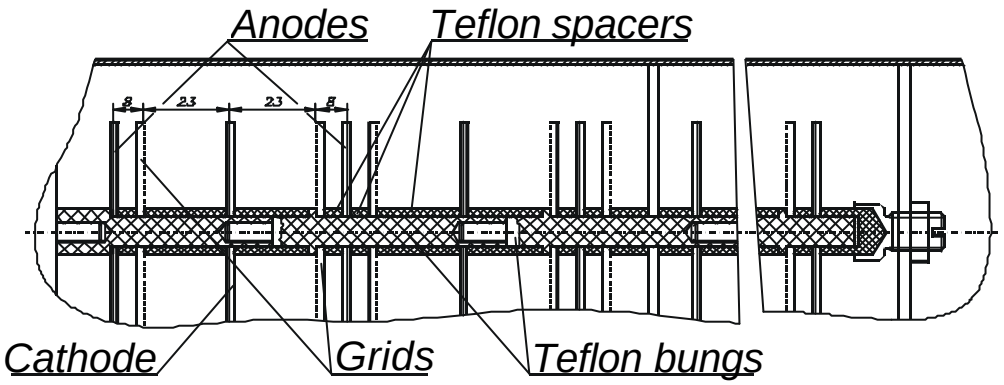


**Fig. 2-13.** Electrode assembly of the multi-section ionization chamber.

Now we will describe briefly working principle of the Frisch-gridded ionization chamber. The fission fragments emitted from the cathode are stopped in the space between the cathode and the anode, creating ion-electron pairs along their tracks. The drift velocity of the ionized gas molecules is much less than that of electrons, so ions can be treated as being static for a short time while free electrons drift towards the anode. The charge induced on the anode (or pulse height on charge-sensitive pre-amplifier output $P_{anode}$) is proportional to the number of produced electron-ion pairs, which to the first approximation is proportional to the fission fragment kinetic energy deposited in the gas. At the end of the electron drift, the charge induced on the cathode is proportional to $P_{anode}$ and is a function of the emission angle – $J$ with respect to the cathode normal:

$$P_{cathode} = P_{anode}\left(1 - \frac{\overline{X}}{D}\cos J\right).$$

Here $\overline{X}$ is the distance of the center of gravity of the electron-ion pair track from the origin of the trace and $D$ is the cathode-anode distance. In general $\overline{X}$ is a function of fragment energy, mass and charge. Assuming that $\overline{X}$ is a function of fragment energy only, the ratio $\overline{X}/D$ can be found experimentally for any arbitrary $P_{anode}$. Indeed, at given $P_{anode}$ the ratio $P_{cathode}/P_{anode}$ is distributed between 1- $\overline{X}/D$ and 1. Thus, the $\overline{X}/D$ is given by:

$$\overline{X}/D = 1 - P^{\min}_{cathode}/P_{anode},$$

where $P^{\min}_{cathode}$ is the minimum $P_{cathode}$ value for a given $P_{anode}$. In this way the $\cos J$ can be obtained as:

$$\cos J = \frac{P_{anode} - P_{cathode}}{P_{anode} - P^{\min}_{cathode}}.$$

In practice, the grid does not perfectly screen the anode from the induction of charges in the space between the cathode and the grid. To take this into account, the $\cos J$ should be corrected (to the first approximation) by the factor $1 + \sigma\,(1-\cos J)$, where $\sigma$ is the Frisch grid inefficiency, which is determined from the grid and chamber dimensions. For the chamber described $\sigma$ equals 0.027.

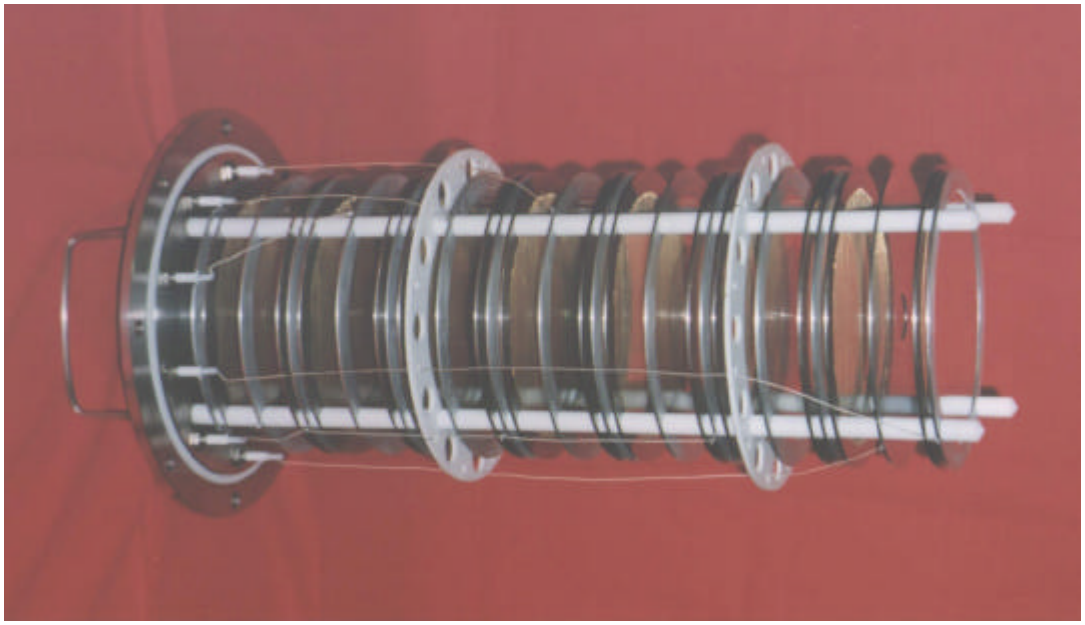

**Fig. 2-14.** Intrinsic arrangement of the multi-section ionization chamber with Frisch grids.

**2.2.3.** Targets.

For experiments with the multi-section Frisch-gridded ionization chamber the fissile samples have been prepared from the following materials: $^{205}$Tl, $^{nat}$Pb, $^{204,206-208}$Pb (enriched in basic isotope), $^{209}$Bi, and $^{nat}$U. The materials were deposited by vacuum evaporation on each side of 50 μm thick duralumin foils stretched between the supporting rings (see the chamber construction). A diameter of each target was 80 mm.

According to experimental requirements the deposit uniformity should be better than 20%, while the uncertainty in the mass no more than 2%. In addition, a loss of expensive materials should be reduced to minimum.

To meet these requirements the thermal evaporation technique developed at the KRI has been used. By this method the evaporator located at a height H above the backing plane is shifted at a distance S from the rotational axis of the backing. The calculations revealed that the best result (for target of 80 mm in diameter) is achieved with S = 32 mm and H = 27 mm.

The evaporation procedure was done with the use of UVR-3? setup. Natural uranium was deposited in the form of $^{nat}UF_4$, while the other targets in the form of metal. Before the evaporation all the backings were cleaned with $CCl_4$.

For metallic targets the fissile mass was obtained by weighting. For this purpose we have used the balance Mettler AE-163. Uncertainty of these measurements was about 0.1 mg for masses within 160 g.

The mass of uranium deposit was obtained by alpha-counting with Si-detector of 20 cm$^2$ in area. The detector equipped with diaphragm of 46.57 mm in diameter was installed at a distance of 81.3 mm from the uranium target, so the required statistics has been accumulated for an hour.

**2.2.4.** Installation of ionization chamber with targets on neutron beam.

The measurements were performed at the neutron beam facility at the The Svedberg Laboratory (TSL) in Uppsala, Sweden, described above (sect. 2.1.1).

For the fission fragment detection we have used the multi-section ionization chamber described in detail in section 2.2.2. The chamber was located near SCANDAL setup (see Fig. 2-1). The back-to back targets were deposited on the seven cathodes using a vacuum evaporation technique. The masses of deposits were determined by weighting with accuracy of 1%. The seventh section with the reference target (natural uranium) was sandwiched between other ones to reduce the effect of the neutron beam divergence. The masses of the forward- and backward-facing targets are given in Table 2-3. The targets are listed in order of arranging along the neutron beam direction.

**Table 2-3.** Target masses.

| Target | Abundance (%) | Mass, mg (Forward) | Mass, mg (Backward) |
|---|---|---|---|
| $^{204}$Pb | 66.5 | 26.0 | 27.7 |
| $^{205}$Tl | 99.8 | 69.6 | 70.4 |
| $^{208}$Pb | 99.0 | 44.4 | 54.1 |
| $^{238}$U | 99.3 | 7.89 | 7.73 |
| $^{209}$Bi | 100 | 57.2 | 43.8 |
| $^{206}$Pb | 90.4 | 49.3 | 55.3 |
| $^{207}$Pb | 93.2 | 48.3 | 49.2 |

The photograph of the multi-section ionization chamber with mounted preamplifiers is shown in Fig. 2-15.

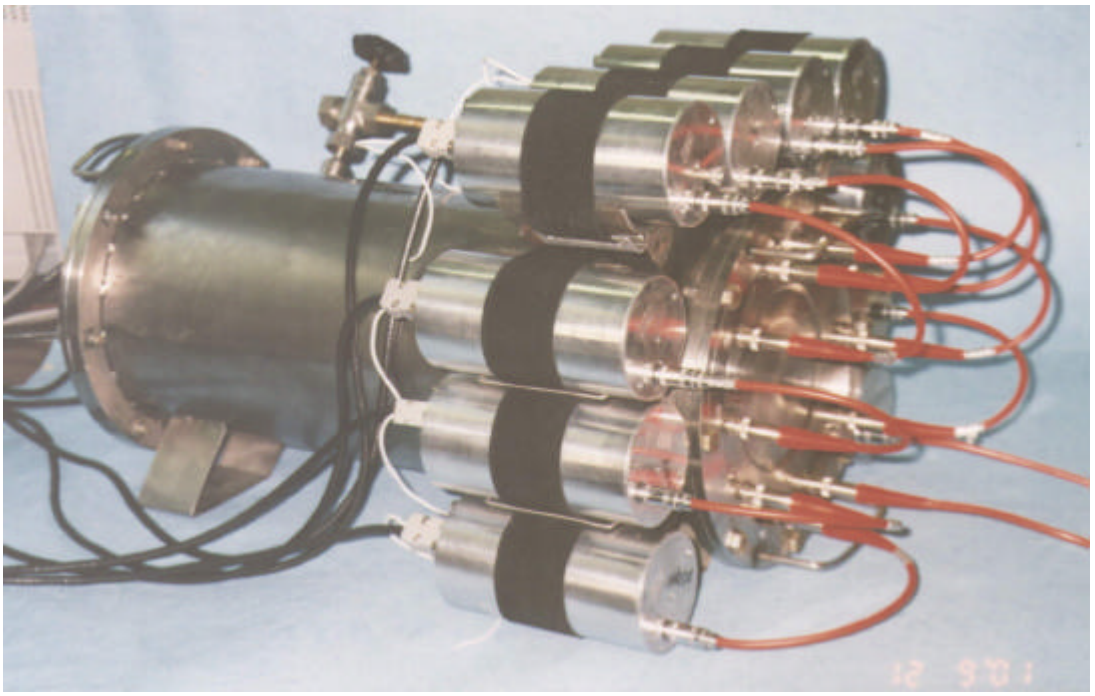

**Fig. 2-15**. Outward appearance of the ionization chamber with preamplifiers.

**2.2.5.** Data taking and processing system.

Fig. 2-16 shows a simplified block diagram of the electronics used to handle the ionization chamber signals. The anodes joined in even and odd groups are connected to two charge-sensitive preamplifiers (PA), which output pulses are amplified and shaped before being fed to an analog-to-digital converter (ADC). Seven fast preamplifiers (FPA) accept the cathode signals and deliver separate preamplifier outputs for timing and pulse-height measurements. The cathode pulse-height signals are treated like the anode signals. The timing

outputs of the FPAs are mixed in linear fan-in/fan-out (LFIFO) and then fed to respective timing filter amplifiers (TFA) with shaping time constants $\tau_{int} = \tau_{diff} = 20$ ns. Three constant fraction discriminators (CFD) follow the TFAs. Their outputs are mixed in logic fan-in/fan-out (FIFO) and then split into two branches. One pulse starts the time-to-digital converter (TDC), while the other one triggers a gate and delay generator (G&DG). The master gate signals with a width of 10-15 μs are fed to the ADCs to ensure that every pulse-height signal will have an associated timing pulse.

The $^{7}$Li(p,n) neutron source is not monoenergetic, but accompanied by a low-energy tail which holds more than a half of all neutrons. The fission and background events induced by non-peak neutrons are discriminated by TOF technique. The neutron time-of-flight is measured with a TDC started by the fast cathode signal and stopped with the RF from the cyclotron. Thus, one fission event generates three parameters: two pulse-heights ($P_{cathode}$ and $P_{anode}$) and the neutron flight time. With knowledge of the ADC channels actuated, it is possible to determine from which target and in which direction (the forward or the backward) the fission fragment was emitted. The data are stored in list mode on a personal computer for off-line analysis. With a typical total event rate of 3-4 sec$^{-1}$, coincidences of fission events from different targets is improbable.

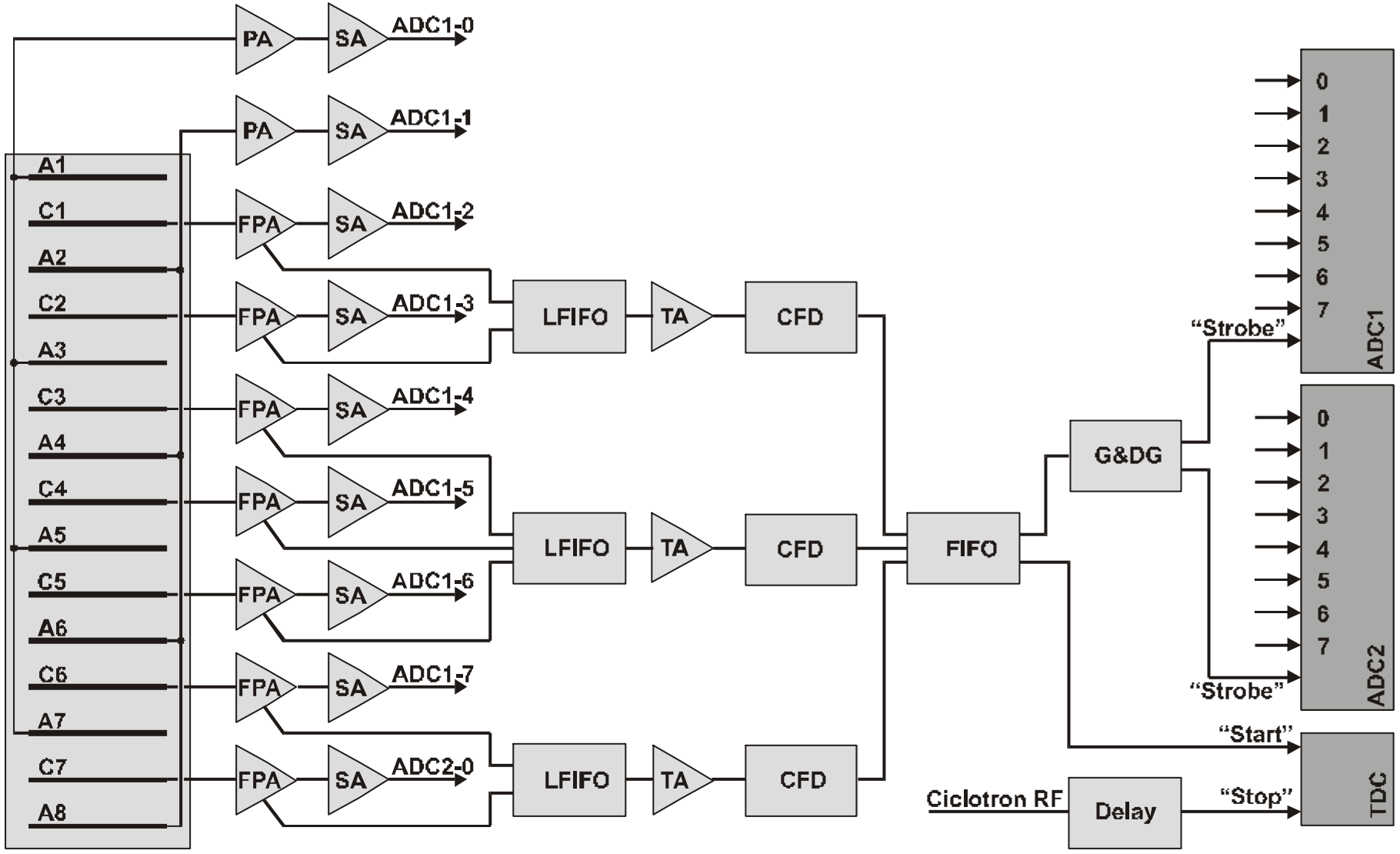


**Fig. 2-16.** The block diagram of the signal processing electronics.

The “On-Line” code for operation with the multi-section ionization chamber consisting of seven double parallel-plane ionization chambers with Frisch grids is created.

In the final version of the code the problems are solved:

1. Primary initialization of functional CAMAC blocks.
2. Reading the registers of these blocks at the event recording, which has occurred in one or several chambers.
3. Providing of the event description control for histogramming.
4. Record of the event description in the file on the hard disk.
5. Representation of measured parameters as the histograms.

In different sessions on the accelerator it is possible to use various types of ADC and TDC. The arrangement ADC and TDC in CAMAC crate also can vary from session to session. Taking into account these features of operation, the program at start gives the experimenter an opportunity to select the type and the addresses of ADC and TDC. Only after that it will carry out primary initialization of functional CAMAC blocks.

At event recording the mode of program expectation of the next event is used. An indication of the event occurrence for the program is the end of TDC conversion. Having fixed that TDC has completed conversion the program goes to sequential reading of all registers of functional blocks irrespective of in what section of the chamber the fission event was detected. Such reading expedient of the register contents provides constant length of the event description. The particular overheads of the making use of the RAM are justified by the fact that length of the event description is rather insignificant. The description of each registered event is located in a buffer file to swap with the hard disk.

Owing to integration of chamber anodes in two groups the algorithm of validation of the event description is some complicated. The results of checkout are used for the output of the histograms and for the definition of failure in operation of CAMAC blocks.

Through the particular periods defined by experimenter, the program copies the data from a RAM buffer in the hard disk in a spool file. Upon termination of an exposure the experimenter has an opportunity to create the file with a unique name from a spool file.

All measuring parameters are represented as the histograms on the monitor screen. For convenience of perception, the histograms of the measuring parameters concerning a particular target are grouped on one tab of the screen shape. To each tab the explored target is assigned. The upgrade of the information occurs through the particular periods defined by experimenter.

On the screen in the recording mode the following quantities are represented: number of the registered events, middle counting rate of events, number of errors and relation of number of errors to number of the registered events.

The “off-line” processing of the binary data files was done with the use of the code “Processing” built on the Windows-98 platform (see Fig. 2-17). As one can see from the table in the first window in Fig. 2-17, the input of the “Processing” code is formed by the energy calibration coefficients (slope, shift) and the angular polynomial coefficients (A0-A5). The energy calibration was done using the precision pulse generator and the energies of alpha-particles from the uranium target. The angular calibration procedure was identical to that described in [24]. The “Processing” code calculates the TOF, energy, angular and mass (for the thin targets) distributions for each target (or group of targets). The selection is done for the respective direction (forward/backward) and for the fixed constrains (see the second window in Fig. 2-17). The distributions retrieved are saved as the text files for the further analysis.

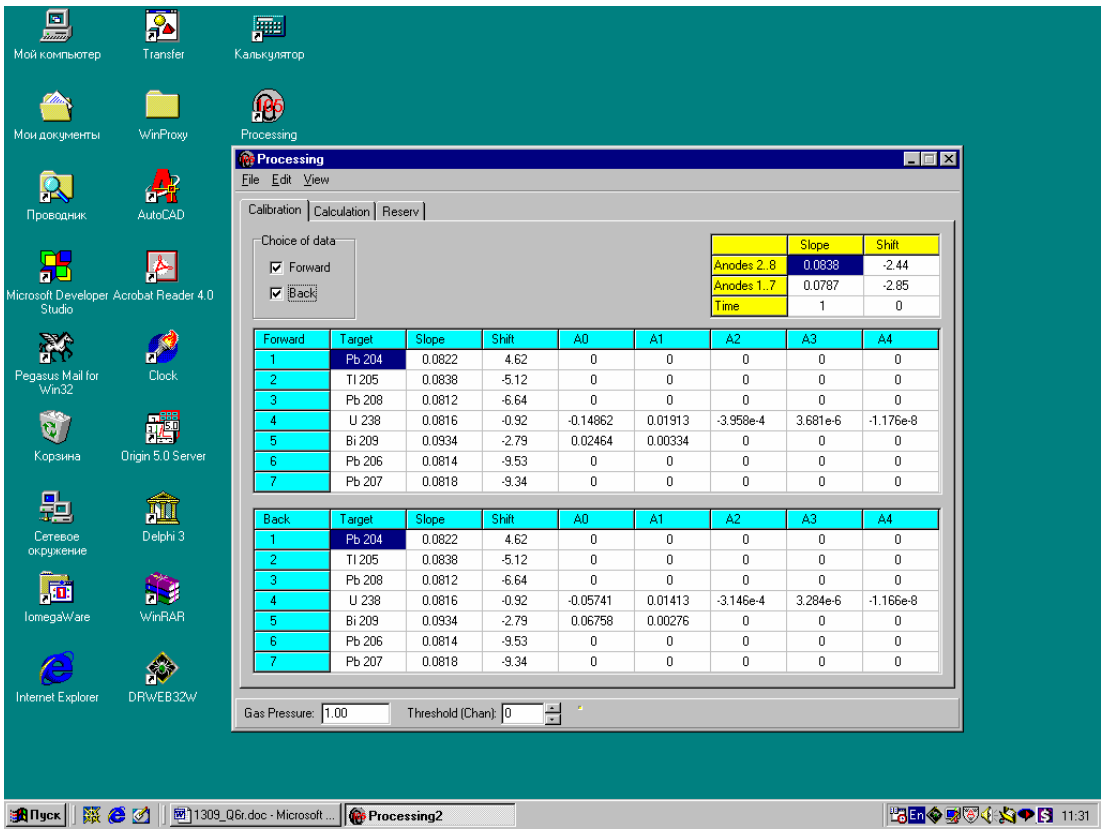


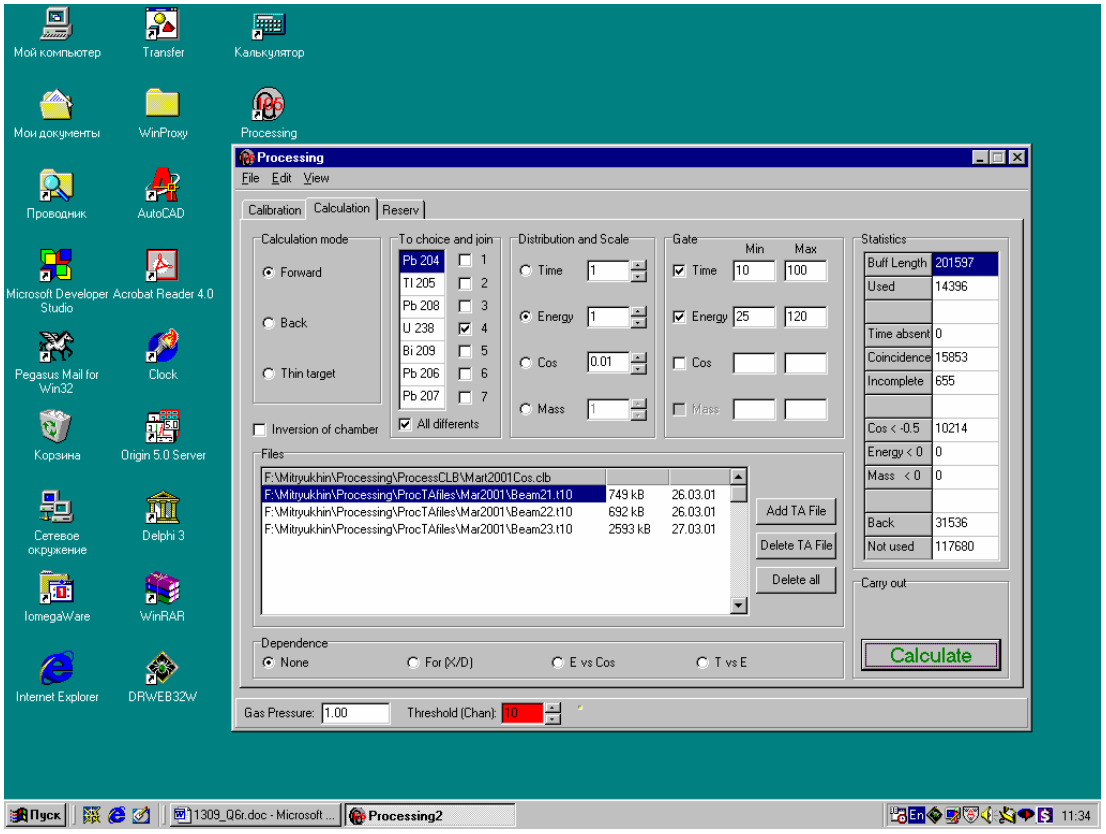


**Fig. 2-17.** Graphic user interface of the “Processing” code.

**2.2.6.** Fission cross section data receiving.

Fig. 2-18 shows an example of fission event distributions over the neutron time-of-flight (TOF) obtained at the quasi-monoenergetic neutron beam with the neutron "peak" energy 96 MeV.

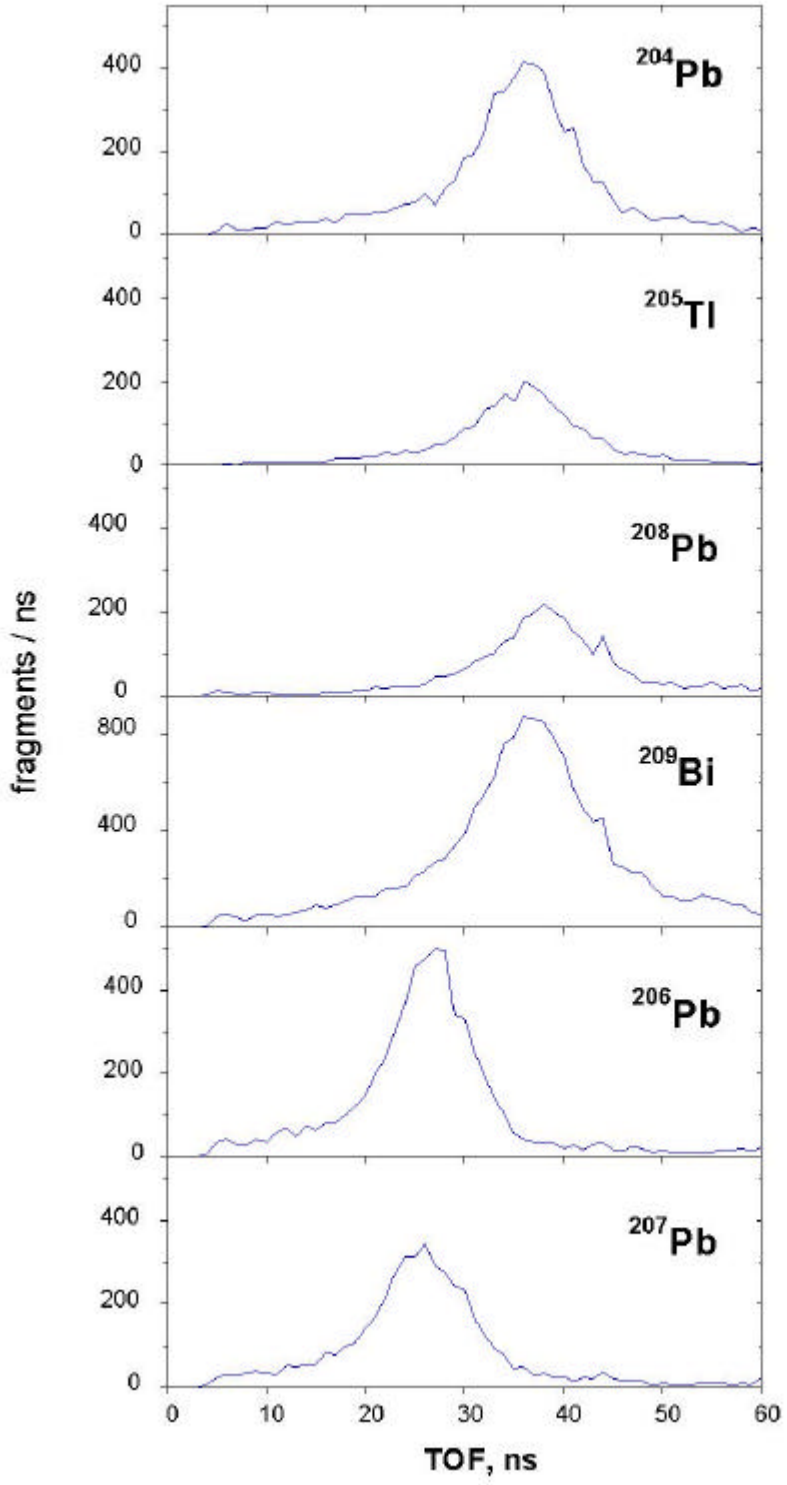


**Fig. 2-18.** Fission event distributions over the neutron time-of-flight obtained at the quasi-monoenergetic neutron beam with the neutron "peak" energy 96 MeV.

To extract from these distributions the number of fission events induced by the “peak” neutrons we have applied the decomposition procedure proposed in [25]. According to this procedure, we have used the composition of the Gaussian and the following step function:

$$y = y_0 + a_0\left(1+\exp\left(\frac{x-x_c}{0.667s}\right)\right)^{-1},$$

to fit the experimental TOF distributions. Here $y_0$ denotes the background level to the right of the peak, $a_0$ is the background "step" value, $x_c$ and σ define the position of the "step" and its width respectively.

In this way the numbers of fission events induced by “peak” neutrons were obtained both for the forward- and backward-facing targets. Then, these data were corrected for the losses due to the pulse height threshold ($K_{th}$) and the self-absorption in the fissile deposits ($K_{abs}$). The later was calculated from the formula:

$$K_{abs} = 1-(t/2R)(1+B/3)^{-1},$$

where $B$ is the anisotropy coefficient ($B = W(0^0)/W(90^0)-1$), $t$ is the thickness of the deposit and $R$ is the average range of fission fragments in the deposit material. Due to the linear momentum transferred (LMT) to the fissioning nuclei the average range of the forward-emitted fragments is larger than that of the backward-emitted ones. For the same reason the forward and the backward anisotropy coefficients differ from each other too. To take the LMT effect into account we have calculated the fragment ranges for both emission directions using our experimental data on fragment energy distributions and the SRIM96 code. These ranges and the experimental anisotropy coefficients were taken to calculate the $K_{abs}$ corrections.

The calculation of $K_{th}$ is complicated by the background from the light charged particles produced by the neutron interactions in the upstream material. As suggested in [26] a Frisch-gridded ionization chamber (apart from a simple parallel-plate one) makes it possible to eliminate the background particles. The principle of so-called angular discrimination lies in the fact that fission fragments and light charged particles give different combinations of anode and cathode signals, and thus may be separated from each other by off-line processing.

Fig. 2-19 shows the total (line) and the “cleared” (line+point) energy spectra of the fission fragments emitted in the direction of 96 MeV neutron beam. One can see that the problem of the extrapolation to the zero fragment energy may be more readily resolved after the background discrimination. The extrapolation procedure was the same for all the targets under study. We have assumed that the “cleared” spectra are free from the background particles at the energies in vicinity of 27 MeV (see Fig. 2-19). From this region we have used

the linear approximation $dN/dE = a + kE, \quad (k > 0)$ to the zero fragment energy. The coefficient $a$ was deduced from the energy spectra from the thin $^{252}$Cf source.

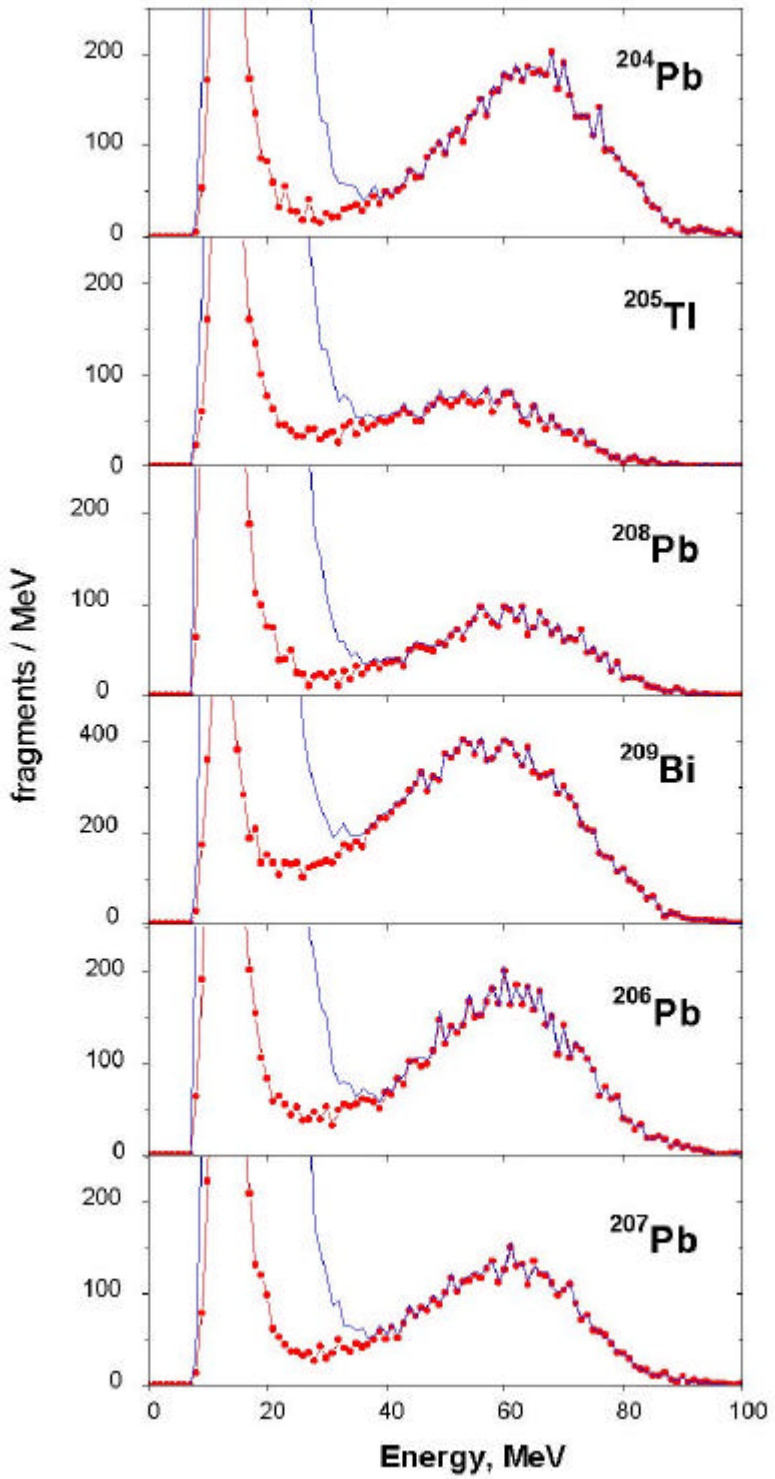


**Fig. 2-19.** The total (line) and the "cleared" (line+point) energy spectra of the fission fragments emitted in the forward hemisphere in respect to the neutron beam of 96 MeV. (The pulse height defect was not taken into account).

Table 2-4, for example, shows the anisotropy coefficients (B), the fragment ranges (R) and the corrections ($K_{abs}$, $K_{th}$) obtained for the forward emitted fragments at 96 MeV.

**Table 2-4.** The anisotropy coefficients (B), the fragment ranges (R), the corrections for the self-absorption ($K_{abs}$) and the pulse height threshold ($K_{th}$) obtained for the forward emitted fragments at the neutron energy 96 MeV.

| Target | B | R, mg/cm$^2$ | $K_{abs}$ | $K_{th}$ |
|---|---|---|---|---|
| $^{205}$Tl | 1.03 | 6.5 | 0.921 | 0.907 |
| $^{204}$Pb | 0.39 | 7.4 | 0.969 | 0.946 |
| $^{206}$Pb | 0.7 | 7.0 | 0.943 | 0.931 |
| $^{207}$Pb | 0.48 | 7.0 | 0.941 | 0.928 |
| $^{208}$Pb | 0.5 | 6.7 | 0.943 | 0.943 |
| $^{209}$Bi | 0.96 | 6.3 | 0.932 | 0.906 |
| $^{238}$U | 0.31 | 5.5 | 0.982 | 0.961 |

The same information is given in Table 2-5, but for the fission fragments emitted in the backward direction.

**Table 2-5.** As in Table 2-4, but for the backward emitted fragments.

| Target | B | R, mg/cm$^2$ | $K_{abs}$ | $K_{th}$ |
|---|---|---|---|---|
| $^{205}$Tl | 1.03 | 5.7 | 0.908 | 0.822 |
| $^{204}$Pb | 0.23 | 6.7 | 0.962 | 0.928 |
| $^{206}$Pb | 0.18 | 6.0 | 0.913 | 0.901 |
| $^{207}$Pb | 0.19 | 6.3 | 0.927 | 0.892 |
| $^{208}$Pb | 0.36 | 6.3 | 0.924 | 0.907 |
| $^{209}$Bi | 0.09 | 5.7 | 0.926 | 0.897 |
| $^{238}$U | 0.13 | 5.1 | 0.981 | 0.951 |

The fission cross-section ratios of $^{205}$Tl, $^{204,206\text{-}208}$Pb to $^{238}$U were calculated both for the forward- and the backward-facing targets as follows:

$$\frac{s_i^{F(B)}}{s_U^{F(B)}} = \frac{N_{f,i}^{F(B)}}{N_{f,U}^{F(B)}} \cdot \frac{m_U^{F(B)}}{m_i^{F(B)}}.$$

In this formula the superscript *F(B)* denotes the forward (backward) direction. $N_f$ is the number of "peak" fission events corrected for the $K_{abs}$ and $K_{th}$, while *m* is the number of target nuclei. Uncertainties in Kabs and Kth we estimate no more than 1.5 and 3 % accordingly. The

resulting ratios were obtained as the average of the corresponding forward and backward ratios:

$$\frac{s_i}{s_U} = \frac{1}{2}\left(\frac{s_i^F}{s_U^F} + \frac{s_i^B}{s_U^B}\right).$$

Table 2-6 contains the neutron-induced fission cross section ratios of $^{205}$Tl, $^{204,206\text{-}208}$Pb and $^{209}$Bi to $^{238}$U multiplied to $10^3$, obtained at the middle neutron energy of 34.7, 46.3, 65.4, 96.0, 133.6 and 173.9 MeV. Fission cross section ratios for lead isotopes $^{204}$Pb, $^{206}$Pb, $^{207}$Pb and $^{nat}$Pb received taking into account the isotope composition of targets used. Statistical uncertainties are shown only.

**Table 2-6.** Neutron-induced fission cross section ratios of $^{205}$Tl, $^{204,206\text{-}208}$Pb and $^{209}$Bi to $^{238}$U multiplied to $10^3$, obtained at the different neutron energy. Statistical uncertainty is shown.

| Target | 34.7 MeV | 46.3 MeV | 65.4 MeV | 96 MeV | 133.6 MeV | 173.9 MeV |
|---|---|---|---|---|---|---|
| **$^{205}$Tl** | 0.015±0.010 | – | 0.63±0.04 | 3.35±0.15 | 6.0±0.4 | 8.5±1.1 |
| **$^{204}$Pb** | 0.29±0.07 | 1.58±0.09 | 7.2±0.3 | 21.6±1.0 | 35.2±1.9 | 47.0±2.7 |
| **$^{206}$Pb** | 0.05±0.02 | 0.47±0.04 | 2.99±0.12 | 10.4±0.4 | 17.8±1.0 | 28.8±1.8 |
| **$^{207}$Pb** | 0.02±0.01 | 0.31±0.03 | 2.1±0.1 | 7.9±0.3 | 13.7±0.8 | 26.3±1.3 |
| **$^{208}$Pb** | 0.018±0.012 | 0.17±0.02 | 1.51±0.08 | 5.8±0.3 | 10.9±0.7 | 18.2±1.1 |
| **$^{209}$Bi** | 0.23±0.04 | 1.65±0.07 | 9.0±0.2 | 20.4±0.9 | 32.9±1.8 | 50.5±2.7 |

**2.2.7.** Receiving of the fission fragment angular distributions.

The "off-line" treating of the experimental data for all investigated nuclei by code "Processing" results fission fragment angular distributions in forward and backward hemisphere with respect to the neutron beam. The events with energy more than 25 MeV have been used. $\overline{X}/D$ value over fragment energy needed to receive a fission fragment angular distribution. It has been obtained experimentally for nuclei $^{238}$U and $^{209}$Bi at neutron energy of 96 MeV by method described in section 2.2.2. A scarce statistics has prevented to receive $\overline{X}/D$ value for lead isotopes and thallium with acceptable uncertainty, so for these nuclei we used $\overline{X}/D$ value obtained for $^{209}$Bi. $\overline{X}/D$ value for given nucleus was considered as independent upon incident neutron energy. For instance in Fig. 2-20 fission fragment angular for the $^{205}$Tl nuclei at the neutron energy of 96 MeV are shown for forward and backward

hemispheres. In Fig. 2-21 are shown the same distributions but for the $^{204}$Pb nuclei at the neutron energy of 96 MeV, in Fig. 2-22 – for the $^{238}$U nuclei at the neutron energy of 46.3 MeV. Dash lines in the Figures show fit function: $dN/d\Omega = A\times(1+B\cos^2 J)$.

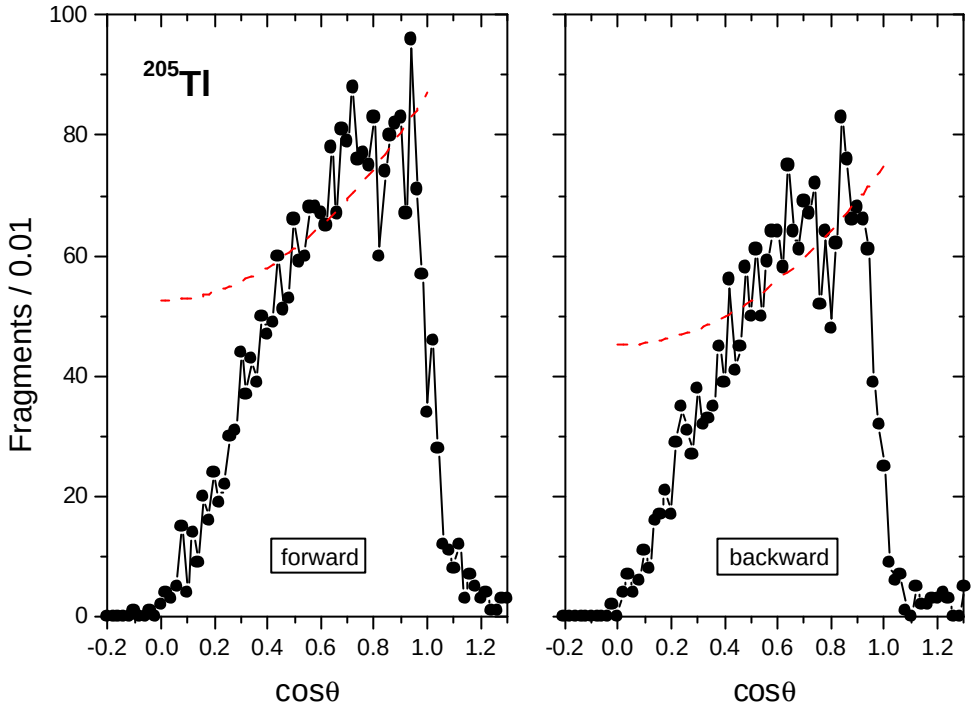


**Fig. 2-20**. Fission fragment angular distributions for $^{205}$Tl nuclei at the neutron energy of 96 MeV. Dash line – fit function.

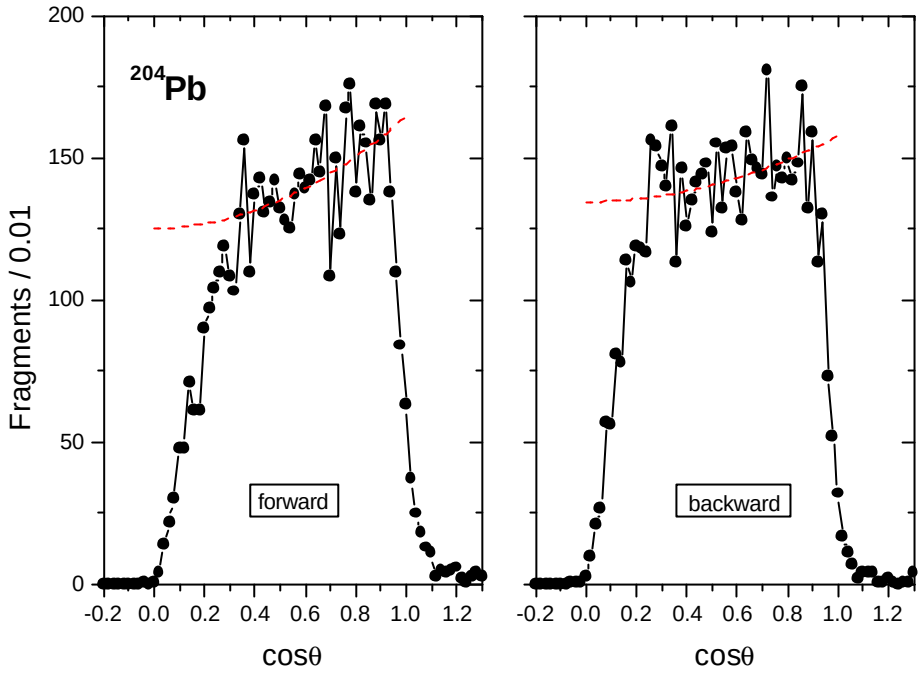


**Fig. 2-21**. Fission fragment angular distributions for $^{204}$Pb nuclei at the neutron energy of 96 MeV. Dash line – fit function.

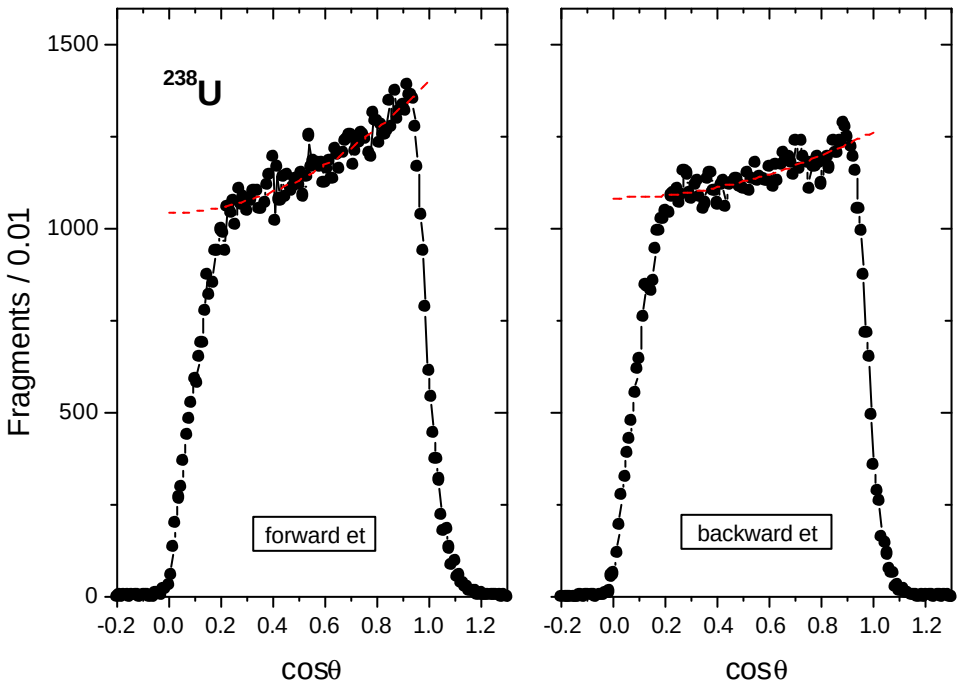


**Fig. 2-22**. Fission fragment angular distributions for $^{238}$U nuclei at the neutron energy of 46.3 MeV. Dash line – fit function.

# 3. Results.

## 3.1. Neutron-induced fission cross sections.

**3.1.1.** Neutron-induced fission cross sections measured with the ionization chamber (IC).

The absolute value of neutron-induced fission cross section for thallium-205, lead isotopes and bismuth-209 at the certain energy was received from fission cross section ratio for this nucleus to uranium (see sec. 2.2.6) and absolute cross section for uranium-238 at the appropriate energy. The uranium-238 fission cross section was recommended as a standard for cross section measurements at the intermediate neutron energy by the Nuclear Data Committee of the International Atomic Energy Agency (IAEA) [7]. The data of the Lisowski group received at Los-Alamos on the "white" spectrum neutron source (WNR/LAMPF) has been laid in the base of this standard.

In the Table 3-1 the absolute fission cross sections of thallium-205, lead isotopes and bismuth-209 nuclei at the quasi-monoenergetic neutrons with different energy of "peak" neutrons are presented in the energy range of 35÷175 MeV: in all 35 experimental values at energies 35, 46, 65, 96 134 and 174 MeV. In the separate column the natural lead nucleus fission cross section is presented. It has been received by summing up of the separate lead isotope cross sections with the appropriate weight. The fission cross section uncertainties shown include both uncertainty of the measured cross section ratio and uncertainty of the standard cross section. In column with the mean "peak" energy of neutrons pointed out half-width of spectral distribution of "peak" neutrons, not an uncertainty of mean energy. (thallium-205 target has not been used in the experiments at the neutron energy of 46.3 MeV and so data in this cell miss).

**Table 3-1.** Absolute neutron-induced fission cross sections of thallium-205, lead isotopes and bismuth-209 nuclei at the intermediate energy.

| En | $^{205}$Tl | $^{204}$Pb | $^{206}$Pb | $^{207}$Pb | $^{208}$Pb | $^{nat}$Pb | $^{209}$Bi |
|---|---|---|---|---|---|---|---|
| **MeV** | **mb** | **mb** | **mb** | **mb** | **mb** | **mb** | **mb** |
| **34.7±1.4** | 0.025±0.017 | 0.46±0.13 | 0.08±0.04 | 0.035±0.024 | 0.029±0.022 | 0.048±0.025 | 0.37±0.07 |
| **46.3±1.1** | – | 2.58±0.15 | 0.79±0.06 | 0.51±0.04 | 0.28±0.04 | 0.49±0.05 | 2.70±0.12 |
| **65.4±0.9** | 0.97±0.08 | 11.1±0.7 | 5.1±0.3 | 3.28±0.22 | 2.33±0.17 | 3.32±0.24 | 12.3±0.7 |
| **96.0±1.4** | 4.73±0.26 | 30.3±1.7 | 15.2±0.9 | 11.2±0.6 | 8.2±0.5 | 10.9±0.7 | 28.8±1.7 |
| **133.6±1.9** | 7.9±0.7 | 46.2±3.4 | 24.2±1.8 | 18.2±1.4 | 14.3±1.1 | 18.0±1.5 | 43.3±3.3 |
| **173.9±1.9** | 11.1±1.6 | 61.7±4.8 | 38.7±3.1 | 35.3±2.5 | 23.9±1.8 | 30.5±2.4 | 66.6±3.8 |

In Fig. 3-1 in double logarithmic and linear scale the fission cross sections of thallium-205, lead isotopes and bismuth-209 nuclei versus energy of neutrons are shown.

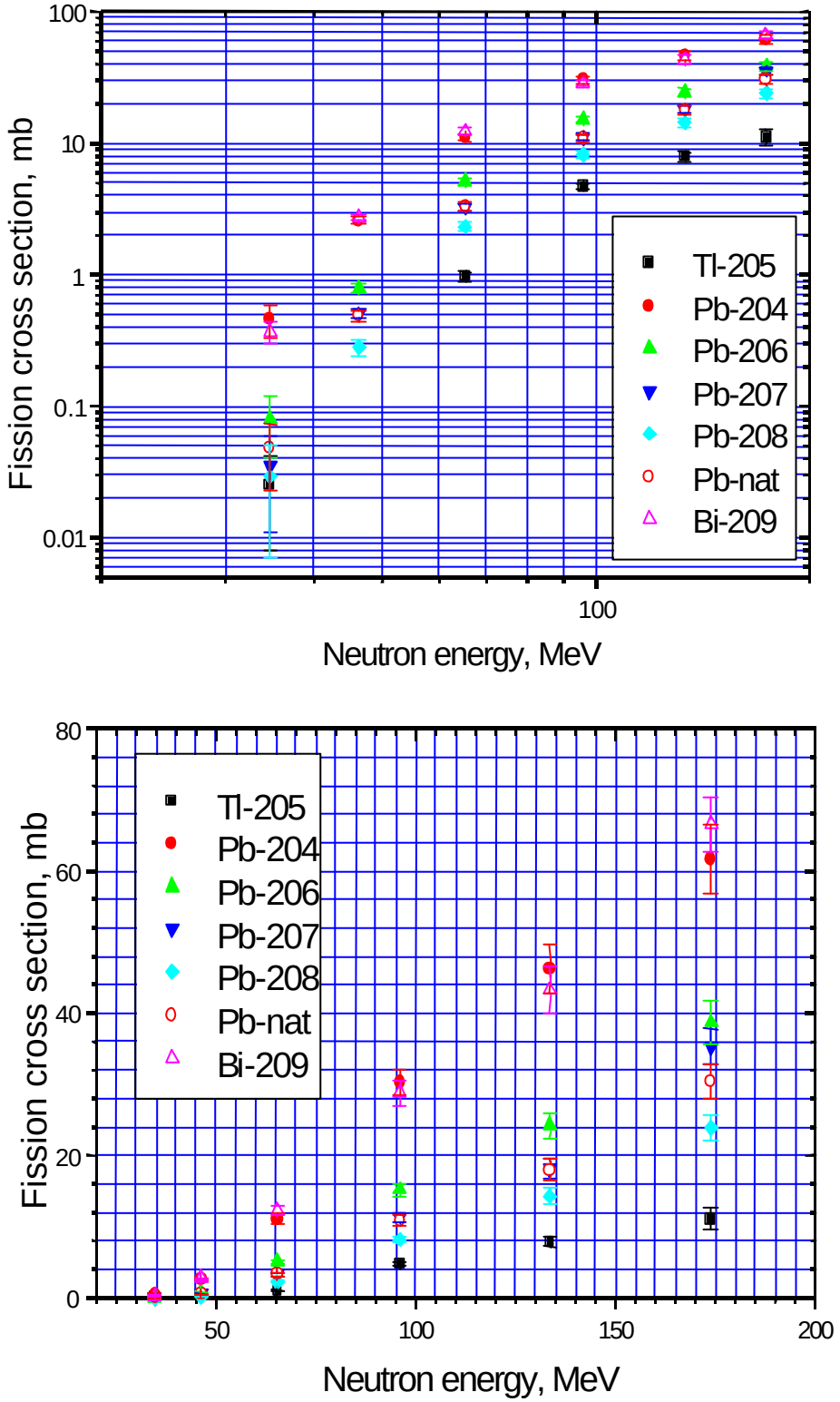


**Fig. 3-1.** Fission cross sections of thallium-205, lead isotopes and bismuth-209 nuclei versus energy of neutrons in double logarithmic (top) and linear (bottom) scale.

The energy dependence of fission cross section looks like function growing with energy. The velocity of grow diminish with removal from a barrier of fission. The value of cross section decreases with diminution of fissility parameter $Z^2/A$. These qualitative regularities appear similar to ones established earlier for protons.

**3.1.2.** Neutron-induced fission cross sections measured using TFBC.

The results on the relative fission cross sections obtained using the TFBC method are presented in the tables 3-2 and 3-3. The ratios of the cross sections of the nuclides under study to the $^{209}$Bi(n,f) cross section are presented in the table 3-2.

These ratios do not undergo to the influence of corrections on detector's efficiency because the difference of detection efficiency for such similar nuclei as $^{209}$Bi, lead isotopes, $^{205}$Tl is about 1% (see 2.1.5.1.). In table 3-3 the fission cross section ratios of $^{209}$Bi to $^{238}$U are given. The values of the corrections are about 5%. Possible uncertainty of the calculated value and the impossibility of direct testing in neutron measurements (due to low values of neutron fluxes) put restrictions on use of these ratios for determination of these cross sections with 10% accuracy.

63 values of the (n,f) cross section ratios of different nuclei to $^{209}$Bi and of $^{209}$Bi to $^{238}$U at 10 and 11 values of the neutron energy correspondingly have been obtained in all. The $^{209}$Bi(n,f)/ $^{238}$U(n,f) ratios measured earlier at the neutron energies 34.5, 46, 66, 74, 96, 133, 160 and 174 MeV [10, 15] have been revised using new approach to the corrections $d_e$ and $k_{peak}$ and have been taken into account at processing of the results of the present work.

**Table 3-2**. Neutron induced fission cross sections of $^{204,206,207,208}$Pb, $^{nat}$Pb and $^{205}$Tl relative to the $^{209}$Bi measured using the TFBC method.

| $E_n$ [? ??] | $^{204}$Pb | $^{206}$Pb | $^{207}$Pb | $^{208}$Pb | $^{nat}$Pb | $^{205}$Tl |
|---|---|---|---|---|---|---|
| **34.7±1.4** | 1.04±0.09 | 0.17±0.02 | 0.13±0.02 | 0.029±0.007 | | 0.020±0.007 |
| **46.1±1.2** | 1.06±0.05 | 0.32±0.02 | 0.19±0.01 | 0.082±0.005 | 0.20±0.01 | 0.067±0.004 |
| **66.4±0.9** | 1.02±0.05 | 0.45±0.02 | 0.29±0.01 | 0.202±0.008 | 0.30±0.01 | 0.105±0.005 |
| **73.4±1.0** | | | | 0.219±0.019 | 0.32±0.03 | |
| **89.5±0.8** | 1.06±0.08 | 0.49±0.03 | 0.37±0.03 | 0.28±0.02 | | 0.16±0.01 |
| **95.0±1.4** | 0.98±0.05 | 0.49±0.02 | 0.36±0.02 | 0.30±0.01 | 0.38±0.01 | 0.164±0.006 |
| **111.0±1.1** | 1.06±0.09 | 0.55±0.04 | 0.46±0.03 | 0.33±0.02 | | 0.204±0.016 |
| **133.0±1.9** | 1.00±0.06 | 0.59±0.03 | 0.44±0.02 | 0.31±0.01 | 0.42±0.02 | 0.23±0.01 |
| **144.0±1.8** | 1.02±0.07 | 0.65±0.04 | 0.50±0.03 | 0.39±0.02 | 0.46±0.03 | 0.25±0.01 |
| **173.9±1.9** | 1.00±0.04 | 0.61±0.02 | 0.47±0.02 | 0.37±0.01 | 0.51±0.02 | 0.25±0.01 |

**Table 3-3.** Neutron induced fission cross sections of $^{209}$Bi to the $^{208}$U measured using the TFBC method.

| $E_n$ [? ??] | $^{209}$Bi |
|---|---|
| **34.7±1.4** | $1.32\times10^{-4}\pm7\times10^{-6}$ |
| **46.1±1.2** | $1.07\times10^{-3}\pm7\times10^{-5}$ |
| **66.4±0.9** | 0.0053±0.0003 |
| **73.4±1.0** | 0.0083±0.0004 |
| **89.5±0.8** | 0.0131±0.0007 |
| **95.0±1.4** | 0.0143±0.0003 |
| **111.0±1.1** | 0.023±0.002 |
| **133.0±1.9** | 0.026±0.001 |
| **144.0±1.8** | 0.030±0.002 |
| **160.0±1.8** | 0.040±0.001 |
| **173.9±1.9** | 0.039±0.001 |

**3.1.3.** Comparison of the results of both methods of measurements, isotopic dependence of cross sections.

To compare results received by both methods and to rise a precision of definition of relative fission cross section the ratios of cross section of different nuclei to fission cross section of $^{209}$Bi were retrieved also from data in the Table 3-1 obtained using an ionization chamber and are listed in Table 3-4.

**Table 3-4.** Neutron-induced fission cross section ratios of lead isotopes and thallium to $^{209}$Bi (IC).

| $E_n$[MeV] | $^{205}$Tl | $^{204}$Pb | $^{206}$Pb | $^{207}$Pb | $^{208}$Pb | $^{nat}$Pb |
|---|---|---|---|---|---|---|
| **34.7±1.4** | 0.067±0.047 | 1.260±0.440 | 0.223±0.120 | 0.098±0.069 | 0.077±0.059 | 0.133±0.080 |
| **46.3±1.1** | - | 0.970±0.060 | 0.303±0.014 | 0.193±0.017 | 0.105±0.015 | 0.183±0.018 |
| **65.4±0.9** | 0.079±0.006 | 0.904±0.048 | 0.414±0.022 | 0.266±0.016 | 0.189±0.012 | 0.270±0.017 |
| **96.0±1.4** | 0.164±0.008 | 1.050±0.055 | 0.526±0.026 | 0.394±0.017 | 0.290±0.015 | 0.380±0.018 |
| **133.6±1.9** | 0.181±0.012 | 1.070±0.054 | 0.557±0.029 | 0.418±0.023 | 0.331±0.020 | 0.415±0.024 |
| **173.9±1.9** | 0.17±0.023 | 0.934±0.056 | 0.580±0.034 | 0.529±0.031 | 0.360±0.024 | 0.458±0.030 |

The results of both methods are shown in Fig. 3-2. One can see, that in uncertainty limits the data coincide. The weighted means of the cross section ratios represented by solid lines.

The neutron-induced fission cross section for enriched isotopes of lead and also for $^{205}$Tl are obtained for the first time. The essential expansion, twice, of a line of the investigated

isotopes of lead: from Δ? =2 (? =208÷206) to Δ? =4 (? =208÷204) reached over the plan, is obviously important. In Fig. 3-2 it is visible, that the indicated expansion results in noticeable change of the energy dependence shape of the relative cross sections. Against other isotopes of lead, an isotope 204 has fission cross section close to fission cross section of bismuth-209 in all energy range. The isotopic dependence of fission cross section of lead isotopes measured in a broad energy range is one of the main results of work having essential value for build-up of an adequate theoretical model.

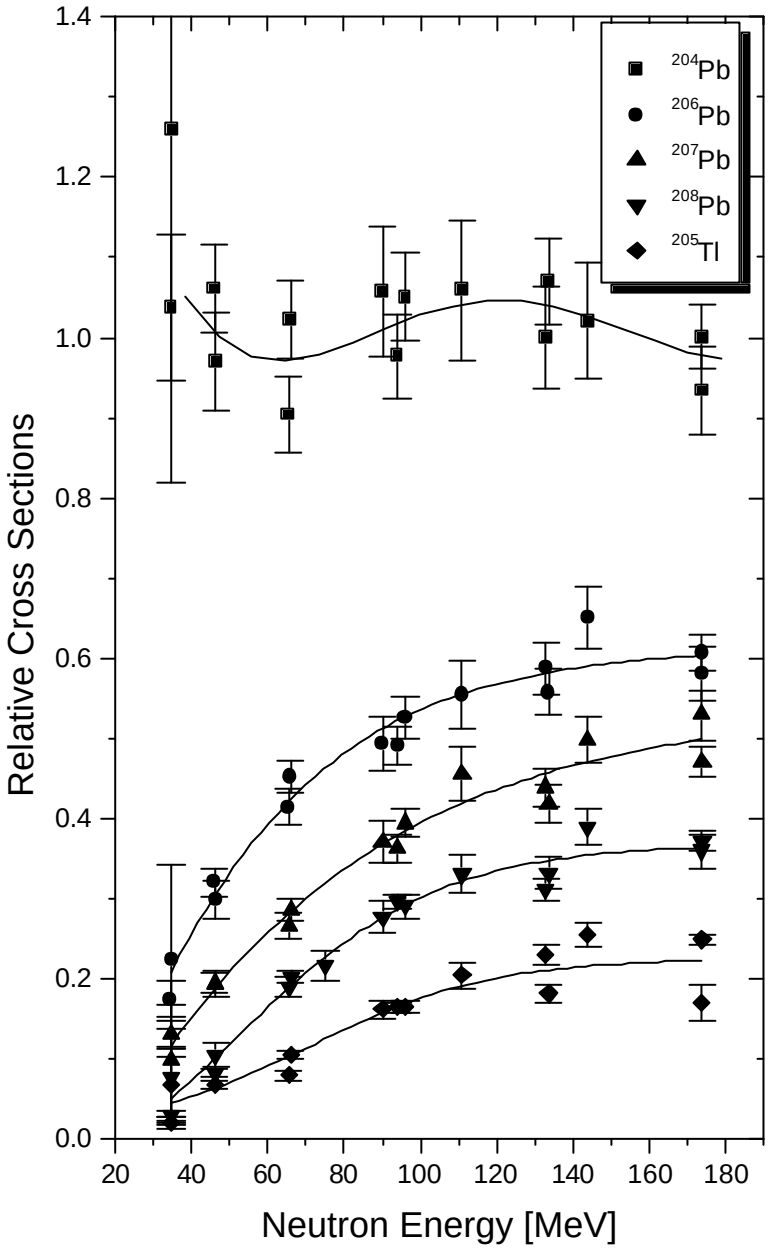

**Fig. 3-2.** Relative fission cross sections of lead isotopes and thallium-205 to fission cross section of bismuth-209.

**3.1.4.** Comparison of our results with the data of other works.

For an estimation of reliability of the obtained results on neutron-induced fission cross sections it is obviously important to carry out comparison with the data of other authors available in the literature, where it is possible. Those data now are available only for $^{209}$Bi nucleus and Pb nucleus of a natural isotope composition ($^{nat}$Pb). The basic data array on $^{209}$Bi and $^{nat}$Pb in the neutron energy range of 30-200 MeV obtained with a "white" spectrum neutron source in Los-Alamos by Staples et al. [27] in 1996 and quite recently within the framework of the project ISTC 609-97 in Gatchina by Shcherbakov et al. [28]. There are the data on $^{209}$Bi and upper limits of fission cross-section of $^{nat}$Pb, obtained at the monoenergetic neutron source at the energies of 18-23.3 MeV by Vorotnikov and Larionov in 1984 [29], and recent data on $^{209}$Bi and $^{nat}$Pb, obtained on a quasi-monoenergetic source at the neutron energy of 46, 61, 97 and 145 MeV by Nolte et al. [30]. All aforesaid data for $^{209}$Bi nucleus together with our data are represented in Fig. 3-3. In the same figure the line represents recommended value of the secondary standard of fission cross section for $^{209}$Bi [7]. As the value of viewed cross sections in neutron energy range of 18-200 MeV varies on more than 6 orders, the data in Figure both in logarithmic and in linear scale are shown. In Fig. 3-4 the data for $^{nat}$Pb nucleus are represented. Our earlier data [26, 31] are not shown in figures, as the error in operation of the equipment is discovered there. It results in the underestimated cross sections.

It is possible to approve, that our data obtained both for $^{209}$Bi and for $^{nat}$Pb coincide well with the data by Shcherbakov et al. practically in all neutron energy area. Unfortunately, in the data of Shcherbakov et al. the statistical errors of the ratio of cross-sections are given only. At comparison of the absolute cross-sections it is necessary to add, as a minimum, uncertainty of reference cross-section ($^{235}$U) to the statistical errors. However taking into account circumstance that in work of Shcherbakov et al. the neutron-induced fission cross section of nucleus $^{238}$U in the energy range of 35-200 MeV is obtained on ~6-8 % lower, than recommended reference cross-section $^{238}$U [7], which we used as the standard, the coincidence can be casual.

The data of Staples et al. [27] at the neutron energy > 50 MeV as for $^{209}$Bi, and $^{nat}$Pb in the uncertainty limits conform to our data (and data of Shcherbakov et al. [28]). At the neutron energy < 50 MeV the data of Staples et al. start to exceed ours, so at the energy of 35 MeV their exceeding achieves twofold for $^{209}$Bi and fourfold for $^{nat}$Pb.

The data of Nolte et al. [30] with indicated uncertainty limits are consistent with our data, thus on the average they are a little bit lower, except for value of the fission cross section of $^{209}$Bi at 97 MeV, which is lower on ~20 % than ours.

The data of Vorotnikov and Larionov [29] are unique in the neutron energies < 25 MeV, however they do not contradict a smooth extrapolation of our data in low neutron energy area both for $^{209}$Bi and for $^{nat}$Pb.

The data for $^{nat}$Pb and $^{209}$Bi have large practical interest, because they are considered as the most perspective materials of neutron production targets for accelerator driven systems. For possible practical usage of the results of fission cross section approximations for data obtained by means of the ionization chamber are given as follows:

for $^{nat}$Pb: $\sigma_f = 50.1 \times \exp\text{-}(127/E)^{1.5}$ [mb],

for $^{209}$Bi: $\sigma_f = 101 \times \exp\text{-}(109/E)^{1.5}$ [mb],

where ? – a neutron energy, MeV.

The formulas are available for the region ?=25-180 MeV, mean-weighted deviation of the experimental points from the curve is not more than the uncertainties of the measurement.

About probable restrictions of usage of data obtained with the help of TFB? , shown in figures 3-3 and 3-4 by squares see 3.1.2.

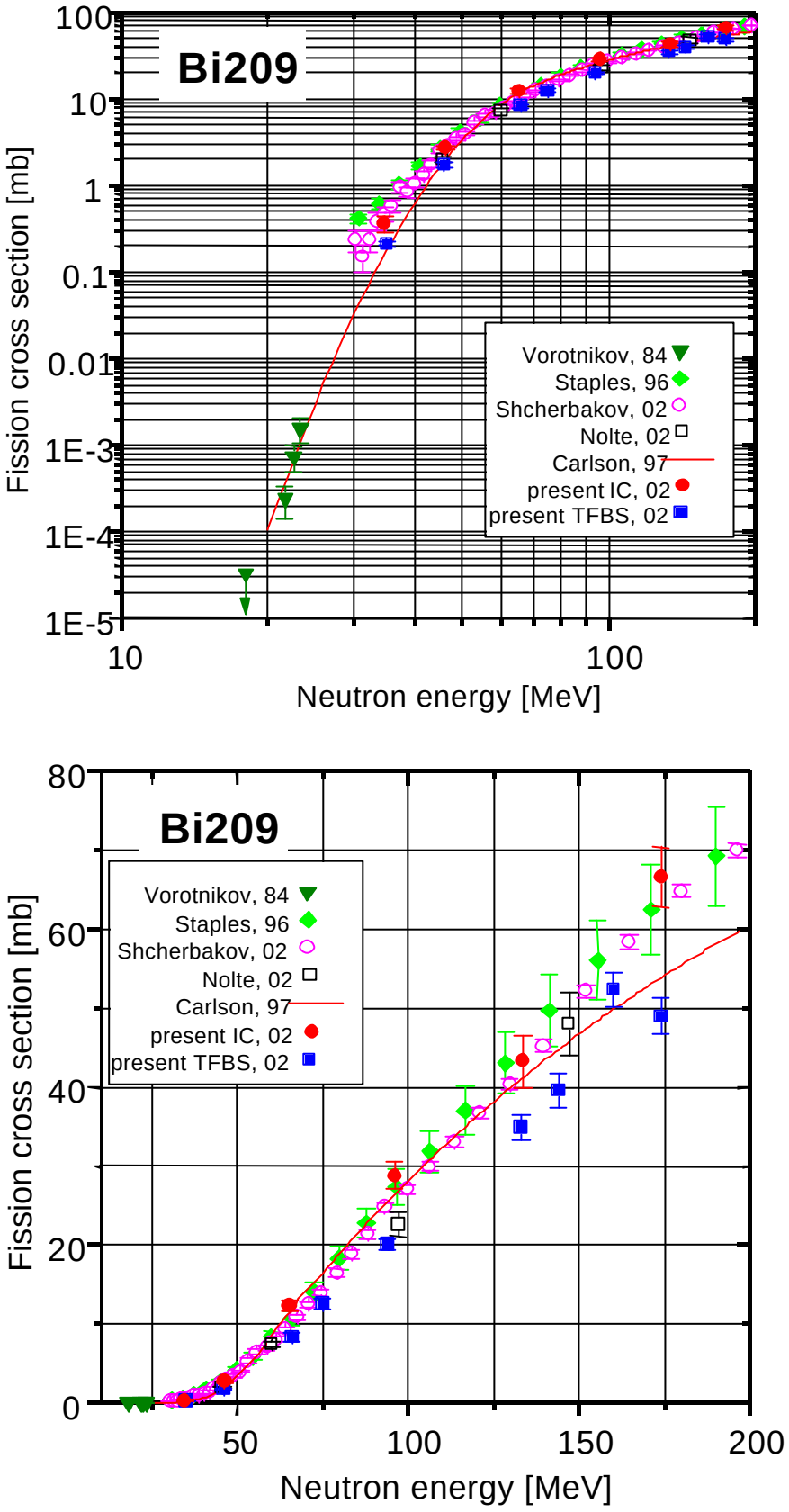


**Fig. 3-3.** Comparison of neutron-induced fission cross sections of bismuth-209 with available data [27-30] and recommended standard [7] in double logarithmic (top) and linear (bottom) scale.

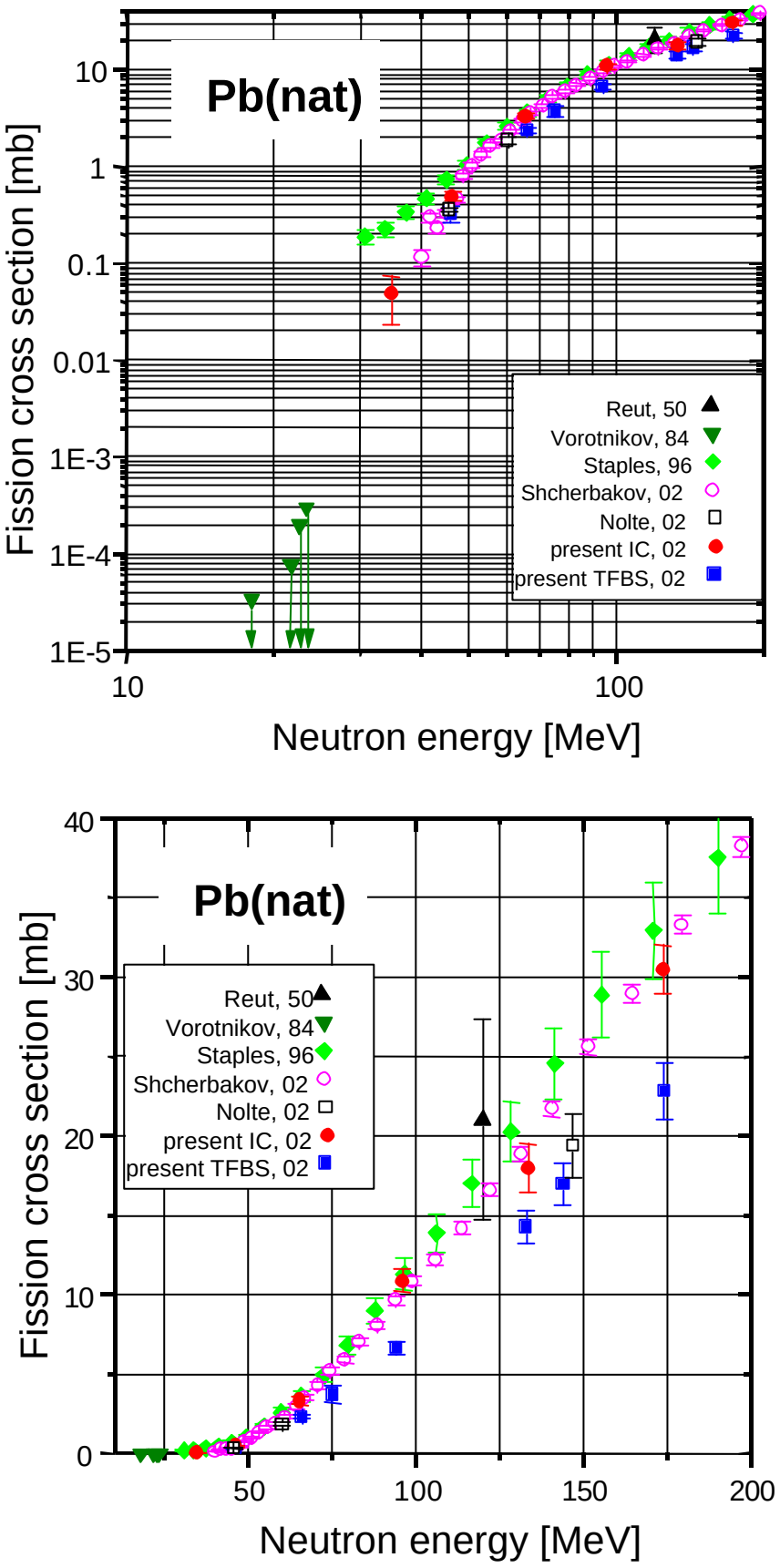


**Fig. 3-4.** Comparison of neutron-induced fission cross sections of natural lead with available data [27-30] in double logarithmic (top) and linear (bottom) scale.

### 3.2. Proton-induced fission cross sections.

**3.2.1.** Description of the results.

All measurements of the proton-induced fission cross sections are carried by the TFBC technique.

The proton-induced fission cross sections for $^{204,206,207,208}$Pb, $^{nat}$Pb and $^{205}$Tl nuclides have been measured relative to $^{209}$Bi and for $^{209}$Bi relative to $^{238}$U. 18 values of the (p,f) cross sections at the proton energies 64, 94 and 167 MeV have been obtained. The results are presented in tables 3-5 and 3.6.

**Table 3-5**. Proton-induced fission cross sections of $^{204,206,207,208}$Pb, $^{nat}$Pb and $^{205}$Tl relative to the $^{209}$Bi.

| $E_p$ [? ??] | $^{204}$Pb | $^{206}$Pb | $^{207}$Pb | $^{208}$Pb | $^{nat}$Pb | $^{205}$Tl |
|---|---|---|---|---|---|---|
| **64±2** | 1.12±0.09 | 0.52±0.04 | 0.36±0.03 | 0.25±0.02 | -- | 0.17±0.01 |
| **94±2** | 1.05±0.12 | 0.58±0.06 | 0.52±0.06 | 0.37±0.04 | -- | 0.20±0.03 |
| **167±2** | 1.05±0.06 | 0.57±0.08 | 0.52±0.02 | 0.44±0.03 | 0.54±0.04 | 0.34±0.02 |

**Table 3-6**. Proton-induced fission cross sections of $^{209}$Bi to the $^{208}$U.

| $E_p$ [? ??] | $^{209}$Bi |
|---|---|
| **64±2** | 0.018±0.001 |
| **167±2** | 0.086±0.004 |

The absolute (p,f) cross sections for $^{209}$Bi, $^{204,206,207,208}$Pb and $^{205}$Tl have been measured too. Results of the measurements are presented in table 3-7.

**Table 3-7.** Proton-induced fission cross sections of $^{209}$Bi $^{204,206,207,208}$Pb and $^{205}$Tl.

| $E_p$ | $^{209}$Bi | $^{204}$Pb | $^{206}$Pb | $^{207}$Pb | $^{208}$Pb | $^{205}$Tl |
|---|---|---|---|---|---|---|
| **MeV** | **mb** | **mb** | **mb** | **mb** | **mb** | **mb** |
| **47.5±0.5** | 9.3±0.9 | -- | -- | -- | -- | 0.86±0.09 |
| **49.2±0.5** | 11.3±1.1 | -- | -- | ---- | -- | 1.14±0.11 |
| **97.5±2.0** | 100±10 | 106±10 | 49±5 | -- | -- | 18±2 |
| **177.3±1.2** | 162±16 | 179±18 | 97±10 | 79±8 | 73±8 | 50±5 |

**3.2.2.** Isotope dependence of the proton-induced fission cross section.

The energy dependences of the proton-induced fission cross section ratios of lead isotopes and $^{205}$Tl to the $^{209}$Bi have been obtained using the data of the table 3-5 and the data extracted from datasets of other authors (see sect. 3.2.3). The results are shown in Fig. 3-5.

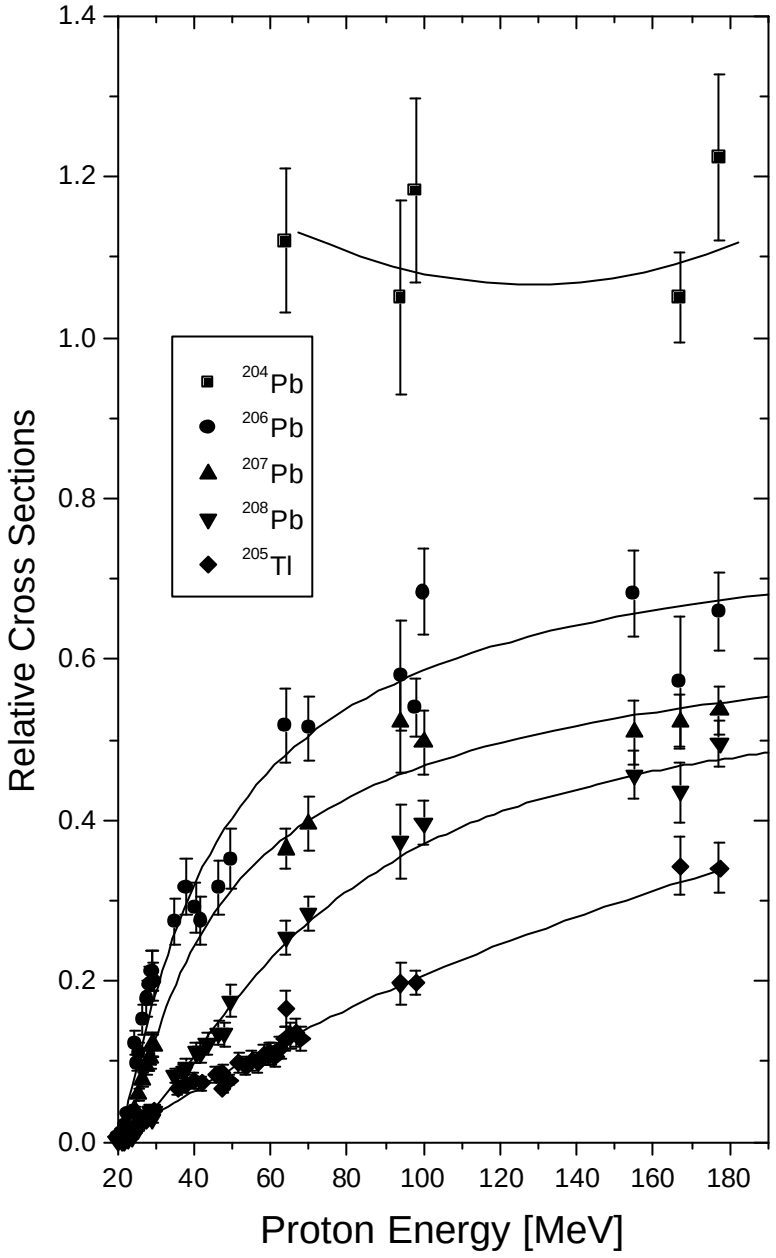


**Fig. 3-5.** Proton-induced fission cross section ratios of lead isotopes and $^{205}$Tl to the $^{209}$Bi.

If in the case of neutron-induced fission (Pb+n), shown in fig. 3-2, the dependence for lead isotopes is traced, in this case (Pb+p) a talk is about dependences for bismuth isotopes. It is correct at least at low energies of protons and neutrons ($E_{p,n} < 50$ MeV), when the fission is going from a compound states of nuclei. From a comparison of fig. 3-2 and 3-5 it is seen that the shape of the energy dependences and their changes from one isotope to another is similar for both cases, while the values of the ratios is somewhat higher for protons than for neutrons. This fact can reflect an exponential character of the dependences of the fissilities on the

parameter $Z^2/A$. As a whole, it gives additional material for study of the influence of the nuclear structure near closed shells on the fission process.

**3.2.3.** Comparison with results of other works.

The absolute values of the (p,f) cross sections at the proton energies 64, 94 and 167 MeV have been obtained from the relative ones presented in tables 3-5 and 3-6 using compiled from literature data on absolute $^{nat,238}$U(p,f) and $^{209}$Bi(p,f) cross section in the proton energy range from about 40 to 200 MeV [11]. The values of the absolute $^{209}$Bi(p,f) cross section obtained in this work at the proton energies 47.4, 49.2, 98 and 177.3 MeV (see table 3-7) were used for absolutisation of the (p,f) cross sections for lead isotopes and thallium too.

For comparison and analysis of the results of measurements of the (p,f) cross sections for $^{209}$Bi, $^{206,207,208}$Pb and $^{205}$Tl the data from all known works in the proton energy range from about 20 to 200 MeV have been attracted [32-42]. Data for $^{204}$Pb are obtained for the first time. It is necessary to note that the group of datasets from works [39-42], lying in the energy range from about 15 to 68 MeV and being of relative character because of unreliable outdated normalization [43], have been renormalized taking into account the data of the present work for $^{209}$Bi and $^{205}$Tl at proton energies 47.4 and 49.2 MeV. Fig. 3-6 presents all up-to-date experimental data on (p,f) cross sections for $^{209}$Bi, $^{204,206,207,208}$Pb and $^{205}$Tl in the proton energy range from 20 to 200 MeV. Comparative analysis has shown that results of the absolute (p,f) cross section measurements agree well with the absolute values of (p,f) cross section obtained from the relative data within uncertainties (≈10%). Results of the present work as a whole are in good compatibility with the reference data in the all over proton energy range.

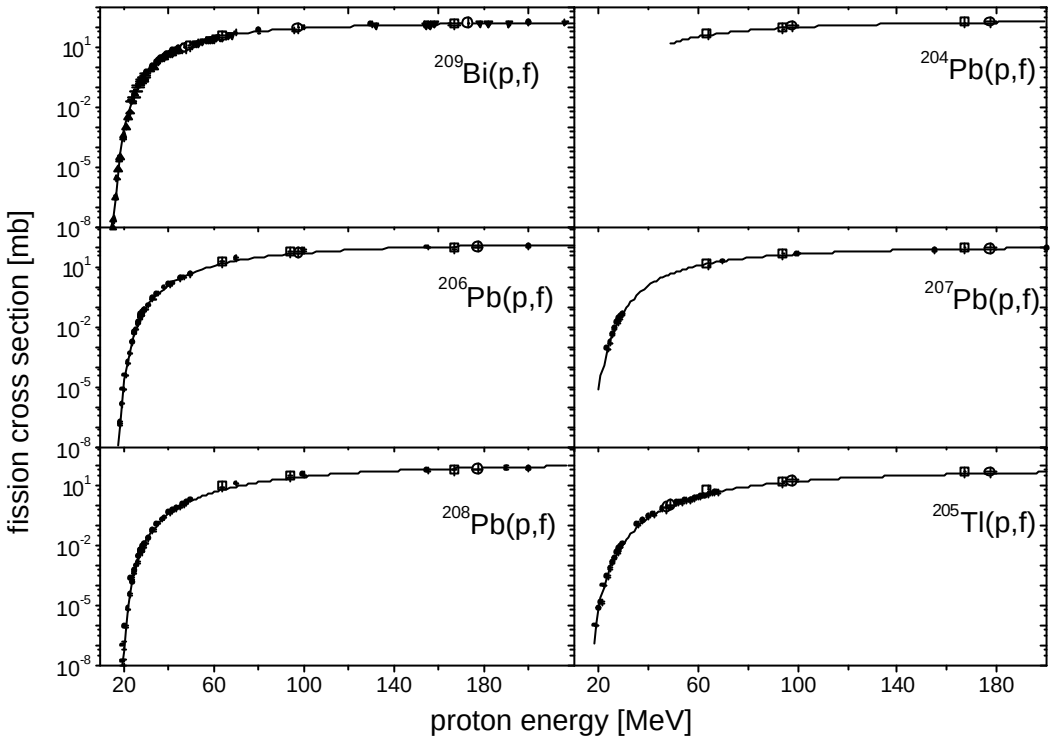


**Fig. 3-6.** Proton-induced fission cross sections of $^{209}$Bi, $^{204,206,207,208}$Pb and $^{205}$Tl. Open symbols are results of the present work (open circles are the results of the absolute measurements); solid symbols are compilation of works [32-42]; curves are the exponential-polynomial parameterizations.

Energy dependence of the (p,f) cross section for natural lead is of importance for applications. All up-to-date data on the $^{nat}$Pb(p,f) cross section in the proton energy range from about 20 to 200 MeV are shown in Fig. 3-7. It is necessary to note that in this energy region only three values have been obtained with the targets made from natural mixture of lead: 156 MeV [37], 190 MeV [38] and 167 MeV (present work). The other data were obtained by the linear combination of the data on separate isotopes of lead taking into account their partial weights in the natural mixture. The data are approximated by the following curves:

$\sigma_f = 113 \times \exp-(99.9/E)^{1.7}$ [mb] – for $^{nat}$Pb

$\sigma_f = 197.0 \times \exp-(86.2/E)^{1.7}$ [mb] for $^{209}$Bi,

where ? – a proton energy, MeV.

The formulas are available for the region ?=25-200 MeV, weight-average deviation of the experimental points from the curve is not more than the uncertainties of the measurements.

The uncertainty of the results for $^{nat}$Pb and $^{209}$Bi is about 10%.

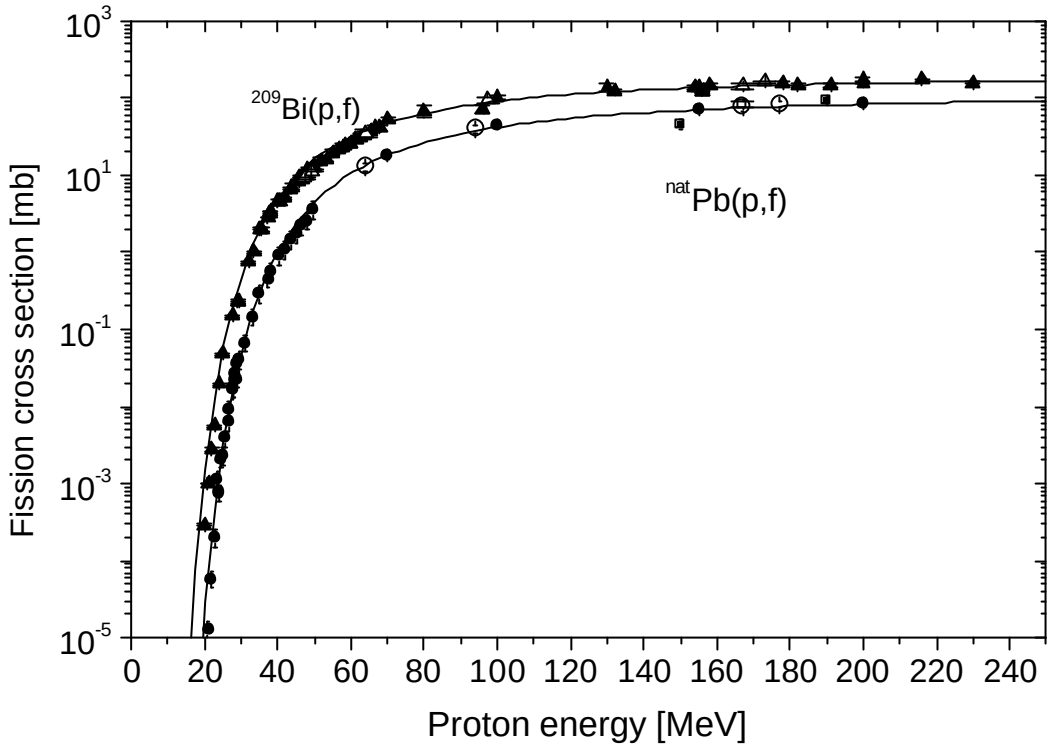


**Fig. 3-7.** Proton-induced fission cross section of $^{nat}$Pb and $^{209}$Bi. Open symbols are the results of the present work, solid symbols are the compilation from works [33, 38-41]. Squares represents the data obtained with targets made from natural lead.

### 3.3. Comparison of the proton- and neutron-induced fission cross sections.

The first comparison of the (p,f) and (n,f) cross sections (as well as the (γ,f) cross section) have been undertaken for the incident particle energy region up to 100 MeV [44]. It has been found that for all nuclei from $^{232}$Th to $^{239}$Pu at nucleon energies E well above the proton Coulomb barrier of these nuclei (V≈15 MeV), where the Coulomb factor, 1-V/E, is close to unity, the (p,f) cross sections are higher than the (n,f) cross sections at the same energies. Moreover the difference between the cross sections increases with the decrease of the mass of the fissioning nuclei. In further comparisons [8, 45-49] the range has been widened to lighter nuclei – down to $^{197}$Au. It has been found that the (p,f)/(n,f) cross section ratios continue to increase with the decrease of the fissility parameter $Z^2/A$ of the target nuclei reaching a value of about 2-3 or more.

In this report this effect is considered for nuclei close to lead, i.e., for $^{205}$Tl, $^{204,206,207,208}$Pb and $^{209}$Bi. The $^{208}$Pb is of special interest as being a double-magic nucleus with closed neutron (N=126) and proton (Z=82) shells. Its special energy stability and absence of

deformation can influence both the mechanism of nucleon-nucleus interaction (via the properties of the optical potential) and the fission probability and its dependence on excitation energy. Measurements for different isotopes allow investigation of the role of the isospin both for the incident particle and the target nuclei (so-called “double isospin effect”).

The main characteristic of the measurements was that in order to improve the reliability of the results, the measurements with both protons and neutrons were carried out in as identical beam conditions as possible, using the same fission chambers based on thin film breakdown counters (TFBC).

The (p,f) and (n,f) cross sections as well as their ratios depend on the incident nucleon energy. Fig. 3-8 shows examples of the $\sigma_{pf}/\sigma_{nf}$ energy dependence for nuclei ranging from $^{181}$?? to $^{237}$Np.

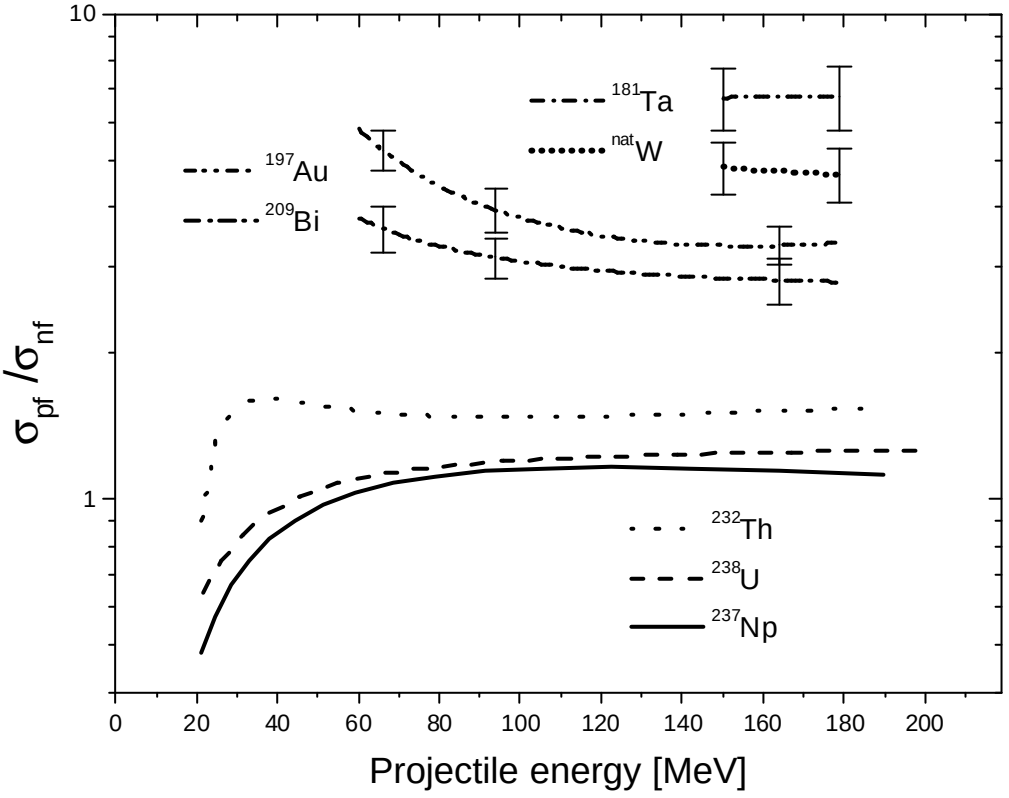


**Fig. 3-8.** Cross section ratios for heavy nuclei.

It is seen that for the heaviest nuclei ($^{237}$Np and heavier), for which the (p,f) and (n,f) cross sections are close to the inelastic cross sections, the cross section ratio increases with the projectile energy to overcome the Coulomb barrier and reaches unity at energies above about 100 MeV. The $\sigma_{pf}/\sigma_{nf}$ ratio for $^{238}$U is sometimes higher than for $^{237}$Np, and further higher for $^{232}$Th. For lighter nuclei ($^{197}$Au – $^{209}$Bi) the energy dependence of the $\sigma_{pf}/\sigma_{nf}$ ratios have

another shape. Having a maximum value at the energy near the fission barrier, the ratios decrease sharply with energy increase and reach a plateau in the energy range above about 100 - 150 MeV. The value of the $\sigma_{pf}/\sigma_{nf}$ ratios at the plateau is about 3. The ratios for $^{nat}$W and $^{181}$Ta at energies of 150 – 200 MeV are even higher (the data on the (p,f) cross sections for lower energies are absent for these nuclei).

The same dependences on the energy of the $\sigma_{pf}/\sigma_{nf}$ ratios for the lead isotopes are shown in Fig. 3-9. It is seen from the figure that the shapes are the same as for the $^{197}$Au and $^{209}$Bi, but the dependence on the mass is opposite – the $\sigma_{pf}/\sigma_{nf}$ ratios for lighter isotopes are lower than for the heavier ones. This is clearly noticeable at the lower energies but it is almost justified also for the higher energies within the uncertainties - the ratios for $^{204,206}$Pb are lower than for $^{207,208}$Pb.

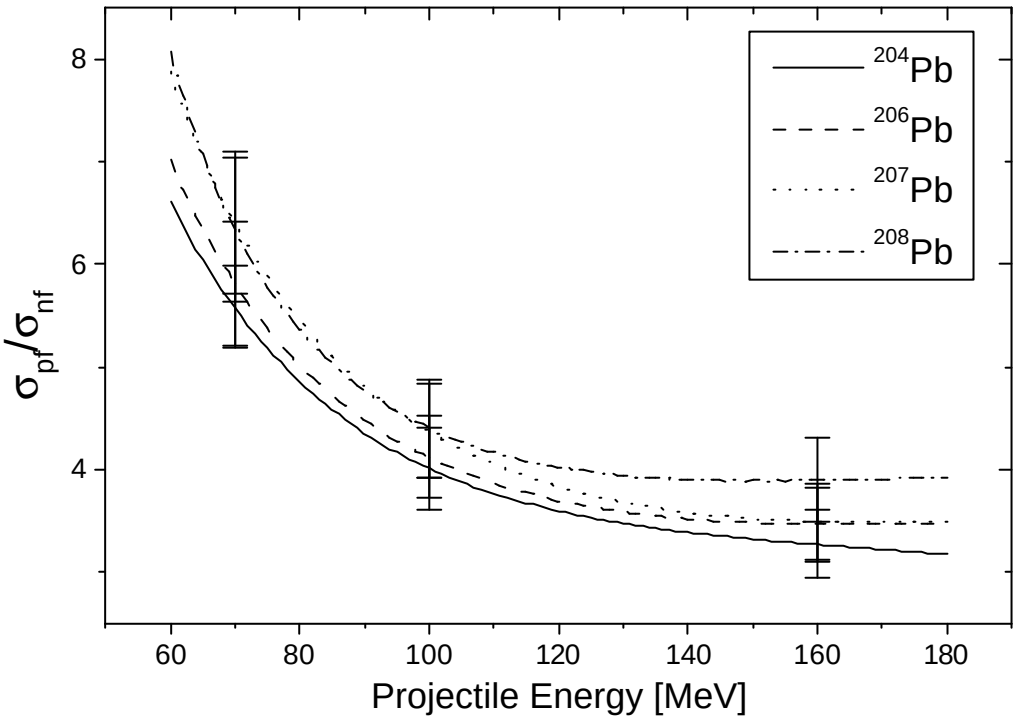


**Fig. 3-9.** Cross section ratios for lead isotopes.

However, if one chooses the fissility parameter $Z^2/A$ of a target nucleus as a variable quantity, the results on the cross section ratios are found to be non-contradictory. As is seen from Fig. 3-10, the $\sigma_{pf}/\sigma_{nf}$ ratio decreases with the fissility parameter increase from about 7 for $Z^2/A$ =29 to 1 for $Z^2/A$ =36.6:

$$s_{pf} / s_{nf} \approx \exp[0.26(36.6 - Z^2 / A)].$$

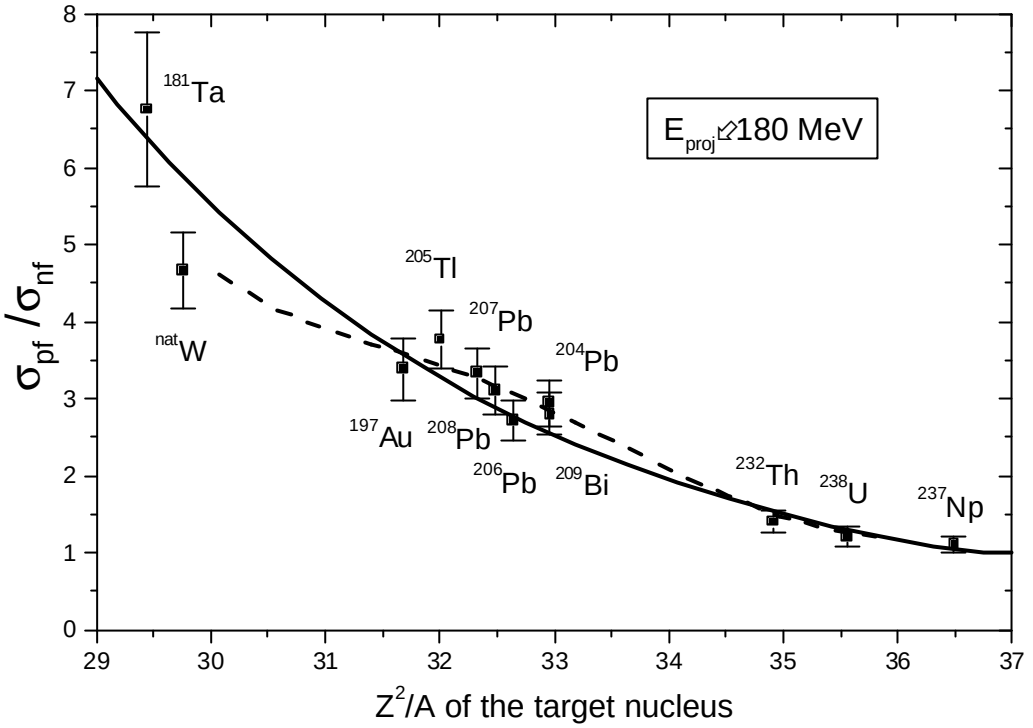


**Fig. 3-10.** Cross section ratios vs $Z^2/A$.

The fission cross section $\sigma_f$ is determined by the cross section of an inelastic interaction $\sigma_{in}$ with a target nucleus and by the decay probability of the created nuclei by means of fission: $\sigma_f = \sigma_{in} \cdot P_f$. Though influence of both factors is possible, the connection of $\sigma_{pf}/\sigma_{nf}$ to $Z^2/A$ gives a reason to consider the fission probability, which depends on $Z^2/A$, as the main factor determining the observed behavior of the $\sigma_{pf}/\sigma_{nf}$ ratio. A more detailed analysis has to take into account that, in the energy region under study, not only the compound nucleus undergoes fission but there is also a wide range of nuclei resulting from the processes of intranuclear cascade and pre-equilibrium emission. Taking these processes into account, the total fission probability can be expressed:

$$P_f = \sum_A \sum_Z \int_{E^*} W(A, Z, E^*, T_Z) P(A, Z, E^*) dE^*,$$

where P(A,Z,E*) is the fission probability of the residual nucleus with mass A, charge Z and excitation energy E*, W(A,Z,E*,$T_Z$) is the distribution of residual nuclei, which may depend on the projection of isospin of the incident particle, $T_Z$. Calculations performed with use of the cascade-exciton model [48] show that the distribution of the residual nuclei keeps a "memory" about isospin of the incident particle: the average value of the $Z^2/A$ parameter is higher for protons than for neutrons. Thus, the fission probability, and therefore the fission cross section,

for protons is found to be higher than for neutrons. One can say that the total fission probability is a function of the fissility parameter of the composite nucleus (target nucleus + incident particle). It is interesting to note that accordingly to ref. [44] the probability of fission of $^{232}$Th by γ-quanta has an intermediate value between the fission probabilities for protons and neutrons, which corresponds to the following fissility parameters:

$$(Z+1)^2/A > Z^2/A > Z^2/(A+1).$$

As far as the fission probability is determined by the ratio of the fission and neutron evaporation widths,

$$P_f \approx \Gamma_f / \Gamma_n + \Gamma_f,$$

$$\frac{s_{pf}}{s_{nf}} \approx \frac{P_f^p}{P_f^n} \approx \frac{\Gamma_f^p}{\Gamma_f^n} \approx \exp\left(\frac{B_f^n - B_f^p}{T}\right),$$

where $B_f^n$ and $B_f^p$ are the fission barriers, and $T$ is the temperature of the nucleus, $T \sim E_{proj}^{1/2}$.

This means that $\sigma_{pf}$ and $\sigma_{nf}$ are almost equal for heavy nuclei, where $B_f^p \approx B_f^n$, and differ strongly for subactinide nuclei, where $B_f^p < B_f^n$, which explains the stated empirical dependence of $\sigma_{pf}/\sigma_{nf}$ on the fissility parameter. As far as the temperature $T$ of the nuclei has its lowest value near the fission barrier, the $\sigma_{pf}/\sigma_{nf}$ ratio is especially high near the barrier, which explains the observed energy dependence of $\sigma_{pf}/\sigma_{nf}$ (with the exception of weak Coulomb factor).

An analogous interpretation of the $\sigma_{pf}/\sigma_{nf}$ dependence on the fissility parameter was given in ref. [50]. However, in the opinion of the authors of ref. [51], the possible difference between the measured (p,f) and (n,f) cross sections might be attributed to the influence of the isovector term of the nucleon-nucleus optical potential. The latter interpretation may, however, result in inconsistencies if a wide range of elements and different isotopes of the same element is considered.

It seems as additional information about the nature of the effect under study can be obtained with more complete measurements of the $\sigma_{pf}/\sigma_{nf}$ for tungsten and of separate isotopes of this element. The fission barrier changes weakly for heavy actinide nuclei. In the region of lighter nuclei the barrier increases rapidly with decreasing mass and charge of the nucleus and reaches a maximum value for $^{208}$Pb due to the large (15 MeV) shell correction to the liquid-drop barrier. As the shell correction decreases (for tungsten this correction is close to zero) the barrier reaches a plateau, that can lead to slowing down of the $\sigma_{pf}/\sigma_{nf}$ rise in the region of tungsten, as is shown in Fig. 3-10 by the dashed curve.

### 3.4. Fission fragment angular distributions

**3.4.1.** Fission fragment angular distributions at neutron-induced fission.

Fission fragment angular distributions for uranium-238, thallium-205, isotopes of lead and bismuth-209 by neutrons with energy of 35-175 MeV were obtained using multisection ionization chamber.

In the "off-line" processing of the experimental data the fission fragment angular distribution of all explored nuclei in forward and backward hemispheres with regard to the direction of neutron beam have been obtained. The angular distribution was simulated by function of a view: $dN/d\Omega = A\times(1+B\cos^2 J)$, where $B=W(0^?)/W(90^?)-1$ – anisotropy coefficient, $W(J)$– probability of emission of a fragment under angle $J$ with regard to the selected direction. Fit of the data by the least squares method was fulfilled in area, where the distribution is not distorted by the self-absorption of fragments in a target layer close to $\cos J$ =0 and definite angular resolution close to $\cos J$ =1 (usually 0.4 < $\cos J$ < 0.9). The anisotropy coefficients are not identical to fission fragments of the given nucleus at the given neutron energy for angular distributions in forward and backward hemispheres. The transferred momentum to the fissionable nucleus causes it. We have supposed, that fission anisotropy coefficient in the centre of mass system of fissionable nucleus is equal to the mean of anisotropy coefficients in forward and backward hemispheres in the laboratory system.

In Table 3-8 the anisotropy coefficients obtained for fission of thallium-205, isotopes of lead, bismuth-209 and uranium-238 by neutrons with different energy are represented. The small number of the registered fission events of thallium and lead nuclei has not allowed receiving fragment angular distributions at the neutron energies of 34.7 and 46.3 MeV.

**Table 3-8.** Fission anisotropy coefficients (B) of thallium-205, isotopes of lead, bismuth-209 and uranium-238 by neutrons with energy 35-175 MeV.

| En, [MeV] | $^{205}$Tl | $^{204}$Pb | $^{206}$Pb | $^{207}$Pb | $^{208}$Pb | $^{209}$Bi | $^{238}$U |
|---|---|---|---|---|---|---|---|
| **34.7±1.4** | – | – | – | – | – | 5.0±9.0 | 0.30±0.04 |
| **46.3±1.1** | – | 0.26±0.28 | 0.41±0.41 | 0.84±0.75 | 1.5±1.2 | 1.1±0.5 | 0.25±0.02 |
| **65.4±0.9** | 0.75±0.52 | 0.07±0.16 | 0.48±0.24 | 0.48±0.36 | 0.41±0.32 | 0.93±0.24 | 0.29±0.02 |
| **96.0±1.4** | 0.92±0.24 | 0.32±0.11 | 0.44±0.12 | 0.34±0.12 | 0.50±0.16 | 0.54±0.11 | 0.22±0.02 |
| **133.6±1.9** | 0.95±0.24 | 0.37±0.08 | 0.43±0.10 | 0.43±0.11 | 0.45±0.11 | 0.55±0.09 | 0.16±0.02 |
| **173.9±1.9** | 0.82±0.20 | 0.10±0.10 | 0.29±0.11 | 0.35±0.14 | 0.30±0.12 | 0.31±0.09 | 0.03±0.03 |

In Fig. 3-11 the fission anisotropy coefficients of thallium-205, isotopes of lead, bismuth-209 and uranium-238 versus neutron energy are shown.

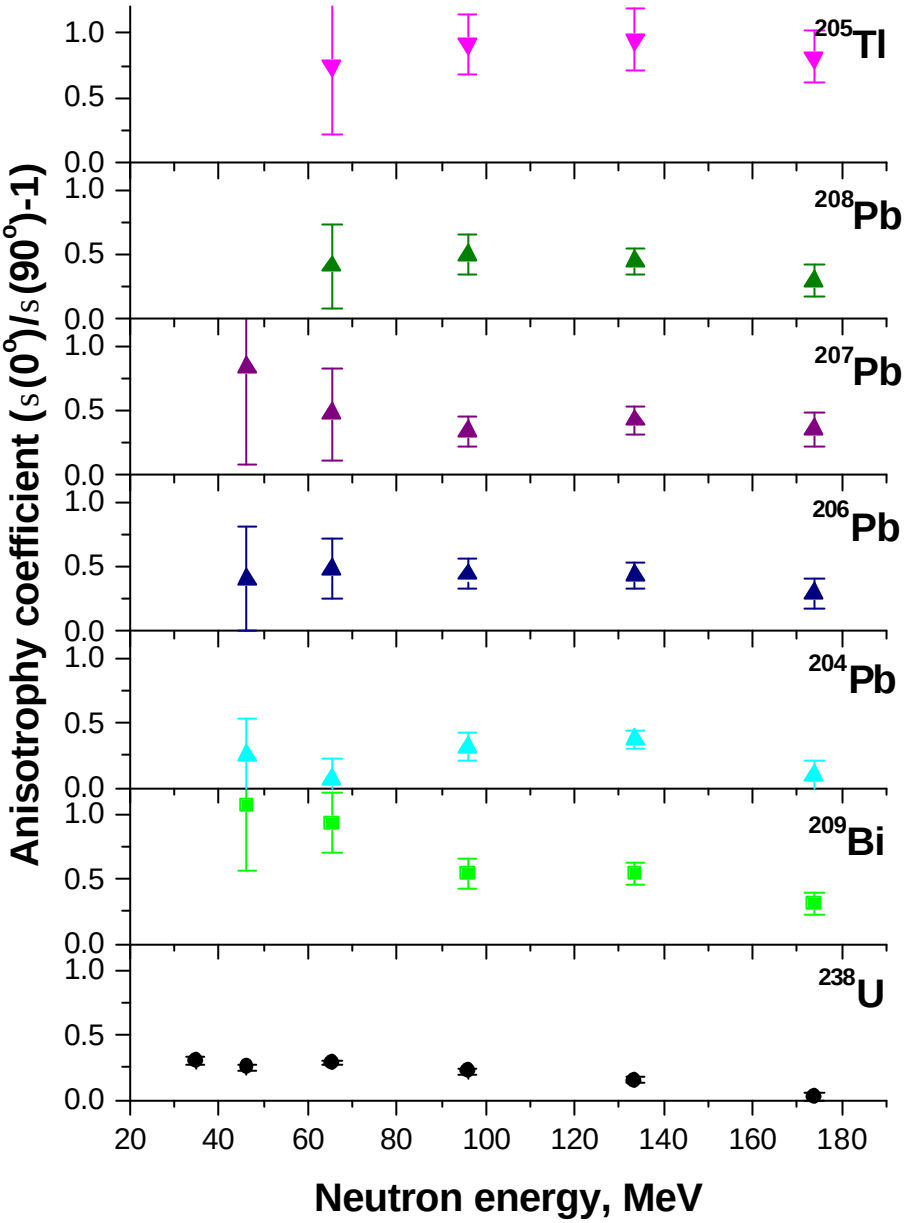


**Fig. 3-11**. Fission anisotropy coefficients of thallium-205, isotopes of lead, bismuth-209 and uranium-238 versus neutron energy. Some points at energy 34.7 and 46.3 MeV are not shown on the diagram.

In Fig. 3-11 it is visible, that like for $^{238}$U nucleus, the anisotropy coefficient for all nuclides decreases with neutron energy and does not depend on a nucleon composition (Z, A) of nuclides in a range from $^{204}$Pb up to $^{209}$Bi in experimental uncertainty limits (~30 %).

All neutron-induced fission anisotropy data are obtained for the first time.

**3.4.2**. Fission fragment angular distributions in proton-induced fission.

As a result of processing of experimental angular distributions of fission fragments for $^{209}$Bi, $^{204,206,207,208}$Pb and $^{205}$Tl at proton energies 49, 98 and 177 MeV the anisotropy factors have been obtained, presented in Table 3-9.

**Table 3-9.** The anisotropy factor for proton-induced fission fragments.

| $E_p$ [MeV] | $^{209}$Bi | $^{204}$Pb | $^{206}$Pb | $^{207}$Pb | $^{208}$Pb | $^{205}$Tl |
|---|---|---|---|---|---|---|
| **48±1** | 0.35±0.05 | 0.42±0.07 | 0.35±0.07 | 0.4±0.1 | 0.35±0.10 | 0.55±0.10 |
| **98±2** | 0.22±0.05 | 0.25±0.1 | 0.4±0.1 | -- | -- | 0.29±0.06 |
| **177.3±1.2** | 0.11±0.05 | 0.15±0.04 | 0.17±0.03 | 0.12±0.03 | 0.17±0.05 | 0.36±0.10 |

The results for $^{209}$Bi and $^{206,207,208}$Pb are shown in the Fig. 3-12 together with earlier results of other authors [37, 39,41, 42, 52]. As it is seen from the figure, results of the present work are in good agreement with the earlier data within stated errors. The data for $^{204}$Pb and $^{205}$Tl have been obtained for the first time.

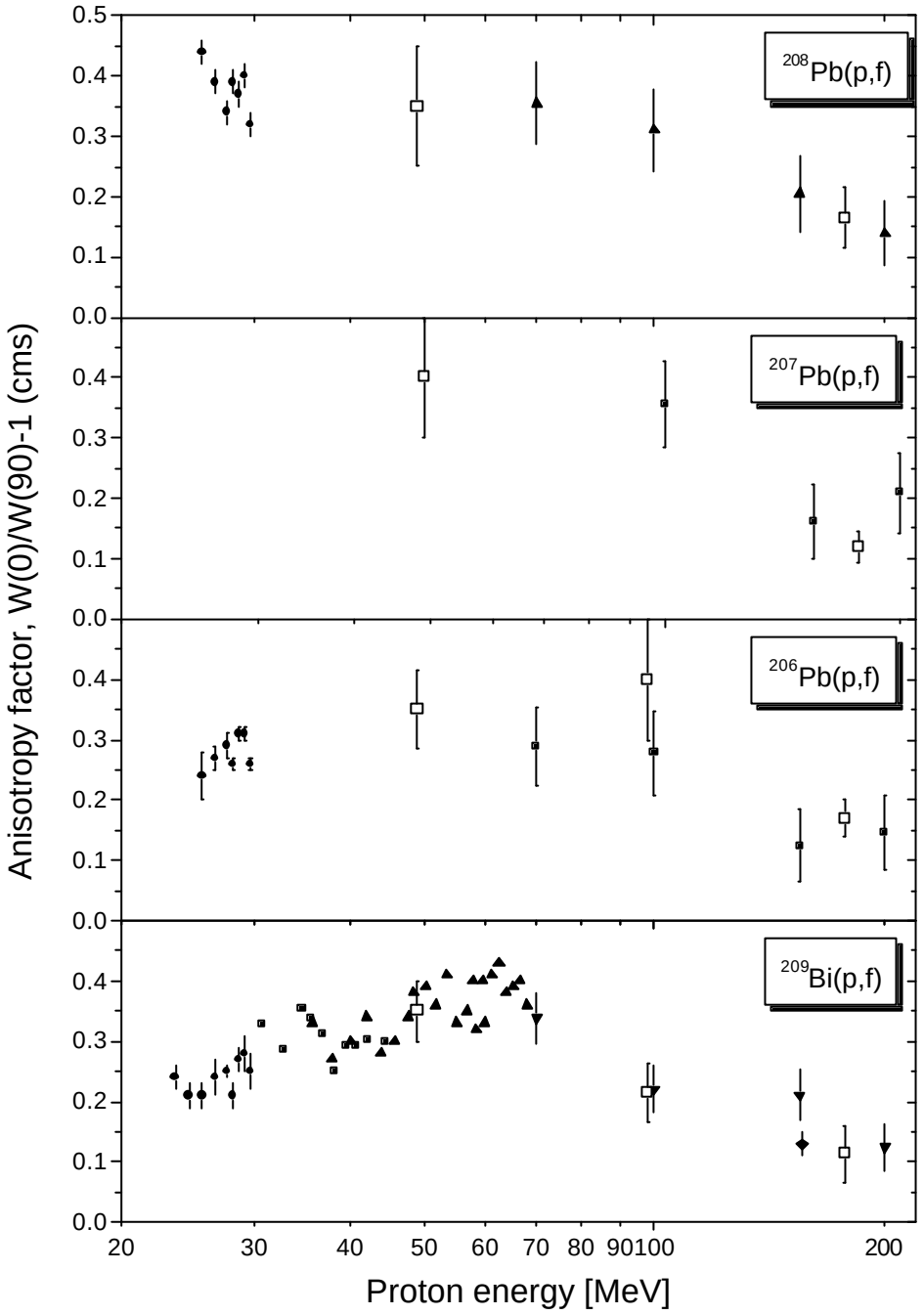


**Fig. 3-12.** Experimental values of the anisotropy factors for proton-induced fission of $^{209}$Bi, $^{206}$Pb, $^{207}$Pb and $^{208}$Pb versus proton energy. Open symbols represent the results of the present work, solid symbols represent the earlier data from [37, 39,41, 42, 52].

All the data are presented in Fig. 3-13.

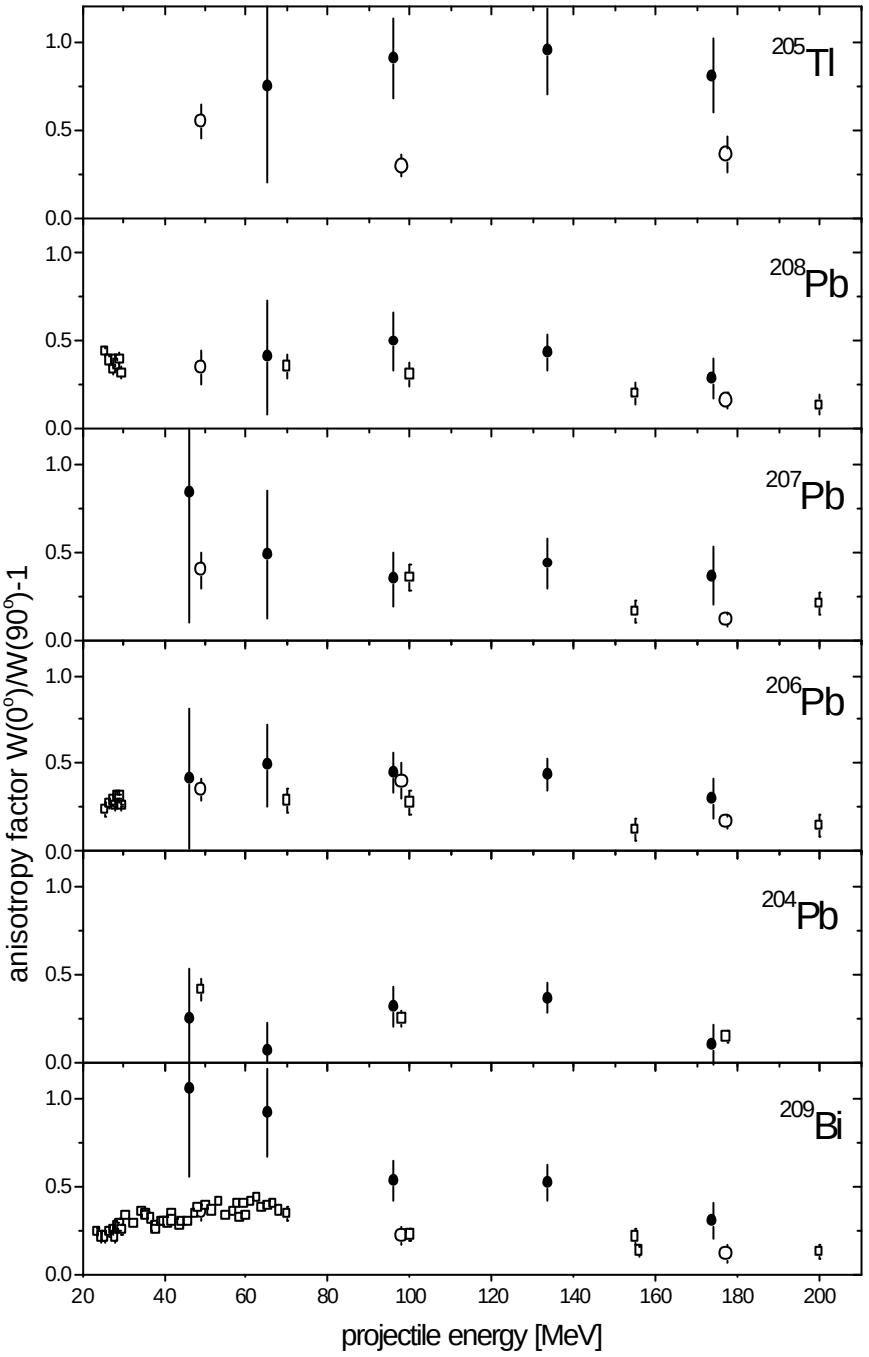


**Fig. 3-13.** Experimental values of the anisotropy factors for neutron- (solid symbols) and proton-induced (open symbols) fission of $^{209}$Bi, $^{206}$Pb, $^{207}$Pb and $^{208}$Pb versus the projectile energy.

**3.4.3.** Comparison of fragment angular distributions in fission induced by protons and neutrons.

According to statistical model of an anisotropy $? = \langle I^2 \rangle / 4JT$, where $\langle I^2 \rangle$ - mean square of an angular momentum of fissioning nucleus in a saddle point, J and ? - effective momentum of inertia and temperature of a nucleus in the same point. One can think, that the angular momentum for nuclei close on a mass number A and, hence, sizes, does not differ from one nucleus to another. Therefore distinction in an anisotropy coefficient of different nuclei can be caused either distinction in temperature ? or in momentum of inertia J. At excitation energies, not too far from the barrier of fission, when emissive fission has a low probability the temperature of nuclei are approximately equal because the difference of their fission barriers, about 5 MeV, is small compare with the excitation energy, ~50 MeV. Calculations [53] indicate, that for investigated nuclei which fissility parameter $Z^2/A$ lies in area of $Z^2/A \sim 32\text{-}34$, the momentum of inertia J in a saddle point also is close to each other. Therefore, small distinction in anisotropy coefficients of different nuclei is not surprising.

Because of distinction in angular momentum brought in by neutrons $\langle I_n^2 \rangle$ and protons $\langle I_p^2 \rangle$ caused by Coulomb barrier V and described by a relation $\langle I_n^2 \rangle / \langle I_p^2 \rangle = E_n/(E_p - V)$, the anisotropy of fission by neutrons can be higher, than for fission by protons. However, as one can see from this expression, the distinction can be appreciable only at small energies of bombarding particles (V~12? ??). Unfortunately, small value of fission cross section at low energies and small intensity of neutron fluxes do not make opportunities to obtain the statistically provided data in this case. It is difficult to explain also distinction observed in anisotropy coefficients on neutrons and protons for $^{209}$Bi and $^{205}$Tl.

### 3.5. Physical aspects of the results.

Physical aspects of the results of the comparison of the proton- and neutron-induced fission cross sections are worded in p. 3.3, a model explanation of the data on angular distributions of the fission fragments is presented in p. 3.4. In this section the physical sense is discussed of the behavior of the cross sections of the lead isotopes and possible conclusions from the experimental data on excitation function about energy dependence of the fission barrier as one of the fundamental parameters of the model.

Double magic nucleus $^{208}$Pb with closed proton (Z=82) and neutron (N=126) shells, being formed in our case in the reaction $^{207}$Pb+n at relatively low energies of the bombarding neutrons (≤50? ??), has the highest fission barrier. However, as it is seen from fig. 3-1, the minimal fission cross section is observed for the $^{208}$Pb(n,f) reaction, i.e. for the composite nucleus $^{209}$Pb. Most probably it is connected with the competition between the fission and emission of neutrons which determines the value of the fission cross section.

$$\sigma_f=\sigma_c\times\Gamma_f/\Gamma_t\approx\sigma_c\times\Gamma_f/\Gamma_n,$$

where $\Gamma_t$, $\Gamma_f$ and $\Gamma_n$ are the total, fission and neutron widths correspondingly. At the medium excitation energies

$\Gamma_f \sim\exp(-B_f/T)$, and

$\Gamma_n\sim\exp(-B_n/T)$, and therefore

$\sigma_f\sim\exp[-(B_f - B_n)/T]$.

The value of the difference of the fission barrier and the bound energy, $B_f - B_n$, changes from 18 to 23 MeV with the increase of the mass of the lead isotope (composite nucleus) from 205 to 209 that explains its lowest cross section. For the bismuth isotopes the difference, $B_f - B_n$, changes by the similar way too. It increases from 13 to 17 MeV for isotopes from ? =205 to ? =209 that explains the minimal value of the cross section observed for $^{208}$Pb+p.

Data on fission of the lead isotopes are of important interest from the point of view of the value of the shell effects. In this range of nuclei the “microscopic” (shell) corrections to the “macroscopic” (liquid-drop) energy of the nucleus have the especial large value: the contribution of the shells to the fission barrier for the double magic nucleus $^{208}$Pb is about 13-14 MeV and approximately equal to the second, liquid-drop component. Each component of the barrier: the shell, $B_{sh}$, and the liquid-drop, $B_{ld}$, depend on the temperature (excitation energy of the nucleus) and their sum determines the dependence of the barrier on the temperature $B_f(T)= B_{sh}(T)+ B_{ld}(T)$.

Dependence of the shell component on temperature, $B_{sh}(T)$, which, as it has been shown in [54], corresponds to the energy dependence of the shell effects in the level density parameter at the barrier, determines the energy dependence of the barrier in the excitation energy range $?^{*} \leq 50$ MeV, while the dependence $B_{ld}(T)$ – at higher energies.

Determination of these dependences from the data on fission cross sections of nuclei in the lead region and their comparison with both the dependence for superheavy nuclei, for which the total barrier is conditioned by the shells, $B_f = B_{sh} \approx 6$ MeV, and for the tungsten isotopes, for which the barrier is clearly liquid-drop, $B_f = B_{ld} \approx 25$ MeV, could be consider as important stage in studying of the nuclear structure.

## 4. Conclusion.

1. The database on the intermediate energy neutron- and proton-induced fission cross section for lead and neighbouring nuclei is widened in considerable power:

- neutron-induced fission cross section of all stable isotopes of lead – 208, 207, 206, and 204 - and $^{205}$Tl are measured for the first time;
- new data on fission cross section of $^{209}$Bi (monoisotope) and $^{nat}$Pb at quasi-monoenergetic neutrons are obtained;
- proton-induced fission cross section of $^{204}$Pb and $^{205}$Tl are measured for the first time using up-to-date level;
- additional data on proton-induced fission cross section of $^{209}$Bi and $^{nat}$Pb are obtained.

2. As a result it can be concluded that for practically important elements being considered as prospective materials for the neutron-production targets of accelerator driven systems (ADS) - $^{nat}$Pb and $^{209}$Bi – in the practically important energy region of bombarding particles, i. e. above 50 MeV, the accuracy is attained of about 10% of determination of the both neutron- and proton-induced fission cross sections, that is satisfactory up-to-date.

3. As a result it can be concluded that new important information is obtained on isotopic dependences of the neutron- and proton-induced fission cross sections, necessary for building of adequate theoretical models, which, in the last analysis, are also directed on the practical application.

The results of detailed comparison of the neutron- and proton-induced fission cross sections will further to development of our conceptions on mechanism of nucleon-nucleus interactions and fission process too.

4. Experimental data on the fission cross sections and fission fragment angular distributions are documented for the presentation in the international data format EXFOR.

5. Measurement of the fission cross section of tungsten and its enriched isotopes using the created setups would be a natural development of the carried out works, that would have both practical (tungsten is one of the elements of neutron-production target of ADS) and theoretical (isotopes of tungsten are in the range of deformed nuclei) importance.

## 5. References.


1. M.Blann et al., OECD/NEA, 1994.
2. R.Michel, P. Nagel, NEA/PT Report ? 14, OECD/NEA, 1997.
3. A.J.Koning, NEA/PT Report ? 4, OECD/NEA, 1992.
4. F. Carminati et al., CERN/AT/93-47 (ET), 1993.
5. J.L. Anderson et al., Nucl. Instr.& Meth. in Phys. Res. A320 (1992) p. 336-367.
6. Y.N. Shubin et al., Proc 2nd Conf. on ADTT, Kalmar, Sweden, June 3 - 7, 1996, p. 953
7. A.D. Carlson, S. Chiba , F.-J. Hambsch, N. Olsson and A.N. Smirnov. IAEA Report INDC (NDC) - 368, Vienna (1997).
8. H. Condé, V. P. Eismont, A. N. Smirnov et al. Proc. 2nd Conf. on ADTT, Kalmar, Sweden, June 3-7, 1996, ed. H. Condé, v.2, p.599
9. A. N. Smirnov, I. Yu. Gorshkov, A. V. Prokofiev, V. P. Eismont. Total and Differential Cross Sections of 10 to 95 MeV Proton-Induced Fission of Actinide Nuclei. - Proc. 21st International Symposium on Nuclear Physics. From Spectroscopic to Chaotic Features of Nuclear Systems. Castle Gaussig, Germany, Nov. 4-8, 1991, pp. 214-222.
10. V.P. Eismont, A.V. Prokofiev, A.N. Smirnov, K. Elmgren, J. Blomgren, H. Condé, J. Nilsson, N. Olsson, T. Rönnqvist, and E. Tranéus. Phys. Rev. C53, 2911 (1996).
11. V. P. Eismont, A. I. Obukhov, A. V. Prokofiev and A. N. Smirnov. Proc. 2nd Conf. on ADTT, Kalmar, Sweden, June 3-7, 1996, pp. 592-598.
12. P. W. Lisowski et al., in Proc. Specialists' Meeting on Neutron Cross Section Standards for the Energy Region above 20 MeV, Uppsala, Sweden, 1991 May 21-23, 1991, OECD/NEA report NEANDC-305 'U', p.177
13. H. Condé, S. Crona, A. Håkansson, O. Jonsson, A. Lindholm, L. Nilsson, P-U. Renberg, G. Tibell, I. Bergqvist and P. Ekström, Can. J. Phys. 65 (1987) 643.
14. O. Jonsson , P.-U. Renberg, A. Prokofiev, and A. Smirnov. TSL Progress Report 1998-1999, ed. A. Ingemarsson, Uppsala University (2000), p. 43.
15. V. P. Eismont (Project Manager), "Measurements of neutron induced fission cross sections in energy region $15<E_n<160$ MeV for basic and applied researches", Final Project Technical Report of ISTC 540-97, V.G.Khlopin Radium Institute, St.-Petersburg, 1999.
16. V. P. Eismont, A. N. Smirnov Thin-film breakdown counters (review). Prybory I tehnika experimenta (Sov. Journ. On Experimental Technique and Devices) No. 6, (1983) 5-9.
17. Yu. P. Gangrskiy, B. Dalhsuren and B.N. Markov. Nuclear fission fragments. Moskow, Energoatomizdat, 1986.
18. V.E. Viola, K. Kwiatkowski, and M. Walker. Phys. Rev. C31, 1550 (1985).
19. L.C. Northcliffe and R.F. Schilling, Nuclear Data Tables, Section A, V.7, N 3-4, January 1970.
20. V. P. Eismont, H. Condé, A. N. Smirnov et.al. Proc. Int. Conf. on Accelerator-Driven Transmutation Technologies and Applications, Praha, Czech Republic, June 7-11, 1999 (CD ROM publication, paper P-23).
21. N. Nakao et al. Nucl. Instr. and Meth. in Phys. Res. A420 (1999) 218; N. Nakao, private communication, 1998..
22. K. Johansson, P. Dyreklev, B. Granbom, N. Olsson, J. Blomgren, and P.-U. Renberg. - IEEE Transactions on Nuclear Science I 45, 2195 (1998)
23. A. Michalowicz. Cinématique des réactions nucléaires, Paris, 1964.
24. G.A. Tutin, I.V. Ryzhov, V.P. Eismont, A.V. Kireev, H. Condé, K. Elmgren, N. Olsson, P.-U. Renberg, "An ionization chamber with Frisch grids for studies of

high-energy neutron-induced fission", *Nucl. Instr. and Meth.* **A457,** No 3, (2001) pp.646-652.
25. V.P. Eismont, A.V. Kireev, I.V. Ryzhov, G.A. Tutin, H. Condè, K. Elmgren and S. Hultqvist; "Measurement of the neutron-induced fission cross sections of $^{209}$Bi at 45 and 73 MeV", *Proceedings of the 2nd International Conference on Accelerator Driven Transmutation Technologies and Applications*, Kalmar, Sweden, 3-7 June 1996, ed. Henri Condè, Uppsala University, vol. 2, pp. 618-623, (1997).
26. V.P. Eismont, A.V. Kireev, I.V. Ryzhov, S.M. Soloviev, G.A. Tutin, H. Condè, K. Elmgren, N. Olsson, and P.-U. Renberg; "Neutron-induced fission cross section ratios of $^{209}$Bi to $^{238}$U at 75 and 96 MeV," *Proceedings of the 3rd International Conference on Accelerator Driven Transmutation Technologies and Applications*, Praha, Czech Republic, 7-11 June 1999, (available as CD-ROM, paper Mo-O-C7) (1999).
27. Staples, P.W. Lisowski, and N.W. Hill, "Fission cross section ratios of $^{nat}$Pb and $^{209}$Bi relative to $^{235}$U for neutron energies from threshold to 400 MeV", *Presented in APS/AAPT Conference*, Washington, April 18-21, 1995; *Bull. Am. Phys. Soc.* **40**, 962 P. (1995); Updated data, Private communication by P. Staples (1996).
28. O. Shcherbakov, A. Donets, A. Evdokimov, A. Fomichev, T. Fukahori, A. Hasegawa, A. Laptev, V. Maslov, G. Petrov, S. Soloviev, Y. Tuboltsev and A. Vorobyev, "Neutron-induced fission of $^{233}$U, $^{238}$U, $^{232}$Th, $^{239}$Pu, $^{237}$Np, $^{nat}$Pb and $^{209}$Bi relative to $^{235}$U in the energy range 1-200 MeV", *Journal of Nuclear Science and Technology*, Supplement 2, August 2002, pp.230-233, Proceedings of the International Conference on Nuclear Data for Science and Technology, October 7-12, 2001, Tsukuba, Japan, vol.1.
29. P.E. Vorotnikov and L.S. Larionov, "Cross sections for neutron fission of Pb and Bi," *Yad. Fiz.*, **40**, 867 (1984); *Sov. J. Nucl. Phys.*, **40**, 552 (1984).
30. R. Nolte, M.S. Allie, P.J. Binns, F.D. Brooks, A. Buffler, V. Dangendorf, K. Langen, J.-P. Meulders, W.D. Newhauser, F. Ross and H. Schuhmacher, "Measurement of $^{235}$U, $^{238}$U, $^{209}$Bi and $^{nat}$Pb fission cross sections using quasi-monoenergetic neutrons with energies from 30 MeV to 150 MeV", *Journal of Nuclear Science and Technology*, Supplement 2, August 2002, pp.311-314, Proceedings of the International Conference on Nuclear Data for Science and Technology, October 7-12, 2001, Tsukuba, Japan, vol.1.
31. I.V. Ryzhov, G.A. Tutin, V.P. Eismont, A. Mitryukhin, V. Oplavin, S. Soloviev, H. Condé, N. Olsson, P.-U. Renberg, "Measurements of Neutron-Induced Fission Cross Sections of Pb and Bi at Intermediate Energies"; *Journal of Nuclear Science and Technology*, Supplement 2, August 2002, pp.1410-1413, Proceedings of the International Conference on Nuclear Data for Science and Technology, October 7-12, 2001, Tsukuba, Japan, vol.2.
32. O.E. Shigaev, V.S. Bychenkov, M.F. Lomanov, A.I. Obukhov, N.A. Perfilov, G.G. Shimchuk, and R. M. Yakovlev, V.G. Khlopin Radium Institute, Preprint RI-17 (1973) (in Russian).
33. E.V. Beljaikin, S.P. Borovlev, M.F. Lomanov, V.E. Lukjashin, Yu.E. Titarenko, and G.G. Shimchuk, presented at the Workshop of ISTC Project #17, February 5-8, 1996, Saint-Petersburg, Russia; Yu.E. Titarenko, private communication.
34. C. Stephan, F. Maury, J. Peter, and H. Langevin-Joliot, Institut de Physique Nucleaire, Facultes des Sciences de Paris, et d'Orsay, p. 13 (1965).
35. H.M. Steiner and J.A. Jungerman, Phys. Rev. 101 (1956) 807.
36. M. Maurette and C. Stephan, Proc. IAEA Conf. on Physics and Chemistry of Fission, Salzburg, Austria, 22-26 March, 1965, v. 2, p. 307.
37. L. Kowalski and C. Stephan, J. de Physique 24 (1963) 901.

38. M.C. Duijvestijn, A.J. Koning, J.P.M. Beijers, A. Ferrari, M. Gastal, J. van Klinken, and R.W. Ostendorf, Phys. Rev. C59 (1999) 77.
39. V.N. Okolovich, O.A. Zhukova, M.G. Itkis, and S.I. Mulgin, Institute of Nuclear Physics, Kazakhstan Academy of Sciences, Preprint P-112, Alma-Ata, 1974 (in Russian).
40. Khodai-Joopari, Ph. D. thesis, UCRL-16489, Berkeley, 1966.
41. A.V. Ignatyuk, M.G. Itkis, I.A. Kamenev, S.I. Mulgin, V.N. Okolovich, and G.N. Smirenkin, Yadernaya Fizika 40 (1984) 625 (in Russian); Sov. J. Nucl. Phys. 40 (1984) 400.
42. E. Gadioli, I. Iori, N. Molho, and L. Zetta, Lettere Al Nuovo Cimento 2 (1969) 904.
43. A.V. Prokofiev. Compilation and Systematics of Proton-Induced Fission Cross Section Data. - In: Nucl. Instr. and Meth. A, Special Issue on Accelerator Driven Systems, Ed. H.S. Plendl, in press
44. V.P. Eismont, A.V. Prokofiev and A.N. Smirnov, "Cross sections of intermediate energy proton induced fission of heavy nuclei and fissility of exited nuclei", Proc. Int. Conf. on Nuclear Data for Science and Technology, Gatlinburg, Tenessee, USA, May 9-13, 1994, ed. J.K. Dickens, ANS, USA, 1994, v.1, p. 397
45. V. P. Eismont, "Nuclear data for accelerator transmutation of radioactive waste", Proc. Intern. Conf. on Nuclear Spectroscopy and Nuclear Structure, S-Petersburg, June 1995, Izv. Akademii Nauk (in Russian). v. 60, p. 2
46. V. P. Eismont, A. A. Rimski-Korsakov, A. N. Smirnov et al. "Up-to-date status of data on nucleon induced fission cross section of heavy nuclei at intermediate energies", Proc. Int. Conf. on Nuclear Data for Science and Technology, Trieste, Italy, May 19 - 24, 1997, v.59, part 1, p.681
47. V. P. Eismont, A. A. Rimski-Korsakov and A. N. Smirnov. "Fission cross sections of heavy nuclei at intermediate energies for hybrid nuclear technologies". Proc. Int. Conf. on Future Nuclear Systems - GLOBAL'97, October 5-10 1997, Yokohama, Japan , p. 1365-1370
48. V. P. Eismont, H. Condé, A. N. Smirnov et al. "Fission cross sections of lead and heavier nuclei for accelerator transmutation", Proc. 9th International Conference on Emerging Nuclear Energy Systems, Tel-Aviv, Israel, June 28- July 2, 1998, v.2, p.753.
49. V. P. Eismont, H. Condè, A. N. Smirnov et. "Up-to-date status a nd problems of the experimental nucleon-induced fission cross section data base at intermediate energies". Proc. Int. Conf. on Accelerator-Driven Transmutation Technologies and Applications, Praha, Czech Republic, June 7-11, 1999 (CD ROM publication, paper P-23).
50. V. E. Bunakov, L. V. Krasnov and A. V, Fomichev. "Possible explanation of the difference in nuclear fission induced by the intermediate energy protons and neutrons". European Physical Journal A8, 447-450 (2000) European Physical Journal A8, 447-450 (2000)
51. V. M. Maslov, Yu. V. Porodzinskij and A. Hasegava. "Actinide nucleon-induced fission reactions up to 150 MeV". In "Neutron Spectroscopy, Nuclear Structure, Related Topics" Proc. VIII International seminar on Interactions of Neutrons with Niclei. Dubna, May 17-20, 2000, p. 277-287.
52. V.S. Bychenkov, M.F. Lomanov, AI. Obukhov, N.A. Perfilov, O.E. Shigaev, G.G. Shimchuk, and R.M. Yakovlev. Sov. J. Nucl. Phys. (1974) 17, 496.
53. V.M. Strutinskiy, Yadernaya Phisika (in Russian) (1965) 1, 221
54. A.S. Zubov, G.G. Adamian, N.V. Antonenko, S.P. Ivanova and W. Scheid. "Survival probability of superheavy nuclei". Phys. Rev. C, V65, p.024308.

## 6. List of published articles with resumes.

### 1. "Measurement and Comparison of Proton- and Neutron-Induced Fission Cross-section of Lead and Neighboring Nuclei in the 20-200MeV Energy Region for Improvement of Nuclei Models and Concepts of Accelerator Driven Systems".

[1]V.P. Eismont, [1]A.G. Mitryukhin, [1]V.S. Oplavin, [1]I.V. Ryzhov, [1]A.N. Smirnov, [1]S.M. Solovjev, [1]G.A. Tutin, [2]H. Condè, [2]N. Olsson, [3]O. Jonson, [3]P.-U. Renberg.

*[1]V.G. Khlopin Radium Institute, Saint-Petersburg, Russia*

*[2]Department of Neutron Research, Ångström Laboratory, Uppsala University, Uppsala, Sweden*

*[3]The Svedberg Laboratory, Uppsala University, Uppsala, Sweden*

Unique possibilities of TSL - producing not only intermediate energy proton beams, but neutron ones too - were used in this work for the measurements and comparison of proton and neutron fission cross sections. The motivation for such measurements is our previous revealing of the difference between proton and neutron cross sections and their dependence on the fissility parameter [1,2]. These facts could not be explained by coulomb repulsion. It was especially interesting to study these effects in reactions with separated isotopes of lead and isotopes near lead, i.e. nuclei with closed neutron and proton shells ($^{208}$Pb) and near they. The results may bring new tests nuclear reaction and fission models. This region of nuclei and energies is also of the interest of the ADS applications.

TSL Progress Report 2000-2001 Ed. A. Ingemarsson, Uppsala University (2002), p. 42.

### 2. "An ionization chamber with Frisch grids for studies of high-energy neutron-induced fission".

[1]G.A. Tutin, [1]I.V. Ryzhov, [1]V.P. Eismont, [1]A.V. Kireev, [2]H. Condé, [2]K. Elmgren, N. Olsson, [3]P.-U. Renberg.

*[1] V.G. Khlopin Radium Institute, Saint-Petersburg, Russia*

*[2] Department of Neutron Research, Uppsala University, Uppsala, Sweden*

*[3] The Svedberg Laboratory, Uppsala University, Uppsala, Sweden*

A gridded ionization chamber for fission fragment detection is described. The chamber has been specially designed for use at the quasi-monoenergetic $^{7}$Li(p,n) neutron source at the The

Svedberg Laboratory, Uppsala, Sweden. The detector permits measurements of fission fragment energy and emission angle for two targets with diameter of up to 10 cm. The time response of the chamber (≤5 ns FWHM) is adequate to apply time-of-flight discrimination against background events induced by non-peak neutrons. Results of angular anisotropy measurements for the $^{232}$Th (n,f) and $^{238}$U(n,f) reactions in the 20-160 MeV energy range are given.

Nuclear Instruments and Methods in Phys. Res., A 457(2001), p. 646.

## 7. List of published reports made at conferences and workshops with resumes.

**1. "Proton- and Neutron-Induced Fission Cross Sections and Fission Probability in the Intermediate Energy Region".**

[1]A.N. Smirnov, [1]V.P. Eismont, [1]I.V. Ryzhov, [2]H. Condè, [2]N. Olsson, [3]P.-U. Renberg [3] and [3]A.V. Prokofiev.

*[1]V.G. Khlopin Radium Institute, , Saint-Petersburg, Russia*

*[2]Department of Neutron Research, Ångström Laboratory, Uppsala University, Uppsala, Sweden*

*[3]The Svedberg Laboratory, Uppsala University, Uppsala, Sweden*

New results are presented of the intermediate energy neutron- and proton-induced fission cross sections of nuclei in the lead region. These results, together with earlier ones, are used for comparison of the fission probability of nuclei induced by protons and neutrons. Possible physical reasons of observed differences in proton- and neutron-induced fission cross sections are discussed .

Journal of NUCLEAR SCIENCE and TECHNOLOGY, Supplement 2. Proc. of Intern Conf. On Nuclear Data in Science and Technology 7-12 Oct, 2001, Tsukuba, Ibaraki, Japan, ed. K. Shibata, Atomic Energy Society of Japan, Japan Atomic Energy Research Institute vol. 1, p. 238.

**2. "Measurements of Neutron-Induced Fission Cross Sections of Pb and Bi at Intermediate Energies".**

[1]I.V. Ryzhov, [1]G.A., Tutin, [1]V.P. Eismont, [1]A.G. Mitryukhin, [1]V.S. Oplavin, [1]S.M. Solovjev, [2]H. Condè, [2]N. Olsson and [3]P.-U. Renberg.

[1]*V.G. Khlopin Radium Institute, Saint-Petersburg, Russia*

[2]*Department of Neutron Research, Ångström Laboratory, Uppsala University, Uppsala, Sweden*

[3]*The Svedberg Laboratory, Uppsala University, Uppsala, Sweden*

Neutron-induced fission cross sections of $^{nat}$Pb and $^{209}$Bi have been measured relative to the $^{238}$U(n.f) cross section at energies 96 MeV for lead and 133 MeV for bismuth. The measurements were performed at the quasi-monoenergetic neutron beam facility of The Svedberg Laboratory in Uppsala using Frisch-gridded ionization chamber. The results obtained are compared with other experimental data. The present state of the Bi standard recommended by IAEA is discussed.

Journal of NUCLEAR SCIENCE and TECHNOLOGY, Supplement 2. Proc. of Intern Conf. On Nuclear Data in Science and Technology 7-12 Oct, 2001, Tsukuba, Ibaraki, Japan, ed. K. Shibata, Atomic Energy Society of Japan, Japan Atomic Energy Research Institute vol. II, p 1410.

**3. "Angular Anisotropy of Nucleon-Induced Fission of Heavy Nuclei at Intermediate Energies".**

[1]V. P. Eismont, [1]I. V. Ryzhov, [1]G. A. Tutin, [2]H. Condè, [2]N. Olsson.

*1V.G. Khlopin Radium Institute, , Saint-Petersburg 194021, Russia*

*2Department of neutron research, Angström Laboratory, Uppsala University, Uppsala, Sweden*

In the frame of the statistical model a semi-empirical description of the angular anisotropy of fission fragments induced by intermediate energy nucleons is given. The dependence of angular anisotropy on nucleon energy and the fissility parameter of the composite nucleus, the temperature of the fissioning nucleus at the transition state and the role of nonstatistical effects are discussed.

Journal of NUCLEAR SCIENCE and TECHNOLOGY, Supplement 2. Proc. of Intern Conf. On Nuclear Data in Science and Technology 7-12 Oct, 2001, Tsukuba, Ibaraki, Japan, ed. K. Shibata, Atomic Energy Society of Japan, Japan Atomic Energy Research Institute vol. 1, p. 299.

**4. "Fragment Angular Anisotropy in the $^{232}$Th(n,f) and $^{238}$U(n,f) Reactions at Intermediate Energies".**

[1]I.V. Ryzhov, [1]G.A. Tutin, [1]V.P. Eismont, [2]M.S. Onegin, [3]H. Condé and [3]N. Olsson.

[1]*V.G. Khlopin Radium Institute, 2oi Murinsky Prospect 28, Saint-Petersburg 194021, Russia*

[2]*Petersburg Nuclear Physics Institute of Russian Academy of Science, Leningrad district, Gatchina 188350, Russia*

[3]*Department of Neutron Research, Ångström Laboratory, Uppsala University, Box 525, S-751 20 Uppsala, Sweden*

Results of fragment angular anisotropy measurements are given for the $^{232}$Th (n,f) and $^{238}$U (n,f) reactions in the energy range 20-160 MeV. The energy dependence of the anisotropy is calculated in the context of the Halpern-Strutinsky's formalism. The observed difference in the fragment anisotropy of $^{232}$Th and $^{238}$U is discussed.

Journal of NUCLEAR SCIENCE and TECHNOLOGY, Supplement 2. Proc. of Intern Conf. On Nuclear Data in Science and Technology 7-12 Oct, 2001, Tsukuba, Ibaraki, Japan, ed. K. Shibata, Atomic Energy Society of Japan, Japan Atomic Energy Research Institute vol. 1, p 295.

**5. "Intermediate Energy Neutron Induced Fission Cross Sections for Perspective Neutron Production Target in ADS".**

[1]A.N. Smirnov, [1]V.P. Eismont, [1]A.V. Prokofiev, [1]I.V. Ryzhov, [1]G.A. Tutin, [2]H. Conde, [2]N. Olsson.

[1]*V.G. Khlopin Radium Institute – Russia,*

[2]*Department of Neutron Research, Uppsala University – Sweden.*

Up-to-date status is considered of the experimental database on neutron-induced fission cross sections of tantalum, tungsten, lead, mercury, gold and bismuth nuclei in the neutron energy range from the fission threshold to 175 MeV. Most of the listed elements are either already used or considered as potential candidates for neutron production target materials in accelerator driven systems (ADS). Data on gold are included because of their methodical and theoretical importance.

Recently published preliminary results, obtained at the quasi-monoenergetic neutron beam facility of The Svedberg Laboratory of the Uppsala University are analyzed. Necessary corrections have been introduced on the neutron spectrum and fission excitation function shapes. Comparative analysis is carried out of the results obtained for the $^{209}$Bi(n,f) cross

section with the use of two different techniques: thin film breakdown counters (TFBC) and a twin Frish-gridded ionisation chamber (TFIC), at the same neutron beam facility. The results for $^{209}$Bi, natPb and $^{197}$Au are compared also with the data obtained earlier at the white neutron source in Los Alamos.

At present, our results are the basis of the considered (n,f) cross section experimental database. Experimental data sets are presented as fission excitation functions of the corresponding nuclides. The data sets are parameterized for the use in engineering calculations.

The perspective of creating a more complete database is discussed, including (n,f) cross sections for separated isotopes of lead and tungsten, in particular $^{208}$Pb(n,f) and $^{184}$W(n,f). These nuclei are included in the High Priority Request List of nuclear data for the nucleon energy region up to 200 MeV. The data are needed for development of adequate nuclear fission models, as well as computer codes for ADS.

The necessity is noted of fission cross section measurements for the above mentioned nuclides, not only with neutrons, but also protons, in the same projectile energy region. These proton induced fission cross section measurements are of interest for both applied and basic research in a comparison with (n,f) cross sections, with the goal of creating a common data base built on a general physical basis.

Sixth Information Exchange Meeting on Actinide and Fission Product Partitioning and Transmutation, Madrid, Spain, 11-13 December,2000, OECD-NEA(NDS), p.117 and CD ROM publication: paper P-36.

**6. "Nucleon-Induced Fission Cross Sections for ADS Needs".**

[1]V.P. Eismont, [1]N.P. Filatov, [1]I.V. Ryzhov, [1]A.N. Smirnov, [1]G.A. Tutin, [2]J. Blomgren, [2]H. Condé, [2]N. Olsson.

[1] *V.G. Khlopin Radium Institute, Saint-Petersburg, Russia*

[2] *Department of Neutron Research, Uppsala University, Sweden*

A program for the development of the experimental nucleon-induced fission cross section data base at the intermediate energies (20-200 MeV) is implemented by the KRI-UU collaboration in frame of the successive ISTC projects. The fission cross section measurements and systematization are carried out for nuclei from the high priority request list for ADS needs.

At the 6$^{th}$ Information Exchange Meeting (Madrid, 2000) we presented our results on the (n,f) cross section measurements for nuclei of Ta, W, Hg, Pb and Bi, which are considered now as the most prospective materials for neutron-producing target. The present report is mainly devoted to both proton- and neutron-induced fission cross section measurements, which have

been performed not only for natural lead, but also for its partitioned isotopes: $^{204}$Pb, $^{206}$Pb, $^{207}$Pb, $^{208}$Pb. The data on partitioned isotopes are of prime interest for the conceptual analysis of ADS, because they form the most credible basis for validation of dedicated nuclear reaction models. The data on lead isotopes are of particular interest, because these isotopes constitute the isotope chain opening up the unique opportunity to study the neutron shell effects when one approaches the double magic nucleus $^{208}$Pb (Z=82, N=126). These effects play an important role in the intermediate energy fission of nuclei in the vicinity of lead and should be taken into account for the adequate modeling. Also a comparison of (p,f) and (n,f) cross sections is of practical and theoretical interest. Our previous experiments revealed that the proton-induced fission cross sections are significantly higher (by factors) than the neutron-induced ones in the incident energy (E) region, where the Coulomb factor 1-V/E (V is Coulomb barrier) is close to 1. The (p,f) to (n,f) cross section ratio increases strongly with decreasing of the fissility parameter of target nucleus. This fact has to be taken into consideration if one wants to calculate the nuclear reactions in the neutron-producing target. The reason for this difference should be interpreted in frame of the reaction models either as a peculiarity of input reaction channel (optical potential) or as a characteristic of output channel (competition between neutron and fission widths). The data to be presented for the partitioned isotopes of lead may give the key information in this respect.

Seventh Information Exchange Meeting on Actinide and Fission Product Partitioning and Transmutation, Jeju, Korea, October 14-16, 2002, program and abstracts, p. 153.

## Application.

Results on fission cross section and fission fragment angular distributions prepared for the data EXFOR format.

RESULTS OF THE MEASUREMENT FISSION CROSS SECTIONS AND ANGULAR DISTRIBUTION OF FISSION FRAGMENTS DOCUMENTED FOR PRESENTATION IN EXFOR

```
ENTRY            ONNN1   20021015                                    ONNN100000001
SUBENT        0NNN1001   20021015                                    ONNN100100001
BIB                12         25                                    ONNN100100002
TITLE       MEASUREMENT AND COMPARISON OF PROTON AND NEUTRON         ONNN100100003
            INDUCED FISSION CROSS SECTION OF LEAD AND NEIGH          ONNN100100004
            BOURING NUCLEI IN THE 20-200 MEV ENERGY REGION           ONNN100100005
AUTHOR      (V.P.EISMONT,G.N.TUTIN,A.N.SMIRNOV,I.V.RIZHOV,           ONNN100100006
            V.S.OPLAVIN, S.M.SOLOVIEV)                               ONNN100100007
INSTITUTE   (4RUSRI,02)                                              ONNN100100008
REFERENCE   (PROG,1309,9,ISTC,20020203)INTERNATIONAL SCIENCE         ONNN100100009
            AND TECHNOLOGY CENTRE                                    ONNN100100010
REL-REF                                                              ONNN100100011
FACILITY    (CICLO,2SWDUPP) GUSTAV WERNER CYCLOTRON AT THE           ONNN100100012
            SWEDBERG LABORATORY,TSL),UPPSALA UNIVERSITY              ONNN100100013
COMMON             3          6                                      ONNN100100014
E                          ONNN100100015
MEV                                                                  ONNN100100016
180         P,30-180 MEV, FLUX DENSITY 10+5-10+6 CM2/SEC             ONNN100100017
INC-SOURSE  (P-LI7) 4-15 MM THICK LITHIUM TARGET, 7-LI-99.98%        ONNN100100018
            FLUX DENSITY (1-3)*10+5 CM2/SEC                          ONNN100100019
METHOD      (FISCT)(TOF)                                             ONNN100100020
ENDCOMMON          6                                                 ONNN100100021
DETECTOR    (FISCH), REACTION CHAMBER                                ONNN100100022
            (IOCH) MULTISECTION FRICSH-GRIDDED IONISATION CHAMBER    ONNN100100023
            (THRES),THIN FILM BREAKDOWN COUNTERS OF FISSION          ONNN100100024
            FRAGMENTS.                                               ONNN100100025
HISTORY     (20020507C) ++Compiled at the center –Cjd++              ONNN100100026
            (20020507U)                                              ONNN100100027
ENDBIB             25                                                ONNN100100028
ENDSUBENT          29                                                ONNN100199999
SUBENT        0NNN1002   20021015                                    ONNN100200001
BIB                10         25                                    ONNN100200002
INC-SOURCE  FLUX QUASI-MONOENERGETIC NEUTRONS AT THE POSITIONS       ONNN100200003
            OF FISILE TARGETS,10-12 M FROM THE LITIUM TARGET,        ONNN100200004
            WAS ABOUT 10+6 N/SEC; DURATION OF PULSE WAS 3-6 NSEC     ONNN100200005
DETEKTOR    MULTISECTION FRICSH-GRIDDED IONISATION CHAMBER           ONNN100200006
SAMPLE      VACUUM EVAPORATED ON 50 MK THICK AL-FOILS                ONNN100200007
            82-PB-204,66.5%; 82-PB-206,90.4%;82-PB-207,93.2%         0NNN10O2OO008
            99.0 %;81-TL-205,99.8%; 83-BI-209,100%                   ONNN100200009
          92-U-238,99.3 % DIAMETR ALL TARGETS WERE 80 MM.          ONNN100200010
            PB,TL,BI,-METAL,U-CMP(UF4),U-METAL                       ONNN100200011
PART-DET    (FF)                                                     0NNN100200012
MONITOR     ((MONIT)((92-U-238(NF))                                  ONNN100200013
MONIT-REF   (A.D.KARLSON AT ALL,INDC(NDS)-368 (199704)               0NNN100200014
ANALYSIS    (INTAD INTED)                                            ONNN100200015
CORRECTION  PERFORMED:ANISOTROPY OF FISSION,LINEAR MOMENTUM          ONNN100200016
            TRANSFER FROM THE FISSIONING INCIDENT PARTICLE TO THE    ONNN100200017
            NUCLEUS,SELF-ABSORBTION IN THE TARGET LAYER,ALTERATION   ONNN100200018
            FLUX DENSITY ALONG CHAMBER,ISOTOP ABUDANSE OF TARGET,    ONNN100200019
            TARGET MASS,                                             ONNN100200020
            NEGLIGIBLE: IMPURITY OTHER ELEMENTS IN SAMPLE,           ONNN100200021
ERR-ANALYS  (ERR-S) THE CONTRIBUTION ARE NEGLIGIBLE FROM             ONNN100200022
            NEUTRON BEAM PROFILE DATA,UNHOMOGENOUS OF TARGETS        ONNN100200023

STATUS      (TABLE)(PRELM)                                           ONNN100200024
ENDBIB             24                                                ONNN100200025
```

```
NOCOMMON                                                                ONNN100200026
ENDSUBENT           27                                                  ONNN100299999
SUBENT        ONNN1003   20021015                                       ONNN100300001
BIB                 1          1                                       ONNN100300002
REACTION   ((81-TL-205(N,F),,SIG))/(92-U-238(N,F),,SIG))               ONNN100300003
ENDBIB              1                                                   ONNN100300004
COMMON                                                                  ONNN100300005
           FISSION CROSS SCTION RATIO * 1E-3                            ONNN100300006
ENDCOMMON                                                               ONNN100300007
DATA                                                                    ONNN100300008
EN         DATA       ERR-S                                            ONNN100300009
MEV        NO-DIM     NO-DIM                                           ONNN100300010
       34.7      0.015      0.010                                       ONNN100300011
       65.4       0.63       0,04                                       ONNN100300012
       96.0       3.35       0.15                                       ONNN100300013
      133.6       6.00       0.40                                       ONNN100300014
      173.9       8.5        1.10                                       ONNN100300015
ENDDATA             8                                                   ONNN100300016
ENDSUBENT          13                                                   ONNN100399999
SUBENT        ONNN1004   20021015                                       ONNN100400001
BIB                 1          1                                       ONNN100400002
REACTION  ((82-PB-204(N,F),,SIG)/(92-U-238(N,F),,SIG))                 ONNN100400003
ENDBIB              1                                                   ONNN100400004
NOCOMMON                                                                ONNN100400005
DATA                3          4                                       ONNN100400006
EN         DATA       ERR-S                                            ONNN100400007
MEV        NO-DIM     NO-DIM                                           ONNN100400007
       34.7       0.29       0.07                                       ONNN100400008
       46.3       1.58       0.09                                       ONNN100400009
       65.4       7.20       0,30                                       ONNN100400010
       96.0      21.60         1.                                       ONNN100400011
      133.6       35.2        1.9                                       ONNN100400012
      173.9       47.0        2.7                                       ONNN100400013
ENDDATA             8                                                   ONNN100400014
ENDSUBENT          13                                                   ONNN100499999
SUBENT        ONNN1005   20021015                                       ONNN100500001
BIB                 1          1                                       ONNN100500002
REACTION  ((82-PB-206(N,F),,SIG)/( 92-U-238(N,F),,SIG))                ONNN100500003
ENDBIB                                                                  ONNN100500004
NOCOMMON                                                                ONNN100500005
DATA                3          4                                       0NNN100500006
EN         DATA       ERR-S                                            ONNN100500007
MEV    NO-DIM   NO-DIM                  ONNN100500008
       34.7       0.05       0.02                                       ONNN100500009
       46.3       0.47       0.04                                       ONNN100500010
       65.4       2.99       0,12                                       ONNN100500011
       96.0       10.4        0.4                                       ONNN100500012
      133.6       17.8        1.0                                       ONNN100500013
      173.9       28.8        1.8                                       ONNN100500014
ENDDATA             8                                                   ONNN100500015
ENDSUBENT          12                                                   ONNN100599999
SUBENT        ONNN1006   20021015                                       ONNN100600001
BIB                 1          1                                       ONNN100600002
REACTION  ((82-PB207(N,F),,SIG)/(92-U-238(N,F),,SIG))                  ONNN100600003
ENDBIB             1                                                    ONNN100600004
NOCOMMON                                                                ONNN100600005



DATA               3          4                                       ONNN100600006
EN         DATA       ERR-S                                            ONNN100600007
```

```
MEV        NO-DIM     NO-DIM                                                ONNN100600008
       34.7       0.02       0.01                                          ONNN100600009
       46.3       0.31       0.03                                          ONNN100600010
       65.4       2.10       0,10                                          ONNN100600011
       96.0       7.90        0.3                                          ONNN100600012
      133.6       13.7        0.8                                          ONNN100600013
      173.9     26.3          1.3                                          ONNN100600014
ENDDATA             8                                                      ONNN100600015
ENDSUBENT          12                                                      ONNN100699999
SUBENT        ONNN1007   20021015                                          0NNN100700001
BIB                 1          1                                          0NNN100700002
REACTION  ((82-PB-208(N,F),,SIG)/ (92-U-238(N,F),,SIG))                   0NNN100700003
ENDBIB              1                                                      0NNN100700004
NOCOMMON                                                                   0NNN100700005
DATA                                                                       ONNN100700006
EN         DATA       ERR-S                                               ONNN100700007
MEV        NO-DIM     NO-DIM                                              ONNN100700008
       34.7       0.02       0.01                                          ONNN100700009
       46.3       0.31       0.03                                          ONNN100700010
       65.4       2.10       0,10                                          ONNN100700011
       96.0       7.90        0.3                                          ONNN100700012
      133.6       13.7        0.8                                          ONNN100700013
      173.9       26.3        1.3                                          ONNN100700014
ENDDATA             8                                                      ONNN100700015
ENDSUBENT          12                                                      ONNN100799999
SUBENT        0NNN1008   20021015                                          0NNN100800001
BIB                                                                        ONNN100800002
REACTION   ((81-TL-205(N,F),,SIG))                                         ONNN100800003
ENDBIB                                                                     ONNN100800004
NOCOMMON                                                                   ONNN100800005
DATA                                                                       ONNN100800006
EN         DATA       ERR-S                                               ONNN100800007
MEV        MB           MB                                                ONNN100800008
       34.7      0.025      0.017                                         ONNN100800009
       46.3          -          -                                         ONNN100800010
       65.4       0.97       0,08                                         ONNN100800011
       96.0       4.73       0.26                                         ONNN100800012
      133.6        7.9        0.7                                         ONNN100800013
      173.9       11.1        1.6                                         ONNN100800014
ENDDATA             8                                                      ONNN100800015
ENDSUBENT          12                                                      ONNN100899999
SUBENT        0NNN1009   20021015                                          0NNN100900001
BIB                                                                        ONNN100900002
REACTION   ((82-PB-204(N,F),,SIG))                                         ONNN100900003
ENDBIB                                                                     ONNN100900004
NOCOMMON                                                                   ONNN100900005
DATA                                                                       ONNN100900006
EN         DATA       ERR-S                                               ONNN100900007
MEV        MB           MB                                                ONNN100900008
       34.7       0.46       0.13                                          ONNN100900009
       46.3       2.58       0.15                                          ONNN100900010
       65.4       11.1        0,7                                          ONNN100900011
       96.0       30.3        1.7                                          ONNN100900012
      133.6       46.2        3.4                                          ONNN100900013
      173.9       61.7        4.8                                          ONNN100900014
ENDDATA             8                                                      ONNN100900015
ENDSUBENT          12                                                      ONNN100999999

SUBENT        0NNN1010   20021015                                          0NNN101000001
BIB                                                                        ONNN101000002
REACTION   ((82-PB-206(N,F),,SIG))                                         ONNN101000003
```

```
ENDBIB                                                          ONNN101000004
NOCOMMON                                                        ONNN101000005
DATA                                                            ONNN101000006
EN         DATA       ERR-S                                     ONNN101000007
MEV        MB           MB                                      ONNN101000008
       34.7       0.08       0.04                              ONNN101000009
       46.3       0.79       0.06                              ONNN101000010
       65.4        5.1        0.3                              ONNN101000011
       96.0       15.2        0.9                              ONNN101000012
      133.6       24.2        1.8                              ONNN101000013
      173.9       38.7        3.1                              ONNN101000014
ENDDATA              8                                          ONNN101000015
ENDSUBENT           12                                          ONNN101099999
SUBENT        0NNN1011   20021015                               0NNN101100001
BIB                                                             ONNN101100002
REACTION   ((82-PB-207(N,F),,SIG))                             ONNN101100003
ENDBIB                                                          ONNN101100004
NOCOMMON                                                        ONNN101100005
DATA                                                            ONNN100600006
EN         DATA       ERR-S                                     ONNN101100007
MEV        MB           MB                                      ONNN101100006
       34.7      0.035      0.024                              ONNN101100009
       46.3       0.51       0.04                              ONNN101100010
       65.4       3.28       0.22                              ONNN101100011
       96.0       11.2        0.6                              ONNN101100012
      133.6       18.2        1.4                              ONNN101100013
      173.9       35.3        2.5                              ONNN101100014
ENDDATA              8                                          ONNN101100015
ENDSUBENT           12                                          ONNN101199999
SUBENT        0NNN1012   20021015                               0NNN101200001
BIB                                                             ONNN101200002
REACTION   ((82-PB-208(N,F),,SIG))                             ONNN101200003
ENDBIB                                                          ONNN101200004
NOCOMMON                                                        ONNN101200005
DATA                                                            ONNN100600006
EN         DATA         ERR-S                                   ONNN101200007
MEV        MB           MB                                      ONNN101200008
       34.7      0.029      0.022                              ONNN101200009
       46.3       0.28       0.04                              ONNN101200010
       65.4       2.33       0.17                              ONNN101200011
       96.0       8.2         0.5                              ONNN101200012
      133.6       14.3        1.1                              ONNN101200013
      173.9       23.9        1.8                              ONNN101200014
ENDDATA              8                                          ONNN101200015
ENDSUBENT           12                                          ONNN101299999
SUBENT        0NNN1013   20021015                               0NNN101300001
BIB                                                             ONNN101300002
REACTION   ((82-PB-O(N,F),,SIG))                               ONNN101300003
ENDBIB                                                          ONNN101300004
NOCOMMON                                                        ONNN101300005
DATA                                                            ONNN101300006
EN         DATA       ERR-S                                     ONNN101300007
MEV        MB           MB                                      ONNN101300008
       34.7      0.048      0.025                              ONNN101300009
       46.3       0.49       0.05                              ONNN101300010
       65.4       3.32       0.24                              ONNN101300011
       96.0       10.9        0.7                              ONNN101300012
      133.6       18.0        1.5                              ONNN101300013
      173.9       30.5        2.4                              ONNN101300014
ENDDATA              8                                          ONNN101300015
ENDSUBENT           12                                          ONNN101399999
```

```
SUBENT        0NNN1014   20021015                                    0NNN101400001
BIB                                                                  ONNN101400002
REACTION   ((83-BI-209(N,F),,SIG))                                   ONNN101400003
ENDBIB                                                               ONNN101400004
NOCOMMON                                                             ONNN101400005
DATA                                                                 ONNN101400006
EN         DATA       ERR-S                                          ONNN101400007
MEV        MB           MB                                           ONNN101400008
       34.7       0.37       0.07                                    ONNN101400009
       46.3       2.70       0.12                                    ONNN101400010
       65.4       12.3        0.7                                    ONNN101400011
       96.0       28.8        1.7                                    ONNN101400012
      133.6       43.3        3.3                                    ONNN101400013
      173.9       66.6        3.8                                    ONNN101400014
ENDDATA             8                                                ONNN101400015
ENDSUBENT          12                                                ONNN101499999
SUBENT        0NNN1015   20021015                                    0NNN101500001
BIB                                                                  ONNN101500002
ADD-RES    FROM ANGLE DISTRIBUTIONS FISSION FRAGMENTS IN THE         0NNN101500003
           FRONT AND BACK HALFSPHERES (RELATIVE TO DIRECTION         ONNN101500004
           NEUTRONBEAM) WERE CALCULATE ANISOTROPY COEFICIENT (B)     ONNN101500005
           AS B=W(0°)/ W(90°)-1                                      ONNN101500006
ELEMENT    81-TL-205                                                 ONNN101500007
ENDBIB                                                               ONNN101500008
NOCOMMON                                                             ONNN101500009
DATE                                                                 ONNN101500010
EN         DATE       ERR-S                                          ONNN101500011
MEV        NO-DIM     NO-DIM                                         ONNN101500012
65.4       0.75              0.52                                    ONNN101500013
96.0       0.92              0.24                                    ONNN101500014
133.6      0.95              0.24                                    ONNN101500015
173.9      0.82              0.20                                    ONNN101500016
ENDDATA             8                                                ONNN101500017
ENDSUBENT          12                                                ONNN101599999
SUBENT        0NNN1016   20021015                                    0NNN101600001
BIB                                                                  ONNN101600002
ELEMENT    82-PB-204                                                 ONNN101600003
ENDBIB                                                               ONNN101600004
NOCOMMON                                                             ONNN101600005
DATE                                                                 ONNN101600006
EN         DATE       ERR-S                                          ONNN101600007
MEV        NO-DIM     NO-DIM                                         ONNN101600008
46.3       0.26              0.28                                    ONNN101600009
65.4       0.07              0.16                                    ONNN101600010
96.0       0.32              0.11                                    ONNN101600011
133.6      0.37              0.08                                    ONNN101600012
173.9      0.10              0.10                                    ONNN101600013
ENDDATA             8                                                ONNN101600014
ENDSUBENT          12                                                ONNN101699999
SUBENT        0NNN1017   20021015                                    0NNN101700001
BIB                                                                  ONNN101700002
ELEMENT    82-PB-206                                                 ONNN101700003
ENDBIB                                                               ONNN101700004
NOCOMMON                                                             ONNN101700005
DATE                                                                 ONNN101700006
EN         DATE       ERR-S                                          ONNN101700007
MEV        NO-DIM     NO-DIM                                         ONNN101700008
46.3       0.41              0.41                                    ONNN101700009
65.4       0.48              0.24                                    ONNN101700010
96.0       0.44              0.12                                    ONNN101700011
133.6      0.43              0.10                                    ONNN101700012
```

```
173.9      0.29              0.11                                ONNN101700013
ENDDATA             8                                          ONNN101700014
ENDSUBENT          12                                          ONNN101799999
SUBENT        0NNN1018   20021015                              0NNN101800001
BIB                                                           ONNN101800002
ELEMENT    82-PB-207                                          ONNN101800003
ENDBIB                                                        ONNN101800004
NOCOMMON                                                      ONNN101800005
DATE                                                          ONNN101800006
EN         DATE       ERR-S                                   ONNN101800007
MEV        NO-DIM     NO-DIM                                  ONNN101800008
46.3       0.84              0.75                             ONNN101800009
65.4       0.48              0.36                             ONNN101800010
96.0       0.34              0.12                             ONNN101800011
133.6      0.43              0.11                             ONNN101800012
173.9      0.35              0.14                             ONNN101800013
ENDDATA             8                                          ONNN101800014
ENDSUBENT          12                                          ONNN101899999
SUBENT        0NNN1019   20021015                              0NNN101900001
BIB                                                           ONNN101900002
ELEMENT    82-PB-208                                          ONNN101900003
ENDBIB                                                        ONNN101900004
NOCOMMON                                                      ONNN101900005
DATE                                                          ONNN101900006
EN         DATE       ERR-S                                   ONNN101900007
MEV        NO-DIM     NO-DIM                                  ONNN101900008
46.3        1.5               1.2                              ONNN101900009
65.4       0.41              0.32                             ONNN101900010
96.0       0.50              0.16                             ONNN101900011
133.6      0.45              0.11                             ONNN101900012
173.9      0.30              0.12                             ONNN101900013
ENDDATA             8                                          ONNN101900014
ENDSUBENT          12                                          ONNN101999999
SUBENT        0NNN1020   20021015                              0NNN102000001
BIB                                                           ONNN102000002
ELEMENT    83-BI-209                                          ONNN102000003
ENDBIB                                                        ONNN102000004
NOCOMMON                                                      ONNN102000005
DATE                                                          ONNN102000006
EN         DATE       ERR-S                                   ONNN102000007
MEV        NO-DIM     NO-DIM                                  ONNN102000008
34.7        5.0               9.0                              ONNN102000009
46.3        1.1               0.5                              ONNN102000010
65.4       0.93              0.24                             ONNN102000011
96.0       0.54              0.11                             ONNN102000012
133.6      0.55              0.09                             ONNN102000013
173.9      0.31              0.09                             ONNN102000014
ENDDATA             8                                          ONNN102000015
ENDSUBENT          12                                          ONNN102999999
SUBENT        0NNN1021   20021015                              0NNN102100001
BIB                                                           ONNN102100002
ELEMENT    92-U-238                                           ONNN102100003
ENDBIB                                                        ONNN102100004
NOCOMMON                                                      ONNN102100005
DATE                                                          ONNN102100006
EN         DATE       ERR-S                                   ONNN102100007
MEV        NO-DIM     NO-DIM                                  ONNN102100008
34.7       0.30              0.04                             ONNN102100009
46.3       0.25              0.02                             ONNN102100010
65.4       0.29              0.02                             ONNN102100011
96.0       0.22              0.02                             ONNN102100012
```

```
133.6      0.16             0.02                                    ONNN102100013
173.9      0.03             0.03                                    ONNN102100014
ENDDATA             8                                               ONNN102100015
ENDSUBENT          12                                               ONNN102199999
SUBENT        0NNN1022   20021015                                    0NNN102200001
BIB                 5         37                                    ONNN102200002
DETECTOR   (TFBC) THIN FILM BREAK DOWN COUNTERS.                     ONNN102200003
           TWO SETS OF DETECTORS WERE USED SIMULTANEOUSLY.          ONNN102200004
           THE FIRST SET CONSISTED OF A DETECTORS WITH SENSITIVE    ONNN102200005
     SQUARE = 40 CM**2 INTENDED FOR PRECISE COUNTING      ONNN102200006
     FISSION FRAGMENTS. THE SECOND SET INCLUDED          0NNN102200007
     DETECTOR MOSAICS WITH A SENSITIVE SQUARE =          ONNN102200008
           26*1.0 CM**2 INTENDED FOR RELATIVE TOF MESUREMENTS.      ONNN102200009
           THE DETECTORS WERE PLACED CLOSE TO THE SAMPLES AT        ONNN102200010
           A NONE-GERMETIC CHAMBERS.                                ONNN102200011
           THE DETECTORS WERE CALIBRATED USING 252-CF SAMPLES       ONNN102200012
           AT THE SAME GEOMETRI                                     ONNN102200013
INC-SOURCE FLUX QUASI-MONOENERGETIC NEUTRONS AT THE POSITIONS       ONNN102200014
           OF FISILE TARGETS,1-2 M FROM THE LITIUM TARGET,          ONNN102200015
           WAS ABOUT (1-3)*10^5 N/SEC; DURATION OF PULSE WAS       0NNN102200016
           3-6 NSEC                                                 0NNN102200017
METHOD     UNIVERSAL FISSION CHAMBERS BASED ON TFBC USED FOR THE    0NNN102200018
           RELATIVE MEASUREMENTS BOTH AT NEUTRONS AND WIDE PROTON   0NNN102200019
           BEAM.THE CHAMBER INCLUDES 6 SANDWICHEES PLACED SIMMET-   0NNN102200020
           RICALLY IN A PLANE THAT IS PERPINDICULAR TO THE          0NNN102200021
           INCIDENT PARTICLE BEAM DIRECTION.EACH SANDWICH           0NNN102200022
           CONSISTS OF A FISSIONNING TARGET AND A TFBC PLACED       0NNN102200023
           CLOSE TO THE TARGET SURFACE.                             0NNN102200024
           FROM 10 TO 15 CHAMBERS WERE PLACED ONE AFTER ANOTHER     0NNN102200025
           IN THE NEUTRON FLUX AND UP TO 4 CHAMBER IN THE PROTON    0NNN102200026
           BEAM AND THUS TO PERFORM RELATIVE FISSION CROSS          0NNN102200027
           SECTION MEASUREMENTS FOR A FEW DIFERENT TARGET NUCLIDES0NNN102200028
CORRECTION PERFORMED:ANISOTROPY OF FISSION,LINEAR MOMENTUM          ONNN102200029
           TRANSFER FROM THE FISSIONING INCIDENT PARTICLE TO THE    ONNN102200030
           NUCLEUS,A CONTRIBUTION OF LOW ENERGY NEUTRONS DERIVED    ONNN102200031
           FROM THE TOF MEASUREMENT.                                ONNN102200032
           NEGLIGIBLE: IMPURITY OF THE BI-209 SAMPLE,CHARGE         ONNN102200033
           PARTICLE BACKGROUND                                      ONNN102200034
ERR-ANALYS (ERR-S) THE CONTRIBUTION ARE NEGLIGIBLE FROM:            ONNN100200035
            TARGET WEIGHTING, NEUTRON BEAM PROFILE DATA, DIRECT     ONNN102200036
           MEASUREMENTS OF THE FASILITE GEOMETRY, CORRECTIONS FOR   ONNN102200037
           ANISOTROPY OF FISSION AND FOR LINEAR MOMENTUM TRANSFER.ONNN102200038
ENDBIB              37                                              0NNN102200039
COMMON     NEUTRON INDUCED FISSION CROSS SECTION RELATIVE TO THE    0NNN102200040
           83-BI-209                                                0NNN102200041
ENDCOMMON            2                                              0NNN102200042
ENDSUBENT           29                                              0NNN102299999
SUBENT        0NNN1023   20021015                                    0NNN102300001
BIB                                                                 ONNN102300002
REACTION    ((82-PB-204(P,F),,SIG))/((83-BI-209(P,F),,SIG))         ONNN102300003
ENDBIB                                                              ONNN102300004
NOCOMMON                                                            ONNN102300005
DATE                                                                0NNN102300006
EN         DATE       ERR-S                                        ONNN102300007
MEV        NO-DIM     NO-DIM                                       ONNN102300008
34.7       1.04             0.O9                                    ONNN102300009
46.1       1.06             0.05                                    ONNN102300010
66.4       1.02             0.05                                    ONNN102300011
89.5       1.06             0.08                                    0NNN102300012
95.0       0.98             0.05                                    ONNN102300013
111.0      1.06             0.09                                    0NNN102300014
```

```
133.0      1.00             0.06                                    ONNN102300015
144.0      1.02             0.07                                    0NNN102300016
173.9      1.00             0.04                                    ONNN102300017
ENDDATA           11                                                ONNN102300018
ENDSUBENT                                                           0NNN102399999
SUBENT        0NNN1024   20021015                                   0NNN102400001
REACTION    ((82-PB-206(P,F),,SIG))/((83-BI-209(P,F),,SIG))       ONNN102400003
ENDBIB                                                              ONNN102400003
NOCOMMON                                                            ONNN102400004
DATE                                                                0NNN100400006
EN         DATE       ERR-S                                        ONNN102400007
MEV        NO-DIM     NO-DIM                                       ONNN102400008
34.7       0.17             0.O2                                    ONNN102400009
46.1       0.32             0.02                                    ONNN102400010
66.4       0.45             0.02                                    ONNN102400011
89.5       0.49             0.03                                    0NNN102400012
95.0       0.49             0.02                                    ONNN102400013
111.0      0.55             0.04                                    0NNN100400014
133.0      0.59             0.03                                    ONNN102400015
144.0      0.65             0.04                                    0NNN100400016
173.9      0.61             0.02                                    ONNN102400017
ENDDATA           8                                                 ONNN102400018
ENDSUBENT                                                           0NNN102499999
SUBENT        0NNN1025   20021015                                   0NNN102500001
BIB                                                                 ONNN102500002
REACTION    ((82-PB-207(P,F),,SIG))/((83-BI-209(P,F),,SIG))       ONNN102500003
ENDBIB                                                              ONNN102500004
NOCOMMON                                                            ONNN102100005
DATE                                                                0NNN102500006
EN         DATE       ERR-S                                        ONNN102500007
MEV        NO-DIM     NO-DIM                                       ONNN102500008
34.7       0.13             0.O2                                    ONNN102500009
46.1       0.19             0.01                                    ONNN102500010
66.4       0.29             0.01                                    ONNN102500011
89.5       0.37             0.03                                    0NNN102500012
95.0       0.36             0.02                                    ONNN102000013
111.0      0.46             0.03                                    0NNN102500014
133.0      0.44             0.02                                    ONNN102500015
144.0      0.50             0.03                                    0NNN102500016
173.9      0.47             0.02                                    ONNN102500017
ENDDATA           8                                                 ONNN102500018
ENDSUBENT                                                           0NNN102599999
SUBENT        0NNN1026   20021015                                   0NNN102600001
BIB                                                                 ONNN102600002
REACTION    ((82-PB-208(P,F),,SIG))/((83-BI-209(,PF),,SIG))       ONNN102300003
ENDBIB                                                              ONNN102600004
NOCOMMON                                                            ONNN102600005
DATE                                                                0NNN102600006
EN         DATE       ERR-S                                        ONNN102600007
MEV        NO-DIM     NO-DIM                                       ONNN102600008
34.7      0.029            0.0O7                                    ONNN102600009
46.1      0.082            0.005                                    ONNN102600010
66.4      0.202            0.008                                    ONNN102600011
73.4      0.219            0.019                                    ONNN102600013
89.5       0.28             0.02                                    0NNN102600014
95.0       0.30             0.01                                    ONNN102600015
111.0      0.33             0.02                                    0NNN102600016
133.0      0.31             0.01                                    ONNN102600017
144.0      0.39             0.02                                    0NNN102600018
173.9      0.37             0.01                                    ONNN102600019
ENDDATA           8                                                 ONNN102600020
```

```
ENDSUBENT                                                          0NNN102699999
SUBENT        0NNN1027   20021015                                  0NNN102700001
BIB                                                                ONNN102700002
REACTION    ((82-PB-O(P,F),,SIG))/((83-BI-209(P,F),,SIG))          ONNN102300003
ENDBIB                                                             ONNN102700004
NOCOMMON                                                           ONNN102700005
DATE                                                               0NNN102700006
EN         DATE       ERR-S                                       ONNN102700007
MEV        NO-DIM     NO-DIM                                      ONNN102700008
46.1       0.20             0.01                                  ONNN102700009
66.4       0.30              0.01                                 ONNN10270010
73.4       0.32              0.03                                 ONNN102700011
95.0       0.38              0.01                                 ONNN102700012
133.0      0.42              0.02                                 ONNN102700013
144.0      0.46              0.03                                 0NNN100700014
173.9      0.51              0.02                                 ONNN10270015
ENDDATA             8                                              ONNN102700016
ENDSUBENT                                                          0NNN102799999
SUBENT        0NNN1028   20021015                                  0NNN102800001
BIB                                                                ONNN102800002
REACTION    ((81-TL-2O5(P,F),,SIG))/((83-BI-209(P,F),,SIG))        ONNN102800003
ENDBIB                                                             ONNN102800004
NOCOMMON                                                           ONNN102800005
DATE                                                               0NNN102800006
EN         DATE       ERR-S                                       ONNN102800007
MEV        NO-DIM     NO-DIM                                      ONNN102800008
34.7       0.20             0.007                                 ONNN102800009
46.1      0.067             0.004                                 ONNN102800010
66.4      0.105             0.005                                 ONNN102800011
89.5       0.16              0.01                                 ONNN102800012
95.0      0.164             0.006                                 ONNN102800013
111.0     0.204             0.016                                 ONNN102800014
133.0      0.23              0.01                                 ONNN102800015
144.0      0.25              0.01                                 0NNN102800016
173.9      0.25              0.01                                 ONNN102800017
ENDDATA             8                                              ONNN102800018
ENDSUBENT                                                          ONNN102899999
SUBENT        0NNN1029   20021015                                  0NNN102900001
BIB                                                                ONNN102900002
REACTION   ((83-BI-209(P,F),,SIG))/((92-U-238(P,F),,SIG))         ONNN102900003
ENDBIB                                                             ONNN102900004
COMMON     (NO-DIM)E-4                                             0NNN102900005
ENDCOMMON                                                          0NNN102900006
DATE                                                               0NNN102900007
EN         DATE       ERR-S                                       ONNN102900008
MEV        NO-DIM     NO-DIM                                      ONNN102900009
34.7       1.32              0.07                                 ONNN102900010
46.1       10.7               0.7                                 ONNN102900011
66.4       53.0                3.                                 ONNN102800012
73,4       83.0                4.                                 ONNN102900013
89.5      131.0                7.                                 ONNN102900014
95.0      143.0                3.                                 ONNN102900015
111.0     230.0               20.                                 0NNN102900016
133.0     260.0               10.                                 ONNN102900017
144.0     300.0               20.                                 ONNN102900018
160.0     400.0               10.                                 ONNN102900019
173.9     390.0               10.                                 ONNN102900020
ENDDATA             8                                              ONNN102900021
ENDSUBENT                                                          ONNN102999999
SUBENT        0NNN1030   20021015                                  0NNN103000001
BIB                                                                ONNN103000002
```

```
INS-SOURSE PROTON BEAM                                                  ONNN103000003
REACTION   ((81-TL-205(P,F),,SIG))/((83-BI-209(P,F),,SIG))              ONNN103000003
ENDBIB                                                                  ONNN103000005
COMMON                                                                  ONNN103000006
DATE                                                                    0NNN103000007
EN         EN-ERR     DATE       ERR-S                                 ONNN103000008
MEV        MEV        NO-DIM     NO-DIM                                ONNN103000009
64         2          0.17            0.01                             ONNN103000010
94         2          0.20            0.03                             ONNN103000011
167        2          0.34            0.02                             ONNN103000012
ENDDATA             8                                                   ONNN103000021
ENDSUBENT                                                               ONNN103099999
SUBENT        0NNN1031   20021015                                       0NNN103100001
BIB                                                                     ONNN103100002
REACTION    ((82-PB-204(P,F),,SIG))/((83-BI-209(P,F),,SIG))             ONNN102100003
ENDBIB                                                                  ONNN103100004
NOCOMMON                                                                ONNN103100006
DATE                                                                    0NNN103100007
EN         EN-ERR     DATE       ERR-S                                 ONNN103100008
MEV        MEV        NO-DIM     NO-DIM                                ONNN103100009
64         2          1.12            0.09                             ONNN103100010
94         2          1.05            0.12                             ONNN103100011
167        2          1.05            0.06                             ONNN103100012
ENDDATA             8                                                   ONNN103100013
ENDSUBENT                                                               ONNN103199999
SUBENT        0NNN1032   20021015                                       ONNN103200001
BIB                                                                     ONNN103200002
REACTION    ((82-PB-206(P,F),,SIG))/((83-BI-209(P,F),,SIG))             ONNN103200003
ENDBIB                                                                  ONNN103200004
NOCOMMON                                                                ONNN103200005
DATE                                                                    0NNN103200006
EN         EN-ERR     DATE       ERR-S                                 ONNN103200007
MEV        MEV        NO-DIM     NO-DIM                                ONNN103200008
64         2          1.12            0.09                             ONNN103200009
94         2          1.05            0.12                             ONNN103200010
167        2          1.05            0.06                             ONNN103200011
ENDDATA             8                                                   ONNN103200012
ENDSUBENT                                                               ONNN103299999
SUBENT        0NNN1033   20021015                                       ONNN103300001
BIB                                                                     ONNN103300002
REACTION    ((82-PB-207(P,F),,SIG))/((83-BI-209(P,F),,SIG))             ONNN103300003
ENDBIB                                                                  ONNN103300004
NOCOMMON                                                                ONNN103300005
DATE                                                                    0NNN103300006
EN         EN-ERR     DATE       ERR-S                                 ONNN103300007
MEV        MEV        NO-DIM     NO-DIM                                ONNN103300008
64         2          0.52            0.04                             ONNN103300009
94         2          0.58            0.06                             ONNN103300010
167        2          0.57            0.02                             ONNN103300011
ENDDATA             8                                                   ONNN103300012
ENDSUBENT                                                               ONNN103399999
SUBENT        0NNN1034   20021015                                       ONNN103400001
BIB                                                                     ONNN103400002
REACTION    ((82-PB-208(P,F),,SIG))/((83-BI-209(P,F),,SIG))             ONNN103400003
ENDBIB                                                                  ONNN103400004
NOCOMMON                                                                ONNN103400005
DATE                                                                    0NNN103400006
EN         EN-ERR     DATE       ERR-S                                 ONNN103400007
MEV        MEV        NO-DIM     NO-DIM                                ONNN103400008
64         2          0.25            0.02                             ONNN103400009
94         2          0.37            0.04                             ONNN103400010
```

```
167         2           0.44              0.03                        ONNN103400011
ENDDATA               8                                               ONNN103400012
ENDSUBENT                                                             ONNN103499999
SUBENT         0NNN1035   20021015                                    ONNN103500001
BIB                                                                   ONNN103500002
REACTION     ((82-PB-O(P,F),,SIG))/((83-BI-209(P,F),,SIG))            ONNN103500003
ENDBIB                                                                ONNN103500004
NOCOMMON                                                              ONNN103500005
DATE                                                                  0NNN103500006
EN          EN-ERR      DATE        ERR-S                             ONNN103500007
MEV         MEV         NO-DIM      NO-DIM                            ONNN103500008
167         2           0.54              0.04                        ONNN103500009
ENDDATA               8                                               ONNN103500010
ENDSUBENT                                                             ONNN103599999
SUBENT         0NNN1036   20021015                                    ONNN103600001
BIB                                                                   ONNN103600002
REACTION     ((81-BI-209(P,F),,SIG))/((92-U-238(P,F),,SIG))           ONNN102600003
ENDBIB                                                                ONNN103600004
NOCOMMON                                                              ONNN103600005
DATE                                                                  0NNN103600006
EN          EN-ERR      DATE        ERR-S                             ONNN103600007
MEV         MEV         NO-DIM      NO-DIM                            ONNN103600008
64          2           0.018             0.001                       ONNN103600009
167         2           0.086             0.0O4                       ONNN103600011
ENDDATA               8                                               ONNN103600012
ENDSUBENT                                                             ONNN103699999
SUBENT         0NNN1037   20021015                                    ONNN103700001
BIB                                                                   ONNN103700002
ELEMENT     83-BI-209(P,F),,SIG))                                     ONNN103700003
ENDBIB                                                                ONNN103700004
NOCOMMON                                                              ONNN103700005
DATE                                                                  0NNN103700006
EN          EN-ERR      DATE        ERR-S                             ONNN103700007
MEV         MEV          MB          MB                               ONNN103700008
47.5        0.5          9.3               1.0                       ONNN103700009
49.2        0.5         11.3               1.2                       ONNN103760010
97.5        2.0          100               11                        ONNN103700011
177.3       1.2          162               17                        ONNN103700012
ENDDATA               8                                               ONNN103700013
ENDSUBENT                                                             ONNN103799999
SUBENT         0NNN1038   20021015                                    ONNN103800001
BIB                                                                   ONNN103800002
ELEMENT     82-PB-204(P,F),,SIG))                                     ONNN103800003
ENDBIB                                                                ONNN103800004
NOCOMMON                                                              ONNN103800005
DATE                                                                  0NNN103800006
EN          EN-ERR      DATE        ERR-S                             ONNN103800007
MEV         MEV          MB          MB                               ONNN103800008
97.5        2.0          106                11                       ONNN103800009
177.3       1.2          179               19                        ONNN103800010
ENDDATA               8                                               ONNN103800013
ENDSUBENT                                                             ONNN103899999
SUBENT         0NNN1039   20021015                                    ONNN103900001
BIB                                                                   ONNN103900002
ELEMENT     82-PB-206(P,F),,SIG))                                     ONNN103900003
ENDBIB                                                                ONNN103900004
NOCOMMON                                                              ONNN103900005
DATE                                                                  0NNN103900006
EN          EN-ERR       DATE        ERR-S                            ONNN103900007
MEV         MEV          MB          MB                               ONNN103900008
97.5        2.0           49               6                         ONNN103900009
```

```
177.3      1.2          97             17                          ONNN103900010
ENDDATA             8                                             ONNN103900011
ENDSUBENT                                                         ONNN103999999
SUBENT        0NNN1040   20021015                                 ONNN104000013
BIB                                                               ONNN104000002
ELEMENT    82-PB-207(P,F),,SIG))                                  ONNN104000003
ENDBIB                                                            ONNN104000004
NOCOMMON                                                          ONNN104000005
DATE                                                              0NNN104000006
EN         EN-ERR     DATE       ERR-S                           ONNN104000007
MEV        MEV         MB         MB                             ONNN104000008
177.3      1.2          79             9                          ONNN104000010
ENDDATA             8                                             ONNN104000011
ENDSUBENT                                                         ONNN104099999
SUBENT        0NNN1041   20021015                                 0NNN104100013
BIB                                                               ONNN104100002
ELEMENT    82-PB-O(P,F),,SIG))                                    ONNN104100003
ENDBIB                                                            ONNN104100004
NOCOMMON                                                          ONNN104100005
DATE                                                              0NNN104100006
EN         EN-ERR     DATE       ERR-S                           ONNN104100007
MEV        MEV         MB         MB                             ONNN104100008
177.3      1.2        73.8            8                          ONNN104100010
ENDDATA             8                                             ONNN104100011
ENDSUBENT                                                         ONNN104199999
SUBENT        0NNN1042   20021015                                 0NNN104200013
BIB                                                               ONNN104200002
ELEMENT    81-TL-205(P,F),,SIG))                                  ONNN104200003
ENDBIB                                                            ONNN104200004
NOCOMMON                                                          ONNN104200005
DATE                                                              0NNN104200006
EN         EN-ERR     DATE       ERR-S                           ONNN104200007
MEV        MEV         MB         MB                             ONNN104200008
47.5       0.5        0.86           0.09                        ONNN104200009
49.2       0.5        1.14           0.12                        ONNN104200010
97.5       2.0          18           2                           ONNN104200011
177.3      1.2          50           6                           ONNN104200012
ENDDATA             8                                             ONNN104200013
ENDSUBENT                                                         ONNN104299999
SUBENT        0NNN1043   20021015                                 0NNN104300001
BIB                                                               ONNN104300002
ADD-RES    FROM ANGLE DISTRIBUTIONS FISSION FRAGMENTS IN THE      0NNN104300003
           FRONT AND BACK HALFSPHERES (RELATIVE TO DIRECTION      ONNN104300004
           PROTON BEAM) WERE CALCULATE ANISOTROPY COEFICIENT      ONNN104300005
           (B) AS B=((W(0°)/ W(90°))-1                            ONNN104300006
ELEMENT    81-TL-205                                              ONNN104300007
ENDBIB                                                            ONNN104300008
NOCOMMON                                                          ONNN104300009
DATE                                                              ONNN104300010
EN         EN-ERR     DATE       ERR-S                           ONNN104300011
MEV        NO-DIM     NO-DIM     NO-DIM                          ONNN104300012
48.        1.         0.55            0.10                       ONNN104300013
98.        2.         0.29            0.06                       ONNN104300014
177.3      1.2        0.36            0.10                       ONNN104300015
ENDDATA             8                                             ONNN104300016
ENDSUBENT          12                                             ONNN104399999
SUBENT        0NNN1044   20021015                                 0NNN104400001
BIB                                                               ONNN104400002
ELEMENT    82-PB-204                                              ONNN104400003
ENDBIB                                                            ONNN104400004
NOCOMMON                                                          ONNN104400005
```

```
DATE                                                                ONNN104400006
EN          EN-ERR     DATE       ERR-S                            ONNN104400007
MEV         NO-DIM     NO-DIM     NO-DIM                           ONNN104400008
48.         1.         0.42             0.07                       ONNN104400009
98.         2.         0.25              0.1                       ONNN104400010
177.3       1.2        0.15             0.04                       ONNN104400011
ENDDATA              8                                             ONNN104400012
ENDSUBENT           12                                             ONNN104499999
SUBENT        0NNN1045   20021015                                   0NNN104500001
BIB                                                                 ONNN104500002
ELEMENT     82-PB-206                                               ONNN104500003
ENDBIB                                                              ONNN104500004
NOCOMMON                                                            ONNN104500005
DATE                                                                ONNN104500006
EN          EN-ERR     DATE       ERR-S                            ONNN104500007
MEV         NO-DIM     NO-DIM     NO-DIM                           ONNN104500008
48.         1.         0.35             0.07                       ONNN104500009
98.         2.         0.4              0.1                        ONNN104500010
177.3       1.2        0.17             0.03                       ONNN104500011
ENDDATA              8                                             ONNN104500012
ENDSUBENT           12                                             ONNN104599999
SUBENT        0NNN1046   20021015                                   0NNN104600001
BIB                                                                 ONNN104600002
ELEMENT     82-PB-207                                               ONNN104600003
ENDBIB                                                              ONNN104600004
NOCOMMON                                                            ONNN104600005
DATE                                                                ONNN104600006
EN          EN-ERR     DATE       ERR-S                            ONNN104600007
MEV         NO-DIM     NO-DIM     NO-DIM                           ONNN104600008
48.         1.         0.4             0.1                         ONNN104600009
98.         2.          -               -                          ONNN104600010
177.3       1.2        0.12             0.03                       ONNN104600011
ENDDATA              8                                             ONNN104600012
ENDSUBENT           12                                             ONNN104699999
SUBENT        0NNN1047   20021015                                   0NNN104700001
BIB                                                                 ONNN104700002
ELEMENT     82-PB-208                                               ONNN104700003
ENDBIB                                                              ONNN104700004
NOCOMMON                                                            ONNN104700005
DATE                                                                ONNN104700006
EN          EN-ERR     DATE       ERR-S                            ONNN104700007
MEV         NO-DIM     NO-DIM     NO-DIM                           ONNN104700008
48.         1.         0.35             0.10                       ONNN104700009
98.         2.          -                -                         ONNN104700010
177.3       1.2        0.17             0.05                       ONNN104700011
ENDDATA              8                                             ONNN104700012
ENDSUBENT           12                                             ONNN104799999
SUBENT        0NNN1048   20021015                                   0NNN104800001
BIB                                                                 ONNN104800002
ELEMENT     83-BI-209                                               ONNN104800003
ENDBIB                                                              ONNN104800004
NOCOMMON                                                            ONNN104800005
DATE                                                                ONNN104800006
EN          EN-ERR     DATE       ERR-S                            ONNN104800007
MEV         NO-DIM     NO-DIM     NO-DIM                           ONNN104800008
48.         1.         0.35             0.05                       ONNN104800009
98.         2.         0.22             0.05                       ONNN104800010
177.3       1.2        0.11             0.05                       ONNN104800011
ENDDATA              8                                             ONNN104899999
ENDSUBENT           12                                             ONNN109999999
ENDENTRAY           46
```

**Ministry of the Russian Federation for Atomic Energy**
**Federal State Unitary Enterprise**
**"STATE SCIENTIFIC CENTER OF THE RUSSIAN FEDERATION – INSTITUTE FOR PHYSICS AND POWER ENGINEERING named after A.I.Leipunsky"**

## PROJECT # 1372

# COMPLEX RADIOCHEMICAL AND ACTIVATION ANALYSIS OF LONG-LIFE NUCLEAR WASTE TRANSMUTATION IN FAST REACTORS AND IN THE BEAMS OF HIGH ENERGY ACCELERATORS

## Scientific/Technical Progress Report
## Three quarters from 01.03.02 till 30.11.02

Leading Institution: **State Scientific Center of the Russian Federation – Institute for Physics and Power Engineering named after academician A.I.Leipunsky**

Address: 1, Bondarenko Sq., Obninsk 249033, Kaluga region

Supporting Institution: **Joint Institute for Nuclear Research**

Address: 6, Jolio-Curie St., 141980 Dubna, Moscow region.

Project Manager: **E.Ya.Smetanin**

Project Duration: **30 months**

Project Commencement Date: **01.03.2002**

**2002**

# I. Summary of Technical Progress.

**Task 1. Radiochemical activities on extraction and purification of individual isotopes, fabrication of targets for the irradiation in beams of the accelerating complex of Laboratory of High Energies (LHE) of JINR.**

The following isotopes were recovered and purified from radionuclide and chemical impurities for carrying out experiments on transmutation of actinide element isotopes: Americium-241, Neptunium-237, Plutonium-238, Plutonium-240, and Uranium-235 of 90% enrichment which was used as a burn-up monitor in these investigations.

The first batch of solid-state detectors made of the depleted uranium-238 was fabricated to investigate the transmutation of actinide element isotopes in proton beams of the accelerating complex of the LHE of JINR. The following radionuclides were re-packed in new targets: I-125, Np-237, Am-241. Targets as ampoules made of aluminum were fabricated from the following radionuclides: I-129 (as NaI, 2 ampoules), Np-237 (as oxide, 2 ampoules), Am-241 (as oxide, 3 ampoules), U-234 (as oxide, 1 ampoule). The targets were delivered to the LHE of JINR.

**Task 2. Research of the samples irradiated in BN-350 reactor with the use of radiochemical and nuclear physical methods.**

Measurements of $\alpha$-, $\beta$-, and $\gamma$-activity of samples of various solutions are performed in order to identify radionuclides, to determine their quantities and purity in radionuclide impurities. An alpha-spectrometer 7184 produced by company "EURISYS MESURES" is used for measuring the alpha-radiation. Special codes "INTER Winner" and "ALPHA VISION" are used for processing the machine spectrum. Metrologic characteristics of a scintillation $\beta$-spectrometer "BETA-1C" were defined during $\beta$-spectrometric measurements.

A gamma-spectrometer with germanium-lithium detector is used for measuring gamma-radiation from samples of the solutions. The energy calibration and the efficiency calibration with the use of **R**eference **S**pectrometric **S**ources of **A**lpha-**R**adiation (RSSAR) were performed for the gamma-spectrometer. We perform activities aimed at calibration of the mass-spectrometer using state standards.

For determining concentrations of alpha-radionuclide in solutions with the help of alpha-activity measurements working standards were made of the specially purified plutonium-239 with the well-known isotopic composition and from neptunium-237 which was pure in plutonium-238.

We have started investigations of $^{241}$Am and $^{237}$Np samples irradiated in BN-350 reactor. $\alpha$- and $\gamma$-spectrometric analysis of the initial solutions (IS) of $^{241}$Am and Np-237 was performed.

**Task 3. Research of actinide transmutation in BN-350 fast reactor.**

We analyzed measurement results on location-finding of radioactive sources of Iridium-192 in the capillaries containing the actinide samples being irradiated. All maps of loading in micro-campaigns were fixed. We worked out in detail the information on burn-up levels of the fuel assemblies surrounded the fuel assemblies with capillaries for all micro-campaigns.

We processed the files ENDF/B-6 with the use of codes GRUCON and NJOY in order to obtain group cross-sections of fission reactions and radiation capture on minor actinides. The decay data library of the system BNAB-93 was analyzed, the radiation yields and their errors were evaluated. A model of BN-350 reactor corresponding to the average stationary state was prepared. Also, we started the analysis of working drawings of the assemblies of BN-350 reactor as of irradiation moment in order to form the specified loading of BN-350 reactor.

Critical loadings of the core of BN-350 reactor were analyzed, calculation models for the mean stationary state of BN-350 reactor were developed for carrying out evaluation calculations. Evaluation calculations of the anticipated activity of media were performed.

The models for calculating the 50th and the 51st micro campaigns have been developed, it is sufficient for calculation of samples of the first batch.

We calculated distributions of neutron fields of BN-350 reactor as of moment of irradiation. The calculations were performed using TRIGEX code on diffusion approximation. Constants for the calculation were prepared on the basis of multi-group (299 multigroups) version of the constant system ????-93 with the further collapse of cross-sections into 18 groups. As a result absolute neutron fluxes for Np-237, Pu-238, and Am-241 samples have been determined. CARE code (developed by the IPPE) and ORIGEN-S code (USA) were used as basic codes for calculating nuclide compositions. The U.S. code "ORIGEN" has been referred to Russian software using constants in ????-93 format.

Nuclide compositions of Np-237, Pu-238, and Am-241 samples will be calculated during the fourth quarter.

**Task 4. Creation of complete data files with the evaluated neutron cross-sections for Pu-240, Np-237 and Am-241 isotopes up to 150 MeV.**

All available experimental data and existing evaluations on reaction cross-sections for $^{240}$Pu, $^{237}$Np, and $^{241}$Am in the energy range up to 200 MeV were complied and also, their consistency and uncertainty were analyzed during the first quarter.

The activities implemented during the second quarter focused on the more precise determination of parameters of optical potential for fission nuclei. The results of precise measurements of total neutron cross-sections for $^{238}$U performed in Los Alamos were published in 2002. These data make it possible to determine reliably parameters of the generalized optical potential enabling calculation of total neutron cross-sections for neighboring nuclei. As differences of total cross-sections of the neighboring nuclei are rather small, such determination of total cross-sections may be more reliable than straight description of the earlier experimental data which errors are considerably higher than the errors obtained for $^{238}$U. We performed the appropriate analysis of all previous calculations and evaluations of neutron cross-sections for $^{240}$Pu and obtained the optimum description of all the experimental data on total cross-sections and differential elastic neutron scattering cross-sections in the total neutron energy range up to 150 MeV. On the basis of the obtained set of the optical potential parameters inelastic neutron scattering cross-sections as well as cross-sections of (n,xn)-reactions have been specified.

The analysis of all the experimental data on cross sections of $^{240}$Pu fission by neutrons has been performed. New experimental data obtained during the last decade conform well to the previous evaluations within the neutron energy up to 15 MeV, and they require certain specification of the recommended cross-sections only above this energy. Unfortunately, data on the energies above 20 MeV for $^{240}$Pu were measured when implementing the single research work, and the errors were rather considerable. The final evaluation of cross-section of $^{240}$Pu fission by neutrons in the neutron energy range up to 200 MeV has been obtained on the basis of fractionally rational approximation of all experimental data and the calculation curve. Such approach makes it possible to provide for optimum description of the experimental data as well as to determine evaluation errors together with the correspondent covariance matrix of errors.

The analysis and evaluation of fission neutron spectra and multiplicity as a function of incident neutron energy have been carried out. The yields of "hard" (pre-equilibrium) and "soft" (evaporated) neutrons have been estimated for the events with and without fission. The energy distributions of the hard neutrons of both kinds are parameterized with the evaporation spectrum, which temperature is determined by the average energy of the pre-equilibrium neutrons. Madland-Nix model was used for describing the evaporated neutrons at incident neutron energy up to 30 MeV and Maxwellian approximation of spectra – at the higher energies. Energy-angular distributions of secondary neutrons have been described with Kalbach-Mann model.

The calculations of cross-sections, spectra, and angular distributions of protons, deuterons, tritons, and α-particles emitted by heavy fission nuclei in the reactions with neutrons of different energies have been performed. The comparison with the available experimental data for the spectra of light charged particles in the reactions of neutrons of the initial energy of 62.7 MeV with nuclei of uranium and lead enables to make a conclusion that the parameters of the optical-static model have been chosen correctly. The calculations performed have served as a basis for the integral yields and light charged particle spectra evaluation for $^{240}$Pu.

The complete file of the recommended evaluated data for $^{240}$Pu for the neutron energy up to 150 MeV has been formed in the ENDF/B-VI format on the basis of the performed calculations. The format verification of the file is being carried out now, and the file will be submitted to the collaborators after the completion of it.

Based on the results of the performed work a presentation was given at the International Conference on new nuclear energy systems: A. V. Ignatyuk, V. P. Lunev, Yu. N. Shubin, E.V. Gai, N. N. Titarenko. "Neutron Cross Section Evaluations for Actinides at Intermediate Energies." Proc. International Conference on Emerging Nuclear Energy Systems, Albuquerque, New Mexico, USA, 29 September - 4 October 2002.

**Task 5. Transmutation research in proton beams of the accelerating complex of the Laboratory of High Energies (LHE) of JINR.**

Spectra measurements of gamma-quanta of activation detectors and transmutation samples were completed at a complex consisting of 4 germanium spectrometers.

The gamma-spectra obtained out of measurements of transmutation samples (Iodine-129 and Neptunium-237) have been processed.

The irradiation of lead target with paraffin moderators and long-lived radioactive waste (Iodine-129, Neptunium-237, and Plutonium-239) in the nuclotron was prepared and implemented in July 2002. The irradiation was made for investigating waste transmutation at three energies of bombarding protons: 0,53, 2,0, and 4,3 GeV.

A moderator design has been developed and made of high purity graphite.

A goniometric system intended for positioning the lead target and the moderator on the beam has been developed and manufactured.

Radiation safety documentation has been issued for carrying out a session of irradiation of $^{129}$I, $^{237}$Np, $^{239}$Pu, $^{241}$Am samples with neutrons from the lead target with paraffin moderator.

We process results of the irradiation session of the lead target with paraffin moderator on proton beam with the energy of 0.5; 2.0 and 4.0 GeV which took place in July 2002.

The system consisting of five fast scintillation detectors on the base of ? ? ? -87, an auxiliary target of 1 g/cm$^2$ in thickness for scattering a part of the primary flux, software programmable controller for transferring data through ETHERNET has been assembled and adjusted.

Gamma-spectra of the sample made of radioactive waste of Iodine-129 have been processed. This sample was exposed in the field of electro-nuclear neutrons generated when irradiating U/Pb-assembly with nuclotron's proton beam at the energy of 1.5 GeV.

A new algorithm for calculating total and inelastic cross-sections of interactions of mesons and nucleons with nuclei at energies E > 10 MeV – 10 TeV has been developed.

The more accurate algorithm of simulation of the excited nuclei fission has been developed. A programming module describing the geometry and the nuclear composition of the facility "Energy plus Transmutation" has been prepared.

The results on neutron spectra in the inter-sectional space of 2-section and 4-section assemblies and on the uranium blanket surface of the facility "Energy plus Transmutation" at proton incident energy 1.5 GeV have been obtained. The obtained results were preliminary compared with the available experimental data.

Program moduli in the language C++ were developed for description of lattice structure of the facility blanket. Test calculations were preformed. The calculated neutron spectra were compared with the data that had been obtained when unfolding spectra.

Two versions of the facility "Energy plus Transmutation" were simulated mathematically on the basis of the program complex "CASCADE": separately for the lead target and the lead target with paraffin blanket.

In-put files were prepared and preliminary Monte Carlo calculations were made for 9-section facility with uranium blanket taking into account peculiarities of the experimental chamber where the facility is supposed to be located.

Neutron spectra as a function of depth of a sample immersion in the paraffin moderator layer and neutron spectra as a function of energy of incident proton beam upon the primary lead target were investigated in the facility configuration being researched.

Codes on the basis of cascade-evaporating model were developed, and calculations of isotope yields in radioactive nuclei samples, irradiated by direct proton beams, were started. A comparison with the available experimental data was started.

The experimental data on neutron yields in hadron-nuclear reactions at different energies were collected by means of digitizing graphs; the data were presented in different files. The files are accessible to each project participant for testing codes and evaluating experimental conditions.

The calculation code on a model of quantum molecular dynamics was advanced. Test calculations of neutron yields in the reaction $p + Fe$ at the energy of 113 MeV were performed.

Neutron yields were calculated in the following reactions within the framework of the model of quantum molecular dynamics (CHIMERA) and the cascade-evaporating model as well:

$^{27}Al(p,xn)X$ $E_p$=800 MeV, PR C47 p.1647, fig.3
$^{56}Fe(p,xn)X$ $E_p$=113 MeV, PR C52 p.2620, fig.10
$^{56}Fe(p,xn)X$ $E_p$=597 MeV, PR C52 p.2620, fig.12
$^{58}Ni(p,xn)X$ $E_p$=120 MeV, PR C53,p.1824, fig.21
$^{208}Pb(p,xn)X$ $E_p$=256 MeV, PR C52,p.2620, fig.11
$^{208}Pb(p,xn)X$ $E_p$=800 MeV, PR C52,p.2620, fig.13

The analysis of calculations of neutron and proton spectra in proton-induced reactions has been performed.

A version of QMD model for nucleus-nuclear interactions has been developed.

## REFERENCES:

1. A. V. Ignatyuk, V. P. Lunev, Yu. N. Shubin, E.V. Gai, N. N. Titarenko.
"Neutron Cross Section Evaluations for Actinides at Intermediate Energies. Pu." *Proceedings of International Conference on Emerging Nuclear Energy Systems*, Albuquerque, New Mexico, USA, 29 September-4 October 2002.

2. 2nd meeting of BASTRA Cluster (Basic Studies for Transmutation)
(HINDAS / n_TOF-ND-ADS / MUSE/ISTC/OECD-NEA). Uppsala, Sweden, 12-14 September 2002.

3. V.S. Barashenkov, A. Polyanski, I.A. Shelaev. ?/? ?2-2-2002-190, JINR, Dubna, 2002 "Parameters of uranium electronuclear assembly (ISTC Project #3721)"

4. V.S.Barashenkov, H. Kumawat, U. Gayal, V. Kumar. Atomic Energy Symposium, BARC, Bombey, Dec. 2002."Modelling of an experiment for the study of neutron spallation source at JINR"

5. V.S.Barashenkov, H.Kumawat, U.Gayal, V.Kumar. Atomic Energy Symposium, BARC, Bombey, Dec. 2002. "Modelling of an experiment INSS and paraffin moderator at JINR".

6. Youri Khomjakov, Andrei Kotchetkov, Mikhail Semenov, Anatolii Tsiboolia, Nikolai Nerozin, Vadim Pavlovich, Eduard Smetanin "Evaluation of the activation and burn-up experiments made on the BN-350 reactor", this presentation was given at the conference "PHYSOR-2002", Seoul.
7. Chultem D., Ts.Tumendelger, M.I.Krivopustov, Sh.Gerbish, B.Tumendemberal, A.B.Pavliouk, O.S.Zaverioukha «Research of the Mass Spectra of the Fission Products and Yields of (n, γ)- and (n, 2n) Reactions in a Model Subcritical Uranium Blanket of the Electronuclear System «Energy plus Transmutation» on Proton Beam of the JINR Synchrophasotron at 1,5 GeV Energy». Preprint JINR ?1-2002-16, Dubna, 2002.
8. B.A.Martsynkevich, A.M.Khilmanovich, S.V.Korneev, I.L.Rakhno, S.E.Chigrinov, M.I.Krivopustov, A.N.Sosnin, Ts.Tumendelger, D.Chultem, O.S.Zaverioukha, A.V.Pavliouk «Unfolding of Fast Neutron Spectra in the Wide Energy Range (to about 200 MeV) in a Heterogeneous Subcritical Assembly of an Electronuclear System «Energy plus Transmutation» Preprint JINR P1-2002-65, Dubna, 2002.
9. I.V.Zhuk, M.K.Kievets, M.I.Krivopustov, A.N.Sosnin, C.Tumendelger, D.Chultem, V.Westmeier, O.S.Zaveryukha, A.V.Pavlyuk. "Investigation of space-energy distribution of neutrons in lead target and uranium blanket of an electronuclear system "Energy plus transmutation" when bombarding by protons with the energy of 1,5 GeV". JINR, ?1-2002-184, Dubna, July 2002.

**II. Description of Significant Travel.**

International Conference PHYSOR 2002 on reactor physics including transmutation problems and high-performance computing was held on 7-10 October in Seoul, Republic of Korea. E.Ya. Smetanin, O.Yu. Vtorova, and Yu.S. Khomyakov participated in the conference and made presentation "Evaluation of the activation and burn-up experiments made on the BN-350 reactor".

Yu.N. Shubin, project participant, presented a report on the course of activities on the ISTC Project #1372 at the Second BASTRA Cluster Meeting (BAsic Science for TRAnsmutation), Uppsala, 12-14 September. Also he made presentation "Neutron cross section evaluations for actinides at intermediate energies. Pu." at the 11th International Conference on Emerging Nuclear Energy Systems ICENES 2002, Albuquerque, New Mexico, USA, 29 September-4 October 2002.

A.N. Sosnin, project participant from JINR, Dubna, was on business trip in Germany on 16-22 September 2002. He met with Dr. C.Broeders, project collaborator, for discussing possibility of application of the multi-group constant system being under development for sub-critical blanket characteristic calculation used in the experiments carried out in the frames of the Project 1372.

**III. Current Technical Status.**

The Project activities are carried on schedule in accordance with the Work and Calendar plans with implementation of the activities in accordance with the sub-task 5.5 ahead of schedule.

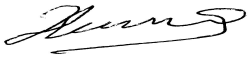

Project Manager E.Ya. Smetanin

# *ISTC-1606 progress development meeting – 16-18 December, 2002 at Moscow*

## *Minutes of t he meeting (Draft)*

*Short reminder on the project #1606:*

Title: Experimental Mock-Up of Molten Salt Loop of Accelerator-Based Facility for Transmutation of Radioactive Waste and Conversion of Military Plutonium.

Stage 2: Experimental Study of Molten Salt Technology for Safe, Low-Waste and Proliferation Resistant Treatment of Radioactive Waste and Plutonium in accelerator-driven and critical systems.

Main participants: Russian Federal Nuclear Center - Institute of Technical Physics ( VNIITF ), Snezhnisk (before – Chelyabinsk) one of the main weapon laboratories in the Soviet Union and currently in Russia as well.
Russian Research Center – Kurchatov Institute ( RRC-KI )

Agenda for the meeting – see Appendix A.

**M. Hugon** (EC) presented the EC projects of the 5th framework program in the transmutation and separation field. The links of the EC projects with the ISTC projects was underlined. Information on the time schedule and the fields of interest for the 6$^{th}$ framework program was given.

**M. Delpech** (CEA) presented briefly the status of the MOST project : the document on scenarios and main characteristics of the MSR projects is written. The table of content and some draft of thematic documents (chemistry, reactor physics, dynamic behaviour, salt processing, ...) are done and final documents are due for June 2003. MOST will finish end of October 2003. The link with the ISTC 1606 project and the contribution of V. Ignatiev is appreciated by the MOST partners.

**A. Gagarinski** (KI) presented the studies on innovative systems in the frame of INPRO and GEN IV. For Gen IV concepts, the Russian experience was presented : SCWR (20 years of R&D), VHTR (30 years of R&D, maximum temperature reached : 3000°K), MSR (30 years of R&D), Na FBR (50 years of R&D, BN350, BN600 and soon, BN800), LBE FR (30 years of R&D and 80 reactor.year of operation), Gas FBR (20 years of R&D).

A. Lopatkin (Minatom) presented the status of the studies : for the short term : use of existing technology and then implementation of the Fast Spectrum reactors for transmutation in 2050. The thorium in a thermal spectrum is foreseen for after 2050. This will leave time for R&D for the FBR (reactor technology and cycle facilities) and the MSR. The curium will be store during 50-100 years. The scenarios were studied on this hypothesis and taking into account the uranium resources with a lower cost than 130$ per tons ????. In these conditions, VVER can produce 650 tons of Pu. For Minor actinide recycling, homogeneous recycling, using nitride fuel is foreseen as a reference in a FBR. The alternatives are ADS, MSR.

V. Ignatiev and K. Grebenkine presented the status of the ISTC-1606 project. The project ...

**Neutronic calculations :**
One scenario was studied : Pu and MA transmutation without uranium or thorium support in a MSR. After validation of the code by doing comparison with the results obtained for AMSTER project, the DMSR (ORNL) project and with the calculation done at ISN, the sensitivity study used input data provided by CEA and EDF for the Plutonium and MA compositions. The optimisation of the concept is a MSR without graphite moderator in the core, with salt processing period of one year.

**Prediction of the physicochemical properties :**
The properties of the 3 salts were calculated for the density, viscosity, heat capacity, thermal conductivity using interpolation of the binary fluorides properties. These calculations were validating by some experimental measurements.

**Preparation of the molten salt components:**
The elements are prepared under argon and $HF/H_2$ atmosphere in order to get low impurities content.

**Phase diagram verification**

Three salts were chosen for salt characteristics measurements:

| in mol % | LiF | NaF | $BeF_2$ |
|---|---|---|---|
| Salt A | 7.1 | 64.1 | 28.8 |
| Salt B | 20 | 56.6 | 21.4 |
| Salt C | 14.3 | 59 | 26.7 |

Complementary and in order to determine more precisely the eutectic point, 3 others salts was studied:

| in mol % | LiF | NaF | $BeF_2$ |
|---|---|---|---|
| Salt D | 13 | 58 | 29 |
| Salt E | 15 | 58 | 27 |
| Salt G | 17 | 58 | 25 |

For these salts, the measurement of the phase change was determined using the technique of temperature measurements during heating or cooling with constant rates; a temperature peak shows the phase change. E was determined as the eutectic point (479°C $\pm$ 1 °C);

**Preliminary experiments of An Solubility :**
The salt used in the preliminary step for the first measurements is FLiBe salt. The experimental techniques were presented. It is expected to measure the solubility limit with a precision of 10%. The first measurement will be done in December and, in January for the salt E in a temperature range of 500°C / 700°C.

**Viscosity measurement :**
The experimental techniques were presented in detail (Torsional oscillation of cyclindrical crucible). The measurment is done under inert atmosphere and are done for the salts A and C.

**Thermal conductivity :**
The experimental method was validated on alcohol and on Helium in a large range of temperature. The measures were done for the salt A in a range of temperature between 500°C and 750°C, with a precision of 10%.

**Measurement of the potential for An/Ln separation (electrochemical potential) :**
The formation energy (Gibbs) for the La, Ce, Nd depending on the temperature was measured and calculated. The reduction potential of the Lanthanides in the molten salt was measured by using voltametric techniques and chronopotentiometry, in order to evaluate the Ln extraction from the salt (LiF-NaF-$NdF_3$-$LaF_3$-$ZrF_4$ at 0.5 mol%). Then, the extraction of the Ln was evaluated for a salt with Beryllium, knowing that Be could be extracted before some others F.P. It is also evaluated that An could be extracted before the Be but experimental data are needed for this. The experiment on the FLiBe salt was the extraction of the La from the salt.

**Oxide solubility :**
The order of precipitation of the oxide in the salt is : Zr, U - Pu (+4) – Be – Pu(+3) – Al – Am, Ce – Ln in the FLiBe salt. The base for using oxide separation for salt processing is :

$$LnF_3 + Ln_2O_3 \rightarrow 3\ LnOF$$

It means that by adding some oxide of PF, we could have precipitation of a fluoride oxide in the salt. But the oxidation of Pu is more difficult. The experience will be conducted on the salt FLiBe, the salts A and E on the oxide of Ln solubility.

**Reductive extraction :**
ORNL has used Bi as metallic phase. One alternative could be Cd or Al. The metallic phase is enriched in Li in order to catch the Ln in the metal after Li exchange :

$$EuF_2 + 2\ Li_{(Bi)} \rightarrow 2\ LiF + Eu_{(Bi)}$$

The experiment was done with a FLiBe salt and Bi metal for Ce, Nd, U, Eu in order to determine the decontamination (or separation) factor (D) that is expected to be between 1000 and 300. This part is not included in the ISTC project.

**Corrosion design test loop :**
The loop will integrate control and redox measurements and the purpose is to perform corrosion test on various Nickel alloys or stainlessteel, without or with Pu. The temperature gradient in the loop will be 100°C, the length of the convection part is 1.2m with a diameter of 6 cm. The maximum temperature in the loop will be 750°C. The power is 6 to 8 kW. The material is Nickel (99.9%). The salt mass is 13 kg. The thermohydraulic was validated on the previous loops in KI. The salt specification was given (impurities content). The loop and the tank will be under inert atmosphere (Argon). To fill the loop of salt, the following operations are planned:
loop section : argon to purify the loop and the nickel in cold and then, in hot conditions (600°C) during 2 or 3 hours.
tank section : powder of salt will be cleaned firstly by using argon, then heated to melt the salt and then cleaned by using HF/$F_2$ gas. This operation needs 2 or 3 days ???.

This will allow to have a clean salt and to measure properly the corrosion of the sample. The samples are analysed before (element compositions, mechanical characteristics and structural analysis) and after the corrosion test.

**Redox-potential measurment:**
Different reference electrodes can be used : metallic, gas or ceramic one. The techniques (DRPM) developed for redox control to be used in the loop for the salt chosen (E) has a reference electrode in Mo, a glassy carbon as anode and a Mo cathode (working electrodes). The tests of these techniques were tested with the salt C, using different pulse time and impurities level ($CeF_3$). The precision of the measure is improved by enlarging the pulse period. The working range is from 10mA to 500mA with pulses between 1s to 200s. The precision is $\pm$ 5mV.

**Conclusion :**
The work done in the frame of ISTC-1606 project is evaluated by the European collaborators (A. Rieneski, W. Gudowski, M. Hugon and M. Delpech) as a good work, getting the information, having experimental values for the salt properties, for the processing of the salt. The loop is build seriously and the test program is already defined. The loop will be transfer soon to Snezhnisk/Chelyabinsk. The project is performing what was expected with good exchanges between Russian teams and European teams.

Appendix A.

# PROGRAM

ISTC#1606 progress development meeting

(16-18.12.2002, Moscow, RRC Kurchatov Institute)

***16.12.2002***

$9^{30}$ Pick-up and transfer to RRC KI

$10^{00}$ Welcome, introduction of participants, approval of agenda

$10^{30}$ EC programs on P&T *(Michel Hugon, EC)*

$11^{00}$ Status of MOST Project *(Marc Delpech, CEA)*

*$11^{30}$ Coffe-break*

$11^{45}$ Innovative reactor & fuel cycle concepts studies at KI *(Andrei Gagarinski, KI)*

$12^{00}$ Minatom activities on P & T *(Aleksandr Lopatkin, Minatom)*

$12^{15}$ WP1: # 1606 Status *(Konstantin Grebenkine, VNIITF)*

*$13^{00}$-$14^{30}$ Lunch*

$14^{30}$ WP2: Possible role of MSR in the future nuclear power *(Stas Subbotine, KI)*

$15^{00}$ WP2: Models for neutronics calculations *(Olga Feinberg, Andrei Miasnikov, KI)*

*$16^{00}$-$16^{15}$ Coffe-break*

$16^{15}$ WP5: Preparation of molten salt components *(William Mashirev, VNIIkHT)*

$16^{45}$ Discussion

$17^{00}$ Adjourn

***17.12.2002***

$9^{00}$ Pick-up and transfer to RRC KI

$9^{30}$ WP3: Phase diagram, $AnF_3$ solubility *(Vladimir Subbotine, Alex Panov, VNIITF)*

$10^{30}$ WP3: Prediction of physicochemical properties *(Vladimir Khoklov, IVTEX)*

*$11^{15}$ Coffe-break*

$11^{30}$ WP3: Measurements of heat conductivity and viscosity *(Aleksandr Merzliakov, KI)*

$12^{15}$ WP3: An/Ln standard potentials and RE's recovery *(Raul Zakirov, KI)*

*$13^{00}$-$14^{30}$ Lunch*

$14^{30}$ WP3: Oxides solubility and precipitation *(Vladimir Gorbunov, KI)*

$15^{00}$ WP3: Reductive extraction *(Yuri Vereshagin, KI)*

$15^{30}$ WP4: Corrosion test loop design *(Aleksandr Surenkov, KI)*

$16^{30}$ WP4: Redox-potential measurement *(Valery Afonichkin, IVTEX)*

$17^{00}$ Discussion

$17^{15}$ Adjourn

***18.12.2002***

$9^{00}$ Pick-up and transfer to RRC KI

$9^{30}$ Visit of Molten Salt facilities

$11^{00}$ Visit to Pebble-Bed Gas Cooled Pile - Astra

$12^{00}$ Discussion, Signing the protocol

*$13^{00}$-$14^{00}$ Lunch*

$14^{00}$ Adjourn

Appendix B.

## *LIST of participants*

ISTC#1606 progress development meeting

(16-18.12.2002, Moscow, RRC Kurchatov Institute)

**CEA**
*Marc Delpech*

**EC**
*Michel Hugon*

**FZK**
*Andrei Rineiski*

**KTH**
*Waclaw Gudowski*

**ISTC**
*Gill Won Suh*
*Lev Tocheny*

**RRC-KI**
*N. Ponomarev-Stepnoi*
*A. Gagarinski*
*V. Ignatiev*
*S. Subbotine*
*O. Feinberg*
*M. Kalugin*
*A. Mjasnikov*
*R. Zakirov*
*Yu. Vereschagin*
*A. Merzliakov*
*V. Gorbunov*
*A. Surenkov*
*I. Gnidoi*
*R. Gudimov*
*S. Konakov*

**VNIITF**
*K. Grebenkine*
*V. Subbotine*
*A. Panov*

**IVTEX**
*V. Afonichkin*
*V. Khoklov*

**VNIIkHT**
*W. Mashirev*

**MINATOM**
*A. Lopatkin*

DRAFT

# Conclusions from the first project #1606 progress review meeting in Moscow, Kurchatov Institute, December 16-18, 2002.

***Russian Participants:***

RRC-KI, Moscow
Dr. V. Ignatiev
Prof. A. Gagarinski
Dr. S. Subbotine
Dr. O. Feynberg
Dr. A. Myasnikov
Dr. R. Zakirov
Dr. A. Merzliakov
Dr. V. Gorbunov
Dr. A. Surenkov
Dr. S. Konakov

VNIITF, Snezhinsk
Dr. K. Grebenkine,
Dr. V. Subbotine

IHTE, Ekaterinburg
Dr. V. Afonichkin
Prof. V. Khoklov

VNIIkHT, Moscow
Prof. W. Mashirev

MINATOM
Dr. A. Lopatkin

***Foreign Participants*:**

Dr. Marc Delpech, CEA-Cadarache, EU

Dr. Michel Hugon, CEC, EU

Prof. Waclaw Gudowski, KTH, EU

Dr. A. Rineiski, FZK, EU

Dr. Gill Won Suh, ISTC, Moscow

***1 – Status of the project :***

The project #1606 has 3 years duration since February 1, 2001 till to February 2004. The general mission of the Project # 1606 still remain to perform an integral reevaluation of the Molten salt Technology potential as applied to safe, low-waste and proliferation resistant management of TRUs in critical and subcritical systems.

The project #1606 is carry out in close co-operation with EC MOST project that is focused on analysis of the MSR technology potential to service future Nuclear Power development.
Current stage of #1606 is applied to examine, mainly experimentally, potential of Molten Salt Advanced Reactor Transmuter (MOSART) for TRU in Th-U free FLiBe based stream.

The aim of the meeting was to review with foreign EC collaborators and Russian project participants the project progress as well as co-ordinated actions for its further development.

During the meeting in foreign collaborators contributions, the current and future EC programs on P&T (M. Hugon), including possible role of molten salt technology, as well as the status of EC MOST project (M. Delpech) were explained. From Project side, its management (K. Grebenkine & V. Ignatiev) presented ISTC#1606 Status. After that, key Russian project participants contributed with detailed reports devoted to project subtasks (WP2-WP5), including:

- WP2: Reactor physics & fuel cycle consideration

- WP3: Experimental study of behavior and fundamental properties of Na,Li,Be/F system
- WP4: Experimental verification of candidate structural materials for fuel circuits
- WP5: Preparation of Na,Li,Be/F salt components

List of all presentations and summary of contributions made by key project #1606 experts at progress review meeting is attached. The presentations were accompanied by detailed discussions, and foreign collaborators had opportunity to ask any questions on the project execution.

The collaborators visited project workplaces at RRC-KI site. Experimental facilities used for the project execution were demonstrated, including the natural convection corrosion loop, which is now under construction and preliminary testing at RRC-KI. According workplan test section should be filled by Na,Li,Be/F salt and moved to Snezhinsk for further studies at VNIITF site by April 2003.

It was concluded that:

- The project is conducted on schedule.
- The technical results of the project are delivered according to project workplan.
- In general, the project implementation is successful.

***2 – Recommendation on the project further development:***

Agreement has been achieved between the project management and the foreign collaborators to continue the further project development after the current stage ISTC#1606 completion in Feb.2004.

It was decided to explore possible two options (G.W. Suh, K. Grebenkine, V. Ignatiev) for support of continuation of the project team efforts:

1. Prolongation of the existing project 1606, according the scope of work prepared for first version of the project #1606 proposal and taking into account new knowledge received within current project stage execution. Remind, that due to budget available about half of scope proposed initially (particularly, significant part of experiments with salts, containing actinide trifluorides) was avoid at current stage of the project execution. The budget requested for project proposal at that time was one million Euros.
2. Development of the new project proposal. Certainly, this option will need more time for next stage of project start up.

The discussions with foreign collaborators on workplan for the prolonged project 1606 as well as new project proposal will be continued by electronic mail. It is proposed for option (1): to get approval of workplan for prolonged project from foreign collaborators (M. Delpech, M. Hugon) during the next MOST project meeting in June. If option (1) will not supported by EC, discussion on option (2) can be finalized by approval of new proposal during the next ISTC#1606 project review meeting in Snezhinsk.

***3 – The next project progress meeting:***

It was suggested that the next project progress review meeting will take place in Snezhinsk, in 4$^{th}$ quarter, 2003.

***4 – The project 1606 budget correction:***

In the 2$^{nd}$ quarter of the project execution its budget had been reduced by 25% due to the conversion rate between Dollar and Euro existed at that time. Dr. G.W. Suh informed the project management that now ISTC is reimbursing part of the reduced funding of the projects supported by EC. It is performed by means of the budgets correction that should be made 2 quarters before the project completion date.

It has been concluded that in July 2003 ISTC will inform the project about the ultimate amount of the returned funding, and appropriate correction of the project workplan and budget will be implemented, immediately.

## *Appendix1. List of presentations made at project #1606 progress review meeting*

1. Welcome, introduction of participants, approval of agenda
2. EC programs on P&T (Michel Hugon, CEC)
3. Status of MOST Project (Marc Delpech, CEA)
4. Innovative reactor & fuel cycle concepts studies at KI (Andrei Gagarinski, KI)
5. Minatom activities on P & T (Aleksandr Lopatkin, Minatom)
6. Project # 1606 Status (Konstantin Grebenkine, VNIITF & Victor Ignatiev, KI)
7. Models for neutronics calculations (Olga Feynberg, Andrei Myasnikov, KI)
8. Prediction of physicochemical properties (Vladimir Khoklov, IHTE)
9. Possible role of MSR in the future nuclear power (Stas Subbotine, KI)
10. Phase diagram, $AnF_3$ solubility (Vladimir Subbotine, VNIITF)
11. Measurements of heat conductivity and viscosity (Aleksandr Merzliakov, KI)
12. An/Ln standard potentials and RE's recovery (Raul Zakirov, KI)
13. Oxides solubility and precipitation (Vladimir Gorbunov, KI)
14. Corrosion test loop design (Aleksandr Surenkov, KI)
15. Preparation of molten salt components (William Mashirev, VNIIkHT)
16. Redox-potential measurement (Valery Afonichkin, IHTE)
17. Visit of Molten Salt facilities and accompanying talks (V. Ignatiev, A. Surenkov, R. Zakirov, A. Merzliakov, V. Subbotin).

## *Appendix2. Summary of presentation made by key Project participants*

<u>WP2: Models used for neutronics calculations (Olga Feynberg, Andrei Myasnikov -KI)</u>

Adaptation and development of theoretical models and methods for neutronics calculations of MSR cores fuelled by TRU's trifluorides and operating in different fuel processing modes have been discussed. Particularly, test calculations, including verification of the codes basing on the available data (e.g. for MSBR, DMSR, AMSTER concepts) were made.

The optimization calculations included three "double component" scenarios of the MOSART start up loading and feeding by TRU from spent PWR fuel. The cell optimization calculations were done for different core configurations depending on volume fraction of salt in the core (salt / graphite ratio 5-100%), solvent system (Li,Na,Be/F; Li,Be,Zr/F and Na,Zr/F), reactor spectrum, neutron flux density (taking into account fuel inventories outside core), feed material composition, the duration of the fuel cycle.

Adaptation and development of theoretical models and methods also, included the work on improving of the schemes (MCU+ORIGEN-S and MCNP4B+ORIGEN-2) in order to provide codes ability for the TRU's recycling and soluble fission products removal in batch or on-line modes.

Claim is made that it is feasible to design single stream Na,Li,Be/F critical reactor fueled only by TRU from PWR spent fuel while equilibrium An+Ln concentration is truly below solubility limit (<1.0-1.5mole% depending on fueling scenario and removal times for soluble fission products). The optimal spectrum is fast with significant epithermal component (homogeneous core). In order to decrease losses to waste removal times for soluble fission products should be increased up to 3-5 years.

Finally, on the base of transmutation effectiveness, comparison for MOSART core loadings will be developed. Note, that for closed fuel cycle to give the realistic evaluation of MOSART transmutation efficiency for different scenarios, calculation scheme at the next stage of the Project should carefully take into account the actinide's losses to waste in multiple recycling.

WP3: Phase diagram, actinide trifluorides solubility (Vladimir Subbotine - VNIITF)

The measurements on phase behavior were carried out for five Na,Li,Be/F salt compositions. Measured melting temperatures of initial components and standard substance are in good agreement with ORNL published data. It confirms applicability of our technique.

Phase transition behavior studies reccommended to place main experimental emphasis in further studies within the WP2-WP4 on salt composition 15LiF-58NaF-27$BeF_2$ with liquidus temperature 479°C. Salt composition 17LiF-58N aF-25$BeF_2$ with melting temperature of 494.. 496 $^{o}$C could be also of interest for further studies.

The technique and first preliminary results of experiments underway on measurement of plutonium and lanthanides trifluorides solubility for selected salt composition were discussed in details.

WP3: Prediction of physicochemical properties for selected salt compositions (Vladimir Khoklov- IVTEX)

The computation technique and experimental data on binary salt compositions were successfully used for prediction of the transport properties for different ternary and quaternary salt compositions. Main result is estimation of the transport properties (density, heat capacity, viscosity, thermal conductivity as well as expansivity) for chosen solvent compositions in the temperature range of 800-1000K.

WP3: Measurements of heat conductivity and viscosity (Aleksandr Merzliakov - KI)

The technique of measurements was presented. Experimental data on kinematic viscosity measurement of two Na,Li,Be/F salt compositions are processed in the temperature range from liquidus up to 800 $^{0}$C. Correlation dependences are proposed. Accuracy of measurement (dispersion) 4 - 6 %. Comparison of the KI experimental data with the modeling estimations (dashed lines) executed by IHTE in previous section, has shown coincidence of estimations to experimental data at high temperatures ($800^{0}C > T > 600^{0}C$), and significant deviation at temperatures close to liquidus temperature. Note, that KI experimental data in that temperature range are in good agreement with the earlier ORNL data for close Na,Li,Be/F compositions, where viscosity measurements were done in the temperature range of 600-800 $^{0}$C with three different instruments.

Thermal conductivity of Na,Li,Be/F molten salt composition is measured in temperature range 500-750 $^{0}$C with accuracy (dispersion) 15 %. It is interesting to compare the results received in the present work with results of modeling estimations done by IHTE in previous Section as well as ORNL experimental data. ORNL paper gives the thermal conductivity value of 1 W/ m/K for two compositions NaF-$BeF_2$ and NaF-LiF-$BeF_2$. KI experimental data are in a good agreement with IHTE modeling estimations. Also, at high temperatures (about 750 $^{0}$C) KI data closely correlate with the ORNL experimental data, but the discrepancy increase with the temperatures decrease down to $500^{0}$C.

WP3: An/Ln standard potentials and RE's recovery (Raul Zakirov - KI)

The experimental technique and results of experiments on measurement of standard potentials in the system lanthanide / lanthanum trifluoride / lead difluoride in temperature range 300-$500^{0}$C for cerium and neodymium were presented. The received experimental data as well as further program for further experiments with actinides were discussed.

The results on electrochemical measurements of electrolysis of lanthanides trifluorides from Na,Li/F and zirconium tetrafluoride from Na,Li,Be/F composition were presented.

WP3: Oxides solubility (Vladimir Gorbunov - KI)

The behaviour of molten fluoride system such as Na,Li,Be/F, is markedly affected by appreciable concentration of oxide ion. The technique of measurement of plutonium and lanthanides oxides solubility in a salt compositions by a method of isothermal saturation were presented and discussed in details. Oxides solubility for 58NaF-15LiF-27$BeF_2$ (mole%) at 650-750 $^oC$ and 40NaF-60LiF (mole%) at 800 $^oC$ have been measured within ISTC#1606. The solubility of tetravalent metals (U, Pu, Zr, Ce) oxides in both systems is low. Differ from Na,Li/F system for Na,Li,Be/F system concentration of trivalent rare earths $La_2O_3$ and $Nd_2O_3$ increased with oxides addition according to reaction: $3BeF_2 + Ln_2O_3 \longrightarrow 3BeO + 2LnF_3$.
It was not found tendency for plutonium as $PuF_3$ to precipitate as oxide.

WP4: Corrosion test loop design (Aleksandr Surenkov - KI)
The technical working project of facility (including its already manufactured components) for investigation process of corrosion and mass transfer of structural materials in dynamic non-isotherm conditions with control of changing salt solvent redox potential of composition 15LiF-58NaF-27BeF2 with further addition of $PuF_3$ were presented and discussed. It was confirmed that corrosion studies will involve 3 types of container material samples: RF HN80MTY, US Hastelloy NM and Czech MONICR. Last one were provided within EC MOST and ISTC#1606 co-operation. The developed facility permits to lead tests of candidate structural materials for MOSART with minimal temperature of circulated fuel salt up to 550-600oC, temperature salt heat up 80-100oC and salt flow rate up to 5 cm/s (Re > 3000).
All designed systems of facility important for reliable control of parameters and facility operation were considered. Development of system and devices allowing to provide purity of salt required and make sampling of the melt as well correction of salt composition by the addition of $PuF_3$ and fission product simulators, gas, solid oxidants (HF-$H_2$, $FeF_2$), reducers ($H_2$, Be, Zr) and perhaps buffers for control of salt redox potential were described. Draft of corrosion tests program for chosen nickel-molybdenum alloys was discussed.

WP4: Technique for redox-potential measurement (Valery Afonichkin, IVTEX)
Developments on the technique for redox potential maintenance and control in the corrosion test loop was discussed. Preliminary tests of the laboratory model of the device for redox potential measuring (DRPM) in the Na,Li,Be/F solvent system and in mixture with addition of 0.1 mole % $CeF_3$ (simulator of $PuF_3$) at 600 °C allowed to determine optimal conditions for formation of the dynamic beryllium reference electrode, which ensures reproducibility of the redox potential values for the melt (h = 3 mm, I = 10-100 mA, $\tau$ = 1- 50 sec). It was shown that the proposed DRPM has a high sensitivity to changes in the redox potential of the melt and provide measurement of these changes within ±5 mV.
Test section fabricated for corrosion loop is delivered to KI and presented to meeting participants. Recommendation for further studies on DRPM, including experiments with active salt containing $PuF_3$ were also given.

WP5: Preparation of molten salt components (William Mashirev, VNIIkHT)
The technique of salt components (LiF, NaF, $BeF_2$) as well $PuF_3$ and fission product simulators preparation, including its purification procedure, for experiments within WP3-WP4 was presented. The schedule as well as optimal procedure for additional purification at VNIIkHT and transfer of salt composition for corrosion loop to KI were discussed and approved.

# Minutes
# Of the St.Petersburg meeting 25.03.02 – 26.03.02

**Participants:**

Dr.F. Balbaud - CEA/Saclay (France);

Dr.D.Gomez Briceno - CIEMAT-DFN (Spain);

Prof.W.Gudowski – RIT (Sweden);

Dr.G.Mueller, Dr.G.F.K.Heusener, Dr.A.Weisenburger - FzK (Germany);

Acad.V.Glukhikh, Dr.B.Yatsenko, Dr.V.Engelko, Dr.K.Tkachenko, Dr.A.Yudin - D.V.Efremov Institute of Electriphysical Apparatus, St.Petersburg;

Dr.A.Rusanov, Dr.G.Khorasanov – IPPE, Obninsk;

Prof.G.Karzov, Dr.V.Markov, Dr.V.Yakovlev -CRISM "Prometey", St.Petersburg.

**Agenda**

23.03 – Arrival. Diner at 19.30.

25.03 – Working day in Efremov Institute:

- 10.00. V.Glukhikh, Director of the Efremov Inst. Welcome.
- 10.15. V.Engelko. General description of the ISTC project No.2048. Work plan.
- 11.00. A.Rusanov. IPPE project activities.
- 11.30. V.Markov. PROMETEY project activities.
- 12.00. Break.
- 12.30. Dolores Gomez Briceno. Ciemat participation in the project.
- 13.00. Fanny Balbaud. CEA participation in the project.
- 13.30. G.Mueller. FzK participation in the project.
- 14.00. Lunch.
- 15.00. Visit to the laboratory of pulsed electron accelerators.
- 16.00. Discussion.
- 17.00. Transport to the Hotel.

26.03. – Working day in PROMETEY:

- 11.00.- 13.00. Visit to corrosion test facilities.

- 13.00. Lunch.
- 14.00. Discussion.
- 15.30. Transport to the Hotel.

**25.03.02.**

Prof. V.Glukhikh presented general information about the Efremov Institute: structure, activities in the fields of particles accelerators, plasma devices, laser facilities, electrotechnical equipment development and manufacture.

Dr.V.Engelko presented information concerning the development of pulsed electron accelerators and application of pulsed intense electron beams for improvement of hardness, corrosion and wear resistance, fatique strength of metals and alloys. These effects were realized in some applications such as: an increase of life-time of turbine blades of electric power generators, wear resistance of elements of automobile engines, corrosion resistance and fatique strength of aircraft engines turbine blades. Then he described the aim and main objectives of the ISTC project No.2048, work plan and roles of participating Institutions.

Dr. A.Rusanov and Dr. V.Markov presented an information about the IPPE and Prometey activities in the ISTC Project No.2048. These Institutions are responsible for corrosion tests. It is planed: to perform the tests of samples with and without surface modification in the flow of Pb and Pb-Bi alloy during up to 10000 hours at temperatures of 550-650 $^{o}$C and in the wide range of the of oxygen content, at stressed and not-stressed conditions; to study of the coatings stability at thermo-cycling in Pb-Bi allow and their behavior under conditions of base spreading. The analysis of properties of materials, coatings and surface alloys before and after modification, before and after testing at liquid-metal loops will be done by all participating Institutions.

Dr. Gomez Briceno informed participants of the meeting about the research center CIEMAT, fields of its activities and in more details about the department of fision (DFN). This department is equiped very good with different types of diagnostics for materials properties investigations. This diagnostics will be used in the frame of the ISTC project for investigation of samples after corrosion tests.

Dr. F.Balbaud presented an information concerning static and dynamic corrosion test of austenitic and martensitic steels in Pb-Bi alloy, performed in CEA Saclay. Participation in the ISTC project No.2048 was discussed.

Information presented by Dr .G.Mueller was devoted to the Karlsruhe Lead Laboratory KALLA – facilities, stagnant and loops experiments, numerical codes, etc. He also informed concerning works performed in IHM on applications of pulsed electron beams (GESA facilities) for an increase of the corrosion resistance of materials in heavy metal coolants. FZK participation in the project is connected with the choice of materials, preparation of samples, investigation of their properties, study of the electron beam interaction with solid materials.

Dr. G.Khorosanov and A.Yudin presented a new ISTC project - "Investigation of processes of high - performance laser separation of lead isotopes by selective for development of environmentally clean perspective power reactor facilities". Summary of this project was passed to interested persons.

**26.03.02.**

Participants of the meeting have visited the Prometey Institute.

Prof. G.Karzov – deputy director of the Institute described main its activities. Special attention was paid to works connected with development of nuclear reactors with water, sodium, lead, lead-bismuth and helium coolants.

Four operating facilities ( X6, X2, X3 and AIMA ) with Pb and Pb-Bi coolants were demonstrated. The facilities are provided with the oxygen control systems. They allow to perform long time tests under stressed and unstressed conditions, creep tests, thermo-cycling, etc.

In the course of discussion the main results of the meeting were formulated in the protocol, signed by representatives of the collaborating Institutions. The protocol is enclosed.

# Protocol of work meting
# under the project ISTC ? 2048
# (St. Petersburg, 23.03.02-26.03.02)

1. Participants of the seminar:
   Dr.G.Mueller, Dr.G.F.K.Heusener, Dr.A.Weisenburger - FZK (Germany);
   Dr.F. Balbaud - CEA/Saclay (France);
   Dr.D.Gomez Briceno - CIEMAT-DFN (Spain);
   Prof.W.Gudowski - RIT (Sweden);
   Dr.B.Yatsenko, Dr.V.Engelko, Dr.K.Tkachenko - D.V.Efremov Institute of Electriphysical Apparatus;
   Dr.A.Rusanov - IPPE;
   Prof.G.Karzov, Dr.V.Markov, Dr.V.Yakovlev -CRISM "Prometei".

2. Dr.V.Engelko has reported about activities in the field of modification of a materials surface in NIIEFA and available equipment for these purposes. Dr.A.Rusanov and Dr.V.Markov have reported about available in IPPE and CRISM "Prometei" facilities for carrying out materials specimens tests. Dr.D.Gomez Briceno has reported about CIEMAT-DFN activity, corrosion tests and capability of realization of researches of material properties.
   Dr.F.Balbaud has reported about CEA/Saclay activities in corrosion tests and researches of material properties.
   Dr.G.Mueller has reported about available in FzK facilities for realization of corrosion tests and activities on material surface modification in FzK.

3. During the discussion the participants have considered the possible directions of collaborators participation in activities under the project. The participants of seminar have agreed about the following:
   1. European steels T91, 1.4970, HT9 are selected for realization of activities under the project.
   2. FzK delivers samples of steels 1.4970 and HT9, and CEA/Saclay - T91.
   3. Samples have form of rods: ∅15 mm (the length is multiple 30 mm) and ∅25 mm (the length is multiple 100 mm).
   4. Part of specimens after pulse electron-beam modification and corrosion tests should be send to collaborators for the analysis of material properties.

Manager of the ISTC project ? 2048

_____ Dr. V.Engelko

Collaborators of the ISTC project ? 2048

_____ Dr. G.Mueller

_____ Dr. F. Balbaud

_____ Dr. D.Gomez Briceno

# Project 2068 - Development and demonstration of HLW partitioning technology with the use of phosphorylated calixarenes.

***Project duration: 3 years, April 2002 - March 2005***

*Objectives planned*

Effective and economic partitioning of waste resulting from nuclear power remains one of the most complicated problems of radiochemical industry. Long-lived isotopes and actinide elements in particular are the most hazardous components of nuclear power waste. Their separation from the waste bulk and individual burial or partitioning (transmutation) will permit significantly to increase the ecological safety and efficiency of nuclear fuel cycle. The extraction technology of radwaste partitioning with the use of organophosphorus extractants is fully suited for solving this problem.
The widely used monodentate extractants such as different-radical phosphine oxide (POR) have low capacity and insufficient selectivity and do not provide recovery of actinides and other hazardous radionuclides from acidic high-level waste (HLW). A promising method for modification of extractant properties is concerned with attachment of donor phosphoryl groups to calixarene rigid platform. In such compounds the extractant donor centers can be best arranged around a metal cation, which considerably increases the efficiency and selectivity of extraction process. In the framework of INCO-COPERNICUS (IC15-CT98-0208) project the Russian and Ukranian specialists have detected the high extraction ability of calix-4-arene with dibutylphosphine oxide groups towards Eu and Am. This result allows to direct lines of studies on development of efficient and selective extractants on the basis of phosphorylated calixarenes.
For realizing the potential of such calixarenes it is necessary to select specific extractants and diluents, to establish conditions of radionuclide extraction and stripping, to arrange a flowsheet providing the needed HLW purification from long-lived radionuclides. Thus, the project is aimed at developing the scientific fundamentals of HLW partitioning technology with the use of new extractants - phosphorylated calixarenes and at checking the efficiency of this technology with actual HLW.
Advantages of such extractants are as follows:
- efficient recovery of target radionuclides from HLW;
- possibility of using the diluted extractant solutions (below 0.1 M) for radionuclide recovery;
- minimal co-extraction of acid and neutral salts;
- possibility for recovery of actinides into an individual fraction by selective stripping;
- possibility for joint recovery of actinides, rare-earth elements, technetium, ruthenium and other platinum elements.

The project execution should results in the following:
- extraction properties of new phosphoryl-containing calixarenes will be studied;
- main factors affecting the efficiency and selectivity of radionuclides extraction by phosphoryl-containing calixarenes will be determined;
- a variant of HLW partitioning flowsheet will be developed with the use of

phosphoryl-containing calixarene as extractant;
- laboratory testing of main operations for recovery and separation of radionuclides by using actual HLW.
Thus, the execution of a series of investigations under the project should permit to propose a new version of HLW extraction partitioning which allows to recover and separate long-lived radionuclides for their subsequent immobilization.

Objectives achieved up to date In accordance with the Work plan in the first year the study on extraction properties of phosphorylated calixarenes and simulated phosphine oxides was started.

The main results presented in quarter reports (see attachment)

Objective altered or changed with or without the consensus of the collaborators
No

Difficulties experienced
No

Already published papers
No

Plans to apply for prolongation or new projects logically related to the current project
Will be determined later.

Igor Smirnov,
Team Leader,
Khlopin Radium Institute,
28, 2-nd Murinskiy, St.-Petersburg, 194021, Russia

tel. 7-812-2475845
fax 7-812-2478095
e-mail: igor_smirnov@atom.nw.ru

**Scientific and Technical Quarter Report**
**Project N 2068**

# Development and demonstration of HLW partitioning technology with the use of phosphorylated calixarenes.

1. Laboratory research on extraction ability of phosphorus-containing calixarenes

1.1. Screening studies

April – June 2002

All the Project participants were engaged in this work.

During the first quarter the following work was carried out in accordance with the Project Work Plan.

## 1.1. Screening studies

In accordance with the Work plan in the first quarter the preliminary studies concerned with preparation of initial aqueous metal solutions, checking of analytical procedures and research on extraction of elements by conventional organophosphorus extractants were conducted.

### Extraction of europium, americium and technetium

The extractants synthesized and purified at Institute of Organic Chemistry of Ukranian Academy of Sciences (Kiev). 3-nitrobenzotrifluoride (NBTF) of "Rhodia" Co (France) was used as a diluent. Other reagents were made by "Vekton" Co (St. Petersburg). $^{152}$Eu, $^{241}$Am, $^{99}$Tc – isotopes were produced by "Isotop" Co (St. Petersburg). Extractant solutions were prepared by precise weighed portions.

In order to determine the metal distribution coefficients, 1.5 ml organic and aqueous phases each with needed composition were placed into a polypropylene stopped flask, were stirred at 22-24$^{o}$C for 5 min, phases were separated by centrifuging and the metal content was determined in both phases by radiometry through γ-emission of corresponding isotope. The radiometric measurements were performed by scintillation γ-spectrometer «DeskTop InSpector» based on NaJ-detector 51×51 mm with a well ("Canberra" Co). Error of radiometric measurements was no more than 10%.

We selected different-radical phosphine oxide ($(C_{7\text{-}9}H_{15\text{-}19})_2C_5H_{11}P(O)$, POR) and diphenyl-N,N-dibutylcarbamoylmethylenephosphine oxide ($Ph_2P(O)CH_2C(O)N(C_4H_9)_2$, CMPO) as reference organophosphorus extractants. According to literary data, these extractants are widely used for recovery of actinide and rare-earth elements from HLW. The data on europium, americium and technetium extraction from $HNO_3$ solutions by these reference organophosphorus extractants are given in Table.

**Extraction of palladium**

The initial (standard) palladium solution was prepared by dissolving a weighed portion of palladium metal in 7 M/ℓ $HNO_3$. To decrease the acidity, the resultant solution was evaporated on water bath with water addition. Thus, the solution containing 6.6 g/ℓ Pd and 2.9 M/ℓ $HNO_3$ was obtained. This solution was used for preparation of process solutions at palladium concentration of about 100 mg/ℓ.

A fast and reliable method for palladium determination in simple solutions is photometry of its complex with thiourea.

The following procedure for determining Pd content in process solutions was used in our work:

- 5 $cm^3$ of concentrated HCl were added to 1.5 g of thiourea and the volume was adjusted to 50 $cm^3$ with water;
- 4 $cm^3$ of the prepared thiourea solution were added to 1 $cm^3$ of a solution to be analyzed and the mixture is kept for no less than 20 min;
- upon keeping, the solution is subjected to photometry in 10 mm cuvette at 400 nm wavelength on SF-16 spectrophotometer. The prepared thiourea solution is used as a reference.

On determining the palladium distribution coefficients, aqueous solutions were mixed with extractant solutions during no less than 30 min to attain the equilibrium state. Pd concentration was determined in the initial and equilibrium aqueous solution. The distribution coefficient was calculated by expression:

$$D = \frac{(C_{initial} - C_{equil.}) \bullet V_{aq.}}{V_{org.} \bullet C_{equil.}}$$

In some tests the equilibrium concentration of palladium in organic phase was determined after its stripping into thiourea solution. In this case the palladium distribution coefficients were calculated by the formula: $D = C_{org}/?_{aq}$.

The data on Pd extraction from $HNO_3$ solutions by standard organophosphorus extractants are presented in Table.

**Preparation of ruthenium solutions**

In our opinion, an approach to attainment of equilibrium by destruction of the most inert ruthenium nitrite complexes in $HNO_3$ with formation of the most stable complexes under established conditions seems to be the best modeling method for preparing the simulated nitrate-nitrite solutions of ruthenium. Analysis of literary data shows that the main groups of ruthenium existence forms in simulated and actual HLW involve nitrosonitrate-, nitrosonitre- and their mixed complexes. Therefore, the procedures for production of three solution types were approbated: the most stable solution of nitrosonitro-form in weakly acidic solution, $[RuNO(NO_2)_4OH]^{2-}$ (solution I); as a result of treatment of this solution, the solution of mixed and nitrosonitrate-forms of ruthenium, i.e. solutions II and III, respectively.

Solution I was prepared by a weighed portion of $Na_2[RuNO(NO_2)_4OH]\cdot 2H_2O$ (**?**) complex synthesized according to modified procedure by fluorination of ruthenium metal. Solution II was produced by keeping 0.1 M solution of **?** complex in 3M $HNO_3$ during three days; solution III was obtained by dissolution of **?** complex in 8M $HNO_3$ on boiling for one hour, by evaporation up to wet salts and by dissolution in 3M $HNO_3$.

**Characterization of ruthenium forms in solutions**

The characterization was carried out by NMR method (Spectrometer MSL-400 Bruker) on $^{14}N$ nuclei (separately the lines of free and coordinated $NO_3$, $NO_2$ and NO -groups), $^{17}$? ($H_2O$, OH-groups) and $^{99}Ru$ (unique measurements due to creation in Novosibirsk of highly-sensitive low-frequency sensors of NMR adapted to ruthenium solutions) and to a lesser extent by IR-spectrometry (Fourrier spectrometer BOMEN M-102). It was found that in solution I being in equilibrium with the main form there are accumulated up to 10% of hydrated $[RuNO(NO_2)_3(H_2O)OH]^-$ form. The sole mixed form of $[RuNO(NO_2)_2NO_3(H_2O)_2]^0$ being stable in 3M $HNO_3$ for a long time prevails in solution II. Solution III contains only a series of nitrosonitratoe-forms, because there are no lines of coordinated $NO_2$-group on NMR-spectra.

**Characteristics of analytical methods**

For analytical provision of screening studies on extraction properties of different phosphorylated calixarenes towards Ru, the procedures of atomic-absorption analysis (AAA) were adapted as applied to solutions in $HNO_3$ and nitrate-nitrite solutions, including those with complicated composition, as well as to ammonia strip products. AAA was conducted on Spectrometer Z-8000 with Zeeman background correction of Hitachi Co at flaming and electrothermal atomization of samples. As to these versions, the detection limits of Ru (μg/mℓ) in aqueous and toluene (in brackets) solutions were equal to 0.5 (0.3) and 0.003 (0.006), respectively. The analytical procedures for nitric acid solutions and ammonia strip products are directly used in the presence of buffer additions; in the case of complicated nitrato-nitrite solutions the preliminary extraction concentration of ruthenium with alkylaniline is applied. Relative standard deviation in analysis of different solutions in the concentration range of $10^{-4}$–1 g/ℓ Ru is 0.02-0.07 (2-7%). Concurrently with ruthenium, these procedures enable also to determine palladium and rhodium with Ru-related metrological characteristics.

**Extraction and analysis of equilibrium phases**

Initial nitrato (0.01-5 M $HNO_3$)-nitrite solutions for ruthenium extraction were prepared by 10-100 fold dilution of solutions I- with adjusting to a needed acidity by corresponding $HNO_3$ solutions and were kept for three days. The analytical procedure of equilibrium phases after Ru extraction was tested on simulated systems (POR and CMPO solutions in NBTF). In analysis of raffinates, to avoid the effect of Ru form and macrobasic elements on the value of analytical signal, ruthenium was preliminarily transformed into the single chemical form of ($RuNOCl_5^{2-}$) which was extracted by alkylaniline solution in toluene with simultaneous separation from all non-noble metals. Raffinates were pre-evaporated repeatedly with concentrated HCl up to wet salts and were dissolved in 6M HCl. The direct determination of Ru in extracts on the basis of MNBTF by atomic-absorption method is impossible because of fluorine effect on spectrophotometer optics. Therefore, ruthenium was previously stripped by ammonia solutions which proved to be most efficient as compared with other stripping agents (NaOH, thiourea).

The data on ruthenium extraction (solution II) from $HNO_3$ by standard organophosphorus extractants are given in Table.

Table

Extraction Eu ([$10^{-5}$ M]), Am (+$10^{-5}$ M Eu), Tc(traces), Ru ([$10^{-3}$ M]) and Pd ([$10^{-3}$ M]) from $HNO_3$ by solutions L in m-nitrobenzotrifluoride (NBTF). Concentration of [L} is 0.01 M, unless otherwise indicated

| L | | [$HNO_3$] M: | | | | |
|---|---|---|---|---|---|---|
| | | 0,1 | 0,3 | 1,0 | 3,0 | 6,0 |
| CMPO | $D_{Eu}$ | 0,02 | 0,06 | 0,41 | 0,70 | 0,54 |
| | $D_{Am}$ | 0,06 | 0,24 | 1,04 | 1,28 | 0,98 |
| | $D_{Tc}$ | 0,5 | 0,34 | 0,14 | 0,02 | <0,01 |
| | $D_{Ru}$ | <0,01 | 0,01 | 0,012 | 0,01 | <0,01 |
| | $D_{Pd}$ | <0,01 | <0,01 | <0,01 | <0,01 | <0,01 |
| POR (0,04 ? ) | $D_{Eu}$ | 0,04 | 0,05 | 0,006 | <0,01 | <0,01 |
| | $D_{Am}$ | 0,04 | 0,04 | 0,01 | <0,01 | <0,01 |
| | $D_{Tc}$ | 45 | 41 | 3,05 | 0,14 | 0,03 |
| | $D_{Ru}$ | 0,04 | 0,04 | 0,01 | <0,01 | <0,01 |
| | $D_{Pd}$ | 2,5 | 1,3 | 0,22 | 0,06 | <0,01 |

It is evident from these data that the routine organophosphorus extractants do no afford the efficient combined recovery of elements to be studied from moderately acidic media (1 ? $HNO_3$). CMPO does not extract Pd and Ru, while POR extracts Am, Eu and Ru very poorly.

Project Manager 2068

I.V. Smirnov

**Scientific and Technical Quarter Report**
**Project N 2068**

# Development and demonstration of HLW partitioning technology with the use of phosphorylated calixarenes.

1. Laboratory research on extraction ability of phosphorus-containing calixarenes

1.1. Screening studies

July – September 2002

All the Project participants were engaged in this work.

During the second quarter the following work was carried out in accordance with the Project Work Plan.

## 1.1. Screening studies

In accordance with the Work plan in the second quarter the study on extraction properties of phosphorylated calixarenes and simulated phosphine oxides was started.

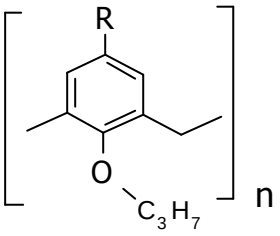


n = 4; 6.

Structural formula of phosphorylated calix[4]- and calix[6]arenes.

Fig. 1

**Extraction of europium, americium and technetium**

The extractants synthesized and purified at Institute of Organic Chemistry of Ukrainian Academy of Sciences (Kiev) were used, 3-nitrobenzotrifluoride (NBTF) of "Rhodia" Co (France) was used as a diluent. Other reagents were made by "Vekton" Co (St. Petersburg). $^{152}$Eu, $^{241}$Am, $^{99}$Tc – isotopes were produced by "Isotop" Co (St. Petersburg). Extractant solutions were prepared by precise weighed portions.

To determine metal distribution coefficients, 1.5 ml organic and aqueous phases each with needed composition were placed into a polypropylene stopped flask and were stirred at 22-24$^{o}$C for 5 min, phases were separated by centrifuging and the metal content was determined in

both phases by radiometry through γ-emission of corresponding isotope. The radiometric measurements were performed by scintillation γ-spectrometer «DeskTop InSpector» based on NaJ-detector 51×51 mm with a well ("Canberra" Co). Error of radiometric measurements was no more than 10%.

Data on europium and americium extraction from $HNO_3$ solutions by above extractants are given in Table 1, those of technetium – in Table 2.

Table 1. Extraction of Eu ([$10^{-5}$ M]) and Am (+$10^{-5}$ M Eu) from $HNO_3$ by L in NBTF. If not specified, [L] = 0.01 M.

| L | R | | [$HNO_3$]M: | | | | |
|---|---|---|---|---|---|---|---|
| | | | 0,1 | 0,3 | 1,0 | 3,0 | 6,0 |
| CIP-2 calix[4] arene | 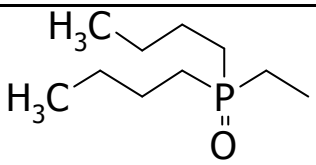 | $D_{Eu}$ | 4,0 | 3,5 | 0,68 | 0,03 | <0,01 |
| | | $D_{Am}$ | 1,5 | 1,3 | 0,27 | 0,01 | <0,01 |
| CIP-31 calix[4] arene | 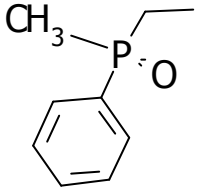 | $D_{Eu}$ | 0,54 | 0,68 | 0,83 | 0,08 | 0,01 |
| | | $D_{Am}$ | 0,28 | 0,32 | 0,4 | 0,04 | <0,01 |
| CIP-34 calix[4] arene | 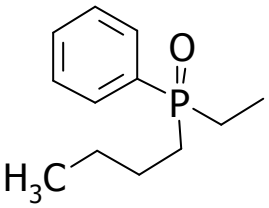 | $D_{Eu}$ | 0,16 | 0,23 | 0,2 | 0,13 | 0,03 |
| | | $D_{Am}$ | 0,25 | 0,4 | 0,4 | 0,15 | 0,04 |
| CIP-35 calix[6] arene | 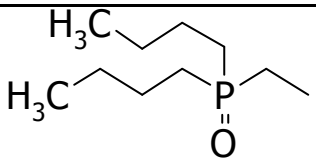 | $D_{Eu}$ | 0,6 | 0,4 | 0,15 | 0,01 | <0,01 |
| | | $D_{Am}$ | 0,2 | 0,23 | 0,1 | 0,01 | <0,01 |
| CIP-36 0,04 M | 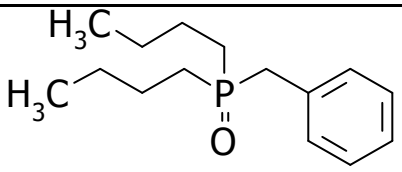 | $D_{Eu}$ | 0,01 | 0,023 | 0,01 | <0,01 | <0,01 |
| | | $D_{Am}$ | 0,004 | 0,008 | <0,01 | <0,01 | <0,01 |
| CIP-36 0,06 M | 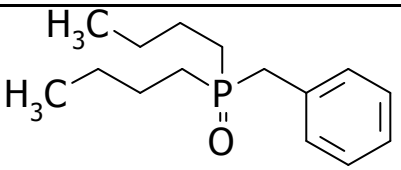 | $D_{Eu}$ | 0,01 | 0,025 | 0,016 | 0,015 | <0,01 |
| | | $D_{Am}$ | 0,007 | 0,026 | 0,008 | <0,01 | <0,01 |

| L | R | | [$HNO_3$]M: | | | | |
|---|---|---|---|---|---|---|---|
| | | | 0,1 | 0,3 | 1,0 | 3,0 | 6,0 |
| CIP-37 0,04 M | 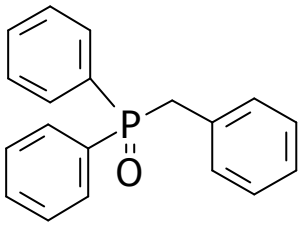 | $D_{Eu}$ | 0,005 | 0,006 | 0,008 | 0,013 | 0,006 |
| | | $D_{Am}$ | <0,01 | <0,01 | <0,01 | <0,01 | <0,01 |

**Extraction of palladium**

Initial solution containing 6.6 g/ℓ Pd and 2.9 M/ℓ $HNO_3$ was used for preparing of process solutions at Pd concentration ~ 100 mg/ℓ ([$10^{-3}$ M]).

On determining the palladium distribution coefficients, aqueous solutions were mixed with extractant solutions during no less than 30 min to attain equilibrium state. Pd concentration was determined in the initial and equilibrium aqueous solutions by photometry of its complex with thiourea. In individual tests the equilibrium palladium concentration was determined upon its stripping into thiourea solution.

Data on palladium extraction from $HNO_3$ solutions are given in Table 2.

Table 2. Extraction of $Tc^{99}$ [traces] and Pd ([$10^{-3}$ M]) from $HNO_3$ by L in MNBTF. If not specified, [L] = 0.01 M.

| L | R | | [$HNO_3$]M: | | | | |
|---|---|---|---|---|---|---|---|
| | | | 0,1 | 0,3 | 1,0 | 3,0 | 6,0 |
| CIP-2 calix[4] arene | 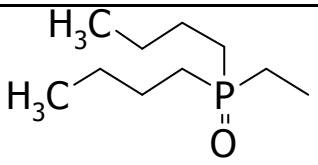 | $D_{Tc}$ | 74,1 | 31,5 | 4,4 | 0,27 | 0,037 |
| | | $D_{Pd}$ | 3,3 | 2,6 | 0,7 | 0,2 | 0,05 |
| CIP-31 calix[4] arene | 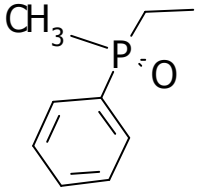 | $D_{Tc}$ | 34,8 | 21,7 | 3,65 | 0,23 | 0,026 |
| | | $D_{Pd}$ | 1,7 | 1,5 | 0,8 | 0,3 | 0,06 |
| CIP-34 calix[4] arene | 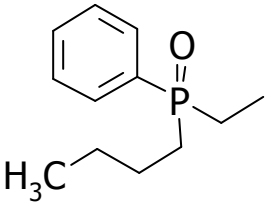 | $D_{Tc}$ | 35,9 | 18,2 | 2,4 | 0,26 | 0,03 |
| | | $D_{Pd}$ | 1,9 | 1,3 | 0,5 | 0,2 | 0,03 |

| L | R | | [$HNO_3$]M: | | | | |
|---|---|---|---|---|---|---|---|
| | | | 0,1 | 0,3 | 1,0 | 3,0 | 6,0 |
| CIP-35 calix[6] arene | 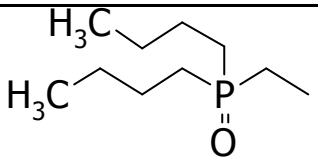 | $D_{Tc}$ | 41,8 | 23,4 | 3,6 | 0,19 | 0,03 |
| | | $D_{Pd}$ | 3,9 | 3,3 | 1,4 | 0,3 | 0,06 |
| CIP-36 0,04 M | 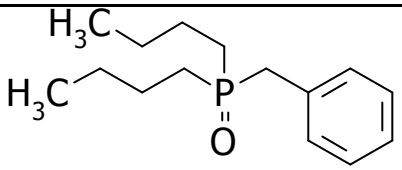 | $D_{Tc}$ | 26,4 | 14,4 | 2,1 | 0,11 | 0,02 |
| | | $D_{Pd}$ | 0,9 | 0,3 | 0,06 | 0.05 | 0,02 |
| CIP-36 0,06 M | 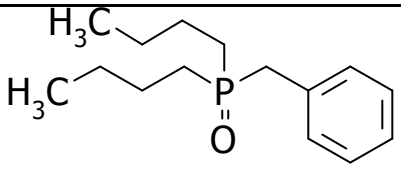 | $D_{Tc}$ | 39,0 | 24,1 | 3,5 | 0,19 | 0,03 |
| | | $D_{Pd}$ | 1,9 | 1,1 | 0,05 | <0,01 | <0,01 |
| CIP-37 0,04 M | 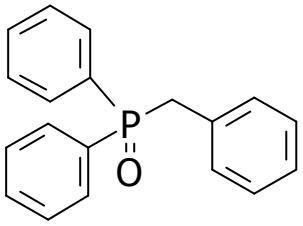 | $D_{Tc}$ | 4,7 | 2,2 | 0,63 | 0,04 | 0,01 |
| | | $D_{Pd}$ | 0,02 | <0,01 | <0,01 | <0,01 | <0,01 |

Phosphorylated calixarenes CIP-2 and CIP-31 were previously characterized as efficient extractants of americium and europium. As seen from Table 2, they extract technetium and palladium rather well.

To assess the effect of calixarenes on extraction properties of phosphine oxide groups, we tested the monodentate compounds CIP-36 and CIP-37. As compared the extraction properties of CIP-2 and CIP-36, it should be noted that the highest combined effect is observed in europium extraction (~ 70); in the case of palladium extraction it is significantly less (12) and is practically absent in technetium extraction.

Phosphorylated calix[6]arene (CIP-35) extracts radionuclides almost to the same extent as calix[4]arene (CIP-2), despite one-and-a-half increased number of phosphine oxide groups.

Substituent value of phosphorus atom exerts a certain effect on extraction properties of phosphorylated calixarenes. Replacing of methyl radical (CIP-31) with butyl one (CIP-34) deteriorates extraction of metals under investigation.

**Preparing of solutions of ruthenium nitrate-nitroforms and their characterization.**

Solutions were obtained by aging of 0,1 ? $Na_2[RuNO(NO_2)_4OH]\cdot 2H_2O$ in 3 ? $HNO_3$ during 3 days at room temperature. Data on $^{14}N$ and $^{99}Ru$ NMR revealed that 2 from 4

coordinated $NO_2$-groups were destroyed after 1 day aging in 3 ? $HNO_3$ and complex $[RuNO(NO_2)_2(NO_3)(H_2O)_2]^0$ is dominated in this solution, for removal of 2 remained $NO_2$-groups long-time heating at high temperature being needed.

Depending on equilibrium concentration of $HNO_3$ and time of solutions aging the complex $[RuNO(NO_2)_2(NO_3)(H_2O)_2]^0$ may undergo some types of transformations:

$[RuNO(NO_2)_2(NO_3)(H_2O)_2]^0 = [RuNO(NO_2)_2(NO_3)(H_2O)(OH)]^- + H^+$ (1);

$[RuNO(NO_2)_2(NO_3)(H_2O)_2]^0 + H_2O = [RuNO(NO_2)_2(H_2O)_3]^+ + NO_3^-$ (2);

$[RuNO(NO_2)_2(H_2O)_3]^+ = [RuNO(NO_2)_2(H_2O)_2(OH)]^0 + H^+$ (3);

$[RuNO(NO_2)_2(NO_3)(H_2O)_2]^0 + NO_3^- = [RuNO(NO_2)_2(NO_3)_2(H_2O)]^-$ (4);

$[RuNO(NO_2)_2(NO_3)_x(H_2O)_{3-x}]^{1-x} + H^+ + H_2O = [RuNO(NO_2)(NO_3)_x(H_2O)_{4-x}]^{2-x} + HNO_2$ (5).

Processes of proton dissociation (1, 3) are most fast and they need no time for equilibrium setting. Processes of substitution of coordinated nitrate ions for water and vice versa (2, 4) take some hours to attain equilibrium. Removal of 1 of 2 remained $NO_2$-groups is possible if to accent the equilibrium (5) due to elimination of nitrous acid from solution. At room temperature this process is extremely slow and may exert noticeable influence on distributing ruthenium on forms during weeks and months after preparing solutions.

**Extraction of ruthenium nitrate-nitroforms from nitric acid solutions.**

The initial solutions were obtained by means of dilution of ($[RuNO(NO_2)_2(NO_3)(H_2O)_2]^0$) solution with $HNO_3$ of corresponding concentration Ru up to content of $10^{-3}$ M. The extraction was carried out immediately after dilution (series I), 3 days later (series II) and 1,5 months later (series III).

Table 3. Effect of preparation method of mixed ruthenium nitrate-nitrocomplexes ($1 \cdot 10^{-3}$ M) solutions on the extraction of Ru by 0,04 M CMPO ($Ph_2Bu_2$) in MNBTF

| $HNO_3$, M | $D_{Ru}$ for method of solution preparation ???????? | | |
|---|---|---|---|
| | I | II | III |
| 0,01 | 0,006 | 0,016 | 0,008 |
| 0,10 | 0,011 | 0,006 | 0,003 |
| 0,30 | 0,019 | 0,009 | – |
| 1,0 | 0,022 | 0,012 | 0,007 |
| 3,0 | 0,017 | 0,008 | 0,006 |
| 6,0 | 0,006 | 0,003 | 0,004 |

It is obvious from Table 3 that Ru recovery is low for the methods of preparing solutions (all series), although the tendency of $D_{Ru}$ decrease with increasing the time of solutions aging is evident.

In freshly prepared solutions the content of uncharged form ($[RuNO(NO_2)_2(NO_3)(H_2O)_2]^0$) increases with increase of acidity according to (1). This fact in combination with concurrent extraction of $HNO_3$ leads to appearance of maximum in $D_{Ru}$. After 3 days aging the equilibriums (2–4) are established in solutions and from diluted $HNO_3$ form $[RuNO(NO_2)_2(H_2O)_2(OH)]^0$ is extracted. Rise of acidity leads to protonation of this form and as a result to decrease of $D_{Ru}$. At the same time the increasing nitrate-ion concentration stabilizes the form $[RuNO(NO_2)_2(NO_3)(H_2O)_2]^0$. However, a fraction of this form becomes noticeable at $C_{HNO_3} > 0,25$ M predetermining the minimum in $D_{Ru}$ values. As evaluations show, the fraction of a form passes through maximum at $C_{NO_3} \sim 0,5–1$ M and decreases in proportion with further increase of its concentration according to (4). At $C_{HNO_3} > 3$ M this equilibrium determines lower values of $D_{Ru}$ as compared with freshly prepared solutions. Data on the extraction from solutions aging for 1,5 months show the same dynamics of $D_{Ru}$ change with the variation of $C_{HNO_3}$ as in series II, excepting the fact that Ru extraction is lower at all values of $C_{HNO_3}$. The reason for this phenomenon is the lowering of nitrosodinitrocomplexes fraction according to the equation (5). In general, there is a observed regularity according to which the neutral Ru forms are more extractable than anionic ones.

**Extraction of ruthenium nitrate-nitroforms by phosphorylated calix[4,6]phosphineoxides.**

Data on Ru extraction from solutions (series II) by phosphorylated calix[4,6]arenas and trialkylphopshine oxide are presented in Table 4. The concentrations of extractants were chosen in such a manner that the content of phosphoryl groups in organic phase the same be identical.

Table 4. Extraction of ruthenium nitrate-nitrocomplexes by POR and phosphorylated calix[4,6]arenes in MNBTF from nitric acid solutions

| $HNO_3$, M | $D_{Ru}$ for extractant | | | |
|---|---|---|---|---|
| | POR; 0,04 M | CIP-2; 0,01 ? | CIP-31; 0,01 ? | CIP-35; 0,007 ? |
| 0,01 | 0,09 | 0,28 | 0,03 | 0,28 |
| 0,10 | 0,04 | 0,17 | 0,02 | 0,13 |
| 0,30 | 0,04 | 0,10 | 0,02 | 0,09 |
| 1,0 | 0,011 | 0,04 | 0,03 | 0,06 |
| 3,0 | <0,01 | <0,01 | <0,01 | <0,01 |
| 6,0 | <0,01 | <0,01 | <0,01 | <0,01 |

On the basis of data obtained following conclusions may be drawn:

- the type of $D_{Ru}$ dependence on nitric acid concentration is identical for polydentate calix[4,6]arenes and monodentate POR;
- in acidity range up to 1 M $HNO_3$ a minor cooperative effect is observed ($D_{Ru}$ for CIP-2 and CIP-35 are approximately 4 times as large as $D_{Ru}$ for monodentate analog);
- there are practically no difference in extraction ability of calix-4 and calix-6-arenes;
- at low acidity $D_{Ru}$ for CIP-31 is almost by order lower than for CIP-2 as a result of decrease of phosphoryl oxygen donating properties on the substitution of butyl radical for phenyl one.

Project Manager 2068

I.V. Smirnov

**Scientific and Technical Quarter Report**
**Project N 2068**

# Development and demonstration of HLW partitioning technology with the use of phosphorylated calixarenes.

1. Laboratory research on extraction ability of phosphorus-containing calixarenes

1.1. Screening studies

October – December 2002

All the Project participants were engaged in this work.

During the third quarter the following work was carried out in accordance with the Project Work Plan.

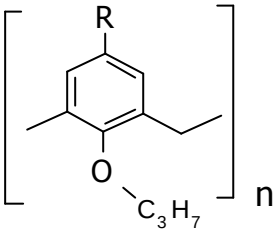


n = 4; 6.

Fig. 1

Structural formula of phosphorylated calix[4]- and calix[6]arenes.

## 1.1. Screening studies

In accordance with the Work plan in the third quarter the study on extraction properties of phosphorylated calixarenes and simulated phosphine oxides was started.

### Extraction of europium, americium and technetium

The extractants synthesized and purified at Institute of Organic Chemistry of Ukranian Academy of Sciences (Kiev) were used, 3-nitrobenzotrifluoride (NBTF) of "Rhodia" Co (France) was used as a diluent. Other reagents were made by "Vekton" Co (St. Petersburg). $^{152}Eu$, $^{241}Am$, $^{99}Tc$ – isotopes were produced by "Isotop" Co (St. Petersburg). Extractant solutions were prepared by precise weighed portions.

To determine metal distribution coefficients, 1.5 ml organic and aqueous phases each with needed composition were placed into a polypropylene stopped flask and were stirred at 22-24$^{o}$C for 5 min, phases were separated by centrifuging and the metal content was determined in

both phases by radiometry through γ-emission of corresponding isotope. The radiometric measurements were performed by scintillation γ-spectrometer «DeskTop InSpector» based on NaJ-detector 51×51 mm with a well ("Canberra" Co). Error of radiometric measurements was no more than 10%.

Data on europium and americium extraction from $HNO_3$ solutions by above extractants are given in Table 1, those of technetium – in Table 2.

Table 1.

Extraction of Eu ([$10^{-5}$ M]) and Am (+$10^{-5}$ M Eu) from $HNO_3$ by solution L in m-nitrobenzotrifluoride (NBTF). Concentration [L] = 0.01 M, unless otherwise specified.

| L | R | | [$HNO_3$]M: | | | | |
|---|---|---|---|---|---|---|---|
| | | | 0,1 | 0,3 | 1,0 | 3,0 | 6,0 |
| CIP-40 calix[4] arene | 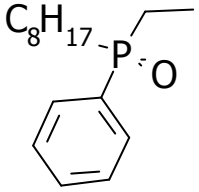 | $D_{Eu}$ | 0,1 | 0,18 | 0,13 | 0,07 | 0,02 |
| | | $D_{Am}$ | 0,09 | 0,11 | 0,11 | 0,04 | 0,01 |
| CIP-42 calix[4] arene | 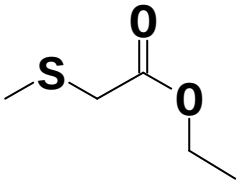 | $D_{Eu}$ | <0,01 | <0,01 | <0,01 | <0,01 | <0,01 |
| | | $D_{Am}$ | <0,01 | <0,01 | <0,01 | <0,01 | <0,01 |
| CIP-44 calix[4] arene | 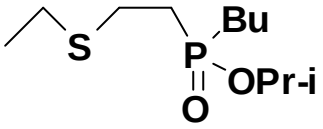 | $D_{Eu}$ | 0,04 | 0,02 | 0,02 | 0,01 | <0,01 |
| | | $D_{Am}$ | 0,05 | 0,03 | 0,01 | 0,01 | <0,01 |
| CIP-45 calix[4] arene | 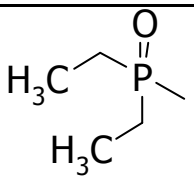 | $D_{Eu}$ | 0,2 | 1,3 | 2,4 | 0,06 | 0,01 |
| | | $D_{Am}$ | 0,1 | 0,42 | 1,1 | 0,03 | <0,01 |
| CIP-46 calix[4] arene | 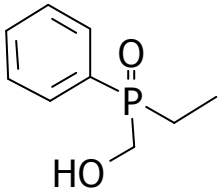 | $D_{Eu}$ | 0,06 | 0,09 | 0,12 | 0,11 | 0,03 |
| | | $D_{Am}$ | 0,05 | 0,08 | 0,09 | 0,07 | 0,03 |

| L | R | | [$HNO_3$]M: | | | | |
|---|---|---|---|---|---|---|---|
| | | | 0,1 | 0,3 | 1,0 | 3,0 | 6,0 |
| CIP-47<br><br>calix[4]arene | 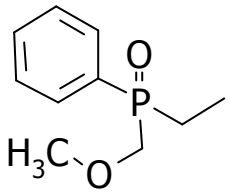 | $D_{Eu}$ | 0,06 | 0,12 | 0,15 | 0,08 | 0,02 |
| | | $D_{Am}$ | 0,07 | 0,1 | 0,1 | 0,05 | 0,01 |
| CIP-48<br>calix[4]arene | 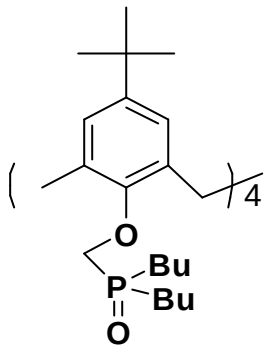 | $D_{Eu}$ | 0,13 | 0,05 | 0,03 | <0,01 | <0,01 |
| | | $D_{Am}$ | 0,04 | 0,05 | 0,03 | <0,01 | <0,01 |
| CMPO ($Ph_2Bu_2$, 0,01 M) | | $D_{Eu}$ | 0,02 | 0,06 | 0,41 | 0,70 | 0,54 |
| | | $D_{Am}$ | 0,06 | 0,24 | 1,04 | 1,28 | 0,98 |
| POR (0,04 M) | | $D_{Eu}$ | 0,04 | 0,05 | 0,006 | <0,01 | <0,01 |
| | | $D_{Am}$ | 0,04 | 0,04 | 0,01 | <0,01 | <0,01 |

**Extraction of palladium**

Initial solution containing 6.6 g/ℓ Pd and 2.9 M/ℓ $HNO_3$ was used for preparing of process solutions at Pd concentration ~ 100 mg/ℓ ([$10^{-3}$ M]).

In determining the palladium distribution coefficients the aqueous solutions were mixed with extractants during no less than 30 min to attain equilibrium state. Palladium concentration was determined in the initial and equilibrium aqueous solutions by photometry of its complex with thiourea. In some experiments the equilibrium concentration of palladium in organic phase was determined upon its stripping into thiourea solution.

Data on palladium extraction from $HNO_3$ solutions are given in Table 2.

Table 2.

Extraction of $Tc^{traces}$ and Pd ([$10^{-3}$ M]) from $HNO_3$ by solutions L in m-nitrobenzotrifluoride (NBTF). Concentration [L] = 0.01 M, unless otherwise specified

| L | R | | [$HNO_3$]M: | | | | |
|---|---|---|---|---|---|---|---|
| | | | 0,1 | 0,3 | 1,0 | 3,0 | 6,0 |
| CIP-40 calix[4] arene | 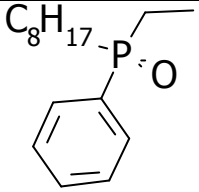 | $D_{Tc}$ | 36,8 | 16,4 | 3,1 | 0,21 | 0,03 |
| | | $D_{Pd}$ | precipitates | | | 0,2 | <0,01 |
| CIP-42 calix[4] arene | 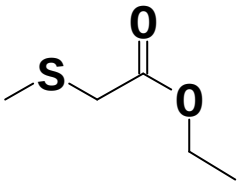 | $D_{Tc}$ | 1,28 | 0,43 | 0,12 | 0,16 | 0,018 |
| | | $D_{Pd}$ | >20 precipitates at interphase | | | | 13 |
| CIP-44 calix[4] arene | 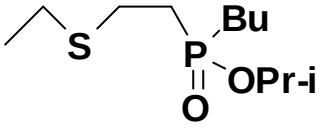 | $D_{Tc}$ | 8,75 | 7,40 | 2,11 | 0,13 | 0,01 |
| | | $D_{Pd}$ | precipitates at interphase | | | | |
| CIP-45 calix[4] arene | 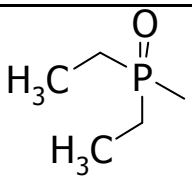 | $D_{Tc}$ | 3,1 | 4,0 | 6,5 | 0,41 | 0,05 |
| | | $D_{Pd}$ | 0,5 | 0,38 | 0,3 | 0,17 | 0,03 |
| CIP-46 calix[4] arene | 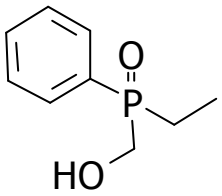 | $D_{Tc}$ | 14,0 | 7,05 | 1,56 | 0,16 | 0,02 |
| | | $D_{Pd}$ | 0,45 | 0,4 | 0,11 | 0,02 | 0,01 |
| CIP-47 calix[4] arene | 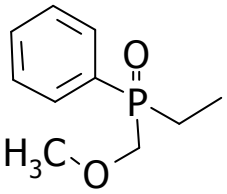 | $D_{Tc}$ | 17,5 | 11,5 | 2,47 | 0,16 | 0,02 |
| | | $D_{Pd}$ | 1,4 | 1,1 | 0,68 | 0,2 | 0,08 |

| L | R | | [$HNO_3$]M: | | | | |
|---|---|---|---|---|---|---|---|
| | | | 0,1 | 0,3 | 1,0 | 3,0 | 6,0 |
| CIP-48 calix[4] arene | 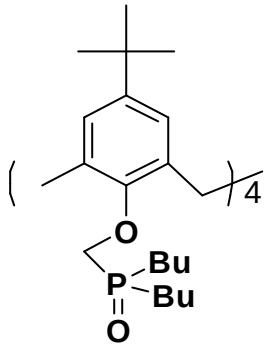 | $D_{Tc}$ | 230 | 88,4 | 10,0 | 0,4 | 0,05 |
| | | $D_{Pd}$ | 2,5 | 1,5 | 0,8 | 0,16 | 0,04 |
| CMPO ($Ph_2Bu_2$, 0,01 ? ) | | $D_{Tc}$ | 0,5 | 0,34 | 0,14 | 0,02 | <0,01 |
| | | $D_{Pd}$ | <0,01 | <0,01 | <0,01 | <0,01 | <0,01 |
| POR (0,04 ? ) | | $D_{Tc}$ | 45 | 41 | 3,05 | 0,14 | 0,03 |
| | | $D_{Pd}$ | 2,5 | 1,3 | 0,22 | 0,06 | <0,01 |

The data presented in Tables 1 and 2 allow to draw some preliminary conclusions about the structure effect of phosphorylated calixarenes on the extraction properties.

**Magnitude of alkyl substituents at phosphorus atom**

Increase of alkyl substituents length at phosphorus atom in a series of alkylphenyl phosphine oxides: $CH_3$ (CIP-31) → $C_4H_9$ (CIP-34) → $C_8H_{17}$ (CIP-40) significantly deteriorates the extraction of europium and americium, but affects the extraction of technetium and palladium only slightly.

**Heteroatoms in substituents at phosphorus atom**

When replacing the alkyl substituents at phosphorus atom (CIP-34) with the alkyl containing hydroxyl (CIP-46) or ether oxygen atom (CIP-47), the extraction of americium and technetium is impaired, while that of technetium remains intact. Palladium is worst of all extracted by the calixarene containing hydroxyl group (CIP-46).

Sulphur-containing calixarenes (CIP-42) and (SIP-44) do not practically extract europium and americium and forms non-soluble precipitates with palladium.

**Phosphorylation at lower ring**

All the compounds previously studied by us were assigned to the class of calixarenes phosphorylated at upper ring. For comparison the calix-4-arene phosphorylated at lower ring (CIP-48) was investigated. As compared to analog phosphorylated at upper ring (CIP-2), it extracts europium and americium, as well as technetium and palladium, much worse. Therefore, on the basis of available data one can suggest that the phosphorylated at upper ring calix[4]arenas with small alkyl substituents at phosphorus atom are of prime interest for group recovery of europium, americium, technetium and palladium.

**The extraction of ruthenium nitrosonitratoaquacomplexes.**

The preparation procedure of solutions of $[RuNO(NO_3)_x(H_2O)_y]^{3-x}$ was developed. This procedure includes dissolution of $Na_2[RuNO(NO_2)_4OH]\cdot 2H_2O$ in $HNO_3$ (1:1), long-time (16 h) heating of the solution on water bath, twice evaporation to moist salts with subsequent dissolution of the residue in 3 M $HNO_3$ on heating. According to NMR data there are some ruthenium nitrosonitratoaquacomplexes (x+y=5) in this solution, probably not only with monomeric structure. There are no signals from coordinated nitrite-ion in $^{14}N$ NMR spectrum of this solution, i.e. coordinated nitrite-ion in conditions of this "hard" treatment is completely destroyed. The extraction was carried out by solutions of POR and CMPO in MNBTF from freshly prepared solutions (the series 1) and 3 days later (the series 2). Experimental data are given in Table 3.

Table 3.

The extraction of ruthenium by 0.04 M POR and CMPO solutions in MNBTF from nitric acid solutions (the concentration of Ru is $1{,}0*10^{-3}$ M).

| ? $NO_3$, ? | Series 1, $D_{Ru}$ | | Series 2, $D_{Ru}$ | |
|---|---|---|---|---|
| | POR | CMPO | POR | CMPO |
| 0.01 | 0,00036 | <0,0002 | <0,0002 | <0,0002 |
| 0.1 | 0,0014 | 0,00024 | 0,00041 | <0,0002 |
| 0.3 | 0,0021 | 0,00036 | 0,0015 | 0,00041 |
| 1.0 | 0,00061 | 0,0013 | 0,00073 | 0,00051 |
| 3.0 | <0,0002 | 0,0003 | 0,00073 | 0,00023 |
| 6.0 | <0,0002 | 0,00024 | 0,00032 | <0,0002 |

Because of low values of $D_{Ru}$ ($10^{-4}$–$10^{-3}$) the concentration of ruthenium in organic phase was determined in ammonia re-extracts by highly sensitive method of atomic absorption in graphite sprayer (the detection limit is 0.003 mcg/ml of Ru).

For both extractants the values of $D_{Ru}$ of $[RuNO(NO_3)_x(H_2O)_y]^{3-x}$ forms are lower almost by order of two than for mixed ruthenium nitrosonitrate-nitrocomplexes $[RuNO(NO_3)_x(NO_2)_y(H_2O)_z]^{3-x-y}$ (Table 4) and slightly reduced with aging of initial solutions during 3 days. The dependence character of $D_{Ru}$ on $HNO_3$ concentration is typical for this extractants: there are maximums at 0.5 ? $HNO_3$ for POR and at 1 ? $HNO_3$ for CMPO.

**The extraction of ruthenium after nitrite treatment of nitrosonitratoaquacomplexes.**

The solution of $[RuNO(NO_3)_x(H_2O)_y]^{3-x}$ forms in 3M $HNO_3$ was treated by solid $NaNO_2$ at room temperature with subsequent solution heating at 60°C during 30 min. After that solution was cooled and all this operations was 5 times repeated. Aliquots of each solutions was diluted with appreciate $HNO_3$ concentration and resulting solutions was used for extraction (series 3). In experiments of series 4 0.15 ? $Zn(NO_3)_2$ was added to the solutions. Data of the extraction experiments are given in Table 4.

Table 4.

The extraction of ruthenium by 0.04 M POR and CMPO solutions in MNBTF from freshly prepared nitric acid solutions after nitrite treatment (the concentration of Ru is $1{,}0*10^{-3}$ M).

| Extractant (series) | $D_{Ru}$ at [? $NO_3$], ? | | | | |
|---|---|---|---|---|---|
| | 0.035 | 0.20 | 1.0 | 1.3 | 1.5 |
| POR (series 3) | 0.33 | 0.22 | – | 0.008 | 0.004 |
| POR (series 4) | 1.30 | – | 0.17 | 0.17 | 0.09 |
| CMPO (series 3) | 0.12 | 0.03 (0.02)* | 0.02 (0.022)* | 0.015 | 0.012 |
| CMPO (series 4) | 0.53 | 0.11 | 0.30 | 0.27 | 0.27 |

* Data on $[RuNO(NO_2)_2(NO_3)(H_2O)_2]^0$ extraction.

In acidity range of 0.2–1.5 ? $HNO_3$ at practically constant nitrate-ion concentration of ~ 3 M the dominating form of ruthenium in solutions is complex $[RuNO(NO_2)_2(NO_3)(H_2O)_2]^0$ with practically equal content. In case of CMPO (series 3) coincidence of $D_{Ru}$ for solutions of $[RuNO(NO_3)_x(H_2O)_y]^{3-x}$ after nitrite treatment with $D_{Ru}$ for solutions of $[RuNO(NO_2)_4OH]^{2-}$ after removal of two coordinated $NO_2$-group indicates to fitting of equilibrium of nitrite-nitrate nitrosoruthenium complexes formation from different sides. Obviously there are only nitrosonitroaquacomplexes of ruthenium in solutions with acidity below 0.2 ? $HNO_3$.

At the whole of $HNO_3$ concentrations range $D_{Ru}$ noticeably increased when $Zn^{2+}$ was added to solutions after nitrite treatment (series 4). This fact was observed for both phosphinoxides (L) (table 4). At the range of Ru nitrosonitrocomplexes domination (up to 0.2 ?

$HNO_3$) it may be explained by formation of heterometallic complexes $[RuNO(NO_2)_4OHZnL_2]$, as we established earlier. At higher acidity the observed effect should be connected with the presence of different anionic forms of ruthenium in solutions. In this case $[ZnL_2]^{2+}$ may to act as a gegenion, because no influence of $Zn^{2+}$ to extraction of uncharged form is observed.

On the basis of data obtained following conclusions may be done:

- The raw of extractability of studied ruthenium complexes is $[RuNO(NO_2)_x(H_2O)_y(? ? )_z]^{3-x-z}$ > $[RuNO(NO_3)_x(NO_2)_y(H_2O)_z]^{3-x-y}$ >> $[RuNO(NO_3)_x(H_2O)_y]^{3-x}$;
- The optimal conditions for ruthenium extraction are subacid solutions (up to 0.2 ? $HNO_3$) after operations of nitrite treatment and $Zn^{2+}$ adding;
- Operation of nitrite treatment in addition to preparing ruthenium forms needed provides the decreasing of $HNO_3$ concentration and put out their competitive influence on ruthenium extraction;
- The studying of extraction properties of phosphorilated calix-arenes should be carried out with using of individual ruthenium form $[RuNO(NO_2)_4OH]^{2-}$ and nitric acid solutions of Ru after nitrite treatment up to 1 ? $HNO_3$.

Project Manager 2068

I.V. Smirnov

**Project # B70 - YALINA**

Title of the project:

**"Experimental Research of Transmutation of Fission Products and Minor Actinides in a Thermal Neutron Spectrum Subcritical Assembly Driven with a Neutron Generator"**

Project duration -30 months ( the project was started in January 2002).

*Objectives planned*

The conclusions from this working meeting and the visit to the actual experimental facility are that this experiment is able to deliver valuable data in the following fields:

studying of the physics of multiplying media with thermal spectrum at different subcriticality levels, large range of different configurations (geometry, composition) and external sources (Cf-252, D (d, n) He-3, D (T, n) He-4);

measurements of transmutation rates of the fission products and minor actinides,

investigation of spatial kinetics of the sub-critical systems with the external neutron sources,

validation of the experimental techniques for, e.g., sub-criticality monitoring, neutron spectra measurement, etc

investigation of dynamics characteristics of the sub-critical systems with the external neutron sources in pulse mode of the neutron generator operation.

*Method:* The constitutive essence of the project is using of low energy accelerators for modeling and investigation of physical characteristics of subcritical target/blanket systems following from mechanism of nuclear reactions in high (~1.0-2.0 GeV) and low (~10-20 MeV) energy ranges, and from features of modern image of nucleon-meson cascade as well. Initiators of the #B-070 have shown up that a spallation neutron source consequences may be simulated by neutrons escaping from heavy element targets bombarded by 14 MeV neutrons.

*Configuration:* The core of the subcritical assembly is a rectangular parallelepiped 40.0cm-width, 40.0cm length and 57.0 cm height. It is assembled from polyethylene blocks with the channels to place the fuel pins and has a square lattice with 2.0-cm pitch. The subcritical assembly has been loaded with UO2 fuel (U-235 enrichment equal to 10 %). Central part of the core is a neutron producing lead target 10-cm diameter and 60 cm length. There are channels for location of detectors of neutron flux monitoring system at the boundaries of the core and experimental channels with diameter of 25 mm for radii 5, 10 and 16 cm for placing different type of samples or Cf source inside the core. The core is surrounded by high purity graphite reflector 40.0-cm thickness and thin 1.5-mm Cd layer.

**The following new equipment have installed around the sub-critical core**

Coaxial HPGe detector 20 % relative efficiency,
resolution (FWHM) –
0.9 keV (122 keV), 1.8 keV (1332 keV).
Low energy germanium detector (active area - 500 ? ? $^2$),
resolution (FWHM) – 550 eV (122 keV).
Portable electronic module with Notebook computer.
Spectroscopy software GENIE-2000.
MGA ? MGAU software for multi group analysis of Uranium and Plutonium.
time analyser Model T914 Turbo-MCS;

standard tritium water samples;
the radioactive samples of Np-237, Am-243 and I-129;
fission chambers (U-238,U-235,Th);
He-3,B-10 detectors;
TiH (TiD) – targets;

Fission chambers without integral cable for in-core use.

| type | Diameter nominal, mm | Detector length nominal, mm | Detector length sensitive, mm | Isotope | Sensitivity to thermal neutron | | Sensitivity to fast neutron $cs^{-1} / n \cdot cm^{-2} \cdot s^{-1}$ | Nominal operating voltage ( V ) | Maximum output current ( μA ) |
|---|---|---|---|---|---|---|---|---|---|
| | | | | | Pulse mode ($cs^{-1} / n \cdot cm^{-2} \cdot s^{-1}$) | Current mode ($A / n \cdot cm^{-2} \cdot s^{-1}$) | | | |
| ? NT-56 | 50 | 750 | 525 | $^{10}$? | – | $4 \cdot 10^{-13}$ | – | +1000 -500 | 500 |
| ? NT-10 | 7 | 70 | 5 | $^{10}$? | – | – | – | 400÷800 | – |
| ? N?-2 | 7 | 70 | 10 | $^{232}$Th | – | – | $6 \cdot 10^{-7}$ | 800 | – |
| ? N?-5 | 7 | 70 | 5 | $^{235}$U | $5 \cdot 10^{-4}$ | – | – | 800 | – |
| ? N?-8 | 7 | 70 | 10 | $^{238}$U | – | – | $2 \cdot 10^{-6}$ | 800 | – |
| ? N?-31 | 32 | 235 | 200 | $^{235}$U | 0,25 | – | – | 800 | 500 |
| ? N?-54 | 50 | 242 | 220 | $^{235}$U | 0,5 | – | – | 500 | 1000 |

| Type | Maximum operating temperature, $^0$? | Sensitive squere, $cm^2$ | Sensitive layer, ($mg \cdot cm^{-2}$) | Detector capacitance, (pF) | Filling gas | Insulating resistance ( Ω ) | | Operating voltage (limit with no radiation, ( V ) | Mass of sensitive layer, ( mg ) |
|---|---|---|---|---|---|---|---|---|---|
| | | | | | | 20 $^0$? | 300 $^0$? | | |
| ? N? -56 | 200 | – | – | 1300 | $BF_3$ | – | – | – | – |
| ? N? -10 | 300 | 1 | 0,5 | 10 | | Min $10^{10}$ | min $10^8$ | min 1800 | $^{10}$B,0,5 |
| ? N? -2 | 150 | 2 | 5 | 10 | 98%Ar + 2%$N_2$ | Min $10^{10}$ | Min $10^8$ | Min 1800 | $^{232}$Th, 6,0 |
| ? N? -5 | 150 | 1 | 1 | 10 | 98%Ar + 2%$N_2$ | Min $10^{10}$ | Min $10^8$ | Min 1800 | $^{235}$U, 1,0 |
| ? N? -8 | 150 | 2 | 5 | 10 | 98%Ar + 2%$N_2$ | Min $10^{10}$ | Min $10^8$ | Min 1800 | $^{238}$U, 6,0 |
| ? N? -31 | 400 | 500 | 1 | 100 | 98%Ar + 2%$N_2$ | – | – | – | – |
| ? N? -54 | 400 | 1000 | 1 | 200 | 98%Ar + 2%$N_2$ | – | – | – | – |

**The basic electronics for pulse and continuous modes of operation**

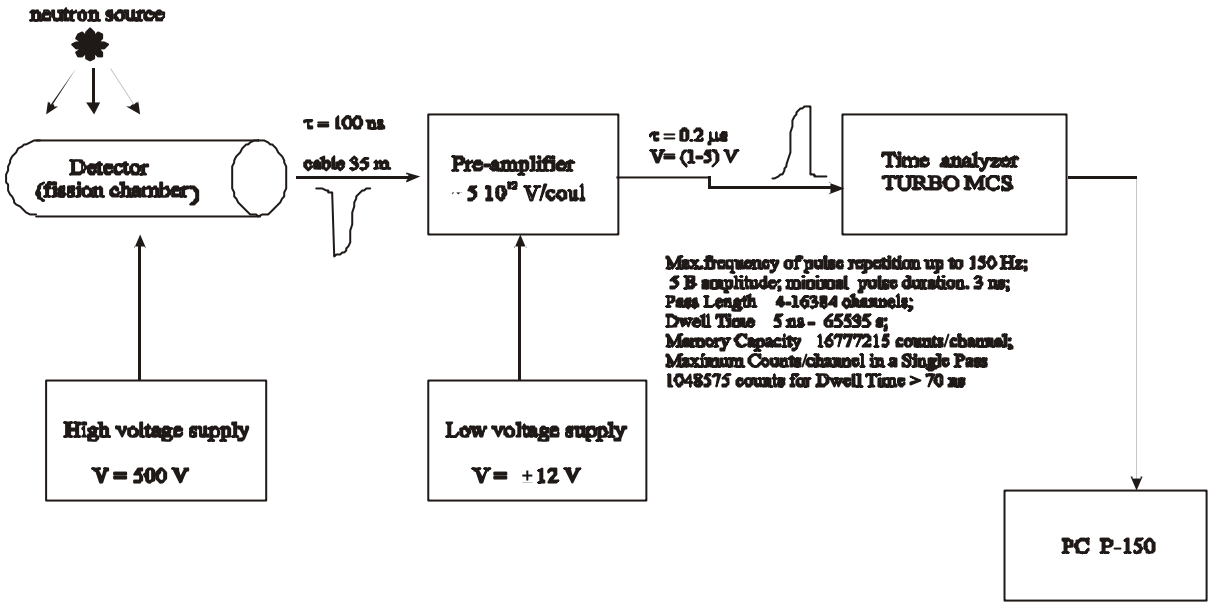


## Objectives achieved up to date.

The following experiments to investigate the physics of subcritical system with thermal spectrum driven with external sources (DD),(DT) have been performed::
1. Measurements of Keff for Nrods equal to 280;
2. Multiplication factors Ksrc for Nrods equal to 280 with different neutron sources S0(E,r,z);
3. Reactivity changes $\Delta\rho$ ($\rho=(k_{eff}-1)/k_{eff}$) due to removal 4 central fuel rods (Nrods= 280 and 276) (The measurements with pulse DT neutrons have been performed, $\tau = 7\mu s$)
4. Measurements of the following reaction rates inside the experimental channels of the core (Nrods = 280) $^{115}In(n,)^{116}In$, $^{19}F(n,2n)^{18}F$, $^{63}Cu(n,2n)^{62}Cu$, $^{27}Al(n,p)^{27}Mg$, $^{27}Al(n,\alpha)^{23}Na$, $^{65}Cu(n,2n)^{64}$ , $^{56}Fe(n,p)^{56}$,Mg, $^{54}Fe(n,p)^{54}Mg$, $^{59}Co(n,p)^{59}Fe$, $^{59}Co(n,\alpha)^{56}Fe$ (external source - DT neutrons).

5.Measurements of neutronics of the assembly without uranium fuel driven with a neutron generator working in (D,D) and (D,T) - modes and with Cf -252 source, placed at different positions of the assembly. (Measurements of spatial distribution of neutron flux density in experimental channels of the core and of the reflector).

6. Measurements of the external source multiplication factor of the sub-critical assembly M = (1-ks)-1 for the DD, DT neutrons and neutrons Cf - 252 source located at different positions in the assembly at the subcriticality level that corresponds to number of fuel pins 280.

At present we carry out researches according to the working plan of the project and the following
measurements is planned to be performed: keff, ksrc for Nrods equal to 216,245,280

with different neutron sources S0(E,r,z),reactivity changes due to removal both the central and the peripheral fuel rods ,transmutation reaction rates 129I(n, )130I, 237Np(n, )238Np, 243Am(n, )244Am, 237Np(n,f), 243Am(n,f) (for Nrods equal to 216,245,280) inside the experimental channels, axial and radial fission reaction rates 235U,238U,232Th,time distributions of fission rates 235U(n,f) for Nrods equal to 216,245,280 with two neutron sources (DD,DT) etc.

**ISTC Project 2002**
**"Experimental and theoretical studies of the yields of residual product nuclei produced in thin Pb and Bi targets irradiated by 40-2600 MeV protons"**

**Report on the 1st Quarter (January 1 – March 31, 2002)**

I. Brief description of the reported work

1. The experimental samples of $^{209}$Bi (five pieces), $^{nat.}$Pb (five pieces) $^{208}$Pb (five pieces), $^{207}$Pb (five pieces), and $^{206}$Pb (five pieces) have been manufactured using certified materials.

2. The CANBERRA GC2518 spectrometer used in the measurements was calibrated weekly by measuring gamma-spectra of the OSGI-3-1-1p $^{152}$Eu calibration source. The measured gamma-spectra were used to locate the main gamma-lines of the source and to determine the absolute effectiveness of the spectrometer. The resultant 7-year long time dependence of the two parameters demonstrates stable performance of the spectrometer.

3. The novel fast extraction system has been adjusted, which makes it possible to extract protons of any energy between 0.04 GeV and 2.6 GeV.

4. The $^{209}$Bi, $^{nat.}$Pb, $^{208}$Pb, $^{207}$Pb, and $^{206}$Pb samples have been irradiated with 2.6 GeV protons extracted by the old slow extraction system, and with 1.2 GeV protons extracted by the new fast extraction system. The $^{27}$Al(p,x)$^{22}$Na reaction was used to monitor the proton flux for both energies. Tentative proton fluences through the samples (see Table 1) have been obtained using the $^{27}$Al(p,x)$^{24}$Na reaction. The final fluences will be obtained after measuring the $^{22}$Na yields (within about 3-6 months after the irradiation).
Besides, $^{197}$Au have been irradiated with 0.8 GeV protons (beyond the Workplan) with the view to later comparison with the GSI inverse kinematics results.

5. The samples irradiated are being gamma-spectrometered. 420 spectra had been measured by the end of the 1st Quarter (see Table 1).

6. 206 spectra measured in the samples have been processed (see Table 1) by the GENIE2000 code in interactive mode.

7. The gamma-lines of the spectra from the 0.8 GeV proton irradiated $^{197}$Au sample have been identified. The yields of radioactive residual nuclei have started being determined.

8. The 2.6 GeV and 1.6 GeV proton-irradiated $^{209}$Bi, $^{nat.}$Pb, $^{208}$Pb, $^{207}$Pb, and $^{206}$Pb product nuclide yields have been simulated by the CEM95, LAHET, INUCL, CASCADE, and YIELDX codes.

9. The divergences of the INC model (CASCADO, LAHET, CEM-95) from the experimental data and from the estimated (p,xn) and (p,xp) reaction cross sections at proton energies 100-250 MeV have been analyzed. The analysis has shown that the divergences arise mainly from

(i) the INC completion condition (as regards energy or accumulation condition of the imaginary part of optical potential);

(ii) the particular description of the probabilities of transitions to more complex exciton configurations (the relations for $\lambda+$) $n \rightarrow n+2$.

The parameters for later calculations will be finally chosen by analyzing the total set of experimental data during the quarters to come.

The effect of the parameters of nuclear level density as a function of excitation energy and the effect of other characteristics of a decaying post-INC nucleus on the residual nuclide yields was also studied. It has been shown that the difference between the calculated and experimental residual nuclide yields cannot be reduced in any way markedly by varying the nuclear level density parameters alone. For that purpose, the decay mechanism of excited nuclei must be specified.

Table 1. Sample irradiation parameters and numbers of measured/processed gamma-spectra.

| Proton energy, GeV | Sample | Irradiation date | Sample mass, mg | Proton Fluence, $p/cm^2$ | Numbers of measured/processed gamma-spectra |
|---|---|---|---|---|---|
| 2.6 | $^{209}$Bi | 29.10.01 | 291.4 | 4.5?10+13 | 31/31 |
| 2.6 | $^{nat.}$Pb | 23.10.01 | 204.5 | 1.5?10+12* | 29/- |
| 2.6 | $^{208}$Pb | 05.11.01 | 126.1 | 3.9?10+13 | 35/35 |
| 2.6 | $^{207}$Pb | 30.10.01 | 136.8 | 2.0?10+13 | 32/32 |
| 2.6 | $^{206}$Pb | 06.11.01 | 123.0 | 3.4?10+13 | 32/32 |
| 1.2 | $^{209}$Bi | 26.02.02 | 290.5 | 6.1?10+13 | 36/20 |
| 1.2 | $^{nat.}$Pb | 22.02.02 | 137.8 | 1.4?10+14 | 61/-** |
| 1.2 | $^{208}$Pb | 04.03.02 | 136.8 | 5.8?10+13 | 38/- |
| 1.2 | $^{207}$Pb | 11.03.02 | 145.0 | 6.7?10+13 | 34/- |
| 1.2 | $^{206}$Pb | 15.03.02 | 138.0 | 8.0?10+13 | 36/- |
| 0.8 | $^{197}$Au | 22.10.01 | 78.7 | 3.4?10+13 | 56/56** |

* This sample is expected to irradiate again because of fluence smallness.
** Two samples were irradiated to examine the impact of the emission of residual product nuclei with a high recoil energy from the samples on the results obtained.

II. The above items conform to the approved Workplan for the 1st Quarter of the 1st year of researches under the Project

III. Summary of the personnel commitments: 39 workers were committed in the researches.

IV. Purchased equipment:

1. Printer HP LaserJat 2200D;
2. Printer Epson Stylus Photo 1290;
3. Monitor 17” LG795FT;
4. PC Athlon XP-1900 DRAM 256Mb, HDD 40Gb/CD-ROM 48x/Video ASUS (2 units).

V. Current status: the researches are made as scheduled.

VI. Delays, troubles, suggestions: none.

Manager of Project 2002

Yu.E.Titarenko

**ISTC Project 2002 Report on the 2nd Quarter (April 1 – June 30, 2002)**

I. Brief description of the reported work

1. Tests are continued of the new system of fast proton extraction to reach extraction of protons of any energy within the 0.04-2.6 GeV range

2. The CANBERRA GC2518 spectrometer used in the measurements was calibrated weekly by measuring gamma-spectra of the OSGI-3-1-1p $^{152}$Eu calibration source. The measured gamma-spectra were used to locate the main gamma-lines of the source and to determine the absolute effectiveness of the spectrometer. The resultant 7-year long time dependence of the two parameters demonstrates stable performance of the spectrometer.

3. During two runs of the accelerator operations (from 1 to 26 April 2002 and from 3 to 28 June 2002), the $^{209}$Bi, $^{nat}$Pb, $^{208}$Pb, $^{207}$Pb, and $^{206}$Pb sample were irradiated with 0.6, 0.8, and 1.6 GeV protons (15 experiments in total) using the new fast extraction system. The tentative proton fluences through the samples (see Table 1) have been obtained using the $^{27}$Al(p,x)$^{24}$Na reaction. The final values of the fluences will be obtained on measuring the $^{27}$Al(p,x)$^{22}$Na yields (in ~3-6 months after the irradiation).

4. Gamma-spectrometry of the samples irradiated during Quarters 1 and 2 is in progress. Some 800 spectra of the samples had been measured by the end of Quarter 2 (see Table 1).

5. 320 gamma spectra of the samples measured have been processed (see Table 1) by the GENIE2000 code interactive mode.

6. The yields of 95 radioactive residual product nuclei in the 0.8 GeV proton-irradiated $^{197}$Au sample have been determined.

7. The gamma lines of the spectra measured in the 2.6 GeV proton-irradiated $^{209}$Bi, $^{208}$Pb, $^{207}$Pb, and $^{206}$Pb samples have been identified. The yields of radioactive residual product nuclei are being determined for the given experiments.

8. The 0.8 and 1.6 GeV proton-irradiated $^{209}$Bi, $^{nat}$Pb, $^{208}$Pb, $^{207}$Pb, and $^{206}$Pb product nuclide yields have been simulated by the CEM95, LAHET, INUCL, CASCADE, and YIELDX codes.

9. The fission cross sections and dispersions of the mass distributions of fragments were analyzed for the Pb and Bi isotopes.

The total set of the experimental data on the integral cross sections for the proton-induced fission of the Pb and Bi isotopes at energies ranging from the threshold to 1 GeV, as well as on the respective dispersions of the mass yields of the fission products, have been accumulated and analyzed. The optimal parameterization of the $^{206,207,208}$Pb isotopes has been obtained in terms of the Fukahori-Prokofiev empirical systematization to supplement the available parameterizations of the fission cross sections for the natural mixture of the Pb and Bi isotopes.

The LAHET and CASCADO codes have been used to analyze the energy dependence of the dispersion of the mass and charge yields of the $^{208}$Pb fission fragments in the 100 MeV – 1 GeV range. Given a consistent normalization of the calculation results to the integral fission cross sections, the calculation results of the two codes prove to correctly reproduce the mass distributions of the fission products observed at the ~80 MeV and 1 GeV proton energies. In the intermediate energy range, any reliable experimental data are still absent, so they must be

obtained under the present Project. The calculations made permit us to predict that the expected energy dependence of the dispersion is proportional to the temperature of nucleus at the effective breake-ip point, i.e., it is proportional to the square root of the mean excitation energy of a fissile nucleus after the INC fast stage.

The differences in the $^{206,207,208}$Pb fission fragment yields have been calculated for the 1 GeV proton energy too. The resultant variations of the mean mass and mass yield dispersion of the fission fragments have been shown to agree with the dependence of the asymmetric deformation rigidity of the saddle-point configurations of fissile nuclei on the $Z^2/A$ ratio predicted by the liquid drop model. The rigidity variations due to the shell effects become only marked at the excitation energies below ~50 MeV. The results obtained will be possible to verify and specify after the relevant measurements are made under the present Project.

The routines BARPOL18, SIGSTOR, CROSTI, SIGHAD, NUCROS, TYPINT,NTPLACE of the CASCADE code have been developed and tested via detailed comparison with experimental data on total, elastic and inelastic cross-sections of nucleon-nucleus interactions, and on inelastic cross sections of nucleus-nucleus interactions. The DELEN and PRECO algorithms that simulate nuclides production via evaporation and fission of high-excited nuclei are optimized. Further improvement of nuclides production simulation requires, first of all, more detailed fitting of the phenomenological constants used. All the routines are well described allowing the user to make further improvements.

Table 1. The sample irradiation parameters and the number of gamma spectra measured/processed.

| Proton energy, GeV | Sample | Irradi-ation date | Sample mass, mg | Proton fluence, p/cm$^2$ | Number of gamma spectra measured/pro-cessed | Measurement state |
|---|---|---|---|---|---|---|
| **I quarter** | | | | | | |
| 2.6 | 209-Bi | 29.10.01 | 291.4 | 4.5?10+13 | 31/31 | Completed |
| 2.6 | nat-Pb | 23.10.01 | 204.5 | 1.5?10+12* | 29/- | Completed |
| 2.6 | 208-Pb | 05.11.01 | 126.1 | 3.9?10+13 | 35/35 | Completed |
| 2.6 | 207-Pb | 30.10.01 | 136.8 | 2.0?10+13 | 32/32 | Completed |
| 2.6 | 206-Pb | 06.11.01 | 123.0 | 3.4?10+13 | 32/32 | Completed |
| 1.2 | 209-Bi | 26.02.02 | 290.5 | 6.1?10+13 | 36/20 | In progress |
| 1.2 | nat-Pb | 22.02.02 | 137.8 | 1.4?10+14 | 61/-** | In progress |
| 1.2 | 208-Pb | 04.03.02 | 136.8 | 5.8?10+13 | 38/- | In progress |
| 1.2 | 207-Pb | 11.03.02 | 145.0 | 6.7?10+13 | 34/- | In progress |
| 1.2 | 206-Pb | 15.03.02 | 138.0 | 8.0?10+13 | 36/- | In progress |
| 0.8 | 197-Au | 22.10.01 | 78.7 | 3.4?10+13 | 56/56** | Completed |
| **II quarter** | | | | | | |
| 1.6 | 209-Bi | 08.04.02 | 342.9 | 3.8?10+13 | 26/- | In progress |
| 1.6 | nat-Pb | 08.04.02 | 205.4 | 5.9?10+13 | 32/- | In progress |
| 1.6 | 208-Pb | 11.04.02 | 143.8 | 5.7?10+13 | 39/- | In progress |
| 1.6 | 207-Pb | 11.04.02 | 143.4 | 3.5?10+13 | 24/- | In progress |
| 1.6 | 206-Pb | 15.04.02 | 135.8 | 6.8?10+13 | 27/- | In progress |
| 0.8 | 209-Bi | 18.04.02 | 286.5 | 5.4?10+13 | 26/- | In progress |
| 0.8 | nat-Pb | 18.04.02 | 191.3 | 8.3?10+13 | 27/- | In progress |
| 0.8 | 208-Pb | 06.06.02 | 138.9 | 8.6?10+13 | 24/- | In progress |
| 0.8 | 207-Pb | 06.06.02 | 139.3 | 8.4?10+13 | 26/- | In progress |

| | | | | | | |
|---|---|---|---|---|---|---|
| 0.8 | 206-Pb | 10.06.02 | 142.0 | 9.2?10+13 | 30/- | In progress |
| 0.6 | 209-Bi | 17.06.02 | 301.6 | 3.8?10+13 | 25/- | In progress |
| 0.6 | nat-Pb | 13.06.02 | 153.7 | 8.3?10+13 | 29/- | In progress |
| 0.6 | 208-Pb | 17.06.02 | 140.1 | 8.0?10+13 | 24/- | In progress |
| 0.6 | 207-Pb | 24.06.02 | 147.8 | 9.0?10+13 | 27/- | In progress |
| 0.6 | 206-Pb | 24.06.02 | 140.3 | 9.8?10+13 | 26/- | In progress |

* The sample is expected to irradiate anew because of the low fluence
** Two samples were irradiated to study the impact of the emission of residual product nuclei of a high recoil energy from the samples on the results obtained.

II. The above items correspond to the approved research schedule of Quarter 2 of the first year of the Project.

III. Personnel commitments.
39 persons were engaged in the researches under the Project.

IV. The equipment purchased.
1. HDD 36 Gb (SCSI) + cable LVD.

V. The current state of the researches.
The researches conform to the schedule.

VI. Delays, troubles, proposals.
None.

Manager of Project 2002

Yury E. Titarenko

**Report on Quarter 3 of the ISTC 2002 Project**
**1 July 2002 – 30 September 2002**

I. Brief description of the reported work

1. As earlier, the CANBERRA spectrometer coupled with a GC2518 Ge detector was calibrated weekly by measuring gamma-spectra of the OSGI-3-1-1r $^{152}$Eu calibration source. The gamma-spectra measured were used to find the position of the main source lines and the absolute spectrometer detection effectiveness at given energies. The resultant time dependence of the two parameters for the last seven years has confirmed that the operations of the spectrometer are actually stable.

2. The accelerator was not committed in the researches during Quarter 3. Preparations are made for two irradiation runs of the accelerator to be realized in Quarter 4 (October-December 2002).

3. The samples irradiated during Quarters 1 and 2 keep being spectrometered. Most of the spectra were measured pending the measurements of relatively long-lived reaction products. Therefore, the spectral measurements lasted mostly for 2-3 days. By the end of Quarter 3, 857 spectra had been measured (see Table 1)

4. The measured 211 gamma-spectra of the samples have been processed (see Table 1) by the interactive mode of the GENIE2000 code. By the end of Quarter 3, 531 spectra had been processed.

5. The spectral gamma-lines are being identified. The yields of residual product nuclei from 1.2 GeV proton-irradiated $^{209}$Bi, $^{208}$Pb, $^{207}$Pb, and $^{206}$Pb samples and from 2.6 GeV proton-irradiated $^{209}$Bi sample are being determined.

6. 581 cross sections for production of product nuclei in (p,x) reactions on 2.6 GeV proton-irradiated $^{208}$Pb, $^{207}$Pb, and $^{206}$Pb and on 0.8 GeV proton-irradiated $^{197}$Au have been determined.

7. The yields of $^{209}$Bi, $^{nat}$Pb, $^{208}$Pb, $^{207}$Pb, and $^{206}$Pb product nuclei at proton energies 0.6 GeV and 1.2 GeV have been simulated by the CEM95, LAHET, INUCL, CASCADE, and YIELDX codes

8. Studies were made with a view of constructing a consistent fission model that would allow for the shell-to-liquid drop fission barrier transition as the excitation energy increases and include the impact of nuclear viscosity on fissility of nuclei.

The effect of different parameterizations of the fission barriers on the Pb and Bi fission cross sections has been analyzed. The calculations were made in terms of different methods for parameterizing fission barriers as proposed by:

a) Sierk, Yukawa. Phys.Rev. v. C33 (1986) p. 2039;
b) Barashenkov, Gereghi, Iljinov and Toneev. Nucl.Phys. v. A206 (1973) p. 131;
c) Barashenkov, Gereghi. Preprint JINR, P4-10781, Dubna, 1977;
d) Myers, Swiatecki. Ark.Phys. v. 36 (1967) p. 343;
e) Pauli, Lederberger. Nucl. Phys. v. A175 (1971) p. 545;
f) Krappe, Nix. Rochester conf. (1973)
g) Krappe, Nix, Sierk. Phys. Rev. v. C20 (1979) p. 992;
h) Cohen, Plasil, Swiatecki. Ann. of Phys. v. 82 (1974) p. 557.

The analysis has shown that the experimental cross sections for proton-induced Pb and Bi isotope fission within a broad proton energy range are reproduced best by parameterizing the fission barriers as proposed by Sierk. The ALICE and CASCADO code simulation results reproduce the Pb and Bi fission cross sections up to proton energies of 120 MeV without modifying the fission barriers, i.e., with the standard-selected parameters. At proton energies above 120 MeV, however, the liquid drop fission barrier has to be lowered by about 10% for the CASCADO code.

At proton energies above 120 MeV, the ALICE code underestimates (by a factor of up to 2) the fission cross section compared with experiment, while the 10% decrease of the fission barriers proves to be insufficient.

Both ALICE and CASCADO allowed for the viscosity of fissile nuclei at excitation energies above 100 MeV in terms of the phenomenological approach to describing the fission widths by introducing the factor of effective suppression of fission probability at high energies of projectiles.

The sensitivity of the integral fission cross section to the shell corrections in the liquid drop fission barriers has proved to be below expectations. At the same time, the impact of the shell corrections on the mass and charge distributions of reaction products is rather significant.

Considering the effects studied, the fission barrier systematization proposed by Sierk can most adequately reproduce the experimental fission cross sections of Bb and Bi isotopes within a broad range of projectile energies from 30 MeV to 1.2 GeV.

The new optimized and minutely-described version of the INELAA subroutine, which governs the inelastic hadron-nucleus and nucleus-nucleus interactions, has been developed and included in the CASCADE code system. The BLPINN subroutine for calculating the coordinates of intranuclear nucleons (newly named COORDN) and the DELTA module for simulating the mass defect have been optimized and described in detail.

The energy dependence of isotope yield in proton interactions with light and heavy nuclei has been studied at energies from 100 MeV to 1 GeV. The mean isotope mass distributions N(A) depend relatively little on the cascade model details, but the separate isotope yields N(A,Z) can be determined only up to a factor of 1.5-3.0.

Allowance for the dependence of the level density parameters on the properties of excited post-cascade nuclei permits the differences from experiment to be reduced by 20-30% at energies of about 1 GeV, and by a somewhat higher percentage at lower energies. At the same time, the CASCADE code system proved to discord significantly with experiment when describing the isotope yields from Th and U nuclei. The discord may be eliminated in terms of some additional hypotheses concerning the properties of the post-cascade nuclei. The hypotheses have been poorly validated, however. The relevant studies are in progress.

Table 1. The current summary of irradiations, gamma-spectrum processing, and determination of residual nuclide yields in the experiments under Project 2002. The data presentation form is **x/y/z**, where **x** is the number of gamma-spectra measured (labeled **+** if all the scheduled spectra have been measured); **y** is the number of the GENIE2000 code-processed gamma-spectra; **z** is the number of the residual nuclide yields determined (**PR** in case the yields are being determined)

| Energy, GeV | $^{208}$Pb | $^{207}$Pb | $^{206}$Pb | $^{nat}$Pb | $^{209}$Bi | |
|---|---|---|---|---|---|---|
| 0.04 | - | - | - | - | - | |
| 0.07 | - | - | - | - | - | |
| 0.1 | - | - | - | - | - | |
| 0.15 | - | - | - | - | - | |
| 0.2 | - | - | - | - | - | |
| 0.4 | - | - | - | - | - | |
| 0.6 | 25/-/- | 28/-/- | 27/-/- | 30/15/- | 26/-/- | |
| 0.8 | 30/-/- | 29/-/- | 32/-/- | 27/-/- | 25/-/- | $^{197}$Au: 56/56/95 |
| 1.2 | 41+/41/PR | 38+/30/PR | 40+/40/PR | 66+**/66/PR | 39+/39/PR | |
| 1.6 | 25/24/- | 25/24/- | 28/26/- | 32/14/- | 27/26/- | |
| 2.6 | 35+/35/162 | 32+/32/162 | 32+/32/162 | 31*/-/- | 31+/31/PR | |

*The sample is expected to irradiate anew because of the low fluence.
**Two samples were irradiated to study the impact of the emission of residual product nuclides from the samples at high recoil energies of the nuclides.

II. The above items conform to the approved workplan of Quarter 3 of the first year of Project 2002.

III. Summary of personnel commitments:
44 persons participated in the research works under Project 2002.

IV. Equipment purchased:
None.

V. The current state of the research works:
The researchers are underway conforming to the schedule.

VI. Troubles, faults, proposals:
None.

Project 2002 Manager

Yu.E.Titarenko

Liquid Metal Target Advisory Committee Meeting

Meeting Minutes

July 31 – August 2 2002
Las Vegas, UNLV

Prepared by Keith Woloshun
Revised by Waclaw Gudowski

## Summary

The target complex TC-1 has arrived at the University of Nevada Las Vegas (UNLV) campus. The intent of UNLV is to utilize this target complex as a significant component of a multi-year lead-bismuth (LBE) technology development program. The goal of UNLV is a research program that contributes to the international programs while remaining true to the fundamental goal of all Universities: The training and education of students. To this end, the function of this meeting was to present to UNLV an overview of LBE work in the US and Europe, and to advise on an appropriate path forward for TC-1. At the same time, it was recognized that many useful University-level research activities could be conducted with small-scale benchtop experiments, independent of and in addition to TC-1. Some of these possibilities were presented and discussed as well.

These minutes do attempt to paraphrase or summarize the presentations made during the meeting. The meeting agenda and attendance list is attached. If there is any need to access presentation materials, the reader of these minutes is urged to directly contact the presenter directly.

These minutes will summarize the recommendations to UNLV. These recommendations are a composite of individual suggestions made by presenters during the course of the meeting as well as free-form discussions by all persons present.

**In the interest of maximizing the benefit of this program to all collaborators, as well as the UNLV team, this Advisory Committee will continue to meet periodically. To minimize inconvenience, these meetings will normally be conducted along with larger conference meetings. The next meeting of this Committee will be held on 12 to 18 months.**

## Initial Program Recommendations to UNLV

The fundamental recommendation to UNLV is to set up the target as it is, without modifications, and operate for nominally 3000 hrs, cumulative. This test program establishes a baseline facility and operating experience for UNLV staff and students, and provides benefit to the ISTC 559 collaborators. Parametric studies within the design envelope of TC-1 are recommended, varying pump power, heat loads, operating temperature, etc. Points of investigation could include:

1) Both steady-state and transient operation.
2) Assure and demonstrate energy balance.
3) Determine system time constants.
4) Monitor stability and reproducibility of system performance over time.
5) Compare performance to model predictions.

In conducting this test, UNLV is reminded of a few key design constraints:

1) Temperatures greater than 150 C everywhere.
2) Heat exchanger pressure no greater than 35 bar on secondary side.
3) No more than 15 cold starts.

The set-up for this test will require proper and safe mounting of TC-1, the design, procurement, installation and testing of all secondary systems, and modification of the controls and data acquisition software to include the secondary systems. It is anticipated that these preparations will take approximately 1 year, and the 3000 hr test program will require another year.

Concurrent with this activity, it is recommended that UNLV develop additional capabilities to do fundamental LBE research and build up special experimental facilities providing such research capabilities. Broadly speaking, this research should encompass the topics of corrosion, thermalhydraulics and instrumentation. Specific suggested areas of academic research are listed below. Such activity is extremely important for engineering personal training, as well as for development of scientific background for TC-1 operation, educational and research activity.

## Subsequent R&D Recommendations

After completing this 2-year combined program of TC-1 operations and supporting fundamental research, UNLV must make decisions based on

its own institutional needs and interests, coupled with available funding and the status of related LBE technology developments outside UNLV. Based on current knowledge the following decision tree is foreseen:

1) Add corrosion chemistry control and measurement capabilities to TC-1.
2) Add a test section to TC-1. Most likely, this entails removing the target itself from TC-1 and replacing it with some geometry suitable for tests of interest that have arisen from the ongoing capabilities development.
3) Perform contaminant transport experiments. Such experiments may permanently exclude future use of TC-1.
4) Visual inspection of the TC-1 primary circuit surfaces, metallography and/or another investigations of primary circuit structure materials.
5) Abandon TC-1 in favor of re-use of key components in another facility (pump, flow meter, heat exchanger, instruments, etc.)

Clearly, 1 and 2 can be performed without destruction, but 3, 4 can limit future use of the system or will lead to TC-1 renewal end 5 means the end of TC-1 life.

**Capabilities Development and Research Recommendations**

During this meeting, a variety of possible research topics were suggested. Some of the topics listed below were extracted from a preliminary Test Plan document for UNLV, crafted by Ning Li, Samir Moujaes and Joachim Knebel.

1) Flow measurement techniques: Magnetic, ultrasonic, and the application of classic or innovative techniques to high temperature liquid metals.
2) Pressure measurements.
3) Continuous level measurements. Currently, point measurements are typically made using continuity-type probes. A continuous measurement using optical or other techniques would improve control and operation of LBE facilities.
4) Gas flow in liquid LBE: The entrainment and movement of bubbles; buoyancy effects.
5) Contaminant species transport and deposition in flowing LBE.
6) Oxygen control and measurement. In advance of possibly installing a system in TC-1, benchtop tests could be performed to

study effects of gas feed rates and temperature on establishing objective oxygen concentrations, and the stability of oxygen concentrations and oxygen sensors with time.

7) Corrosion modelling and mass transfer model verification.
8) Heat transfer measurements including unusual geometries where no correlations have been developed, typical of most window designs. It is a significant fact that in window cooling both thermal and momentum boundary layers are never fully developed.
9) Ultrasonic and radiographic non-destructive inspection of structures.
10) Benchmark experiments for CFD codes and turbulence models for low Pr number flow.
11) Scaled testing of new LBE system concepts, such as gas-assisted pumping and windowless targets.

Liquid Metal Target Advisory Committee Meeting

July 31 – August 2 2002
Las Vegas, UNLV
The Marjorie Barrick Museum of Natural History/Harry Reid Center for Environmental Studies auditorium located in the center of the UNLV campus.

# Agenda

**July 31, 2002**

**Tour to Yucca Mountain for all registered participants**
Departure: 6:00 am from the hotel
Return ~ 4:00 pm (the rest of the day can be spent in casinos..)

**August 1, 2002**

8:30 – Transportation from the hotel to UNLV

**Overview on the LBE Work in the US and at LANL / UNLV**

| | |
|---|---|
| 9:00 – 9:30 | Welcome, organizational details etc. Anthony Hechanova, W. Gudowski |
| 9:30 - 10:30 | Status of the target and "the transfer project" – E. Efimov |
| 10:30 – 11:00 | Coffee break |
| 11:00 – 12:00 | Experimental program at UNLV – A. Hechanova |
| 12:00 – 13:30 | Lunch break |
| 13:30 – 15:00 | Lead-Bismuth project at LANL and collaboration with UNLV - Ning Li |
| 15:00 – 15:30 | US perspective on development of Pb-Bi technology (in the target project context) – F. Goldner |
| 15:30 – 16:00 | Coffee break |
| 16:00 – 17:30 | Discussion. Special issues: Pitting corrosion |
| 17:30 – | Adjourn |

Dinner together

**August 2, 2002**

8:30 – Transportation from the hotel to UNLV

**European projects in Pb-Bi, collaborative potential**

| | |
|---|---|
| 9:00 – 9:40 | Presentation of the TECLA project – C Fazio, ENEA |

9:40 – 10:20 KALLA Laboratory: An Overview – Joachim U. Knebel, FZK
10:20 – 10:50 Coffee break
10:50 – 11:30 Status of MEGAPIE Initiative – Joachim U. Knebel, FZK
11:30 – 12:10 Status of MYRRHA Project – H. Abderrahim

12:10 – 13:30 Lunch

13:30 – 15:00 Formulation of a Joint R&D Programme for UNLV LBE Loop, All (see Appendix 1. - Ning Li's comments for introduction to our discussion)
15:00 – 16:00 Discussion and summary. All participants

**16:00-18:00 Technical visit to UNLV**

# UNLV Transmutation Research Program
## Attendance Sheet
**Molten Metal Advisory Committee**

**Thursday, August 1, 2002**

| Name | Organization | E-mail<br>Phone |
|---|---|---|
| Longzhou Ma | HRC UNLV | lma@unlv.edu |
| Bingmen Fu | Mech Eng | bmtu@nscee.edu<br>702-895-3655 |
| Dale L Perry | LBNL | dlperry@lbl.gov |
| John Farley | UNLV | farley@unlv.edu |
| Samir Moujaes | UNLV | samir@unlv.edu |
| Gary Cerefice | UNLV/HPC | |
| Jim Selser | UNLV Physics | selser@physics.unlv.edu |
| Ajit Roy | HRC/MEG. UNLV | aroy@unlv.edu |
| Konstantin Zabotkin | UNLV/AAA | zabotkin@hotmail.com |
| Kemal Pasamehmetoglu | LANL | kop@lanl.gov<br>505-667-8893 |
| Bill Culbreth | UNLV, Engineering | culbreti@nscee.edu<br>702-896-2817 |
| Julia Maneroue | UNLV | |
| Tom Ward | DOE HQ | Thomas.ward@nnsa.doe.ccov<br>202-586-7255 |
| Valentina Tcharnotskaia | LANL | valentina@lanl.gov<br>505-665-9375 |
| Hamid Ait Abderrahiit | SCK-CEN (Belgium) | Haitabde@sckcen.be<br>+32-14-33-2277 |
| Fazio Concetta | ENEA | Concetta.fazio@brasimone.enea.it<br>+39-0336-801963 |
| Waclaw Gudowski | UTH/RIT | wacek@neutron.kth.se<br>+66-0-553-78200 |
| Joachim Knebel | TZU/ NUCLEAR | Joachim.knebel@psf.fzk.de |
| Evgeni Efimov | IPPE | yefimov@ippe.obninsk.ru<br>007-08439-98703 |
| Alexander Dedoul | IPPE | dedoul@ippe.obninsk.ru |
| Keith Woloshun | LANL | Woloshun@lanl.gov<br>505-665-6822 |
| Dennis Beller | LANL | beller@lanl.gov<br>702-895-2023 |
| Ellen Johnson | UNLV | |

| | | |
|---|---|---|
| Omar Younas | UNLV | uyounas@aol.com |
| Yingtao Tiang | UNLC | yingtao@egr.unlv.edu |
| Woosoon Yim | UNLV | wy@me.unlv.edu |
| Ning Li | LANL | ningli@lanl.gov |
| Anthony Hechanova | UNLV | hechanova@unlv.edu |
| Carter Hull | UNLV | hull@unlv.edu |
| | | |